

**The regulation and function of cortical  
actin remodelling upon entry into  
mitosis**

**André Rosa**

**A thesis submitted to University College of London  
for the degree of Doctor of Philosophy**

**PhD Supervisor: Dr. Buzz Baum**

**MRC Laboratory for Molecular Cell Biology  
UCL**

**October 2013**

## **DECLARATION**

I André Ângelo Sousa Rosa confirm that the work presented in this thesis is my own. Where information has been derived from other sources, I confirm that this has been indicated in the thesis.



## **ABSTRACT**

Entry into mitosis is accompanied by dramatic changes in the morphology and polarity of cells, both of which entail remodelling of the cortical actomyosin cytoskeleton. Here I identified Diaphanous as the main actin nucleator required for the formation of the mitotic actin cortex in the context of a developing epithelium. I also identify the pathway involved, which we show is dependent on Pebble/RhoA and on the apical polarity regulators aPKC/Cdc42/Par6. Strikingly, following the activation of Pbl upon entry into mitosis, Cdc42 RhoGTPase and the polarity proteins aPKC and Par6 extend their domain more basally driving the cortical accumulation of Dia, while Rho directs the accumulation of cortical p-Myosin II. Taken together, these data reveal a new molecular mechanism for the concerted activation and localization of Dia via RhoGTPases and the intimate link between cortical repolarisation and the regulation of actin filament organisation.

## ACKNOWLEDGEMENTS

I would like to acknowledge the financial support from the Fundação para a Ciência e Tecnologia (FCT) to undergo my research. To my PhD program, GABBA, most likely the best PhD program worldwide, where offers students the possibility to learn more about science in the best of environments and then gives them the opportunity to perform their PhD's wherever they want, sounds crazy but its true! Thank you for believing in me.

I want to thank my GABBA year. Those six-seven months in Porto were one of the most amazing times in my life. They are Adriana, Antonio, Bebiana, Bernardo, Bruno, Diana, Diogo, Que-laudia, Cristiana, Joao, Margherita. Best group ever, VINTAGE (title given by Prof. Maria)!! pitty I'm there to ruin the bouquet. Thanks for the moments I shared with you guys. Most definitely one of the best moments in my life and which I will always praise, I love you all (weird this coming from me but you know that deep inside I still have some feelings, deep, deep inside). A special thank to Diana and Antonio for spending most of their time with me during that period, and making Friday nights the most desired night of the all week. Those nights were unutterable!! And Curado for always being a good friend. To Catarina Carona. Minha querida, invejo-te a determinacao e bom humor para aturares todos os anos os estarolas que iniciam mais um ano de GABBA.

To the group of 4 that made the GABBA house in London: Festa do Bigode, nunca mais chegamos a casaaaa!! Poker, Żubrówka, buy guitars at 2 in the morning, dinner by Bruno, cleaning by Calhas, Bernas and the ladies, Toni and - I'm just going for a snooze! You all know what I'm talking about. Good moments! Not forgetting the great apartment of Mornington Crescent! Who doesn't miss the: BELHO, TA TUDO??. Grande SoMatos. My last flatmates: Bruno, Bernardo and Eliana. Thank you for taking up with me during my countless days of grumpiness.

I want to thank my supervisor Dr. Buzz Baum. Most likely I was one of the most challenging PhD students he had to come across with. By being a bit, maybe a lot, negativist, grumpy, stubborn, loud, pointy (a nasty Latin habit of pointing to the listener while expressing an idea) etc, etc. All the best qualities to drive any sane supervisor, mad. Thanks for your patience, guidance, support and knowledge. There are really no words to express my gratitude in the impact you had in my scientific and non-scientific life. Also, thanks for offering me your flat while I was finishing writing and had no place to stay. I wanted to accept but I was a bit scared of breaking something out, everyone in the lab convincing me to do a party in the flat and destroy the place.

I would like to thank Dr. Rui Martinho who had the patience to teach me to do science and to show me what a scientist should be.

I want to thank all the people that make the Buzz lab. A group of extraordinary people (and bright scientists) that make the LMCB a place where I always want to come back. To the past members: Remy, Eliana (which I am thanking a second time, she was really important during my time in London), Arturo, Pato, Marina, Oscar, Mario, Niiiick. To present members: Nelio, my faithful companion in the fly room (I wanted to say something a bit gay for him!) and fundamental colleague in the endless discussions about science and life at late hours in the lab; Scott, latecomer in the fly room, but to who I am very thankful for his friendship. We still have to go to Newcastle. That's going to be amazing! Andrea, the undeniable ladies man! A great privilege to get to know you and be your friend. *Mi casa es tu casa*, any time. Helen, to who I'm sincerely thankful for proofreading my thesis and offering me her spare room when I was homeless. One of the brightest and sweetest scientists I ever came across with. Nunu, my dear, never stop being loud. You are a storm; somebody should add your name to storm definition in Wikipedia. Thank you for your kindness and also offering me your flat when I needed it. Thanks to Ginger Hunter (I just love to say your name, it never gets old), Maxine, Christina, Sergey (also a funny name, only for Portuguese of course), Jigna, Charlotte, Pelin, Thom (he's the living spirit of the 60's). Jo, one of the brightest students I had the pleasure to teach. Clotilde, that

had a brief passage in our lab but to who I believe was the reason for bringing to Britain the hottest summer since 1910. Thank you for showing me happiness and beautifulness in life.

I would like to thank Jacob, a really crazy, but a good, good friend. We had a good run. Nicky, one of the sweetest ladies I ever meet.

I would like to thank Bernardo for taking care of me. A great friend that I will always cherish although he didn't name is new-born after me. Ingrid, thank you so much for taking me out. Best nights and gigs ever, I love your company and to chat with you. Elisa, my sweet friend, we need to get drunk the two of us, seriously! To Bruno, for teaching me to play the guitar and being a great friend. To Cristiana, that keeps challenging me to be a better person and to who I am really grateful to get to know. Um grande beijinho com o meu sincero agradecimento.

A huge, daqueles para entrar nos anais da historia, acknowledgement to all of my estarolas. Matos, o meu gordo, o meu mano Guedes. What can I say, if not what you always say: o que seria de mim sem ti? Xinxas, meu lindo cara-de-alien, one of sweetest, right in your face with no mercy, friends. Batatas meu amor, para ti tudo em Portugues, sabes que te adoro e que as raivas que tenho quando te vejo de te morder e apertar e porque gosto de ti por amor. Monica, my company at late hours while writing or doing experiments in the lab. L for the two of us? We will become the L brothers. Djess! Fade, most definitely the funniest man ever. You're so funny I'm laughing while writing this (seriously). Vitoria, minha afrodita, you know that I will always have a free bed for you and Ultra levur for the next time we go for a British breakfast. Helder, you're funny even when you don't say anything. After Fade you are the funniest guy ever. Irene, the girl with no fear of falling, or maybe just with poor balance. Thank you and Xinxas for Vicky. Patrizia, early arrival but already with so much to offer. Thank you for Sofia and Fade, also, thank you. You're funny! Andre Galvao, o homem que esta sempre a tocar ao bicho. E Bruno, the guy that always says it as it is. I doesn't get any more honest or brutal. Gosto de voces todos por amor.

A minha familia – aos meus avos paternos e maternos que sao as raizes mais antigas que formaram a minha pessoa. Aos meus pais e irmao pelo conforto e carinho que sempre me trataram. Esta jornada teria sido impossivel sem a vossa ajuda.

Finally, I would like not to thank but to dedicate this thesis, for whatever it might worth, to Catarina Fernandes. She is the one who drag my ass out of bed to finish my application for my PhD programme and supported me when I most needed. You're still me support, the inner voice that tells me to do right. She is one of my greatest role models.

## TABLE OF CONTENTS

<b>DECLARATION .....</b>	<b>2</b>
<b>ABSTRACT .....</b>	<b>3</b>
<b>ACKNOWLEDGEMENTS .....</b>	<b>4</b>
<b>TABLE OF FIGURES .....</b>	<b>12</b>
<b>ABBREVIATIONS .....</b>	<b>32</b>
<b>1. INTRODUCTION .....</b>	<b>33</b>
<b>1.1. actin .....</b>	<b>34</b>
<b>1.2. actin dynamics .....</b>	<b>35</b>
1.2.1. Regulation of actin polymerization .....	35
1.2.2. actin nucleators .....	37
1.2.3. actin networks .....	41
<b>1.3. Regulation of actin dynamics in response to external/internal cues. ....</b>	<b>45</b>
1.3.1. Rho .....	46
1.3.2. Rac .....	47
1.3.3. Cdc42 .....	48
1.3.4. actin and Endocytosis .....	49
1.3.5. actin and Cell polarity .....	51
1.3.5.I. Yeast .....	51
1.3.5.II. Cell motility .....	52
1.3.5.III. The regulation of cell polarity in development .....	53
1.3.6. actin and Cell Division .....	55
<b>1.4. The notum as a model system .....</b>	<b>57</b>
1.4.1. Thorax closure .....	58
1.4.2. Patterning and pattern refinement of the notum .....	58

1.5. Aims of the thesis .....	60
<b>2. MATERIALS AND METHODS .....</b>	<b>62</b>
2.1. Genetic techniques .....	62
2.2. Conditions.....	63
2.3. Fly stocks .....	64
2.4. Live imaging and dissections .....	65
2.5. Image processing and analysis .....	66
<b>3. ACTIN-MYOSIN REMODELLING IN MITOSIS.....</b>	<b>68</b>
3.1. Introduction.....	68
3.2. Characterization of actin and Myosin organization in and out of mitosis. ....	69
3.3. Diaphanous versus Arp2/3 localization and function.....	73
3.4. Loss of an actin cortex in mitosis impairs cell size.....	87
3.5. Mitotic cells require an actin cortex to regulate spindle stability.....	91
3.6. Conclusions .....	96
<b>4. REGULATION OF THE ACTOMYOSIN CORTEX.....</b>	<b>98</b>
4.1. Introduction.....	98
4.2. The roles of Pbl, Rho and Cdc42 in the generation of the mitotic actomyosin cortex.....	100
4.2.1. Pebble is required for Myosin II activation and Dia localization and assembly of the mitotic actin cortex.....	100
4.2.2. Rho1 is required for Dia and Myosin II activation in mitosis	110
4.2.3. Cdc42 polarizes Dia at the cell cortex in mitosis. ....	117
4.3. Conclusions .....	126

<b>5. PEBBLE, CELL SHAPE CHANGES AND THE CONTROL OF APKC/CDC42 LOCALIZATION. ....</b>	<b>127</b>
5.1. Introduction.....	127
5.2. Cdc42/Par6/aPKC complex repolarizes in mitosis.....	128
5.3. aPKC/Par6/Cdc42 control mitotic cell shape.....	135
5.4. Pebble and Cdc42 controls aPKC localization in mitosis. ...	145
5.5. aPKC/Cdc42 controls Dia localization in mitosis.....	150
5.6. S.O.P. cells depend on Dia and Cdc42 activity for the remodeling of cortical actin in mitosis.....	153
5.7. Comparing Cdc42 and Dia gain of function.....	157
5.8. Conclusions .....	164
<b>6. CHARACTERIZATION OF APICAL-BASAL POLARITY IN MITOTIC EPITHELIAL CELLS. ....</b>	<b>166</b>
6.1. Introduction.....	166
6.2. Differential positioning of adherens junctions and Baz/Par3 associated with mitosis. ....	167
6.3. Extension of Crumbs domain decorates the cortex of cells in mitosis .....	172
6.4. Lgl depolarization in mitosis .....	175
6.5. Conclusions .....	178
<b>7. DISCUSSION.....</b>	<b>180</b>
7.1. Introduction.....	180
7.2. Cortical actin nucleation in mitosis is a Diaphanous-dependent process .....	181
7.3. Molecular pathway triggering changes in actin dynamics/organization upon entry into mitosis.....	185



7.4. Cortical repolarization in mitosis.....	188
8. OUTLOOK AND FUTURE PERSPECTIVES .....	192
9. BIBLIOGRAPHY .....	193

## TABLE OF FIGURES

Figure 1.2.1. 1. Actin filament elongation and ATP Hydrolysis. The association rate constants have units of  $\mu\text{M}^{-1} \text{s}^{-1}$ . Dissociation rate constants have units of  $\text{s}^{-1}$ . Hydrolysis of ATP bound to each subunit has a half time of 2 seconds. T- ATP-actin monomer. D- ADP-actin monomer. .... 36

Figure 1.2.2. 1. Model of actin nucleation induced by Formins and Arp2/3 complex. Activated Formins bind Profilin-actin-ATP monomers and processively elongate actin filaments. Arp2/3 activated complex nucleates new actin filaments on the side of a pre existing filament making a  $70^\circ$  angle directing filaments against the plasma membrane promoting a pushing force. .... 41

Figure 1.2.3. 1. Actin structures in a motile cell. Lamellipodia in motile cells is rich in branched actin filaments nucleated by Arp2/3 complex. Filopodia is composed of actin bundles nucleated by Formins. Stress fibres composed of actin bundles are associated to adhesion sites of the cell, marked by blue spots. .... 45

Figure 1.3.5. 1. Epithelial cell polarity. Epithelial cells are polarized along their apical-basal axis by the presence of apical microvilli composed of actin bundles, medial actin mesh, junctional actin at the level of adherens junctions and basal protrusions. Polarity proteins play a fundamental role

in establishing and maintaining cell polarity by mutual antagonism or activation of polarity complexes strategically localized along the cell axis. Black punctuated line indicates phosphorylation; red lines indicate mutual or single antagonism. .... 55

Figure 1.4. 1. Thorax closure. 6 hours AP the two epithelial sheets spread inside the pupal case. 8 hours AP fusion of the wing discs at the midline. 9 hours AP the wing discs are attached to the other discs. Abbreviations: ea, eyeantennal disc; dp, dorsal prothoracic disc; a, abdomen; h, haltere disc; s, scutellum. The *pnr* expression domain is indicated in green; in red, oblique flight muscles. Adapted from (Zeitlinger and Bohmann, 1999) ..... 60

Figure 3.2. 1. Filamentous actin accumulate at the cell cortex at the onset of mitosis. (A) Apical, intermediate and basal top views of a lifeactGFP expressing notum with yellow asterisk marking a cell going through different stages of mitosis (single Z-sections). Yellow arrowheads pinpoint medial actin mesh. (B) Live imaging of an intermediate section of a cell expressing lifeactGFP at different stages of mitosis. Yellow arrow: assymetric progression of the furrow from basal to apical. Scale bars: 5µM. .... 71

Figure 3.2. 2. Myosin accumulates at the cell cortex at the onset of mitosis. (A) Apical, intermediate and basal top views of sqh-GFP expressing notum with a yellow asterisk marking a cell going through different stages of mitosis. (B) Live imaging of a intermediate section of a cell expressing sqh-GFP at different stages of mitosis. Note Myosin II

accumulation at the basal part of the cytokinetic ring. Yellow arrow: assymetric progression of the furrow from basal to apical. Scale bars: 5μM.....	72
Figure 3.2. 3. Junctional actin. Actin in the most apical side of epithelial cells of the fly notum localizes with DE-Cadherin .....	73
Figure 3.3. 1. Arp2/3 localizes in punctate at adherens junctions (yellow arrowhead) and at the new interface between daughter cells following cytokinesis. (A) Apical top view of Arp3-GFP and α-tubulin-RFP expressing tissues. (B) Intermediate top view of metaphase cell expressing Arp3-GFP and α-tubulin-RFP. (C) Apical top view of cell performing cytokinesis (yellow arrow) with accumulation of Arp3-GFP and punctae of Arp3-GFP at the level at adherens junctions (yellow arrowhead). Scale bar: 5 μm.....	77
Figure 3.3. 2. RNAi mediated silencing of Arp2/3 does not alter the mitotic actin cortex. Images show actin filaments in apical, intermediate and basal sections of nota at different stages of mitosis, marked with a yellow asterisk. Cells are shown that express lifeact-GFP from the Pnr promoter in the absence (A) or presence (B) of a UAS-Arp3 RNAi transgene. Scale Bars: 5 μM. ....	78
Figure 3.3. 3. Cell deformations of metaphase cells in Arp3 depleted tissues. Intermediate top view of metaphase cell expressing lifeactGFP. Yellow arrow indicates cell bleb in Arp3 RNAi expressing cell. Scale bars: 5μm. ....	79

Figure 3.3. 4. Arp3 RNAi mediated silencing promotes cell blebbing at the furrow canal. Intermediate top view of cell in cytokinesis expressing lifeactGFP. Yellow arrow indicates cell bleb in Arp3 RNAi expressing cell Scale bars: 5µm. ....	79
Figure 3.3. 5. Arp3 RNAi mediated silencing does not alter mitotic cortex of P1 cells. Intermediate top view of metaphase cell expressing Neu-GMAGFP Scale bars: 5µm .....	79
Figure 3.3. 6. Wasp RNAi mediated silencing does not alter mitotic cortex of epithelial cells. Scale bars: 5µm.....	80
Figure 3.3. 7. Scar RNAi mediated silencing does not alter mitotic cortex of P1 cells. Intermediate top view of cells in metaphase and cytokinesis expressing Neu-GMA. Yellow arrow indicates cell bleb in SCAR RNAi expressing cell Scale bars: 5µm .....	80
Figure 3.3. 8. Diaphanous co-localizes with junctional filamentous actin. ....	83
Figure 3.3. 9. Diaphanous accumulates at the cortex of mitotic cells. (A) Intermediate top view of prophase cell. (B) Intermediate top view of metaphase cell with Dia accumulation at the cell cortex. (C) Intermediate top view of anaphase cell. (D) Intermediate top view of cell in cytokinesis with Dia accumulation at the furrow canal (Yellow arrow). ....	83
Figure 3.3. 10. Diaphanous decorates the entire cell cortex of epithelial cells in metaphase. Images show top view stacks from apical to basal sides of a metaphase cell marked with yellow asterisk stained for actin and Dia.....	84

Figure 3.3. 11. Diaphanous is required for the assembly of a mitotic actin cortex. Images show actin filaments in apical, intermediate and basal sections of *nota* at different stages of mitosis, marked with a yellow asterisk. Cells are shown that express lifeact-GFP from the *Pnr* promoter in the absence (A) or presence (B) of a UAS-Dia RNAi transgene. Scale Bars: 5  $\mu$ M. Arrowhead marks basal protrusions. Arrow marks

presumptive cleavage furrow. .... 84

Figure 3.3. 12. Assembly of a mitotic actin cortex in SOP cells is dependent of Dia activity. Intermediate top view of metaphase SOP cells expressing GMAGFP (control cells) and metaphase SOP cells expressing GMAGFP and Dia RNAi..... 85

Figure 3.3. 13. Assembly of an actin cortex is lost in the absence of Dia in epithelial cells entering mitosis. Y values indicate the ratio of mean gray values of filamentous actin intensity at the cortex/cytoplasm of epithelial cells expressing lifeactGFP at interphase and at different times (X time in seconds) in mitosis previously to anaphase. (Values plotted: mean $\pm$ S.D.). .... 85

Figure 3.3. 14. Assembly of an actin cortex is lost in the absence of Dia in SOP cells entering mitosis. Y values indicate the ratio of mean gray values of filamentous actin intensity at the cortex/cytoplasm of epithelial cells expressing Neu-GMAGFP at interphase and at different times (X: time in seconds) in mitosis previously to anaphase. (Values plotted: mean $\pm$ S.D.)..... 86

Figure 3.4. 1. Mitotic cells required an actin cortex to regulate cell size. 89

Figure 3.4. 2. Epithelial mitotic cell perimeter is moderately increased in Diaphanous dsRNA expressing tissues. (Mean±S.D. Control: 30.67±2.78. Diaphanous RNAi: 33.67±4.31 N=30).....	89
Figure 3.4. 3. Sensory organ precursor mitotic cell perimeter is moderately increased in Diaphanous dsRNA expressing tissues. (Mean±S.D. Control: 34.05±1.43. Diaphanous RNAi: 36.25±4.31 N=15). .....	90
Figure 3.4. 4. Nota of cells expressing Dia dsRNA show a decrease in height. (Mean±S.D. Control: 8.78±1.01 µm. Diaphanous RNAi: 7.22±0.94 µm N=3). .....	90
Figure 3.5. 1. Centrosome separation and spindle assembly in Diaphanous RNAi tissues is not impaired. A) NEB of control and Diaphanous RNAi cells marked by α-tubulinGFP B) Metaphase cells of control and Diaphanous RNAi cells marked by α-tubulinGFP displaying a mitotic spindle. Scale bars: 5 µm. ....	93
Figure 3.5. 2. Angle displacement is increased from NEB to anaphase in epithelial cells with Dia compromised function. Absolute values of angle displacement were added in time intervals of 20 seconds in cells progressing from NEB to anaphase. (Mean±S.D. Control: 141±37.3 degrees. Diaphanous RNAi: 189±61.6 degrees N=30).....	94
Figure 3.5. 3. Rate of angle displacement is slightly increased in cells expressing Dia dsRNA. The average of total angle displacement was measured in function of the time (in seconds) of cells progressing from NEB until anaphase. (Mean±S.D. Control: 0.25±0.05 degrees/sec. Diaphanous RNAi: 0.3±0.1 degrees/sec N=30) .....	94

Figure 3.5. 4. Mitotic spindle perform wider angular displacements in cells expressing Dia dsRNA. Events of angular displacement were measured in a single time frame of 20 seconds. ....	95
Figure 3.5. 5. Mediated RNAi silencing of Dia impairs mitotic progression. (Mean±S.D. Control: 9.3±1.3 minutes. Diaphanous RNAi: 11.02±2.2 minutes. N=30).....	95
Figure 4.2.1. 1. RNAi mediated silencing of Pbl impairs the assembly of an actin cortex in mitosis. Images show actin filaments in apical, intermediate and basal sections of nota at different stages of mitosis, marked with a yellow asterisk. Cells are shown that express lifeact-GFP from the Pnr promoter in the absence (A) or presence (B) of a UAS-Pbl RNAi transgene. Scale Bars: 5 $\mu$ M. ....	103
Figure 4.2.1. 2. Pebble controls Dia at the level of junctional F-actin. Apical top view of control interphase cells exhibit Dia at the junctional level. Pbl RNAi cells fail to localize Dia at the level of junctional F-actin. Scale bars: 5 $\mu$ m. ....	103
Figure 4.2.1. 3. Pebble is required for Dia cortical accumulation of cells in mitosis. Intermediate top view of control cells shows a strong accumulation of cortical Diaphanous. Cortical localization of Dia is lost both in tissues expressing Pbl and Dia dsRNA. Scale Bars: 5 $\mu$ m. ....	104
Figure 4.2.1. 4. Dia recruitment to the furrow canal is impaired in Pbl dsRNA expressing tissues. Top view of control cells in cytokinesis show a strong accumulation of Dia at the furrow canal (yellow arrow). Pbl dsRNA expressing cells fail to accumulate Dia at the presumptive furrow canal	



(yellow arrow). Yellow dashed line marks two new daughter cells Scale Bars: 5 $\mu$ m.....	104
Figure 4.2.1. 5. Cortical localization of Dia in metaphase cells is compromised in Pbl RNAi expressing cells. Graph of intermediate single plane ratio of mean gray values of Dia cortex/cytoplasm in control, Pbl and Dia dsRNA expressing metaphase cells. (Mean $\pm$ S.D. Control: 1.32 $\pm$ 0.18. Pbl RNAi: 1.13 $\pm$ 0.13. Dia RNAi: 0.97 $\pm$ 0.13 N=40).....	105
Figure 4.2.1. 6. Pebble is required for activation and cortical accumulation of myosin. Intermediate top view of control cells shows a strong accumulation of cortical activated myosin. Tissues expressing Pbl RNAi are deprived of cortical pMyosin. In Dia RNAi expressing tissues pMyosin is concentrated in the presumptive centrosomes (yellow arrows) indicating that myosin activation is not abrogated. [M.N.] multinucleated cells. Scale Bars: 5 $\mu$ m. ....	108
Figure 4.2.1. 7. Activation of myosin at the furrow canal is compromised in Pbl RNAi expressing cells. Top view of control cells in cytokinesis show a strong accumulation of pMyosin at the furrow canal (yellow arrow). Pbl dsRNA expressing cells show a severe decrease of activated Myosin at the furrow canal (yellow arrow). Scale Bars: 5 $\mu$ m.....	108
Figure 4.2.1. 8. Cortical activation of myosin in metaphase cells is compromised in Pbl RNAi expressing cells. Graph of intermediate single plane ratio of mean gray values of pMyosin cortex/cytoplasm in control, Pbl and Dia dsRNA expressing metaphase cells. (Mean $\pm$ S.D. Control: 1.69 $\pm$ 0.29. Pbl RNAi: 1.25 $\pm$ 0.15. Dia RNAi: 1.19 $\pm$ 0.22 N=40).....	109

Figure 4.2.2. 1. Rho1 controls filamentous actin assembly and Dia at junctional level. Apical top view of control interphase exhibits F-actin and Dia at the junctional level. RhoDN expressing tissues exhibit punctuate accumulation of junctional F-actin and Dia (yellow arrows). Scale bars: 5 $\mu$ m. ....	112
Figure 4.2.2. 2. Cortical localization of Dia is marginally affected in metaphase cells expressing a dominant negative form of Rho. Intermediate top views of metaphase cells expressing RhoDN show an accumulation of cortical Dia in domains with modest actin filaments (yellow arrow). [M.N.] multinucleated cells. Scale Bars: 5 $\mu$ m. ....	112
Figure 4.2.2. 3. Rho1 controls Dia accumulation at the furrow canal. Top view of control cells in cytokinesis show a strong accumulation of Dia at the furrow canal (yellow arrow). RhoDN expressing cells show decreased Dia accumulation at the furrow canal (yellow arrow). Scale Bars: 5 $\mu$ m. ....	113
Figure 4.2.2. 4. Rho1 is required for the activation of myosin at the cell cortex of cells in mitosis. Intermediate top views of metaphase cells expressing RhoDN show impaired accumulation of activated myosin at the cell cortex. [M.N.] multinucleated cells. Scale Bars: 5 $\mu$ m. ....	115
Figure 4.2.2. 5. Phosphorylated Myosin II concentrates at the furrow canal of cells with compromised Rho1 function. Top view of control cells in cytokinesis concentrate pMyosin at the furrow canal (yellow arrow). RhoDN expressing cells performing cytokinesis concentrate pMyosin at the furrow canal (yellow arrow). Scale Bars: 5 $\mu$ m. ....	115

Figure 4.2.2. 6. Cortical localization of Dia in metaphase cells is compromised in RhoDN expressing cells. Graph of intermediate single plane ratio of mean gray values of Dia cortex/cytoplasm in control, Pbl, RhoDN Dia dsRNA expressing metaphase cells. (Mean±S.D. Control:  $1.32 \pm 0.18$ . Pbl RNAi:  $1.13 \pm 0.13$ . RhoDN:  $1.16 \pm 0.11$ . Dia RNAi:  $0.97 \pm 0.13$  N=40). ..... 116

Figure 4.2.2. 7. Cortical activation of myosin in metaphase cells is compromised in RhoDN expressing cells. Graph of intermediate single plane ratio of mean gray values of pMyosin cortex/cytoplasm in control, Pbl, RhoDN and Dia dsRNA expressing metaphase cells. (Mean±S.D. Control:  $1.69 \pm 0.29$ . Pbl RNAi:  $1.25 \pm 0.15$ . RhoDN:  $1.09 \pm 0.16$  Dia RNAi:  $1.19 \pm 0.22$  N=40). ..... 116

Figure 4.2.3. 1. RNAi mediated silencing of Cdc42 compromise cell shape stability. Images show actin filaments in apical, intermediate and basal sections of nota at different stages of mitosis, marked with a yellow asterisk. Cells are shown that express lifeact-GFP from the Pnr promoter in the absence (A) or presence (B) of a UAS-Cdc42 RNAi transgene where metaphase and anaphase/telophase cells exhibit bleb-like deformations (yellow arrows). Scale Bars: 5  $\mu$ M. .... 119

Figure 4.2.3. 2. Cdc42 controls Dia junctional localization. Apical top view of control interphase exhibit Dia at the junctional level. Cdc42 RNAi cells fail to localize Dia at the level of junctional F-actin. Scale bars: 5  $\mu$ m. . 120

Figure 4.2.3. 3. Cdc42 is required for cortical Dia localization in mitosis. Intermediate top view of control cells shows a strong accumulation of

cortical Diaphanous. Cortical localization of Dia is lost in tissues expressing Cdc42 dsRNA. Scale bars: 5 $\mu$ m.....	120
Figure 4.2.3. 4. Dia recruitment to the furrow canal is impaired in Cdc42 dsRNA expressing tissues. Top view of control cells in cytokinesis show a strong accumulation of Dia at the furrow canal (yellow arrow). Cdc42 dsRNA expressing cells show a subtle accumulation of Dia at the furrow canal (yellow arrow). Scale Bars: 5 $\mu$ m.....	121
Figure 4.2.3. 5. Cortical localization of pMyosin is slightly affected in metaphase cells expressing Cdc42 RNAi. Intermediate top views of metaphase cells expressing Cdc42 RNAi show a mild accumulation of cortical pMyosin. Scale bars: 5 $\mu$ m. ....	123
Figure 4.2.3. 6. Phosphorylated myosin concentrates at the furrow canal of cells with compromised Cdc42 function. Top view of control cells in cytokinesis concentrate pMyosin at the furrow canal (yellow arrow). Cdc42 RNAi expressing cells performing cytokinesis concentrate pMyosin at the furrow canal (yellow arrow). Scale Bars: 5 $\mu$ m.....	123
Figure 4.2.3. 7. Cortical localization of Dia in metaphase cells is compromised in Cdc42 RNAi expressing cells. Graph of intermediate single plane ratio of mean gray values of Dia cortex/cytoplasm in control, RhoDN Pbl, Cdc42 and Dia dsRNA expressing metaphase cells. (Mean $\pm$ S.D. Control: 1.32 $\pm$ 0.18. Pbl RNAi: 1.13 $\pm$ 0.13. RhoDN: 1.16 $\pm$ 0.11. Cdc42 RNAi: 1.1 $\pm$ 0.1. Dia RNAi: 0.97 $\pm$ 0.13 N=40).....	124
Figure 4.2.3. 8. Cortical activation of myosin in metaphase cells is slightly compromised in Cdc42 RNAi expressing cells. Graph of single plane ratio of mean gray values of pMyosin cortex/cytoplasm in control, Cdc42, Pbl,	

RhoDN and Dia dsRNA expressing metaphase cells. (Mean±S.D.  
Control: 1.69±0.29. Cdc42 RNAi: 1.42±0.23 Pbl RNAi: 1.25±0.15.  
RhoDN: 1.09±0.16 Dia RNAi: 1.19±0.22 N=40)..... 125

Figure 5.2. 1. Cdc42 and aPKC localize at the apical side of epithelial  
cells in interphase and mitosis. Yellow asterisk marks mitotic cell. Scale  
bars: 5 µm. .... 130

Figure 5.2. 2. Cdc42 extend the apical localization to intermediate  
domains in mitosis. Intermediate top view of cells expressing Cdc42  
tagged with V5 in different stages of mitosis. Yellow arrow indicates  
furrow canal. Scale bars: 5 µm. .... 130

Figure 5.2. 3. Cdc42 extend the apical localization to intermediate  
domains in mitosis. Intermediate top view of wild type cells in different  
stages of mitosis. Yellow arrow indicates furrow canal. Scale bars: 5 µm.  
..... 131

Figure 5.2. 4. aPKC extend the apical localization to intermediate  
domains in mitosis. Intermediate top view of wild type cells in different  
stages of mitosis. Yellow arrow indicates furrow canal. Scale bars: 5 µm.  
..... 132

Figure 5.2. 5. Par6 extend the apical localization to intermediate domains  
in mitosis. Images show Par6 from apical to intermediate sections of nota  
at different stages of mitosis, marked with a yellow asterisk. Cells are  
shown that express Par6GFP from the Pnr promoter. Scale Bars: 5 µM.  
..... 133

Figure 5.2. 6. Par6 extend the apical localization to intermediate domains  
in mitosis. Side view of cells expressing Par6 tagged with GFP in different

stages of mitosis. Yellow asterisk indicates mitotic cell. White double sided arrow indicate Par6 domain. Scale bars: 5  $\mu$ m..... 134

Figure 5.3. 1. Cdc42 is required for cell shape stability in mitosis. Intermediate top view of control cells in metaphase with a round smooth shape and metaphase cells expressing Cdc42 RNAi with shape defects and with heterogenous actin cortex. Scale bars: 5  $\mu$ m. .... 137

Figure 5.3. 2. Cdc42 is required for cell shape stability in mitosis. Intermediate top view of control cells expressing  $\alpha$ -tubulin-GFP in metaphase with a round smooth shape and metaphase cells expressing Cdc42 RNAi and  $\alpha$ -tubulin-GFP with shape defects. Yellow arrow indicates cell bleb. Scale bars: 5  $\mu$ m..... 137

Figure 5.3. 3. aPKC is required for cell shape stability in mitosis. Intermediate top view of control cells in metaphase with a round smooth shape and metaphase cells of hemizygous aPKCs or expressing aPKC RNAi with shape defects and with heterogenous actin cortex. Yellow arrow indicates cell bleb. Scale bars: 5  $\mu$ m..... 140

Figure 5.3. 4. Par6 is required for cell shape stability in mitosis. Intermediate top view of control cells in metaphase with a round smooth shape and metaphase cells expressing Par6 RNAi with shape defects. Scale bars: 5  $\mu$ m. .... 140

Figure 5.3. 5. Percentage of cells with cell shape defects in metaphase for control and Cdc42 RNAi expressing cells. P-value < 0.5. N= 25..... 141

Figure 5.3. 6. Percentage of cells with cell shape defects in metaphase for wild type and heterozygotic and hemizygotic aPKCs nota. P-value < 0.01. N= 25. .... 141

Figure 5.3. 7. Moesin activation and localization is not dependent of Cdc42 activity. Intermediate top view of control cells in metaphase with a round smooth shape and activated moesin decorating the cell cortex and metaphase cells expressing Cdc42 RNAi with shape defects (yellow arrow) and activated moesin decorating the cell cortex. Scale bars: 5  $\mu$ m.

..... 142

Figure 5.3. 8. Moesin activation and localization is not dependent of aPKC activity. Intermediate top view of heterozygous aPKCs cells in metaphase with a round smooth shape and activated moesin decorating the cell cortex and metaphase hemizygous aPKCs cells with shape defects (yellow arrow) and activated moesin decorating the cell cortex.

Scale bars: 5  $\mu$ m. .... 142

Figure 5.3. 9. Cdc42 and aPKC control chromosome segregation.

Intermediate top views of cells in anaphase for control Cdc42 RNAi heterozygous and hemizygous aPKCs. Cells with compromised function for Cdc42 and aPKC show lagging chromosomes in anaphase/telophase (yellow arrow). Scale bars: 5  $\mu$ m. .... 144

Figure 5.4. 1. Apical localization of aPKC is dependent of Pbl activity.

Apical top view of cells in interphase and mitosis (yellow asterisk marks mitotic cells). aPKC localizes at the apical region of control cells. Apical localization of aPKC is compromised in Pbl RNAi expressing cells. Scale bars: 5  $\mu$ m. .... 146

Figure 5.4. 2. Pbl controls intermediate localization of aPKC in mitosis.

Intermediate top view of metaphase cells. aPKC localizes at the cortex of control cells. Intermediate localization of aPKC is compromised in Pbl

RNAi expressing cells. Yellow arrow marks regions of punctuated accumulation of intermediate aPKC in regions severely deprived of filamentous actin. [M.N.] multinucleated cells. Scale bars: 5 $\mu$ m. ....	146
Figure 5.4. 3. Apical localization of aPKC is dependent of Cdc42 activity.	
Apical top view of cells in interphase and mitosis (yellow asterisk marks mitotic cells). aPKC localizes at the apical region of control cells. Apical localization of aPKC is compromised in Cdc42 RNAi expressing cells. Scale bars: 5 $\mu$ m. ....	148
Figure 5.4. 4. Cdc42 controls intermediate localization of aPKC in mitosis.	
Intermediate top view of metaphase cells. aPKC localizes at the cortex of control cells. Intermediate localization of aPKC is compromised in Cdc42 RNAi expressing cells. Scale bars: 5 $\mu$ m. ....	148
Figure 5.4. 5. Cortical localization of aPKC in metaphase cells is compromised in Cdc42 and Pbl RNAi expressing cells. Graph of intermediate single plane ratio of mean gray values of Dia cortex/cytoplasm in control, Pbl, Cdc42 dsRNA expressing metaphase cells. (Mean $\pm$ S.D. Control: 1.44 $\pm$ 0.25. Pbl RNAi: 1.16 $\pm$ 0.13. Cdc42 RNAi: 1.21 $\pm$ 0.30. N=30). ....	
149	
Figure 5.5. 1. Cdc42 is required for cortical Dia localization in mitosis.	
Intermediate top view of control cells shows a strong accumulation of cortical Diaphanous. Cortical localization of Dia is lost in tissues expressing Cdc42 dsRNA. Scale bars: 5 $\mu$ m. ....	151
Figure 5.5. 2. aPKC is required for cortical Dia localization in mitosis.	
Intermediate top view of metaphase heterozygous aPKCts cells shows a	



strong accumulation of cortical Diaphanous. Cortical localization of Dia is lost in hemizygous aPKCs metaphase cells. Scale bars: 5  $\mu$ m. .... 151

Figure 5.5. 3. Cortical localization of Dia in metaphase cells is compromised in hemizygous aPKCs. Graph of intermediate single plane ratio of mean gray values of Dia cortex/cytoplasm in control, RhoDN Pbl, Cdc42, hemizygous aPKCs and Dia dsRNA expressing metaphase cells. (Mean $\pm$ S.D. Control: 1.32 $\pm$ 0.18. Pbl RNAi: 1.13 $\pm$ 0.13. RhoDN: 1.16 $\pm$ 0.11. hemizygous aPKCs: 1.11 $\pm$ 0.15 Cdc42 RNAi: 1.1 $\pm$ 0.1. Dia RNAi: 0.97 $\pm$ 0.13 N=40). .... 152

Figure 5.6. 1. Assembly of a mitotic actin cortex in SOP cells is dependent of Dia activity. Intermediate top view of interphase and metaphase SOP cells expressing GMAGFP (control cells) and SOP cells expressing UAS-GMA, Arp3 and Dia RNAi. Scale bars: 5  $\mu$ m. .... 155

Figure 5.6. 2. Assembly of an actin cortex is lost in the absence of Dia in SOP cells entering mitosis. Y values indicate the ratio of mean gray values of filamentous actin intensity at the cortex/cytoplasm of epithelial cells expressing Neu-GMAGFP at interphase and at different times (X: time in seconds) in mitosis previously to anaphase. (Values plotted: mean $\pm$ S.D.). N=25 ..... 156

Figure 5.6. 3. Partial loss of Dia phenocopies Cdc42 mitotic shape defects in SOP mitotic cells. Intermediate top view of SOP metaphase cells. (A) control cell expressing GMAGFP under the control of *Neu* promoter and Cdc42 and Dia RNAi expressing cells under the control of *pnr*-GAL4. (B) control cell expressing GMA under the control of *Neu*-

GAL4 and Dia RNAi expressing cell also under the control of *Neu*-GAL4.  
 Yellow arrow marks cell shape defects. Scale bars: 5  $\mu$ m. .... 156

Figure 5.7. 1. Constitutively active forms of Cdc42 and Dia promote excessive excessive accumulation of cortical actin. Intermediate top view of control metaphase cells has a defined actin cortex. Cells expressing a constitutively active form of Cdc42 show a thicker actin cortex. Cells expressing a constitutively active form of Dia show a thicker actin cortex and are smaller in size. Scale bars: 5  $\mu$ m. .... 158

Figure 5.7. 2. Cortical localization of Dia in metaphase cells expressing constitutively active forms of Cdc42 and Dia. Graph of intermediate single plane ratio of mean gray values of Dia cortex/cytoplasm in control, Cdc42.V12 and Dia.CA expressing metaphase cells. .... 158

Figure 5.7. 3. Constitutively active forms of Cdc42 and Dia promote excessive excessive accumulation of cortical actin and cell blebbing in SOP cells. Intermediate top view of control metaphase cells has a defined actin cortex. Cells expressing a constitutively active form of Cdc42 show a thicker actin cortex cell blebing (yellow arrow left panel) and intermediate protrusions (yellow arrow right panel). Cells expressing a constitutively active form of Dia show a thicker actin cortex and violent cell blebing (yellow arrow left panel) with cell detachment (yellow arrow right panel). Time frames of 40 seconds apart. Scale bars: 5  $\mu$ m. .... 161

Figure 5.7. 4. Constitutively active forms of Dia impair spindle orientation along apicobasal axis. Images show actin filaments marked by UAS-GMA and centrosomes marked by UAS-CNNGFP in apical, intermediate and

basal sections of a SOP metaphase cell. Yellow arrow marks centrosomes. Scale bars: 5 $\mu$ m. ....	162
Figure 5.7. 5. Constitutively active forms of Cdc42 and Dia are sufficient to drive cell rounding in interphase. Intermediate top view of control cells in interphae show cell protrusions. Cdc42 and Dia constitutively active expression in SOP cells drive cell rounding in interphase cells and assembly of an actin cortex Scale bars: 5 $\mu$ m. ....	163
Figure 6.2. 1. DE-Cadherin shifts position in mitosis. Images show top view of DE-Cadherin apical and intermediate sections of nota at different stages of mitosis, marked with a yellow asterisk. Cells are shown that express DE-CadherinGFP from the Pnr promoter. Scale Bars: 5 $\mu$ M. .	169
Figure 6.2. 2. Cadherin shifts position in mitosis. Side view of cells expressing DE-Cadherin tagged with GFP in different stages of mitosis. Yellow asterisk indicates mitotic cell. White double sided arrow indicates DE-Cadherin localization in interphase and mitotic cells. Yellow arrow marks furrow canal. Scale bars: 5 $\mu$ m.....	170
Figure 6.2. 3. Bazooka localisation undergoes a basal shift in mitosis. Images show top view of Bazooka apical and intermediate sections of nota at different stages of mitosis, marked with a yellow asterisk. Cells are shown that express BazGFP. Scale Bars: 5 $\mu$ M. ....	171
Figure 6.2. 4. DE-Cadherin and Bazooka undergo parallel basal shifts in their localisation during mitosis. Side view of cells co-expressing DE-Cadherin tagged with GFP and Bazooka tagged with mRFP in different stages of mitosis. Yellow asterisk indicates mitotic cell. White double	

sided arrow indicate DE-Cadherin and Bazooka localization. Yellow arrow marks furrow canal. Scale bars: 5  $\mu$ m..... 171

Figure 6.3. 1. PatJ localization is unperturbed in dividing epithelial cells. Intermediate top view of wild type cells in metaphase and surrounding interphase cells. Scale bars: 5  $\mu$ m. .... 173

Figure 6.3. 2. Crumbs extend the apical localization to basal domains in mitosis. Intermediate top view of wild type cells in metaphase and surrounding interphase cells. Scale bars: 5  $\mu$ m. .... 174

Figure 6.4. 1. Dlg domain extends to more basal regions of the cell in mitosis. Images show top view of Dlg apical intermediate and basal sections of nota at different stages of mitosis. Yellow asterisk mark mitotic cells with extended basal domains of Dlg. Cells are shown that express DlgGFP. Scale Bars: 5  $\mu$ M. .... 176

Figure 6.4. 2. Lgl is depolymerized from the cell cortex in mitosis. Images show top view of Lgl junctional and basal sections of nota at different stages of mitosis, Yellow arrow marks mitotic cell in prophase with cortical Lgl in prophase and complete depolymerisation in metaphase. Cells are shown that express LglGFP from the Pnr promoter. Scale Bars: 5  $\mu$ M..... 177

Figure 7.2. 1. Arp3 is present in intermediate and basal filopodia-like projections. Top views of intermediate to basal sections of epithelial cells in interphase with protrusions (Yellow arrow) marked by Arp3GFP. Scale Bars: 5  $\mu$ m..... 184

Figure 7.3. 1. Clustal-W alignment report of ECT2 protein sequences for:  
H. Sapiens; M. musculus; X. laevis and D. melanogaster. Cobalt blue  
match the Consensus within 2 distance units. .... 186

Figure 7.4. 1. A model for actin regulation in mitosis. Epithelial cells when  
entering mitosis change morphology from a columnar like shape to a  
more round shape. These changes are coupled with the disassembling of  
actin bundles and consecutively loss of microvilli at the apical side of cells  
and the assembly of an actin cortex via Diaphanous, downstream of a  
molecular pathway controlled by Ect2 and the activation of Rho GTPases  
Rho1 and Cdc42, which activate and polarize Dia, respectively.  
Junctional actin is maintained. Apico-basal polarity is also remodelled  
with apical polarity factors like Crb extending to more basal sides of the  
cell and the aPKC/Par6/Cdc42 complex also extending their apical  
domains. Baz/Par3 and adherens junctions shift their positions to more  
basal sides of the cell. Lgl is depolarized and Dlg is maintained to the  
basolateral side of cells with a slight extension of its domain to more  
basal sides of the cell..... 191

## **ABBREVIATIONS**

A.B. – Apical Basal  
AJ – Adherens Junctions  
aPKC- atypical protein kinase C  
AP – after pupariation  
Arp2/3 – actin related proteins 2 and 3  
Baz- Bazooka  
CAP- Adenylate Cyclase Associated Protein  
Crb- Crumbs  
Dia – Diaphanous  
Dlg – Discs large  
DE-Cad – Drosophila E-Cadherin  
GEF – Guanine nucleotide exchange factor  
GFP – Green fluorescent protein  
GMA- GFP fused moesin actin domain  
GTP – Guanosine triphosphate  
Lgl – lethal giant larvae  
MHC – Myosin heavy chain  
MLC – Myosin light chain  
Myo-II – Myosin-II  
Neu- Neuralized  
Pnr- Pannier  
RNAi – RNA interference  
Rok – Rho kinase  
Scrib – Scribble  
Sqh – Spaghetti squash  
Svr2- Yeast ortholog of CAP  
ZA – Zonula adherens

## **1. INTRODUCTION**

Here I introduce the background related to my research work. This introduction is divided in three sections.

The first part is focused on actin, which is a fundamental protein of the cytoskeleton in cells. In particular, the regulation of actin polymerization and the actin nucleators that catalyze actin filament nucleation. In the last paragraph I will introduce actin structures localized in precise areas of the cell where perform specific functions in response to several stimuli.

The second part is focused on actin regulators and the coordination of actin structures assembly fundamental for cell processes of endocytosis, polarity and cell division.

The third part introduces the notum as a model system to study the assembly of an actin cortex during cell division in fully polarized epithelial tissue.

## 1.1. Actin

It has already been shown that protein abundance is linked to function, namely that high-abundant proteins are often responsible for core functions, so it comes with no surprise that actin is one of the most abundant proteins ( $>2^7$  protein copies per cell) in eukaryotic cells (Beck et al., 2011; Schwanhaussner et al., 2011). In all eukaryotes studied, with the exception of yeast, highly conserved multigene families whose members are expressed differentially, exhibiting temporal and/or positional specificity, encode different forms of actin (Joseph et al., 2008; Kindle and Firtel, 1978). *Drosophila melanogaster* actin family consists of six highly conserved genes (Fyrberg et al., 1980; Tobin et al., 1980). The expression patterns of the individual genes have suggested differing functional roles for the various actins (Fyrberg et al., 1983; Manseau et al., 1988; Sanchez et al., 1983; Zulauf et al., 1981).

actin is able to perform numerous protein-protein interactions, properties that along with the ability to transition between monomeric (G-actin) and filamentous (F-actin) under the control of nucleotide hydrolysis, ions (Pollard, 1986), and many actin binding proteins make this protein an essential player in a large number of cellular processes. These cell processes can range from cell motility, dividing the cell in to two, maintenance of cell shape and polarity (Aguda et al., 2005; Campellone and Welch, 2010; Chesarone et al., 2010; Chesarone and Goode, 2009; Dominguez and Holmes, 2011; Goley and Welch, 2006; Goode and Eck, 2007; Heng and Koh, 2010; Krause et al., 2003; Kunda and Baum, 2009; Pollard, 1990, 2007; Pollard and Cooper, 2009; Sandquist et al., 2011; Sechi and Wehland, 2004; Wallar and Alberts, 2003; Wang, 1991; Zigmond, 2004).



## 1.2. Actin dynamics

### 1.2.1. Regulation of actin polymerization

Monomeric actin polymerizes in a head to tail arrangement to generate a filament that consists of two intertwined helical strands (Fowler and Aebi, 1983; Smith et al., 1983). The result is a polarised polymer.

Nucleotide hydrolysis within the filament is one of the main factors regulating the actin polymer dynamics. actin filaments tend to lengthen at the barbed end and shorten at the pointed end under steady-state conditions. This treadmilling process is driven by continuous ATP hydrolysis. Actin monomers join the fast-growing barbed end of the filament in the ATP state (Wegner and Isenberg, 1983). As the filament ages, actin-associated ATP decays to ADP+Pi and then to ADP. Near the pointed end depolymerisation occurs releasing G-actin ADP back into the uncharged pool, followed by nucleotide exchange for another round of polymerization.

*In vitro* and under physiological conditions, spontaneous assembly of filaments from pure actin monomers is unfavourable since actin dimers and trimers are unstable, but once started actin polymerization can progress rapidly (Pollard, 1986). Equilibrium constants for ATP-actin differ at the two ends (Figure 1.2.1.1), in steady-state under physiological conditions, growth at the barbed end of actin filaments is limited by dissociation at the pointed end, corresponding to a rate of elongation of 0.04  $\mu\text{m}/\text{min}$  (Blanchoin and Pollard, 2002; Carlier and Pantaloni, 1986; Carlier et al., 1988; Pollard, 1986). This rate of treadmilling *in vitro* is too slow for many actin-dependent cellular processes (e.g keratocytes or “rocketing” microbes, can move at 10  $\mu\text{m}/\text{min}$ ), demonstrating that additional proteins are required to explain the fast polymer dynamics seen in living cells.

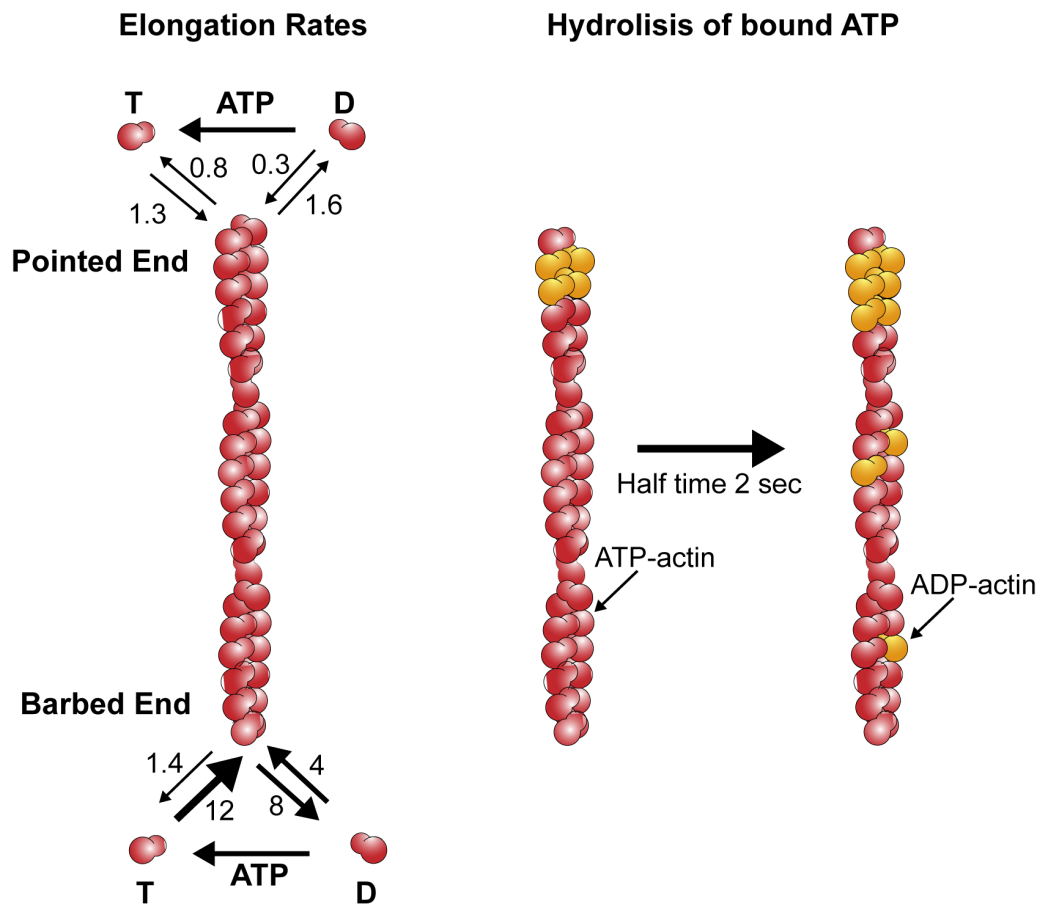


**Figure 1.2.1. 1. Actin filament elongation and ATP Hydrolysis.** The association rate constants have units of  $\mu\text{M}^{-1} \text{s}^{-1}$ . Dissociation rate constants have units of  $\text{s}^{-1}$ . Hydrolysis of ATP bound to each subunit has a half time of 2 seconds. **T**- ATP-actin monomer. **D**- ADP-actin monomer.

### 1.2.2. Actin nucleators

Many cellular processes powered by actin polymerization (e.g. cell motility, endocytosis, and cytokinesis) depend on responsive, rapid bursts of actin filament assembly at specific subcellular locations. Cells typically contain a large pool of actin monomers that is buffered by actin monomer-binding proteins such as CAP/Srv2 (binding ADP-actin) and Profilin (binding ATP-actin). These factors suppress the spontaneous nucleation of new filaments, yet enable rapid mobilization of monomers required for the elongation of existing filament ends (Pollard and Borisy, 2003). This makes nucleation the rate-limiting step in *de novo* filament formation. To overcome this barrier, cells express actin nucleators that catalyze the *de novo* assembly of filaments in response to cellular signals and regulate the precise timing and location of filament formation. There are three classes of nucleation factors distinguished by the mechanism by which each assembles *de novo* actin filaments. These are: Class I, the Arp2/3 complex; Class II, Formins; Class III, non-conventional nucleators composed of Spire, Cordon bleu (Cobl), and Leiomodin (Lmod).

The Arp2/3 complex was initially isolated from *Acanthamoeba* (Machesky et al., 1994) but is found in most eukaryotic cells (Veltman and Insall, 2010). This complex is composed of seven protein subunits including actin related proteins 2 and 3 (Arp2 and Arp3). Active Arp2/3 complex tends to initiate new filaments as branches on the side of pre-existing filaments, making a 70° angle, and acts as a pointed end cap to enable polymerisation of the fast-growing filament barbed end (Blanchoin et al., 2000; Mullins et al., 1998a). By nucleating barbed end filament growth at an angle to the mother filament the complex generates branched networks similar to the ones seen at the leading edge of motile cells (Mullins et al., 1998b) (Figure 1.2.2.1). Activation of Arp2/3 complex is made by nucleation promoting factors like WASp/Scar proteins, which are auto-inhibited unless activated by Rho GTPases and PtdIns(4,5) $P_2$  (Higgs and Pollard, 2000; Rohatgi et al., 2000).

Formins are modular proteins characterized by the presence of two conserved domains: formin homology 1 and 2 (FH1 and FH2). The mechanism of actin nucleation involves high affinity binding of the dimeric FH2 domains to stabilize actin dimers or trimers (Kovar et al., 2003; Maiti et al., 2012; Pring et al., 2003; Pruyne et al., 2002). In contrast to Arp2/3, which caps pointed ends, FH2 domains bind the barbed ends of filaments, where they are thought to act as processive leaky caps that prevent the binding of capping proteins while allowing filament elongation by Profilin-actin (Harris et al., 2004; Romero et al., 2004) (Figure 1.2.2.1). Formins exist in an autoinhibited conformation. Binding of Rho GTPases to the GTPase binding domain (GBD) releases the autoinhibitory interaction between the C-terminal Diaphanous autoregulatory domain (DAD) with the N-terminal Diaphanous inhibitory domain (DID) (Lammers et al., 2005; Li and Higgs, 2003; Rose et al., 2005). Activation of formins enables the formation of a ring-shaped antiparallel dimer, in which the two halves are held together by interactions of “lasso” and “post” segments, generating a flexible tethered dimer (Xu et al., 2004). In many cases, the ability of formins to nucleate actin varies by orders of magnitude depending on the presence of Profilin. For example, a single actin filament bound to an mDia1-coated bead grows rapidly by processive barbed end assembly. In this process, mDia1 increases the rate constant for profilin:actin binding to the barbed end by 15 fold (Romero et al., 2004). In fact, in reconstituted medium containing ADF (ADF/cofilin proteins promotes filament severing and the dissociation of ADP-actin from actin filaments), profilin, ATP and actin, mDia1-coated beads move at a speed of 15  $\mu\text{m}/\text{min}$  (Romero et al., 2004) which is significantly greater than the Arp2/3 dependent beads movement (2  $\mu\text{m}/\text{min}$ ) (Wiesner et al., 2003).

The ability of formins to bind and track actin filament barbed ends also enables them to catalyse processive filament elongation. This tracking mechanism is thought to involve transient, alternating contacts of the two halves of the FH2 dimer with the last actin subunits at the barbed end. During this process the FH2 dimer is thought to alternate between an “open state” that allows the addition of new actin subunits and a

“closed state” which does not (Kovar et al., 2006; Otomo et al., 2005; Vavylonis et al., 2006). The FH1 domain recruits profilin-actin complexes, delivering these to the FH2-capped barbed end. How these actin subunits are transferred from FH1 domain to FH2 dimer is still not fully understood, although it is thought it might involve direct interactions between FH2 dimer and FH1-profilin-actin (Ezezika et al., 2009; Neidt et al., 2009). Interestingly, neither profilin nor ATP hydrolysis are required for formin processivity. The release of free energy that accompanies the addition of new actin subunits at the barbed end seems to be sufficient to drive formin processive movement (Kovar et al., 2006; Mizuno et al., 2011; Paul and Pollard, 2009). FH2 subdomains must alternate between bind and release of actin in order to create accessible site for subsequent actin subunit addition. Given the helical nature of actin filaments, this means that formins need to rotate as the filament elongates. Considering *in vivo* rates of elongation this would mean that formins would need to spin at over 1000 rpm, which might be difficult to achieve for a membrane-bound protein like formins (Breitsprecher and Goode, 2013). This rotation paradox remains controversial. Experiments using single-filament TIRF microscopy and passively mobilized formins suggest that formins do not rotate during filament elongation (Kovar and Pollard, 2004), instead formins may slip around the barbed end to decrease torsional stress (Shemesh et al., 2005). However, this model was recently challenged by a study (Mizuno et al., 2011) where actin filaments were observed to rotate when elongated by immobilized Formins.

Formin associated actin filaments are preferentially coated by Tropomyosins (Skau et al., 2009). Tropomyosins exist as a rod-shaped coiled-coil dimer that forms a head-to-tail polymer along the length of an actin filament (Lin et al., 1997; Phillips et al., 1979). This co-polymerisation of actin and Tropomyosin may provide filaments with a memory of the nucleator used to generate them and that bias their subsequent function. Moreover, *in vitro* Tropomyosin inhibits actin filament branching and nucleation by the Arp2/3 complex and competitively inhibits Arp2/3-dependent nucleation in a reconstituted motility assay (Blanchoin et al., 2001; Bugyi et al., 2010).

Most eukaryotic cells express Tropomyosins from multiple genes and produce multiple isoforms. While certain tropomyosin isoforms show cooperative binding to actin filaments, other isoforms compete for binding to actin filaments. Additionally, different tropomyosin isoforms can also influence myosin activity (Lindberg et al., 2008; Ostap, 2008).

Finally, a third family of proteins, Spire, Cobl, and Lmod, are thought to promote actin nucleation through the recruitment of actin monomers to polymerization seeds. Spire has four tandem actin monomer-binding WASp-homology 2 (WH2) domains separated by short linkers. Electron micrographs supported by hydrodynamic and spectroscopic analyses demonstrate that Spire stably associates with four actin monomers in a prenucleation complex that resembles a short, single-stranded segment of a nascent filament (Bosch et al., 2007; Quinlan et al., 2005). These can bypass the thermodynamic barrier to actin monomer addition, enabling filament elongation. While evidence to support their functioning alone to promote actin filament nucleation *in vivo* is inconclusive, genetic studies in *Drosophila melanogaster* suggest that Spire, along with profilin and the formin Cappuccino, promotes the assembly of cytoplasmic actin meshworks (Kerkhoff, 2006). Cobl's and Lmod nucleation mechanisms are related to that of Spire, but Cobl only has three actin-binding WH2 domains (Ahuja et al., 2007), while Lmod nucleation depends on a single WH2 domain and two unrelated actin-binding domains similar to those found in Tropomodulin (Tmod), a pointed end filament capping protein (Chereau et al., 2008).

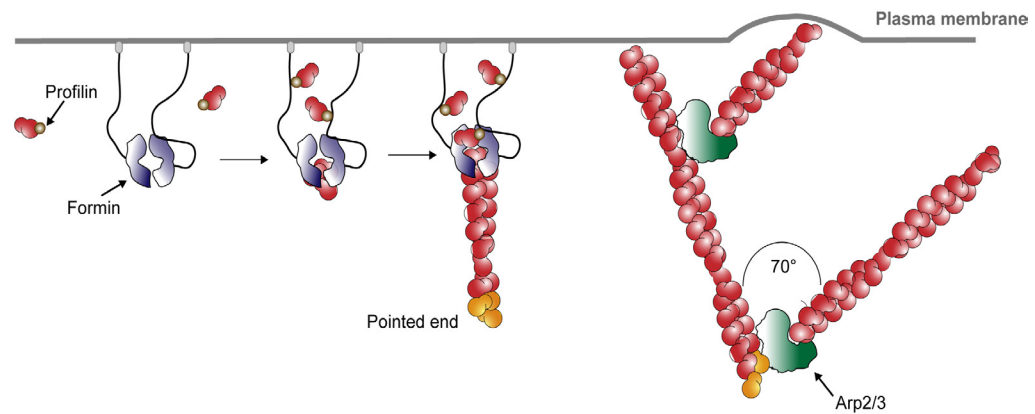


**Figure 1.2.2. 1. Model of actin nucleation induced by Formins and Arp2/3 complex.** Activated Formins bind Profilin-actin-ATP monomers and processively elongate actin filaments. Arp2/3 activated complex nucleates new actin filaments on the side of a pre existing filament making a 70° angle directing filaments against the plasma membrane promoting a pushing force.

### 1.2.3. Actin networks

In cells, actin filaments are found as organized assemblies localized in precise areas of the cytoplasm where they perform specific functions in response to different stimuli. The architecture and functions of these numerous actin-based structures is the product of regulatory proteins that work together to assemble and regulate these networks. One type of actin-based structures is the cross-linked parallel actin bundle, in which actin filaments are aligned axially, packed relatively tightly together and are of the same polarity (Furukawa and Fechheimer, 1997; Matsudaira, 1991). Several actin-binding proteins contribute to the formation of this type of actin filament-based structure. Fascin, Villin and  $\alpha$ -actinin are examples of a group of proteins able to bundle parallel groups of actin filaments. In *Drosophila* these proteins are required for oogenesis and bristle formation (Cant et al., 1998; Cant et al., 1994; Wahlstrom et al., 2004; Zanet et al., 2009). Filamin also plays a fundamental role in oogenesis and bristle formation (Li et al., 1999), however this protein forms looser orthogonal meshworks (Hartwig and Stossel, 1975), that may be a pre-requisite for the later formation of tightly packed arrays bundles (Tilney et al., 1996). All these proteins are also involved in filopodia assembly (Khurana and George, 2011; Stevenson et al., 2012).

Filopodia are protrusions containing 15-20 parallel filaments tightly packed into a bundle with their barbed ends facing the membrane (Lewis and Bridgman, 1992) that are thought to play a role in migration (Figure 1.2.3.1) and in sensing the environment (Cohen et al., 2010). In most studies using cells in culture, formins function to drive the formation of filopodia (Mattila and Lappalainen, 2008). However, a second model has been proposed in which filopodia are formed through the action of bundling proteins like Fascin on Arp2/3 nucleated filaments (Svitkina et al., 2003).

Lamellipodia are thin, sheet-like membrane protrusions found at the leading edge of motile cells moving on a two dimensional substrate (Figure 1.2.3.1). These are composed of a dense and dynamic network of actin filaments. One of the main mediators of actin polymerization in these structures is Arp2/3, which through its side-binding activity is thought to create a spreading network of branched actin filaments strong enough to deform the membrane and to drive forward cell movement (Chesarone et al., 2010; Ridley, 2011); although members of the Formin (Block et al., 2012) and Spire family have been found to contribute to lamellipodia extension.

Microvilli are finger-like projections with a relatively well-defined length emanating from the apical surfaces of epithelial cells (Figure 1.3.3.1). Villin and Fascin are actin bundling proteins that are associated with parallel bundling in microvilli (George et al., 2007; Otto et al., 1980). Additionally, the ERM (Ezrin, Radixin, Moesin) protein family are essential for the anchorage of actin bundles in microvilli to the membrane (Saotome et al., 2004; Yamane et al., 2011; Zwaenepoel et al., 2012).

Stress fibres are composed of bundles of approximately 10-30 actin filaments (Figure 1.2.3.1) (Cramer et al., 1997). These bundles are decorated with Myosin II conferring the character of contractile structures (Cramer et al., 1997) and held together by actin-crosslinking protein  $\alpha$ -actinin (Lazarides and Burridge, 1975). Myosin-II is a double-headed, long rod-like protein capable to bind to actin filaments and produce ATP-dependent motion (Sweeney and Houdusse, 2010). Stress fibres are usually associated with focal adhesions and given their sub-cellular



localization these structures can be divided in three categories. These are: Ventral stress fibres that are typical associated with focal adhesions at both ends and are responsible for tail retraction (Chen, 1981), transverse arcs that flow from the leading edge of migrating cells and which are thought to aid cell movement (Hotulainen and Lappalainen, 2006). These contractile forces are transmitted to dorsal stress fibres. Dorsal stress fibres are actin filament bundles that attach to focal adhesion at one end and rise towards the dorsal section of the cells at the other end. By contrast to ventral stress fibres and transverse arcs, dorsal stress fibres do not typically display periodic  $\alpha$ -actinin–myosin distribution (Naumanen et al., 2008). Interestingly, the assembly of the contractile ring during cytokinesis of the fission yeast *Schizosaccharomyces pombe* also involves coalescence of myosin-II-containing nodes to generate a contractile actomyosin structure (Pollard and Wu, 2010). Thus, this process might also be similar to the assembly of contractile transverse arcs at the leading edge of motile cells.

In tissues stress fibres are found under conditions in which cells are confronted with considerable mechanical stress, for example, in epithelial cells during dorsal closure in *Drosophila* embryos (Jacinto et al., 2002).

The actin cortex is a thin layer of crosslinked actin filaments, actin binding proteins, and myosin-II that underlies the plasma membrane in animal cells (Bray and White, 1988). Compared to lamellipodia and filopodia, our understanding of the cortex is limited (Salbreux et al., 2012). Nevertheless, the actin cortex plays a fundamental role in many important functions of the cell in both interphase and mitosis. Alone the cell membrane is unable to exert extracellular forces or to resist shear stress (Hamill and Martinac, 2001), and therefore cannot maintain cell shape or contribute to cell shape changes. For this reason, the actin cortex functions as a dynamic support that can actively reshape the plasma membrane in animal cells. In this capacity the cortex plays an important role in blebbing cell motility. In 3D environments cells rarely use lamellipodia to move. Instead, they tend to use mesenchymal, amoeboid, or blebbing modes of migration (Friedl et al., 2001; Paluch and Raz, 2013; Salbreux et al., 2012). In blebbing motility, the contractile acto-

myosin cortex has been proposed to help drive forward cell movement by generating internal pressure that is periodically released at the cell front (Bergert et al., 2012; Blaser et al., 2006).

Much remains to be discovered about the structure, assembly and regulation of the cell cortex. At the ultrastructural level, when examined by scanning electron microscopy in detergent extracted cells, the cortex appears as a dense meshwork of actin filaments. According to localization studies the main components in addition to actin at the cortex are actin-membrane linker proteins, actin crosslinking proteins and motor proteins (Charras et al., 2006). These include: ERM proteins that localize to the cell membrane and link the actin cortex to the plasma membrane (Bretscher et al., 2002; Charras et al., 2006; Fehon et al., 2010),  $\alpha$ -actinin, that crosslinks actin filaments (Charras et al., 2006) and Myosin II that drives cortical contraction (Charras et al., 2006). Compared with lamellipodia and filopodia, the actin nucleators driving cortex assembly are poorly understood, although several studies have implicated Formins in cortex assembly (Eisenmann et al., 2007; Hannemann et al., 2008).

Transmission electron microscopy studies suggest a cortex thickness of ~100 nm in *Dictyostelium discoideum* (Hanakam et al., 1996) and ~200 nm in retracting blebs in HeLa cells (Charras et al., 2006). Recently, the cortex of mitotic HeLa cells was shown to be ~190 nm (Clark et al., 2013), using an approach that used a theoretical description of cortex geometry to break the optical resolution limit.

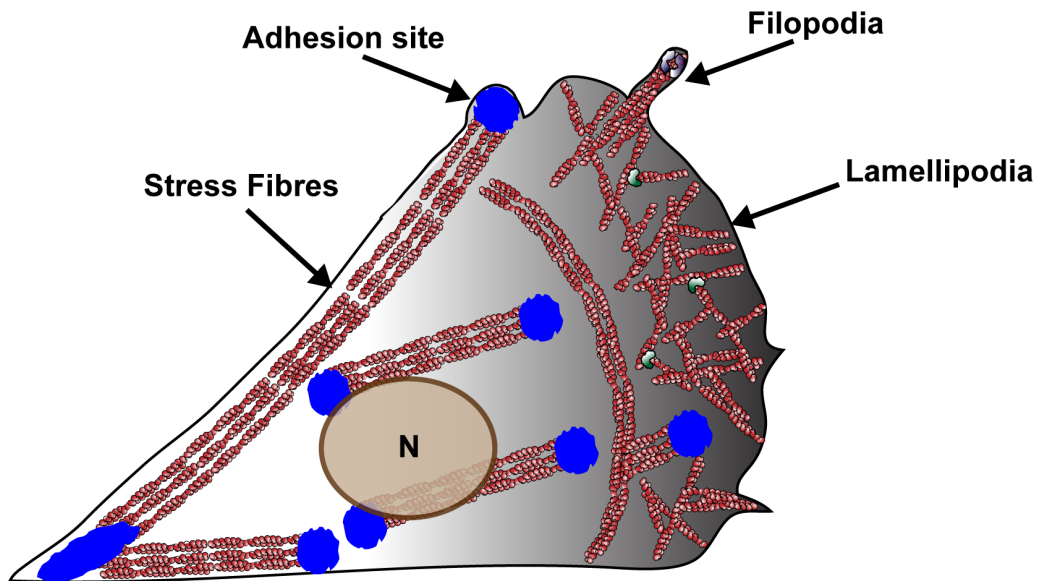


**Figure 1.2.3. 1. Actin structures in a motile cell.** Lamellipodia in motile cells is rich in branched actin filaments nucleated by Arp2/3 complex. Filopodia is composed of actin bundles nucleated by Formins. Stress fibres composed of actin bundles are associated to adhesion sites of the cell, marked by blue spots.

### 1.3. Regulation of actin dynamics in response to external/internal cues.

All cells undergo rapid remodelling of their actin networks to regulate such critical processes as endocytosis, division, cell polarity establishment, and cell morphogenesis. It is not fully understood how cells orchestrate actin filament organisation and dynamics to bring about these very different types of actin-dependent process. However, different members of the Rho GTPase family have been shown to play critical roles through their ability to organise distinct F-actin based structures (Hall, 2005). Thus, the most well-studied members of the Rho GTPase family, RhoA, Rac1, and Cdc42, regulate the formation of F-actin structures, such as stress fibers, lamellipodia, and filopodia, respectively (Nobes and Hall, 1995).

Rho GTPases regulate many important cellular functions through signaling cascades. Rho GTPases cycle between inactive GDP bound and active GTP bound states (Boguski and McCormick, 1993) and are

regulated by three groups of proteins; Rho guanine nucleotide exchange factors (GEFs), Rho GTPase-activating proteins (GAPs) and Rho GDP-dissociation inhibitors (GDIs). GEFs catalyse the exchange of GDP for GTP, and thus promote Rho GTPase activity (Schmidt and Hall, 2002). GAPs enhance the intrinsic slow GTPase capacity of Rho GTPases (Moon and Zheng, 2003). GDIs release Rho GTPases from the membrane, sequester them in the cytoplasm to inhibit nucleotide exchange and GTPase activity (Olofsson, 1999).

### 1.3.1. Rho

Rho GTPase has several downstream effectors, which it associates with in its active GTP-bound state. These include the PKC-related PKN (Amano et al., 1996; Watanabe et al., 1996), PRK2 kinases (Quilliam et al., 1996), the Citron kinase (Madaule et al., 1998) and ROK (Rho kinase) family of serine/threonine kinases (Matsui et al., 1996) and the formin Diaph1 (mammalian homolog of *Drosophila* Diaphanous) (Watanabe et al., 1997).

The function of Rho that is probably best understood is its role in the formation of contractile acto-myosin structures. In many such cases, Rho-GTP is thought to activate ROK, which then activates non-muscle Myosin II, both directly by phosphorylation of MLC and indirectly through the inactivation of Myosin Phosphatase (Amano et al., 1996; Kimura et al., 1996). At the same time, ROK may activate LIM kinase, which phosphorylates ADF/Cofilin (Maekawa et al., 1999), leading to decreased actin filament depolymerisation and severing, and thus to stabilized actin filaments nucleated as the result of Rho-dependent activation of Formins of the Diaphanous family (Lammers et al., 2005; Li and Higgs, 2003; Rose et al., 2005). Together, the activation of Myosin II and Formins results in the generation and contraction of linear anti-parallel actin filaments like the ones in stress fibers (Nobes and Hall, 1995). In a developmental context this has diverse effects all of which appear to be related to the generation of a contractile actomyosin cortex. Thus, the

single Rho GTPase (Rho1) identified in *Drosophila* as homologous to mammalian RhoA (Hariharan et al., 1995; Sasamura et al., 1997) is required at several developmental stages, ranging from oogenesis and embryogenesis (Magie et al., 1999) to eye development (Strutt et al., 1997), where it functions in cell constriction (Fox and Peifer, 2007), wound-healing (Wood et al., 2002) and cytokinesis (Prokopenko et al., 1999).

Interestingly, Rho has also other functions fundamental for cell viability not involving acto-myosin contractility. In the *Drosophila* developing wing disc, Rho1 promotes apoptosis independently of Rho kinase through its effects on c-Jun NH<sub>2</sub>-terminal kinase (JNK) signalling (Neisch et al., 2010).

### 1.3.2. Rac

Rac proteins are Rho family GTPases that are approximately 60% identical to Rho. They are found in diverse eukaryotes, where they regulate actin filament accumulation at the plasma membrane to produce lamellipodia and membrane ruffles. Activation of the heptameric actin-polymerizing complex Arp2/3, by SCAR/WAVE leading to the meshwork of peripheral F-actin induced by Rac. Rac is thought to activate WAVE through binding to Sra1 within the context of a large multiprotein complex (Eden et al., 2002; Kunda et al., 2003; Rogers et al., 2003). The WH2 domain of WAVE then activates Arp2/3, which nucleates actin filaments from the sides of pre-existing filaments to generate a spreading lamellipodial filament mesh (Chen et al., 2010). In *Drosophila*, Rac genes, Rac1, Rac2 and Mtl, have overlapping functions in the control of epithelial morphogenesis, myoblast fusion, and axon growth and guidance, although they are not required for the establishment of planar cell polarity (Hakeda-Suzuki et al., 2002).

### 1.3.3. Cdc42

Cdc42 was first identified in yeast as a critical regulator of actin-based cell polarisation during the cell division cycle. This is the function that remains best understood and is due to a role in Arp2/3-mediated endocytosis and in the generation of actin filament based cables downstream of Formins. In budding yeast, localized activation of Cdc42 induces cell polarization and the emergence of a new bud by triggering the local accumulation of Arp2/3 and Formin nucleated actin structures (Etienne-Manneville, 2004; Moseley and Goode, 2006). Several pathways downstream of Cdc42p orchestrate actin rearrangements. These include the localization and accumulation of Septins downstream of Iqg1p and Bud4p (Briggs and Sacks, 2003; Osman et al., 2002). The regulation of Myosin type I via p21-activated kinase (PAK) family (Wu et al., 1997) and Formin homologues (Bni1p and Bnr1p) that contribute to the formation of actin cables (Evangelista et al., 2003; Sagot et al., 2002). Through the regulation of formin homologues and PAKs, Cdc42p recruits and activates an Arp2/3-activating complex formed by Bee1p/Las17p (the orthologue of mammalian WASp) and Vrp1p, which allows the local assembly of actin filaments (Lechler et al., 2001)

Similarly, in animal cells Cdc42 it has been implicated in both the regulation of cell polarity and actin filament dynamics. First, constitutively active Cdc42 and dominant-negative Cdc42 were implicated in the formation of filopodia in several cell types (Heasman and Ridley, 2008). Several downstream targets for Cdc42 have been implicated in this type of filopodium formation. However, it remains unclear precisely how this works since Wiskott–Aldrich syndrome protein (WASP), which activates the Arp2/3 complex, which was initially thought to be the main contender for a nucleator is not required for filopodia formation (Snapper et al., 2001), and is thought to function primarily in generating the branched filament networks associated with endocytosis. Subsequently, mammalian Diaphanous (mDia) proteins were found to stimulate the polymerization of unbranched actin filaments, and mDia2, a target of

Cdc42, was shown to mediate filopodium formation through studies on mDia1-null cells (Peng et al., 2003). More recently, Cdc42 has been implicated in the control of cell polarity in mammalian cells as was shown for yeast.

In *Drosophila* Cdc42 loss of function, epithelial cells of the embryo fail to establish epithelial polarity and cannot maintain a monolayered epithelial structure (Hutterer et al., 2004). Similarly to Rac, dominant active and negative forms of Cdc42 affect neurite outgrowth in the peripheral nervous system although they do not affect myoblast fusion. Dominant negative Cdc42 has also been shown to disrupt the process of dorsal closure late in embryonic development (Genova et al., 2000). Cdc42 can also regulate adherens junction endocytosis, promoting Dynamin-dependent scission of endocytic vesicles containing junctional components (Georgiou et al., 2008; Leibfried et al., 2008). Two Cdc42 effectors are needed for AJ endocytosis: Cdc42-interacting protein 4 (CIP4) and PAR6. CIP4 and its downstream targets Wiskott–Aldrich syndrome protein (WASP) and ARP2/3 are presumably involved by nucleating actin at the internalization site (Georgiou et al., 2008; Leibfried et al., 2008), and CIP4 associates with Dynamin (Leibfried et al., 2008). Par6 and its binding partner atypical protein kinase C (aPKC) (Georgiou et al., 2008; Leibfried et al., 2008) function in recruiting and maintaining CIP4 at the cell cortex (Leibfried et al., 2008).

#### 1.3.4. Actin and Endocytosis

Endocytosis is the process whereby plasma membrane is internalized into the cell and pinched off to form a vesicle, which can then fuse with endosomes and enter the endolysosomal system. actin plays a fundamental role during endocytosis involving a large number of cell types. Many of our insights into the role of actin in endocytosis have come from studies on the budding yeast *Saccharomyces cerevisiae* (Robertson et al., 2009), where the process is triggered by Cdc42, as it is in animal cells (Georgiou et al., 2008; Harris and Tepass, 2008; Leibfried

et al., 2008). Work in yeast has identified a beautiful stepwise process by which endosomes are generated.

The process of endocytosis begins at multiple independent sites, with the spontaneous assembly of a domain of curved membrane bound to coat proteins, e.g. Clathrin and its adaptor proteins. Next to be recruited are proteins that bind to and/or activate Arp2/3 complex (including WASP family proteins in animal cells (Hussain et al., 2001; Innocenti et al., 2005; Kessels and Qualmann, 2002; McGavin et al., 2001), and certain class I Myosins in yeast, leading to the formation of new filaments as branches on older filaments (Galletta and Cooper, 2009; Kaksonen et al., 2006). Subsequently, the invagination process initiates, involving growth and extension of the membrane into the cell. Associated with this step is the initiation of actin polymerization by Arp2/3 (Kaksonen et al., 2005). Actin polymerization at the plasma membrane, rather than on the surface of the forming vesicle, supports the membrane invagination during growth (Kaksonen et al., 2003). The final steps of endocytosis include scission and movement away from the plasma membrane. In mammalian cells the role of vesicle scission has been ascribed to the large molecular weight GTPase, Dynamin (Song and Schmid, 2003). In yeast, however, vesicle scission is considered to involve the amphiphysin module, comprising Rvs161 and Rvs167 that form a heterodimer (Kaksonen et al., 2005). actin is thought to support this process through the polymerization of a branched actin network around the invaginating vesicle neck (Girao et al., 2008; Song and Schmid, 2003). Following scission, the vesicle is uncoated and moves away from the membrane using actin cables as tracks to guide vesicles to fuse with early endosomes (Toshima et al., 2006). Actin cables are structures made of parallel actin filaments nucleated by formins Bni1p and Bnr1p, assembled in long bundles through the stabilization effect of Tropomyosins and Fimbrin (Adams et al., 1991; Evangelista et al., 2002; Liu and Bretscher, 1989; Sagot et al., 2002).

In *Drosophila*, amphiphysin is found in muscles and is enriched at post-synaptic membranes of neuromuscular junctions (NMJs); however, it does not play a role in synaptic vesicle recycling. Rather, amphiphysin in



fly muscles appears to regulate the organization and structure of the muscle transverse tubule system and possibly the subsynaptic reticulum. Amphiphysin is also involved in membrane organization in both neurons and non-neuronal cells (Leventis et al., 2001; Razzaq et al., 2001; Zehhof et al., 2001).

#### 1.3.5. Actin and Cell polarity

Cell polarity denotes the vectorial axis that directs the asymmetric organization of cellular components and structures. It is essential for the structure and function of most cells. The actin cytoskeleton plays a critical role in the establishment and maintenance of structural cell polarization in all eukaryotes. This is best understood in yeast.

##### 1.3.5.1. Yeast

*S. cerevisiae* can switch from isotropic to polarized growth to form a bud during vegetative proliferation or during the formation of a mating projection. The regulation of this process depends in part on actin cables, which serve as routes for the directed polarised transport of material, including secretory vesicles and protein-RNA complexes (Pruyne et al., 2004). At the same time, actin dependent endocytosis at the bud tip is thought to function to keep the site of cell polarity tightly focused.

How is polarity established? Cdc42 is the master regulator of cell polarity in yeast (Johnson, 1999). It is thought to trigger the nucleation of actin filament based structures at the tip of polarised budding yeast (and in bipolar pombe (Das et al., 2012)). However, genetic analyses suggest that Rho proteins might be the primary GTPases that control formin activation, whereas Cdc42 controls formin localization (Dong et al., 2003). While, Cdc42 performs a similar role in many other eukaryotic cells, it is unclear how it couples actin and polarity in animal cells.

### 1.3.5.II. Cell motility

In motile cells polarization is an important first step through which a cell establishes a leading edge and a contractile rear. Symmetry breaking in motile cells leads to the formation of different actin rich domains at the leading edge and at the opposing contractile cell rear. The leading edge of adherens cells migrating on a hard substrate, as previously introduced, is a protrusive actin-rich structure in which the action of different actin nucleators creates a network of actin filaments that is organized into dendritic or filopodia arrays. At rear end of cells actin is organized into contractile structures that are rich in Myosin-II (Cramer, 2010). These Myosin-II generated forces are necessary to contract the cell rear, driving the forward translocation of the cell body and the disassembly of trailing adhesion complexes (Mitchison and Cramer, 1996; Ridley et al., 2003; Xu et al., 2003; Yam et al., 2007). Rho GTPases act coordinately with other signals to control actin structures in cell migration. Using biosensors, active Rac1, RhoA, and Cdc42 have been shown to localize in lamellipodia during protrusion (Machacek et al., 2009). Rho has predominantly been implicated in tail retraction (Ridley et al., 2003). The role of Cdc42 is actually dual— it not only participates in the protrusive activity but it is also directly involved in cell orientation during directed migration in response to exogenous polarity cues, such as chemotactic signals or cell wounding. Following wounding, Cdc42 is recruited at the wound edge of astrocytes and activated. Interestingly, in this context Cdc42 binds to a set of proteins implicated in polarity in other systems. These include Par6 and atypical protein Kinase C (aPKC). The localized activation of aPKC is then thought to be crucial for microtubule polarized organization and cell orientation, even though it is not required for establishment of the front-rear axis (Etienne-Manneville and Hall, 2001).

### 1.3.5.III. The regulation of cell polarity in development

Remarkably the same protein Cdc42 also plays a fundamental role in the establishment and maintenance of cell polarity in a developmental context in animals. Here, it functions together with Par6 and aPKC (Motegi and Sugimoto, 2006; Nance and Zallen, 2011; St Johnston and Ahringer, 2010). This activity has been best described in the *C. elegans* zygote.

The first breaking symmetry in the development of a *C. elegans* worm occurs shortly after fertilization. At this moment, the introduction of the centrosome associated with the sperm provides the cue that defines the anterior-posterior axis of the embryo. It does this by inducing the local loss of the actomyosin network at the posterior pole (Goldstein and Hird, 1996; Munro et al., 2004). This polarity signal is partially dependent on the regulation of Rho, since Ect2 (a Rho guanine nucleotide exchange factor) is depleted from the cortex adjacent to the sperm/centrosome localization, presumably preventing Rho activation at the posterior side (Jenkins et al., 2006; Motegi and Sugimoto, 2006; Schonegg and Hyman, 2006). Since Rho activates myosin II this leads to hypercontractility of the anterior cortex (Motegi and Sugimoto, 2006). This provides the embryo with smooth and quiescent posterior cortex and a highly contractile anterior cortex (Gonczy and Rose, 2005). This asymmetry in the contractile properties of the cortex results in a long-range flow from posterior to anterior, which in turn entrains the motion of the cell cytoplasm, creating a fluid flow towards the anterior along the inner surface of the membrane (Cowan and Hyman, 2007; Mayer et al., 2010). Given the diffusion properties of anterior Par proteins and Cdc42 at the membrane this cortical flow can drive the redistribution of Par proteins (Goehring et al., 2011). Interactions between anterior and posterior Par domains then fixes this polarity axis, which then serves to guide the future development of the animal head and tail. Thus, polarization of the *C. elegans* embryo involves the intimate association of polarity machines and the actomyosin cortex.

Interestingly, the same process appears to be at work in the establishment and maintenance of epithelial cell polarity. Epithelial cells are characterized by at least four distinct cortical domains: apical, junctional, lateral and basal. These domains are defined by the accumulation of complexes of polarity proteins, adhesion material and different actin structures (Figure 1.3.3.1).

The Crumbs (Crb) complex specifies the apical domain by recruiting other factors like Moesin,  $\beta$ H-spectrin, Stardust and Patj (Izaddoost et al., 2002; Medina et al., 2002). Crb also recruits Par6 and aPKC, which probably also includes active Cdc42 (Sotillos et al., 2004). At the most apical region of epithelial cells actin bundles tethered by ERM proteins to the membrane form short dynamic microvilli structures (Saotome et al., 2004; Zwaenepoel et al., 2012).

A core function of the apical complex is to regulate the junctional domain. The Par protein Par3/Baz and the components of the cell adhesion complexes, specify the junctional domain, and determines where adherent domains can be formed. Thus, regulation of Par3/Baz is extremely important to position adherens junctions during cell morphogenesis (Morais-de-Sa et al., 2010; Walther and Pichaud, 2010). At the site of adherens junctions, a circumferential actin ring is formed, which is dependent of actin nucleators like the Arp2/3 complex and formins regulated by Rho GTPases, which provides the mechanical strength required for epithelial integrity (Carramusa et al., 2007; Kobiela et al., 2004; Kovacs et al., 2002; Ryu et al., 2009), and the forces required for morphogenesis (Martin et al., 2009).

Underneath the apical and junctional domains the polarity proteins Discs large, Scribble, Lethal Giant Larvae and Par1 specify the lateral membrane, restricting the apical and junctional domains (Bilder et al., 2003; Chalmers et al., 2005; Tanentzapf and Tepass, 2003; Yamanaka et al., 2003). At the most basal domain of epithelial cells filopodia-like protrusions is thought to sense the surroundings to control tissue refinement (Cohen et al., 2010). Note that these actin dependent structures were reported to be generated by the Arp2/3 complex,

downstream of polarity regulators and Rho GTPases (Georgiou and Baum, 2010), rather than by formins.

It should be clear from this that epithelial cells are organised into distinct polarised domains each of which is associated with a specific set of actin structures.

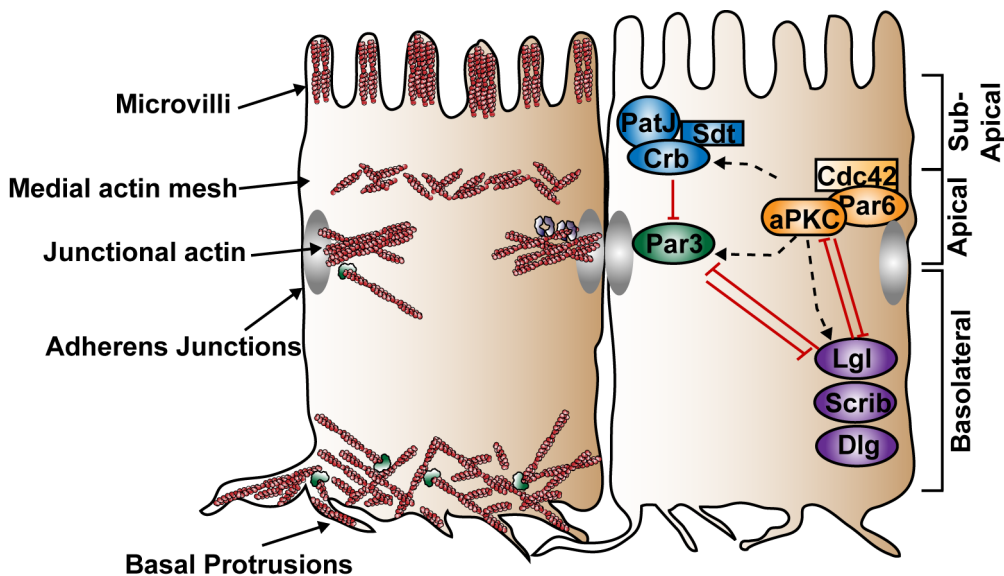


**Figure 1.3.5. 1. Epithelial cell polarity.** Epithelial cells are polarized along their apical-basal axis by the presence of apical microvilli composed of actin bundles, medial actin mesh, junctional actin at the level of adherens junctions and basal protrusions. Polarity proteins play a fundamental role in establishing and maintaining cell polarity by mutual antagonism or activation of polarity complexes strategically localized along the cell axis. Black punctuated line indicates phosphorylation; red lines indicate mutual or single antagonism.

### 1.3.6. Actin and Cell Division

One of the most striking changes in cytoskeletal organization and dynamics occurs in cells entering mitosis. In interphase cells contain an extensive actin network that is rapidly dismantled and rearranged when cells enter mitosis, giving cells their characteristic round shape. At the end of mitosis, actin rearranges at the cleavage furrow and forms part of the contractile ring, vital for the process of cytokinesis (Green et al., 2012). Entry into mitosis begins with the de-adhesion of cells from the substrate (Cramer and Mitchison, 1997). This process requires the

disassembly of focal adhesions and actin stress fibers, a process that is negatively controlled by the small Rho GTPase Rap1 (Dao et al., 2009). During the process of mitotic rounding a mitotic actomyosin cortex is assembled at the plasma membrane. It has been shown that Ect2 (a Cdk1 substrate) activates RhoA and its downstream effectors, ROK, and Myosin II, at the onset of mitosis to induce the actomyosin remodeling that drives both mitotic rounding and cortical stiffening (Maddox and Burridge, 2003; Matthews et al., 2012) a process that is triggered by the release of Ect2 from the nucleus in prophase (Matthews et al., 2012). At metaphase a relatively rigid cortex is assembled in part through ERM family proteins (Carreno et al., 2008; Kunda et al., 2008a) that link the actin cortex to the plasma membrane. This is triggered by Slik activation, inducing the opening of Moesin conformation causing the bind to actin filaments crosslinking to the plasma membrane (Carreno et al., 2008). In addition, the changes in the actomyosin cortex help to direct swelling forces to ensure that cells round up (Stewart et al., 2011).

Although recent work has revealed much about the process of mitotic cortical remodelling, the question of how actin is *de novo* assembled at the cell cortex when cells enter mitosis remains to be investigated. It is clear that this is important for mitosis however, as centrosome separation is dependent of the cortical flow of cortical actin and the myosin network (Rosenblatt et al., 2004), as is spindle alignment (Castanon et al., 2013; Luxenburg et al., 2011; Woolner and Papalopulu, 2012). At mitotic exit, the actomyosin cortex is then remodeled to give rise to a contractile ring.

The mechanism responsible for the positioning of the cytokinetic contractile ring is thought to be dependent of the complexes of a kinesin-like protein and MgcRacGAP/Tumbleweed, which localize to the to the overlapping or juxtaposed plus ends of astral and/or midzone microtubules between anaphase chromosomes. There, through a direct interaction between MgcRacGAP and Pbl/Ect2 (Tatsumoto et al., 1999), the GEF becomes concentrated, generating a cortical ring of activated Rho to regulate the assembly of the actomyosin contractile ring (Chalamalasetty et al., 2006; Grosshans et al., 2005; Nishimura and

Yonemura, 2006; Prokopenko et al., 1999). Rho then recruits Diaphanous, which nucleates actin filament formation (Grosshans et al., 2005) and recruits Rok to activate Myosin (Yuce et al., 2005). At the same time, Sedzinski and colleagues proposed a model whereby polar cortex contractility can lead to shape instabilities, which preclude stable spindle positioning and can lead to division failure if the poles are not correctly controlled (Sedzinski et al., 2011), a process that may be triggered by the movement of the anaphase chromosomes close to the two poles (Kiyomitsu and Cheeseman, 2013). Similarly, in *Drosophila* a contraction-driven asymmetric polar extension of the neuroblast cortex during anaphase contributes to asymmetric furrow position and daughter cell size, (Connell et al., 2011).

#### **1.4. The notum as a model system**

The system chosen for this study is the *Drosophila* notum. The notum forms the dorsal thorax in the adult fly: a very well organized and patterned epithelium that is covered with a set of well-spaced mechanosensory bristles (Simpson, 2007) and that is connected on the basal side via tendon cells to the flight muscles. This tissue arises during pupal development from two distinct epithelial sheets that approach and fuse at the midline to generate a continuous monolayer epithelium (Zeitlinger and Bohmann, 1999) (Figure 1.4.1). Afterwards, a series of morphogenetic events, that include cell division, junctional remodeling and cell delamination (Marinari et al., 2012), contribute to development of the final shape and size of the tissue prior to hatching. Thus, the notum represents a good model system in which to study the process of cell division in a polarized epithelium.

#### 1.4.1. Thorax closure

The pupal notum is formed via a process called thorax closure, as two epithelial sheets of the two wing imaginal discs come together and fuse at the midline between 6 and 8 hours after pupariation (AP) (Zeitlinger and Bohmann, 1999).

The movements of the imaginal discs towards the midline involves actin-myosin cables contraction, elongation of leading edge cells and the formation of extensive thick filopodia that contact the cells of the other wing disc (Martin-Blanco et al., 2000). This process is thought to be regulated by the small GTPase Cdc42, acting upstream of JNK signaling (Agnes et al., 1999), and Dpp signalling. In JNKK (*hep*) mutants, filopodia are rare and cell adhesiveness is compromised (Martin-Blanco et al., 2000), larval cells detach from each other and the wing imaginal discs cannot spread over the larval epidermis. Although Dpp signaling is activated downstream of JNK, Dpp is thought to specifically affect filopodia formation and cell polarity, but not the integrity of the larval epidermis (Agnes et al., 1999; Martin-Blanco et al., 2000).

#### 1.4.2. Patterning and pattern refinement of the notum

The notum is patterned by the activity of Apterous and Dpp, which activates Pannier (Pnr), a transcription factor of the GATA family, in the medial half of the tissue. Pnr restricts the expression of the selector gene Iroquois (Iro) to the lateral half of the notum (Calleja et al., 2000; Cavodeassi et al., 2001; Sato and Saigo, 2000). The Iro complex encodes for homeodomain containing proteins and, together with Pnr, is responsible for patterning most of the notum (Gomez-Skarmeta et al., 1996; Romain et al., 1993).

The dorsal thorax of the adult fly exhibits a very precise and even pattern of mechanosensory bristles. Thus, it has been previously studied as a model of pattern formation in tissue morphogenesis (Cohen et al., 2010; Simpson et al., 1999). Bristles are of two types: macrochaetes and



microchaetes. Macrochaetes are large mechanosensory bristles, which are placed relatively precisely on the thorax during earlier stages of development and are conserved between different species (Usui and Kimura, 1993). Microchaetes spacing instead varies between different species, between different animals within the same species, and between left and right sides of each animal, indicating that it is not precisely pre-patterned but is likely to be self-organizing (Cohen et al., 2010; Simpson et al., 1999; Usui and Kimura, 1993). Microchaetes patterning is mediated by Delta-Notch lateral inhibition (Artavanis-Tsakonas et al., 1999; Hartenstein and Posakony, 1990; Heitzler and Simpson, 1991; Kooh et al., 1993) and the gradual refinement of this pattern is thought to be dependent upon dynamic, basal actin-based filopodia (Cohen et al., 2010) Cohen et al., 2011). Neuralized (Neu) is a conserved regulator of Notch signalling that acts as a cell fate determinant, and in precursor cells of external sensory organ of the notum, Neu works as a cell fate determinant during asymmetric cell divisions (Le Borgne and Schweisguth, 2003). Thus the GAL4/UAS system adapted for genetic manipulation in *Drosophila* (Brand et al., 1994) combined with promoters of genes that pattern the fly notum or determine the cell fate during asymmetric cell division make the notum an ideal system in which to study cell division in an epithelium achieving homeostasis. Additionally, the notum offers a simply model to study tissue dynamics *in vivo* with nearly absent mechanical manipulation during dissection that could influence the normal tissue development (Cohen et al., 2010; Georgiou and Baum, 2010; Le Borgne et al., 2002; Marinari et al., 2012).

**Figure 1.4. 1. Thorax closure.** 6 hours AP the two epithelial sheets spread inside the pupal case. 8 hours AP fusion of the wing discs at the midline. 9 hours AP the wing discs are attached to the other discs. Abbreviations: ea, eyeantennal disc; dp, dorsal prothoracic disc; a, abdomen; h, haltere disc; s, scutellum. The *pnr* expression domain is indicated in green; in red, oblique flight muscles. Adapted from (Zeitlinger and Bohmann, 1999)

## 1.5. Aims of the thesis

During development epithelial tissues go through a series of morphogenetic events to generate the final size and shape of tissues in the adult organism. Tissue morphogenesis is the result of a fine balance between different biological processes like: cell growth and division, cell loss and cell shape changes. Cell division in an epithelium poses a set of novel challenges, since cells have to segregate DNA evenly between two equal-sized daughter cells both of which must maintain an apico-basal polarity axis, without division compromising epithelial integrity. Cells use the actin cytoskeleton to undertake this process however, how is the actin cytoskeleton regulated is not all understood. *Drosophila* notum development constitutes a good model system in which to study actin regulation in dividing cells of a fully polarized epithelium. Thus, in this

study I used this system to characterize the events that regulate the actin cytoskeleton in dividing epithelial cells. In particular, I analyzed the contribution of actin regulators, nucleators and cell polarity factors in the process of *de novo* actin cortex assembly during mitosis.

## 2. MATERIALS AND METHODS

### 2.1. Genetic techniques

Gene over-expression and dsRNA expression were driven using the GAL4/UAS system. The GAL4/UAS system derives from yeast and has been adapted for genetic manipulation in *Drosophila* (Brand et al., 1994). GAL4 is a DNA-binding protein that specifically recognizes target UAS motifs and binds to UAS sites in the genome. Thus, GAL4 expression regulates the expression of target genes downstream of UAS sites. Expression of GAL4 can be driven under the control of an inducible promoter or that of another gene to control gene expression either in different tissues and developmental stages. An additional approach to fine-tune the temporal expression of a UAS-responder is to take advantage of the temporal and regional gene expression targeting (TARGET) technique (Elliott and Brand, 2008). In the TARGET technique a temperature-sensitive version of the GAL80 (GAL80ts) protein (which binds and prevents GAL4 from activating transcription) is expressed in a ubiquitous fashion (in this thesis we used a GAL80ts expression under the control of the *tubulin 1 $\alpha$*  promoter). GAL80 repression of GAL4 can then easily be alleviated by a simple temperature shift (Elliott and Brand, 2008). The generic GAL4/UAS system was used to drive the expression of a hairpin RNA. These double-stranded RNAs are processed within each cell by endogenous Dicer into siRNAs which direct sequence specific degradation of the target mRNA.

Mitotic clones were generated by flp-FRT mediated mitotic recombination (Xu and Rubin, 1993), which generates mosaic patches of mutant cells in a wildtype background. This technique takes the advantage of mitotic recombination between chromosomes within a single dividing cell. Recombination is promoted by flp recombinase activity under the control of a specific promoter (in this thesis we used

heat-shock promoter). Flp induces recombination between specific target FRT sites closely located to the centromere. Mutant cells can be distinguished from the wildtype background by the differential expression of a reporter (GFP, RFP, lacZ).

The *in vivo* model system used in this thesis was notum development. For this reason, most perturbations relied on expression driven by the *pannier* promoter, which is active in the medial notum (Calleja et al., 2000; Simpson, 2007). An additional driver used in this thesis is the NeurGAL4, which is expressed in the sensory organ precursor cells (Bellaiche et al., 2001).

The use of dsRNA technology offers several advantages: RNAi can be induced in a tissue and time specific manner, the RNAi available library targets 88% of predicted protein coding-genes, and the toxicity of the dsRNA expression can be easily modulated (Dietzl et al., 2007; Elliott and Brand, 2008). Moreover, the expression of dsRNA also offers the possibility to image *in vivo* the consequences of gene knockdown, since the tools used as a read out (GFP tagged proteins) are optimized for the GAL4/UAS technology.

## 2.2. Conditions

Stocks of *Drosophila melanogaster* were maintained at 18°C or 25°C. Fly food was made as follows: 39 l dH<sub>2</sub>O, 675 g yeasts, 390 g soy flour, 2.85 kg yellow cornmeal, 224 g agar, 3 l light corn syrup, 188 ml propionic acid. Crosses were kept at 25°C for two days. For RNAi experiments, males from each UAS-IR fly line were crossed with *Neur-GMAGFP*; *pnr-GAL4*, *TubGAL80ts*; *PnrGAL4*, *TubGAL80ts*; *NeurGAL4* or *UAS-GMA*; *Neur-GAL4* virgin females. The F1 progeny was raised at 29°C until 14-16 hours AP. In the case where RNAi expression was toxic *Gal80ts* driver was used and the F1 progeny was kept at 18°C for 14-15 hours AP and subsequently switched to 29°C for an extra 6-7 hours. This same treatment was repeated for *aPKC<sup>ts</sup>* mutants.

## 2.3. Fly stocks

The following stocks used are described in the indicated references: *pnr*-GAL4 (his-tubRFP/CyOGFP; *pnr*-GAL4/TM6b) (3039; Bloomington *Drosophila* Stock Center (BDSC)), *Neur*-GAL4 (*w*; *Neur*GAL4, UAS-GMA/TM6B) (gift from Yohanns Bellaïche), UAS-GMA (gift from Dan Kiehart), *Neur*-GMA (Buzz Baum lab), TubGAL80ts (*w*; TubGAL80ts/CyO; *pnr*GAL4/TM6B and *w*; TubGAL80ts/CyO; *Neur*GAL4,UAS-GMA/TM6B) (gift from Frank Pichaud), *w*; Df(2R)l4, *cn*<sup>1</sup> *bw*<sup>1</sup>/CyO, Ubi-GFP and *w*; aPKCts/CyO, UbiGFP (gift from Rui Martinho), *w*; myc-Cdc42.V12 (Luo et al., 1994), UAS-Dia.CA3 (gift from Nic Tapon), Baz-GFP (CC01941, GFP Fly Trap Stock Center), UAS-Par6-GFP, UAS-Lgl-GFP, UAS-Dlg-GFP, UAS-Crb-GFP (gifts from Frank Pichaud), Rho1.N19,*w* (7327; Bloomington *Drosophila* Stock Center (BDSC)), *w*; Rho1.N19 (7328; Bloomington *Drosophila* Stock Center (BDSC)), *w*, Tub-Gal80 ,hs-Flp, FRT(9-2)/FM7 (gift from Yohanns Bellaïche), *y,w*, P[mw,Ubx-Flp], Cdc42[3], P{ry[+t7.2]=neoFRT}19A / FM7, P[mw,Kr-nls-GFP] (gift from Marios Georgiou), *y,w*, FRT19A; *ey*-FLP5 (gift from Barry Dickson), UAS-*cnn*-GFP, *w* ((7255; Bloomington *Drosophila* Stock Center (BDSC)), SqhAx3; SqhGFP; Gap43Ch (gift from Benedicte Sanson), *w*; *pnr*-Gal4, UAS-lifeActGFP/TM6B (Buzz Baum lab), UAS-*cnn*-GFP (7255; Bloomington *Drosophila* Stock Center (BDSC)), *w*, UAS-GFP-Arp3 and *w*;UAS-GFP-Arp3 (gifts from Lynn Cooley).

All RNAi lines used came from the Vienna *Drosophila* RNAi Center (VDRC) library (Dietzl et al., 2007), excluding the Cdc42 RNAi line (NIG-Fly library, stock ID 12530R-3). The list of RNAi lines used is shown in the table below

<b>Gene name</b>	<b>VDRC ID number</b>
<b>aPKC</b>	105624
<b>Arp3</b>	35260
<b>Diaphanous</b>	103914
<b>Pebble</b>	109305 and 35349
<b>CG32138</b>	34412 and 34413
<b>Baz</b>	2914 and 2915
<b>Crb</b>	39177
<b>Scar</b>	21908
<b>Wasp</b>	13759
<b>Par-6</b>	19731

**Table 2.3. 1. List of RNAi lines used from the VDRC Drosophila stock center.**

## **2.4. Live imaging and dissections**

Live imaging was performed by cutting a window in the pupal case attached to a slide with double-sided tape, and placing a coverslip carrying a drop of injection oil over the notum, supported by coverslips at either end (Georgiou et al., 2008). Notum were imaged from 14 hr AP up to 12 hr during development. For stained tissues, notum from pupae 15 hr after pupariation (AP) were dissected in PBS for direct fixation in 4% formaldehyde for 20 min or paraformaldehyde (Rabbit anti-pERM staining) before being permeabilized by PBS containing 0.1% Triton X-100 (PBT). The notum were then stained 2 hr at RT with DAPI (Sigma) for nuclei and Alexa-568 Phalloidin (Invitrogen) for actin. The acquisition was performed using a Leica SP2 laser scanning SP2 confocal microscope with 40X/1.3 oil objective, with a format of 1024x1024 pixels, frame

average of 3, for live imaging experiments and a SP5 confocal microscope with a 63x/1.3 oil objective with a format of 2048x2048 pixels, line average of 3, for fixed samples, three or more animals were used for each experiment. Primary antibodies were used at the following dilutions: Mouse anti-Dlg 1:10; Rabbit anti-PatJ 1:700; Mouse anti-Crb 1:20; Rabbit anti-Baz 1:2000; Guinea Pig anti-Par6 1:500 (all gifts from Frank Pichaud laboratory); Rabbit anti-aPKC $\zeta$  (c-20) 1:100 (Santa Cruz Biotechnology); Rabbit pMyosin Light Chain II (S19) 1:30 (Cell Signaling Technology); Rabbit anti-pERM 1:100 (Cell Signaling Technology); Mouse anti- $\alpha$ -tubulin (clone DM1A) 1:250 (Sigma); Chicken anti-GFP 1:500 (Abcam); Rabbit anti-Cdc42 1:20 (Eurogentec); rabbit anti-V5 1:100 (Abcam). V5 Epitope Tag is the C-terminal sequence of the P and V proteins of Simian Virus 5. Secondary antibodies from Molecular Probes were labeled with Alexa 488, 546 and 647 dyes.

## **2.5. Image processing and analysis**

The images presented were processed using ImageJ (<http://rsb.info.nih.gov/ij/>) and Adobe Illustrator CS (Adobe Systems, Inc., San Jose, CA). All images are from a single confocal Z-stack section. In the case of live imaging acquisitions were a top to bottom image is shown (from apical to basal) Z-stacks are spaced by 2.2  $\mu$ m acquired by SPE2 Leica confocal microscope. In the case of fixed and stained nota were a top to bottom image is shown (from apical to basal) Z-stacks are spaced by 0.7  $\mu$ m acquired by SP5 Leyca confocal microscope. Protein intensity at the cortex of cells was quantified in a single z intermediate slice using ImageJ. A line of 10 pixels width was drawn by hand around the cortex of the mitotic cell to measure gray mean intensity (Analyze>Measure>mean pixel intensity). To normalize values of gray intensity a region of equal area was drawn inside the same cell and divided to the one obtained at the cell cortex. This process was performed both in live imaging as in stained nota. Due to the challenging conditions to perform live imaging, acquisition was performed in different days, although for each condition



(RNAi, mutants and control) imaging conditions were maintained from the beginning until the end of the experiment. To compare RNAi and mutant conditions with controls in fixed samples, nota were dissected and stained with the same mixture of antibodies on the same day. Image acquisition was performed in two-three consecutive days.

For each case, statistics were calculated with a nonparametrical Mann-Whitney test or a one-way ANOVA test in Prism (GraphPad Software, Inc.) on at least 25 cells of 3 different pupae. p-value<0.05 was represented by \*, p-value<0.01 was represented by \*\*, p-value<0.001 was represented by \*\*\*. Data was plotted in a curve of mean values ( $\pm$  standard deviation-s.d.) or in a box and whiskers plot (tukey plot), depicting median, 25<sup>th</sup> quartile, 75<sup>th</sup> quartile (box), maximum and minimum (whiskers).

### **3. ACTIN-MYOSIN REMODELLING IN MITOSIS**

#### **3.1. Introduction**

The regulation of the actin cytoskeleton and of cell cycle progression are tightly connected. Interphase cells usually contain an extensive actin network, which is rapidly rearranged when cells enter mitosis, altering the geometry of cells to a characteristic round shape (Carreno et al., 2008; Field et al., 2011; Heng and Koh, 2010; Kondo and Hayashi, 2013; Kunda and Baum, 2009; Kunda et al., 2008a; Kunda et al., 2012; Kunda et al., 2008b; Lancaster et al., 2013; Maddox and Burridge, 2003; Matthews et al., 2012; Rosenblatt et al., 2004; Roubinet et al., 2011; Stewart et al., 2011; Thery and Bornens, 2008; Trichet et al., 2012; Werner et al., 2013). At the end of mitosis, actin rearranges at the cleavage furrow and forms the contractile ring, which plays a central process of cytokinesis (Afshar et al., 2000; Cabernard, 2012; Castrillon and Wasserman, 1994; Chalamalasetty et al., 2006; Chang et al., 1997; Fededa and Gerlich, 2012; Green et al., 2012; Herszterg et al., 2013; Lehner, 1992; Mendes Pinto et al., 2012; Pollard, 2007; Sedzinski et al., 2011; Su et al., 2011; Tatsumoto et al., 1999). However, the nature of the molecular mechanism that governs the remodeling of the actin cortex in dividing cells is still poorly understood.

In this chapter I aim to characterize the remodeling of filamentous actin in dividing epithelial cells and investigate which actin nucleators are at work in the process of rearrangement of the actin cortex in mitotic cells, focusing on the function of two well studied molecules; Arp2/3 and Diaphanous, by examining and how cells cope with the loss of these nucleators as they enter and exit mitosis.

### 3.2. Characterization of actin and Myosin organization in and out of mitosis.

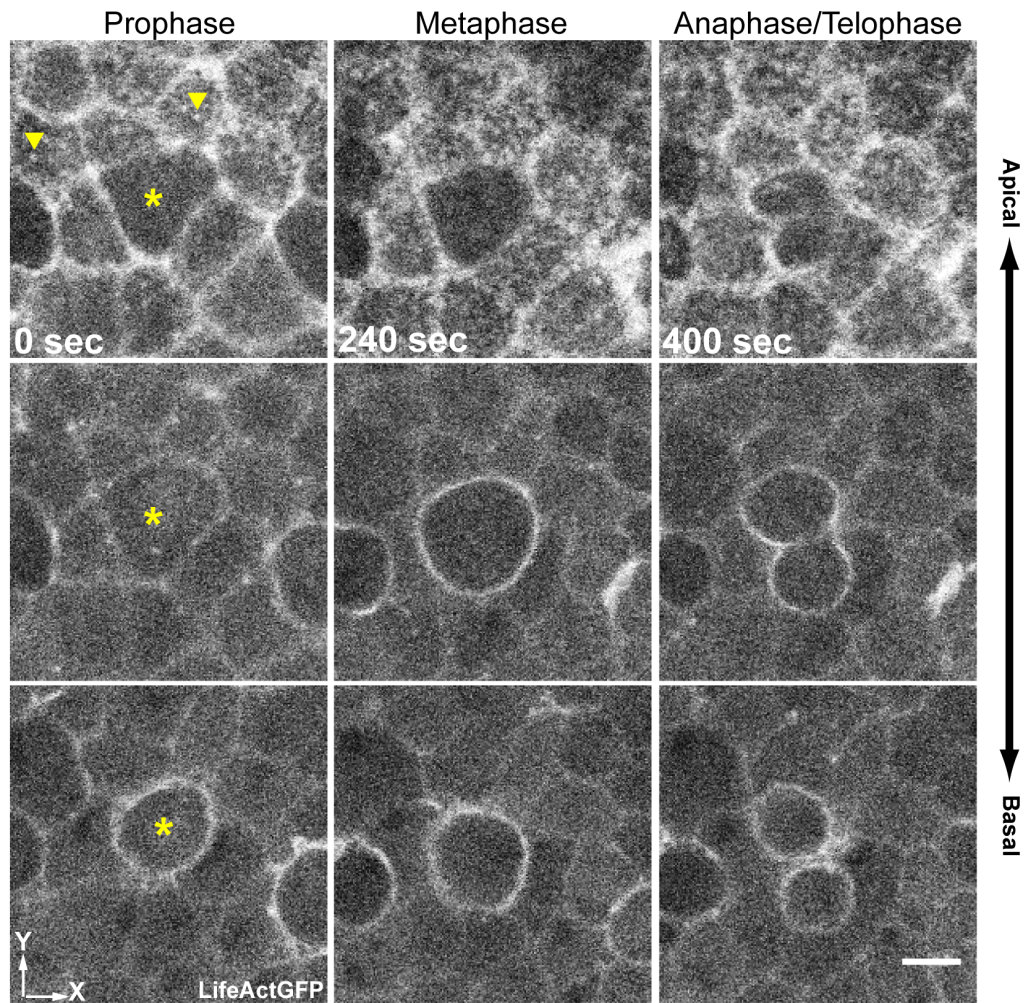
At fourteen to sixteen hours after puparium formation (AP) the *Drosophila* notum goes through several morphogenetic processes including cell division. To analyze the dynamic changes in the organization of the acto-myosin cytoskeleton that accompany cell division we took advantage of flies expressing a lifeact-GFP construct (Riedl et al., 2008), which enables the visualization of filamentous actin without affecting filaments dynamics, and flies expressing a myosin regulatory light chain II (encoded by *spagethi squash*, or *sqh* in *Drosophila*) tagged with GFP (Abreu-Blanco et al., 2011). I imaged epithelial cells in the fly notum from 14 to 16 hours AP. We then compared the organization of the acto-myosin cytoskeleton in mitotic and interphase epithelial cells (Figure 3.2.1 and 3.2.2).

At their most apical side, interphase cells were decorated with a mesh of actin filaments (top panels Figure 3.2.1.A yellow arrowheads), most likely depicting the presence of microvilli (Georgiou and Baum, 2010), common to a variety of epithelial cells (DeRosier and Tilney, 2000; Laster and Mackenzie, 1996). A meshwork of Myosin II was also seen underlying this apical-most cortex (top panels Figure 3.2.2.A). Additionally, at the apical side of cells we observed a high level accumulation of filamentous actin and Myosin at cell edges - demarking adherens junctions (Figure 3.2.3) (Ratheesh and Yap, 2012). At more intermediate and basal levels of epithelial cells, filamentous actin was visible but at lower levels than was seen at adherens junctions (Figure 3.2.1.A, intermediate and basal levels). In the case of Myosin we could not detect any clear accumulation of this protein at intermediate or basal levels, except for small dots corresponding to the remnants of cytokinetic events (Figure 3.2.2 A, intermediate and basal levels).

At the onset of mitosis this polarized acto-myosin cytoskeleton animal cells underwent dramatic remodeling as they rounded up to assume a smooth, stable and spherical shape in metaphase. At the

apical side, the most striking feature was the disappearance of the medial mesh of actin. This was clear both in apical-basal (xy) sections of the notum as well in side views (xz) (Figure 3.2.1 and 3.2.2). At the level of adherens junctions, actin and myosin levels appeared to be unaltered. At the intermediate level we observed a subtle accumulation of cortical actin and Myosin, and there was a strong accumulation of cortical filamentous actin and myosin at the most basal side of cells entering mitosis (Figure 3.2.1.A and 3.2.2.A intermediate and basal sides of the mitotic cell in prophase). At metaphase, while apical actin organization appeared identical to that seen in prophase, filamentous actin and Myosin accumulated across the entire basolateral cortex, beginning immediately beneath adherens junctions (Figure 3.2.1 and 3.2.2, metaphase panels). Interestingly, no cluster of filamentous actin was observed (Mitsushima et al., 2010), as a matter of fact cells in metaphase appear to have less actin at the cytoplasm when compared to neighbouring interphase cells. As cells exited mitosis, microvilli were visible reforming within the apical region as filamentous actin and Myosin accumulated at the presumptive cleavage furrow (Figure 3.2.1 and 3.2.2, anaphase/telophase panels). At more intermediate and basal levels we observed furrow ingression moving asymmetrically (Founounou et al., 2013; Herszterg et al., 2013) (Figure 3.2.1 B and 3.2.2 B, anaphase/telophase panels). Interestingly, within the lateral and basal domains of cells exiting mitosis, filamentous cortical actin remained at high levels in both future daughter cells even though the majority of Myosin re-localized to the cleavage furrow. Given the lack of myosin accumulation at the cortex of the two new daughter cells at mitotic exit, this cortical actin is unlikely to be contractile. Instead it may offer resistance to pressure coming from neighbouring cells while the two new daughter cells settle in their new location. To better test this hypothesis further experimental approaches would be required such as: laser dissection of the cell cortex and quantify cortex displacement would provide better understanding regarding the contractility of the new daughter cells.

**A**



**B**

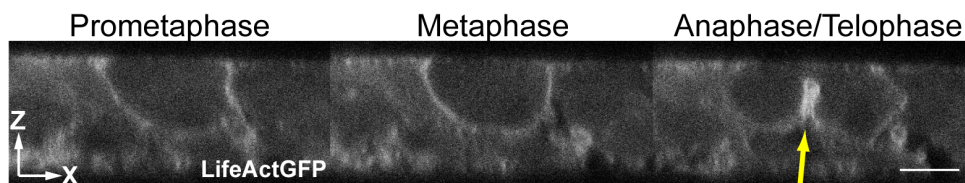
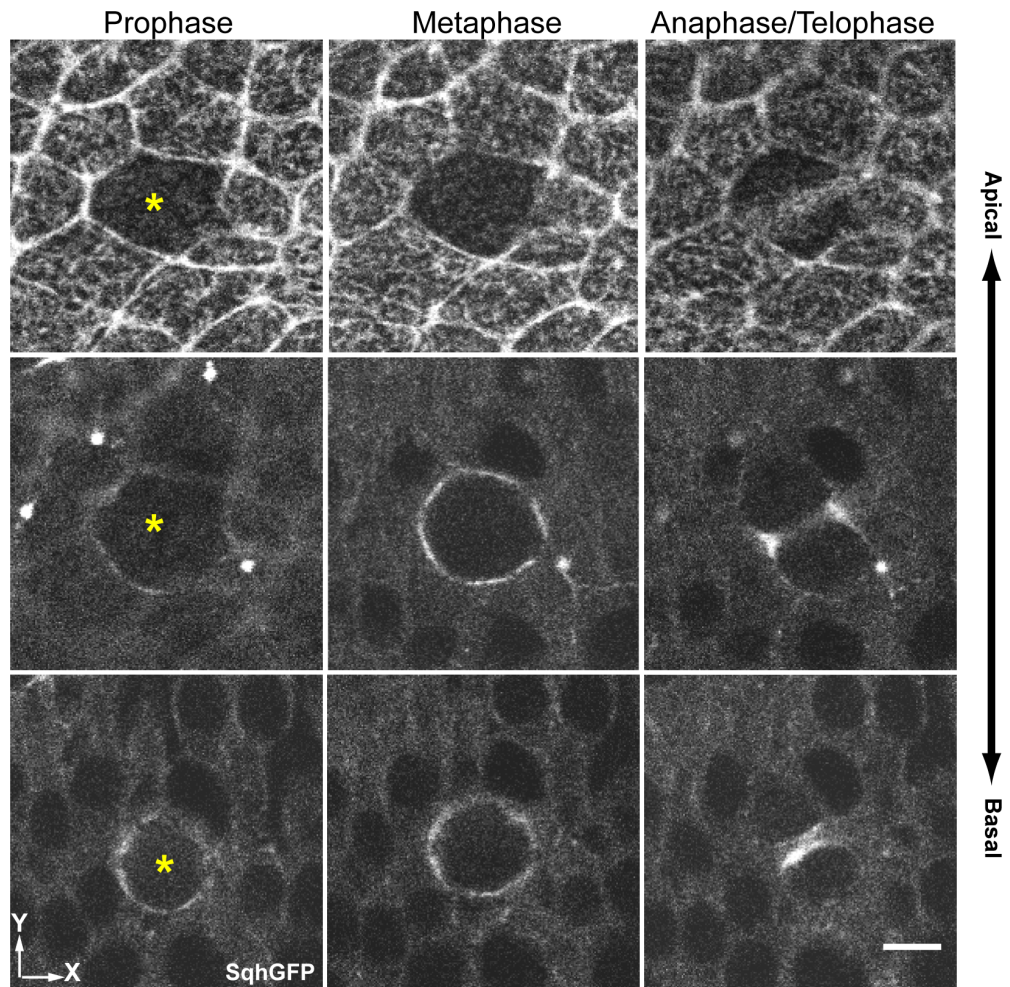


**Figure 3.2. 1. Filamentous actin accumulate at the cell cortex at the onset of mitosis. (A)** Apical, intermediate and basal top views of a lifeactGFP expressing notum with yellow asterisk marking a cell going through different stages of mitosis (single Z-sections). Yellow arrowheads pinpoint medial actin mesh. **(B)** Live imaging of an intermediate section of a cell expressing lifeactGFP at different stages of mitosis. Yellow arrow: assymetric progression of the furrow from basal to apical. Scale bars: 5µM.



**A**



**B**

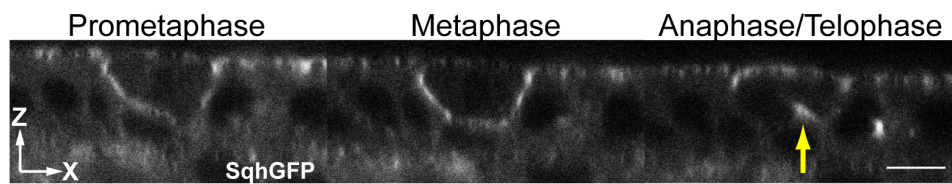


**Figure 3.2. 2. Myosin accumulates at the cell cortex at the onset of mitosis.** (A) Apical, intermediate and basal top views of sqh-GFP expressing notum with a yellow asterisk marking a cell going through different stages of mitosis. (B) Live imaging of a intermediate section of a cell expressing sqh-GFP at different stages of mitosis. Note Myosin II accumulation at the basal part of the cytokinetic ring. Yellow arrow: assymetric progression of the furrow from basal to apical. Scale bars: 5μM.

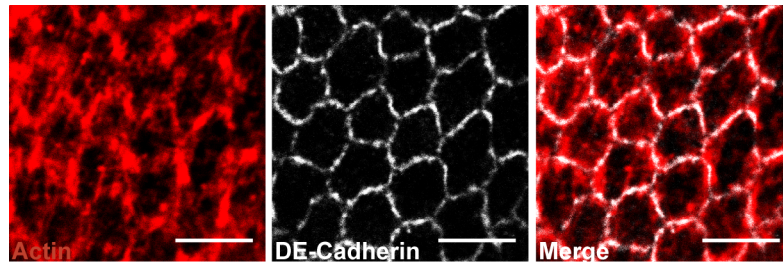


**Figure 3.2. 3. Junctional actin.** Actin in the most apical side of epithelial cells of the fly notum localizes with DE-Cadherin

### **3.3. Diaphanous versus Arp2/3 localization and function.**

Having observed a dramatic alteration in actin organization as cells entered mitosis, we decided to investigate which actin regulators contribute to the formation of the mitotic actin cortex. To address this question we followed a best candidate approach to identify actin nucleators essential for the mitotic actin cortex. Nucleation factors identified to date include: Arp2/3 complex, fomins, Spire, Cordon Bleu (Cobl) and Leiomodin (Lmod) (Campellone and Welch, 2010; Chesarone and Goode, 2009). For our analysis we focused on the two best understood actin nucleators: Arp2/3 complex and Diaphanous.

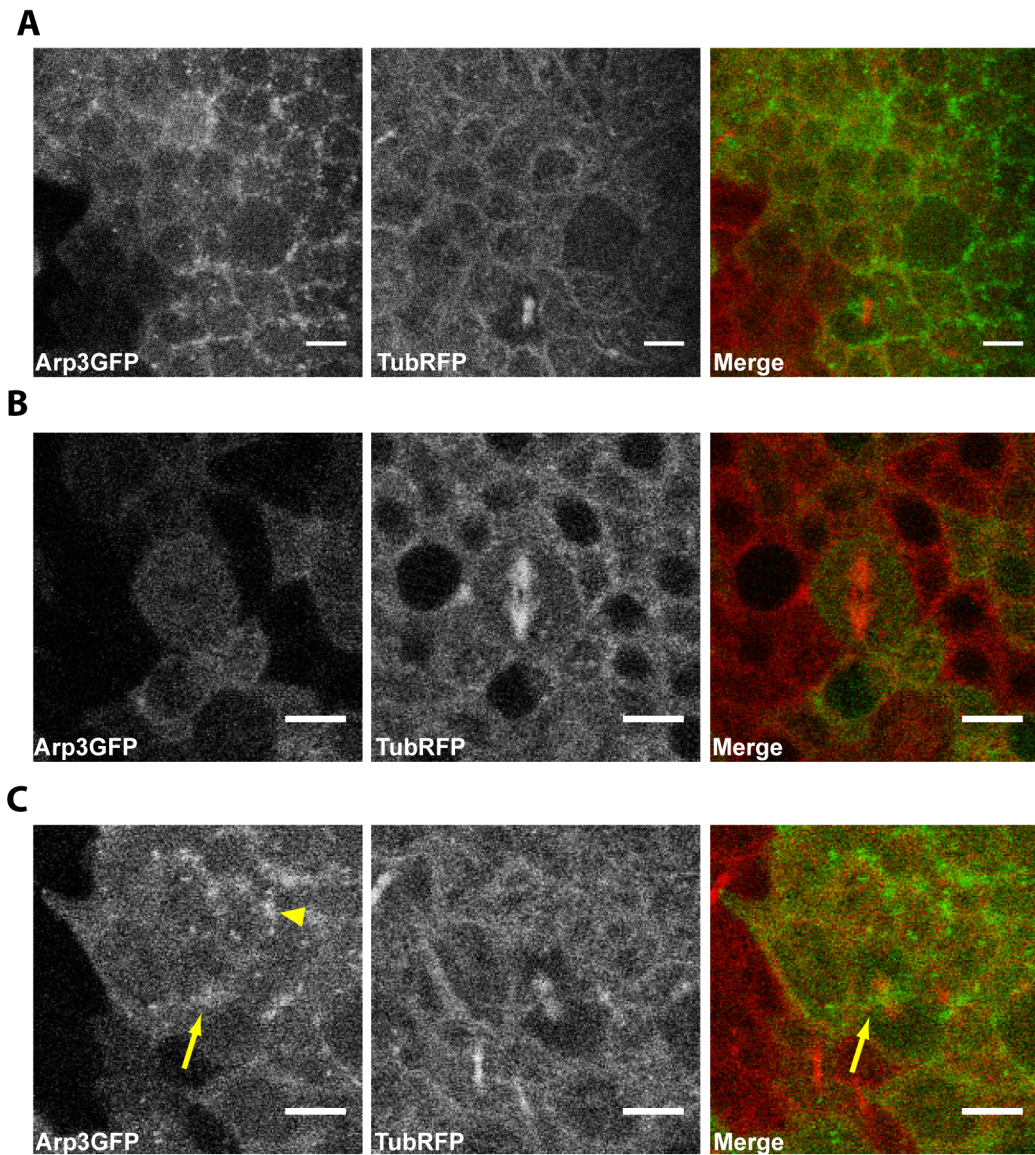
Using flies expressing Arp3 tagged with GFP in combination with Tubulin tagged with RFP we were able to characterize the localization of Arp3 in cells of the notum. We were also able to take advantage of the non-uniform expression induced by the UAS-Arp3-GFP transgene driven by *pnr*-Gal4 to image Arp3-GFP in small clusters of isolated cells. In both mitotic and interphase cells Arp3 was seen accumulating in punctate structures at apical cell-cell junctions (Figure 3.3.1 A). These may correspond to sites of endocytosis (Georgiou et al., 2008). However when cells entered mitosis we failed to detect any other sites of specific Arp3 accumulation (Figure 3.3.1 B), until late in cytokinesis where the protein was found accumulating at the interface between the two new daughter cells (Figure 3.3.1 C), as previously reported (Herszterg et al., 2013). To further investigate the role of Arp2/3 complex in mitosis we expressed an Arp3-specific RNAi hairpin to compromise the function of the Arp2/3 complex. We used the *pnr*-GAL4 driver to induce dsRNA expression, since it defines the intermediate dorsal domain of the tissue and UAS-lifeactGFP or NeuGMA as a read out for actin dynamics. In these movies a reduction in Arp2/3 function did not appear to compromise actin filament formation at adherens junctions in either interphase or mitosis



(Figure 3.3.2). However, interphase Arp3 RNAi cells appeared more stretched along their apical-basal axes, and gaps could be seen between cells at their most basal sides (Figure 3.3.2 B cells surrounding mitotic cell). This defect in basal protrusion formation is similar to that seen in loss of function mutations (Georgiou and Baum, 2010) and confirms that the RNAi-mediated silencing worked in this experiment. Conversely, during mitosis, Arp3 RNAi cells were able to round up to the same extent as control cells (Compare Figure 3.3.2 panel A with panel B), and were able to construct a normal-looking actin cortex. Overall, mitotic actin remodelling, including the disappearance apical-medial actin mesh, appeared to be unaffected by RNAi-induced silencing of Arp3. Though, the accumulation of filamentous actin at the most basal side of cells in prophase was lost. Occasionally, we observed slight cell deformations (Figure 3.3.3) reminiscent of cell blebs within the metaphase cortex (never seen in control cells). However, the average levels of filamentous actin at the mitotic cell cortex appeared to be unaffected by Arp3 depletion (Figure 3.3.12). Nonetheless, after mitosis Arp3 RNAi cells showed cell blebbing in cytokinesis (Figure 3.3.4) (King et al., 2010).

Having assessed the role of the Arp2/3 complex in epithelial cells in the notum, we followed the impact of Arp2/3 silencing on the cortex of sensory organ precursor cells (SOPs). For this we followed actin dynamics using an actin probe UAS-GMA under the *neuralized* promoter. As seen for epithelial cells, mitotic SOP cells expressing Arp3 RNAi assembled a normal actin cortex (Figure 3.3.5) similar to that seen in control cells (Figure 3.3.14). The ubiquitous expression of Arp3 protein in cells progressing through mitosis, allied to the fact that cells with reduced Arp2/3 function were capable of remodelling their cortex to a similar extent as control cells suggest that Arp2/3 does not play a crucial role for cortical actin remodelling during mitosis. Wasp and SCAR are Arp2/3 complex activators (Campellone and Welch, 2010), to better characterize the activity of Arp2/3 in the mitosis we express dsRNA targeting both Wasp (Figure 3.3.6) and Scar (Figure 3.3.7) under the *pnr*-GAL4 expression. In both situations cells were capable to build an actin cortex

in mitosis and no cell shape defects were detected, supporting the evidence that Arp2/3 has a minor role assembling an actin cortex during mitosis. In Scar RNAi expressing tissues we also took advantage of Neu-GMA expressing cells and followed *in vivo* the dynamics of cell division and similar to Arp3 RNAi expressing tissues SCAR inhibition resulted in cell blebbing during cytokinesis (Figure 3.3.7) (King et al., 2010). Although Arp2/3 complex appears not to be required for the assembly of a actin cortex of dividing cells there is still evidence that it might be required for its functionality, since occasionally cells do bleb in the absence of Arp3. It is possible that a fine balance of actin structures are needed at the cell cortex in mitosis and the coordinated function of Dia and Arp2/3 provides the exact mesh of actin structures to provide a functional actin cortex.



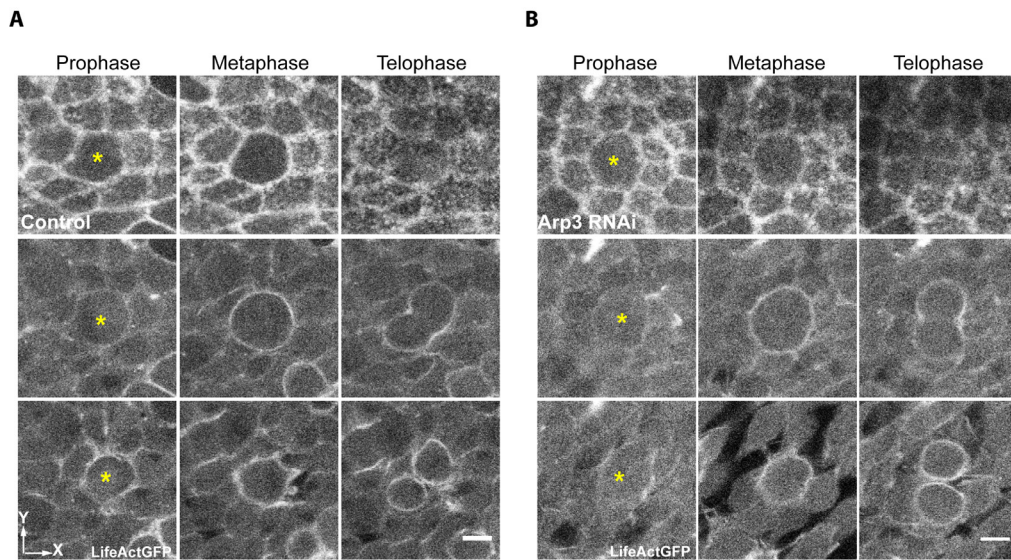


**Figure 3.3. 2. RNAi mediated silencing of Arp2/3 does not alter the mitotic actin cortex.** Images show actin filaments in apical, intermediate and basal sections of nota at different stages of mitosis, marked with a yellow asterisk. Cells are shown that express lifeact-GFP from the Pnr promoter in the absence (A) or presence (B) of a UAS-Arp3 RNAi transgene. Scale Bars: 5  $\mu$ M.



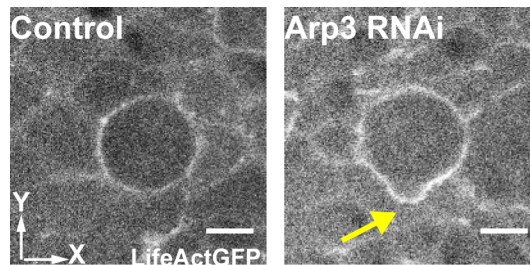


**Figure 3.3. 3. Cell deformations of metaphase cells in Arp3 depleted tissues.** Intermediate top view of metaphase cell expressing lifeactGFP. Yellow arrow indicates cell bleb in Arp3 RNAi expressing cell. Scale bars: 5 $\mu$ m.

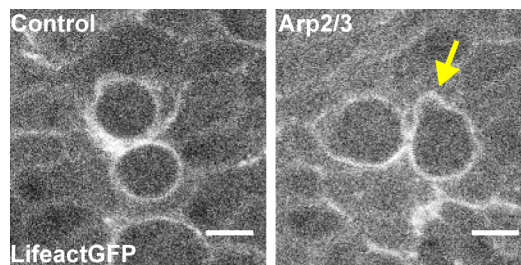


**Figure 3.3. 4. Arp3 RNAi mediated silencing promotes cell blebbing at the furrow canal.** Intermediate top view of cell in cytokinesis expressing lifeactGFP. Yellow arrow indicates cell bleb in Arp3 RNAi expressing cell. Scale bars: 5 $\mu$ m.

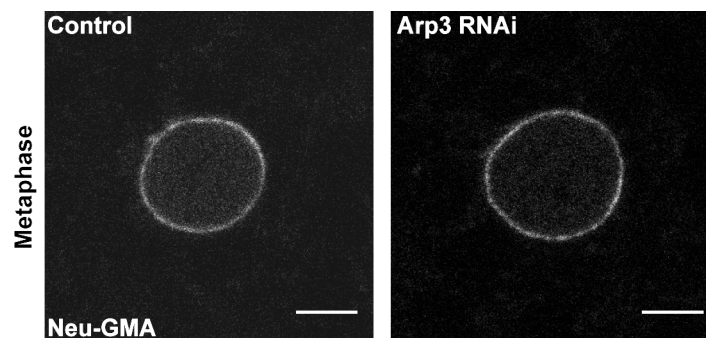


**Figure 3.3. 5. Arp3 RNAi mediated silencing does not alter mitotic cortex of P1 cells.** Intermediate top view of metaphase cell expressing Neu-GMAGFP. Scale bars: 5 $\mu$ m

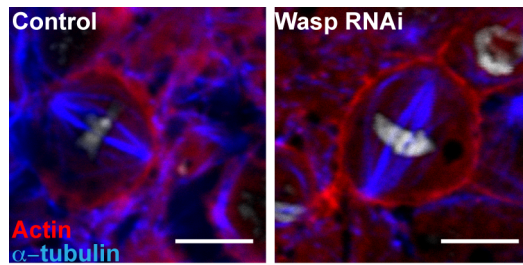


**Figure 3.3. 6. Wasp RNAi mediated silencing does not alter mitotic cortex of epithelial cells.**  
Scale bars: 5 $\mu$ m

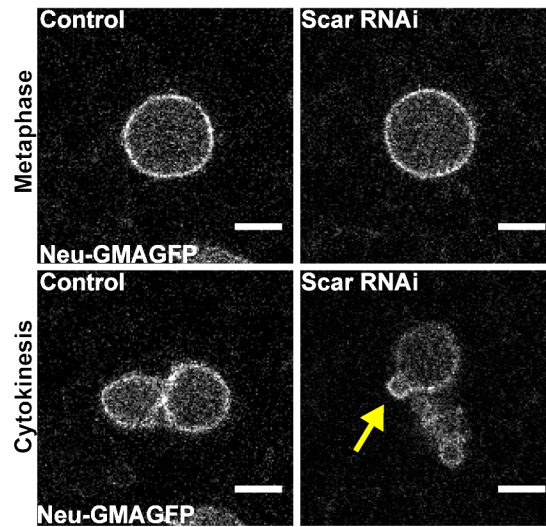


**Figure 3.3. 7. Scar RNAi mediated silencing does not alter mitotic cortex of P1 cells.**  
Intermediate top view of cells in metaphase and cytokinesis expressing Neu-GMA. Yellow arrow indicates cell bleb in SCAR RNAi expressing cell Scale bars: 5 $\mu$ m

To characterize the localization of Diaphanous in mitotic and interphase cells of the fly notum I dissected, fixed and stained nota of control (*w<sup>1118</sup>;pnr-GAL4*) flies using antibodies against Diaphanous protein and  $\alpha$ -tubulin. We also imaged filamentous actin and DNA taking advantage of TRITC-conjugated phalloidin and DAPI. This revealed the co-localization of F-actin and Diaphanous at the level of adherens junctions (Figure 3.3.8) (Homem and Peifer, 2008; Kobiela et al., 2004). Interestingly, I also saw an accumulation of Diaphanous protein at the cell cortex of mitotic cells (Figure 3.3.9). This accumulation was first seen in early prophase (Figure 3.3.9 A), where Diaphanous was seen accumulating at the cell cortex. Interestingly, at this stage, regions of the mitotic cortex with elevated levels of filamentous actin appeared enriched in Diaphanous. At metaphase (Figure 3.3.9 B) the accumulation of F-actin and Diaphanous was enhanced. This accumulation was seen decorating the entire cortex of the cell from apical to basal (Figure 3.3.10). Then levels of cortical Diaphanous appeared to decrease slightly at anaphase (Figure 3.3.9 C). Interestingly, we could observe a mild accumulation of diaphanous at the poles of anaphase cells suggesting a possible role in polar contractions during cytokinesis (Sedzinski et al., 2011). Finally, as expected (Afshar et al., 2000), during cytokinesis Diaphanous was seen accumulating at the cleavage furrow (Figure 3.3.9 D). The accumulation of Diaphanous at the cortex of mitotic cells suggests that it might play a role in remodeling the mitotic actin cortex. To test this hypothesis we induced dsRNA expression under the control of *pnr-GAL4* expression to decrease Diaphanous levels in the fly notum using UAS-lifeact-GFP or NeurGMA as a read out for actin dynamics.

Interphase cells with decreased Diaphanous function still exhibited some medial actin mesh. In addition, they were able to accumulate filamentous actin at the level of adherens junctions (Figure 3.3.11 compare panels A with panels B), indicating that the decrease in Diaphanous activity induced by the hairpin was not sufficient to abrogate these structures, even though Diaphanous has been implicated in junctional actin filament formation (Homem and Peifer, 2008; Ryu et al.,

2009). At intermediate levels, actin was still seen accumulating at cell margins (Figure 3.3.11 B intermediate panels) and at basal levels we observed gaps between neighbouring cells similar to those seen in Arp3 dsRNA expressing tissues. Interestingly, however, cells were still capable of forming dynamic basal protrusions (Figure 3.3.11 B, yellow arrowhead). These phenotypes are all consistent with the dsRNA inducing a partial loss of function RNAi phenotype.

Nevertheless, Diaphanous RNAi cells exhibited profound changes in mitotic actin filament organization. Additionally, in prophase the characteristic accumulation of basal filamentous actin was lost from Diaphanous RNAi cells (Figure 3.3.11 B prophase panels). At metaphase, these mitotic cells failed to recruit an actin cortex. Levels of filamentous actin were similar to those seen in neighbouring non-mitotic cells (Figure 3.3.11 B metaphase panels and figure 3.3.13). Finally, upon exit from mitosis, Diaphanous RNAi cells failed to build a cleavage furrow and failed cytokinesis (Figure 3.3.11 B anaphase/telophase panels), as expected based previous studies (Afshar et al., 2000). Similarly, SOP cells deprived of Diaphanous activity failed to build an actin cortex in mitosis (Figure 3.3.12 and 3.3.14), supporting this being a general phenomenon that is not restricted to symmetrically dividing epithelial cells.



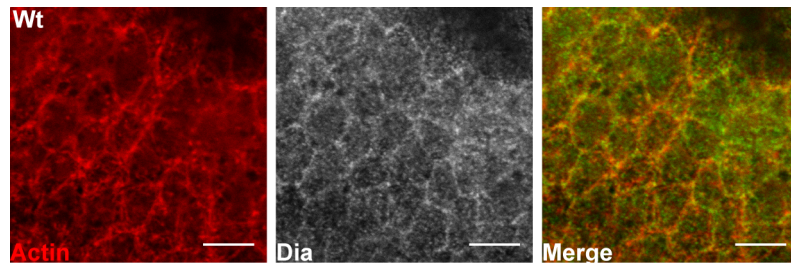


**Figure 3.3. 8. Diaphanous co-localizes with junctional filamentous actin.**

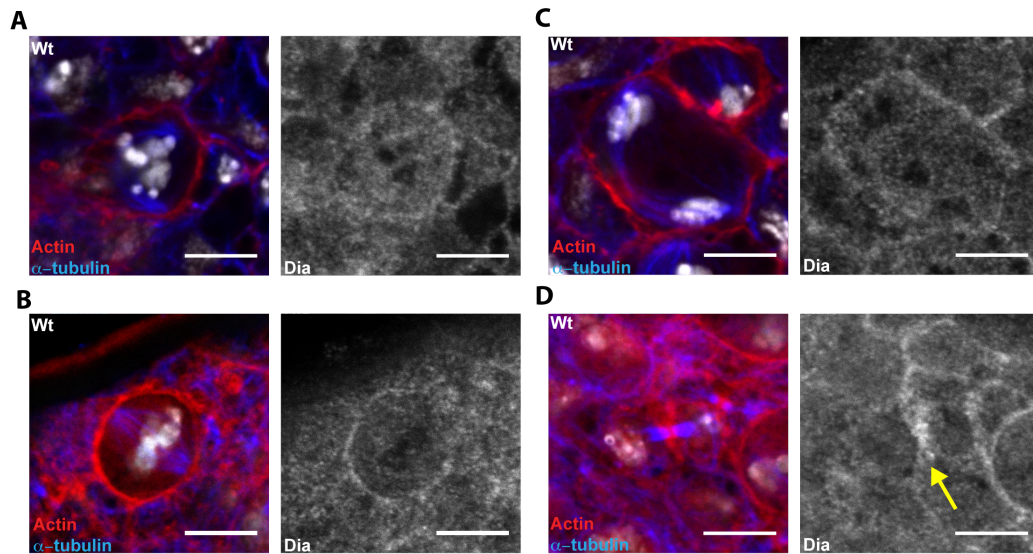


**Figure 3.3. 9. Diaphanous accumulates at the cortex of mitotic cells.** (A) Intermediate top view of prophase cell. (B) Intermediate top view of metaphase cell with Dia accumulation at the cell cortex. (C) Intermediate top view of anaphase cell. (D) Intermediate top view of cell in cytokinesis with Dia accumulation at the furrow canal (Yellow arrow).

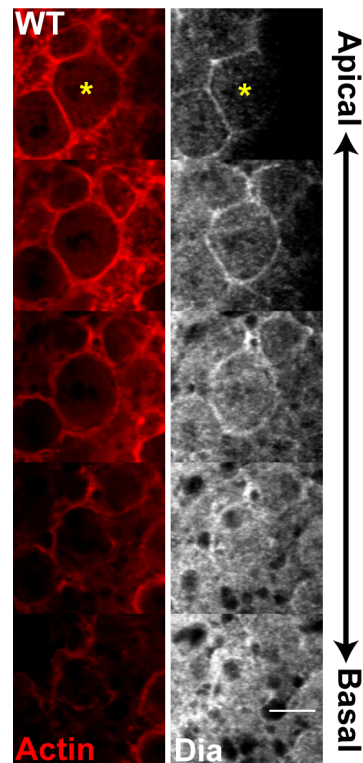


**Figure 3.3. 10. Diaphanous decorates the entire cell cortex of epithelial cells in metaphase.** Images show top view stacks from apical to basal sides of a metaphase cell marked with yellow asterisk stained for actin and Dia.

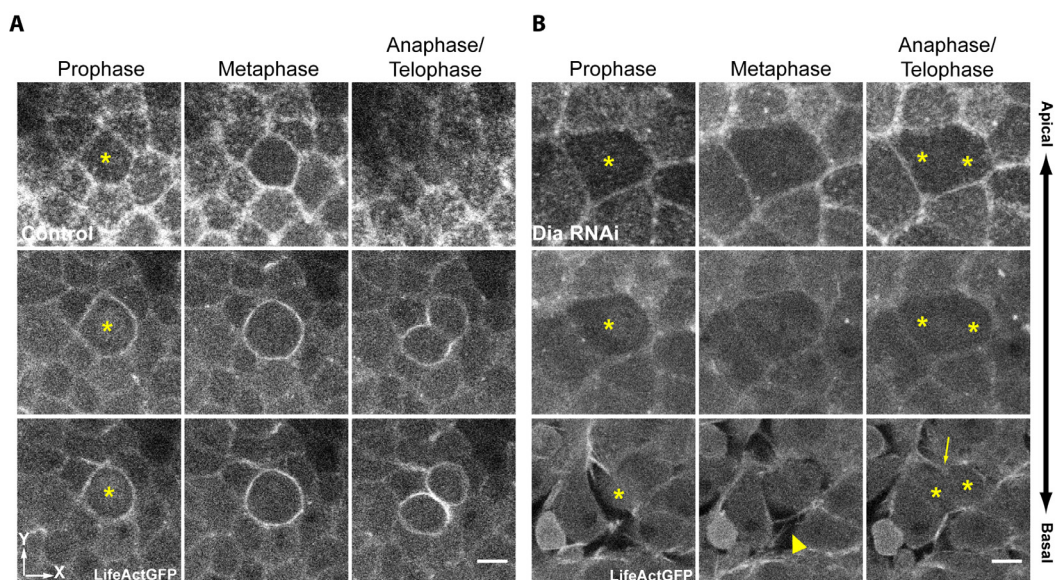


**Figure 3.3. 11. Diaphanous is required for the assembly of a mitotic actin cortex.** Images show actin filaments in apical, intermediate and basal sections of nota at different stages of mitosis, marked with a yellow asterisk. Cells are shown that express lifeact-GFP from the Pnr promoter in the absence (A) or presence (B) of a UAS-Dia RNAi transgene. Scale Bars: 5  $\mu$ M. Arrowhead marks basal protrusions. Arrow marks presumptive cleavage furrow.

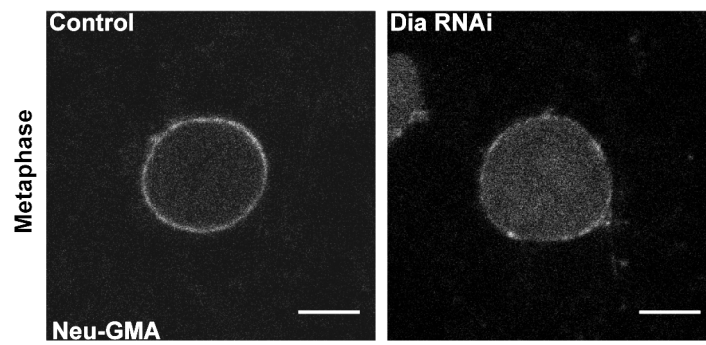


**Figure 3.3. 12. Assembly of a mitotic actin cortex in SOP cells is dependent of Dia activity.** Intermediate top view of metaphase SOP cells expressing GMAGFP (control cells) and metaphase SOP cells expressing GMAGFP and Dia RNAi.

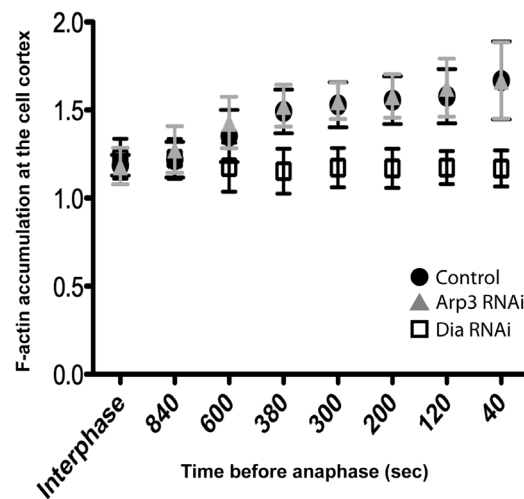


**Figure 3.3. 13. Assembly of an actin cortex is lost in the absence of Dia in epithelial cells entering mitosis.** Y values indicate the ratio of mean gray values of filamentous actin intensity at the cortex/cytoplasm of epithelial cells expressing lifeactGFP at interphase and at different times (X time in seconds) in mitosis previously to anaphase. (Values plotted: mean±S.D.).

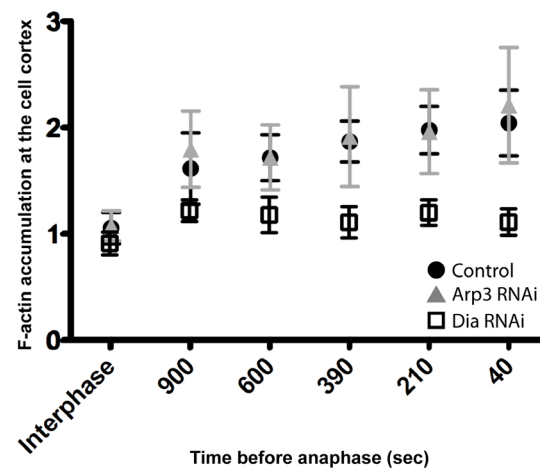


**Figure 3.3. 14. Assembly of an actin cortex is lost in the absence of Dia in SOP cells entering mitosis.** Y values indicate the ratio of mean gray values of filamentous actin intensity at the cortex/cytoplasm of epithelial cells expressing Neu-GMAGFP at interphase and at different times (X: time in seconds) in mitosis previously to anaphase. (Values plotted: mean±S.D.)

### **3.4. Loss of an actin cortex in mitosis impairs cell size.**

Several groups have studied the role of the actin cortex in the regulation of shape, size and mitotic progression in cells and tissues (Salbreux et al., 2012). In particular, a study of Stewart and colleagues (Stewart et al., 2011) demonstrated that differences in cell osmolarity are the driving force for cell rounding in cell culture. Conversely, the actomyosin cortex acts as an opposite force to the expansion of the cell volume. Stewart and colleagues also suggested that disruption of the actin cortex could lead to a volume increase. Given that expression of gene-specific dsRNA against Diaphanous resulted in the depletion of cortical actin in mitotic cells of the notum I wanted to determine whether this would alter mitotic cell size. To test this hypothesis I measured the size of mitotic cells, both in control and Diaphanous RNAi tissues.

Importantly, like the control, Diaphanous RNAi cells were able to take on an almost completely spherical shape as they entered mitosis (Figure 3.3.10 B metaphase panels). This enabled to directly test the effect of the loss of the actin cortex on mitotic cell size being careful not to include multinucleate cells in the analysis. At the level of the mitotic spindle, Diaphanous RNAi cells had a larger perimeter and cross-sectional area than control cells. (Figure 3.4.1). Moreover, this was the case both in epithelial cells and in SOP cells (Figure 3.4.2 and Figure 3.4.3). To determine if the observed increase in the cross-sectional area and perimeter of cells in Diaphanous dsRNA expressing tissues reflected an overall increase in their volume I measured cell height, to rule out the effect being due to a simple change in cell shape. To address this question we imaged the nota of control and Diaphanous dsRNA expressing tissues in an XZ configuration and used UAS-LifeactGFP to measure cell and tissue height (Figure 3.4.1). Using this method, dividing cells were found to have the same height as non-mitotic cells (we verified this result in 6 regions of tissue from at least three different flies

for each condition) This observation enabled us to use the height of the tissue to have a reference of the cell height in control and Dia RNAi expressing tissues. In our quantifications we notice an average height of  $8.78 \pm 1.01 \mu\text{m}$  for control nota and  $7.22 \pm 0.94 \mu\text{m}$  for Dia RNAi cells. Assuming that cells adopt simple spheroid form in mitosis the volume of control and Dia RNAi cells would be on average  $876 \mu\text{m}^3$  and  $869 \mu\text{m}^3$ , respectively (Figure 3.4.4). Although this needs to be verified by 3D reconstruction of the cell volume, these data suggest that the loss of Diaphanous and the consequent loss of the mitotic actin cortex has no major consequences on the cell volume. This is not surprising since osmotic forces are orders of magnitude greater than the contractile forces generated by the actin cortex (Charras et al., 2008).

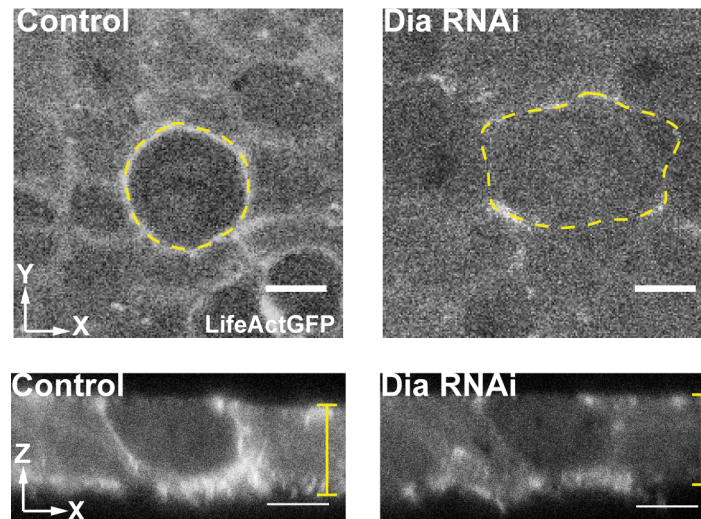


**Figure 3.4. 1. Mitotic cells required an actin cortex to regulate cell size.**

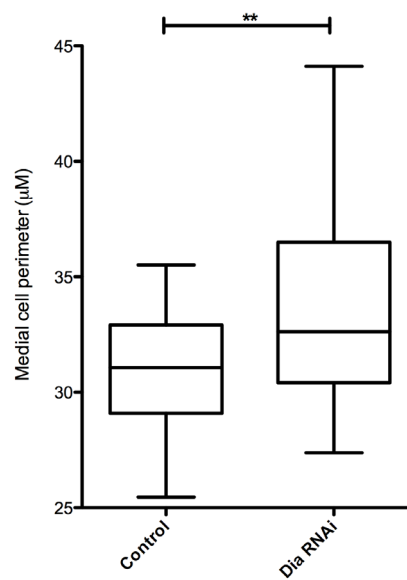


**Figure 3.4. 2. Epithelial mitotic cell perimeter is moderately increased in Diaphanous dsRNA expressing tissues.** (Mean±S.D. Control: 30.67±2.78. Diaphanous RNAi: 33.67±4.31 N=30).



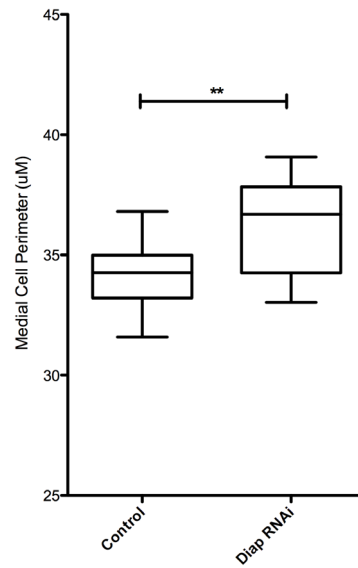


**Figure 3.4. 3. Sensory organ precursor mitotic cell perimeter is moderately increased in Diaphanous dsRNA expressing tissues.** (Mean±S.D. Control: 34.05±1.43. Diaphanous RNAi: 36.25±4.31 N=15).

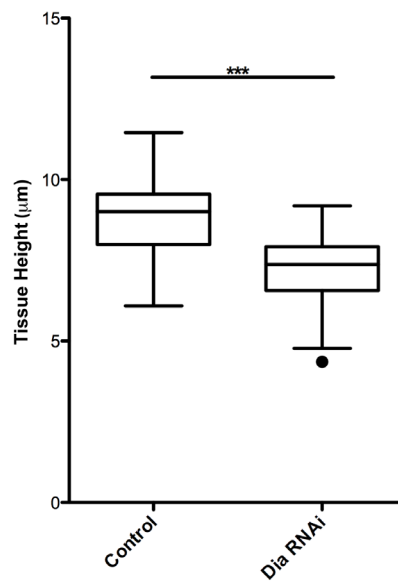


**Figure 3.4. 4. Nota of cells expressing Dia dsRNA show a decrease in height.** (Mean±S.D. Control: 8.78±1.01 μm. Diaphanous RNAi: 7.22±0.94 μm N=3).



### **3.5. Mitotic cells require an actin cortex to regulate spindle stability.**

The mitotic cell cortex has already been shown to be essential in the assembly and orientation of the mitotic spindle (Bompard et al., 2012; Carminati and Stearns, 1997; Carreno et al., 2008; Castanon et al., 2012; Fink et al., 2010; Hwang et al., 2003; King et al., 2010; Kunda et al., 2008a; Lancaster et al., 2013; Matthews et al., 2012; Mattison et al., 2011; Oliferenko and Balasubramanian, 2002; Rosenblatt et al., 2004; Samora et al., 2011; Segal and Bloom, 2001; Stearns, 1997; Vasiliev et al., 2004). Many of these studies, however, did not distinguish between the direct effects of cortical perturbation versus defects in actin-dependent cell shape.

Since mitotic cells deprived of Diaphanous in the fly notum failed to build an actin cortex as they rounded up, this was an ideal system in which to explore this question. To do so, I followed microtubules in Diaphanous RNAi and control cells to investigate how this might influence the mitotic spindle using  $\alpha$ -tubulin tagged with GFP under the control of the *pnr*-GAL4 driver. These movies revealed that mitotic cells in Diaphanous RNAi nota were able to separate their centrosomes to the same extent as control cells (Figure 3.5.1). This differs from findings previously reported for human cells depleted for Myosin II and/or actin (Rosenblatt et al., 2004; Lancaster et al., 2013), most likely because centrosome separation occurs prior to nuclear envelope breakdown in these epithelial cells. As seen in these previous studies, mitotic spindles were assembled with no apparent defects in rounded cells with a compromised mitotic cortex, interestingly, these spindles appear to be longer compared to control cells, presumably due to the differences in cell morphology (Lancaster et al., 2013) (Figure 3.5.1). Since assembly of a mitotic spindle in cells depleted of an actin cortex was not affected, we focused our attention on the dynamics of mitotic spindle orientation in the period after its assembly until anaphase. Spindle orientation along the

apical-basal axis of the cell was not impaired in Dia RNAi and cells always divided along the plane of the tissue we focused our attention to the rotation of the mitotic spindle along the plane of the tissue. We quantified spindle rotation by using images taken every 20 seconds (the minimal time period used for time-lapse image acquisition) to determine the mean angle of spindle displacement relative to a fixed coordinate (the A-P axis of the animal) from NEB until anaphase. This revealed an ~50% increase in total spindle orientation for Diaphanous RNAi cells compared to a control (from  $141 \pm 37.3$  degrees in the control (Figure 3.5.2) to  $189 \pm 61.6$  degrees in Diaphanous RNAi cells (Figure 3.5.2)). This reflected a slight increase in the movements of the spindle in mitotic Diaphanous RNAi cells at each time-step (Figure 3.5.3 and 3.5.4), from an average of  $0.25 \pm 0.05$  degrees/sec in the control to  $0.3 \pm 0.1$  degrees/sec in cells expressing Diaphanous dsRNA (Figure 3.5.3). This increase in the rate of rotation was clearer when we quantified the average rate of angular spindle displacement (Figure 3.5.4). While the mitotic spindle in control cells perform average rotations of 5 degrees every 20 seconds, and spindles were never seen performing rotations larger than 15 degrees, the mitotic spindle of Diaphanous RNAi cells often exhibited large angular displacements of up to 25 degrees in a 20 second period (Figure 3.5.4). It seems likely that these movements are due to an increase in the non-uniformity of the cortex in Dia RNAi cells rather than due to the loss of actin, i.e. similar to the effects of Cytochalasin rather than high dose Latrunculin (Lancaster et al., 2013).

We also noticed that mitotic progression in Diaphanous RNAi cells was slightly impaired (Figure 3.5.5). On average while control cells take  $9.3 \pm 1.3$  minutes to go from NEB to anaphase, Diaphanous RNAi cells take an average of  $11.02 \pm 2.2$  minutes; representing a 22% increase in the time from NEB to anaphase. Since we failed to detect any defects in spindle assembly we can only assume that this delay in mitosis progression may result from the spindle instability induced by these movements, leading to minor defects in attaching kinetochores to the spindle triggering the transient activation of the spindle assembly checkpoint. Similar increases in mitotic timing are seen in cells in culture

with a partial loss of actin filaments, but are not seen in rounded mitotic cells following the treatment with acute high doses of Latrunculin (Lancaster et al., 2013), supporting the idea that these reflect the partial loss of function.

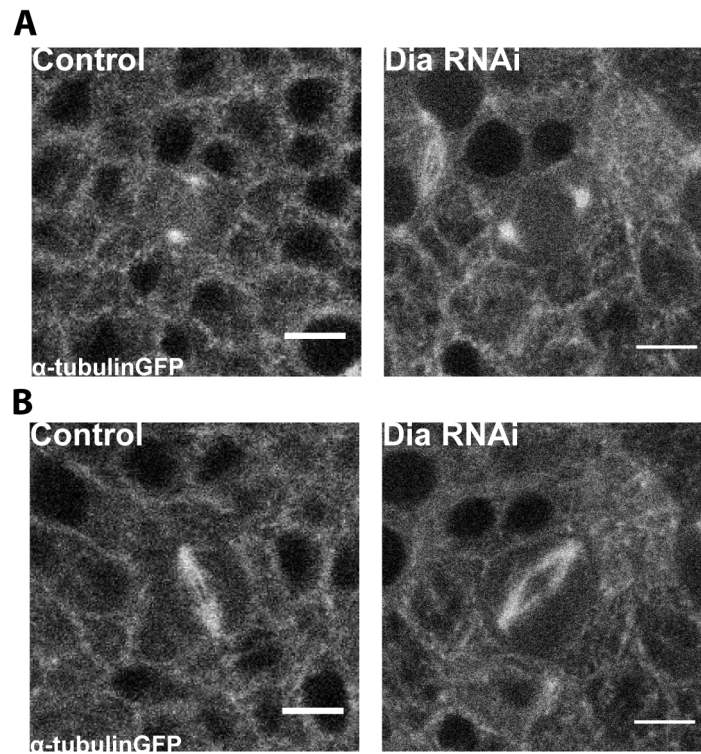


**Figure 3.5. 1. Centrosome separation and spindle assembly in Diaphanous RNAi tissues is not impaired.** A) NEB of control and Diaphanous RNAi cells marked by  $\alpha$ -tubulinGFP B) Metaphase cells of control and Diaphanous RNAi cells marked by  $\alpha$ -tubulinGFP displaying a mitotic spindle. Scale bars: 5  $\mu$ m.

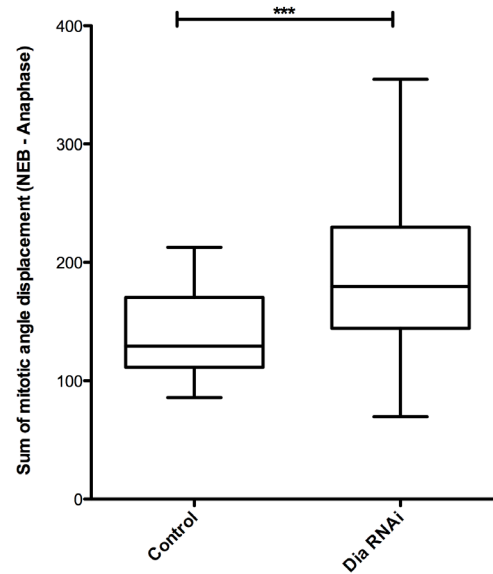


**Figure 3.5. 2. Angle displacement is increased from NEB to anaphase in epithelial cells with Dia compromised function.** Absolute values of angle displacement were added in time intervals of 20 seconds in cells progressing from NEB to anaphase. (Mean±S.D. Control: 141±37.3 degrees. Diaphanous RNAi: 189±61.6 degrees N=30)

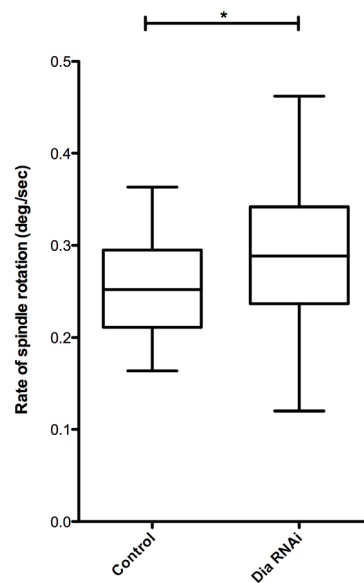


**Figure 3.5. 3. Rate of angle displacement is slightly increased in cells expressing Dia dsRNA.** The average of total angle displacement was measured in function of the time (in seconds) of cells progressing from NEB until anaphase. (Mean±S.D. Control: 0.25±0.05 degrees/sec. Diaphanous RNAi: 0.3±0.1 degrees/sec N=30)

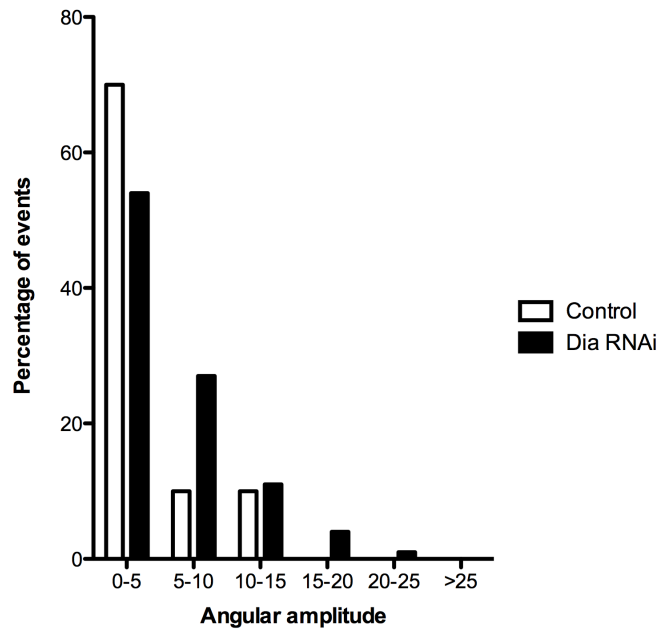


**Figure 3.5. 4. Mitotic spindle perform wider angular displacements in cells expressing Dia dsRNA.** Events of angular displacement were measured in a single time frame of 20 seconds.

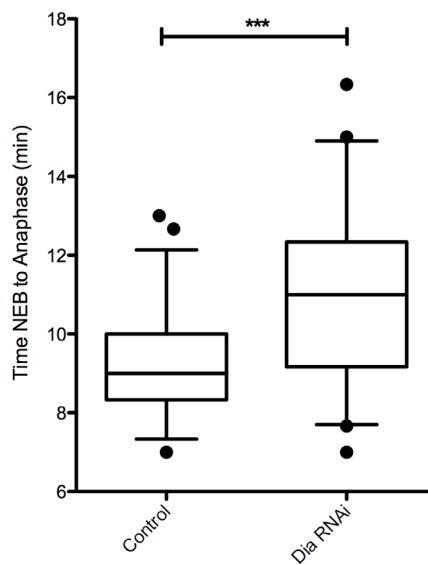


**Figure 3.5. 5. Mediated RNAi silencing of Dia impairs mitotic progression.** (Mean±S.D. Control: 9.3±1.3 minutes. Diaphanous RNAi: 11.02±2.2 minutes. N=30)

### 3.6. Conclusions

In this chapter, I characterize the nucleation of an actin cortex of epithelial cells entering mitosis in a developing notum. The objective of my study was to investigate the reorganization of the cell cytoskeleton entering mitosis specifically, the assembly of a cell cortex rich in F-actin and myosin and the actin nucleators at work in this process. In this chapter I first describe the remodeling of the cell cortex for cells in interphase and entering mitosis. I used transgenic flies that express a marker for F-actin and GFP tagged myosin. In these experiments we could identify microvilli and a meshwork of myosin at the apical side of cells and a strong accumulation of F-actin and myosin at the edges of cells demarking the adherens junctions. Functional epithelial cells form myosin webs and prominent circumferential actin bundles that run parallel to the adherens junctions, and play a fundamental role for cell-cell interactions (Kovacs et al., 2011; Martin et al., 2009; Rauzi et al., 2010). Observing the same cytoskeleton features in cells of the developing notum documented in the epithelia of other systems lead us to conclude that this is an ideal system to study the epithelial cell morphogenesis in the process of cell division.

Entering mitosis, the actin cytoskeleton is completely remodeled and with it the cell shape is altered. This is observed as soon as cells reach prophase where a major alteration is seen at the most apical side of cells with the disappearance of an actin and myosin mesh. In developing eggs the formation of a microvilli-free area is proportionate with the proximity of the meiotic chromosomes (Longo and Chen, 1985). Interestingly, in our system we identify a similar behaviour with the clearance of an apical mesh of actin and possibly microvilli, suggesting a conserved biologic process common to all dividing cells. Also, in prophase we observed an accumulation of both F-actin and myosin at the most basal side of cells. This accumulation we presumed to be due to the loss of substrate adhesion (Dao et al., 2009) since the assembly of this actomyosin cortex occurred ectopically culminating in a rounded cell

completely decorated with F-actin and myosin in metaphase. Later at anaphase/telophase both daughter cells showed high levels of cortical F-actin deprived of myosin, indicating that this cortex is not contractile and the simple cross-linked cortical actin filaments are possibly sufficient to offer resistance from external forces.

The assembly of an actin cortex is an almost universal feature in animal dividing cells (Kunda and Baum, 2009). I first showed that Dia is a fundamental actin nucleator required for the assembly of an actin cortex in mitosis. In these experiments I identified Dia at the cortex of mitotic cells and the compromised function of this protein was sufficient to enable mitotic cells to assemble an actin cortex, both in epithelial cells and SOP cells, strongly suggesting that Dia activity is universal in dividing cells of the fly. I also obtained evidence that when Dia is inactivated cell dimensions are altered but volume appears to be maintained. Fast scanning microscopy like spinning disc microscopy could improve volume measurements in mitotic cells of the fly notum. The use of this technique would increase dramatically the speed of time-lapse acquisition with low toxicity effects, allowing a higher and finer plane of z-stack acquisition which would be fundamental in the 3D reconstruction of dividing cells in different conditions and consequently a realistic measurement of cell volume.

Mitotic spindle instability is possibly due to a cortex with patchy actin, where cells with partial loss of filamentous actin would promote increased mitotic spindle instability (Lancaster et al., 2013). This will be addressed in forthcoming experiments with transgenic flies expressing markers for filamentous actin and GFP tagged tubulin consecutively, with compromised Dia function. Finally, we detect a delay in mitosis progression presumably due to increased spindle instability.

## **4. REGULATION OF THE ACTOMYOSIN CORTEX**

### **4.1. Introduction**

The Rho family of GTPases play important roles in the control of cell morphogenesis (Ridley, 2001). They do so by inducing specific downstream effectors that regulate actin dynamics at several steps to induce structures specific to each GTPase. A good example is the activation of Diaphanous related formins (DRFs) via Rho, which facilitates actin nucleation and polymerization and induces long, straight actin filaments (Etienne-Manneville and Hall, 2002; Hall, 1998, 2005, 2012; Hall and Nobes, 2000). The mitotic roles of Rho Cdc42 and downstream actin nucleators, e.g. Diaphanous/Bni1p, have been studied for some time in different systems (Cabernard, 2012; Evangelista et al., 1997; Fededa and Gerlich, 2012; Glotzer, 2001; Green et al., 2012; Heil-Chapdelaine et al., 1999; Narumiya and Yasuda, 2006; Piekny et al., 2005; Prokopenko et al., 1999; Tolliday et al., 2002; Zhu et al., 2011). In addition, recent work has shed some light on the roles of Rho GEFs and their downstream Rho GTPases in the regulation of changes in mitotic cell shape that accompany mitotic progression (Maddox and Burridge, 2003; Matthews et al., 2012; Rosenblatt et al., 2004; Sakamori et al., 2012; Yoshizaki et al., 2003). However, little is known about the molecular mechanisms responsible for actin remodelling during mitosis. In this chapter I will use the fly notum as a model system in which to investigate the putative role of RhoGEFs, focusing on the role of Pbl/Ect2 (Matthews et al., 2012), and Rho GTPases, focusing on the role of Rho1 (Maddox and Burridge, 2003; Prokopenko et al., 1999) and Cdc42 (Evangelista et al., 1997), in the control of the mitotic cortex. More specifically, building on the work presented in Chapter 3, I will explore the



roles of these upstream regulators in the localization of Diaphanous and in the generation of the mitotic actomyosin cortex.

## **4.2. The roles of Pbl, Rho and Cdc42 in the generation of the mitotic actomyosin cortex.**

### 4.2.1. Pebble is required for Myosin II activation and Dia localization and assembly of the mitotic actin cortex

Rho, Rac and Cdc42 represent the Rho family of small GTPases that control actin remodeling in several biological functions (Hall, 1998). RhoGTPases act as molecular switches being activated by Rho nucleotide exchange factors (GEFs), catalyzing the exchange of bound guanosine diphosphate (GDP) by guanosine triphosphate (GTP) (Hall, 1998). Pebble (the fly ortholog of mammalian Ect2) is a GEF for Rho, Rac and Cdc42 (Tatsumoto et al., 1999) and is active throughout mitosis (Matthews et al., 2012; Niiya et al., 2006; Tatsumoto et al., 1999). Pebble/Ect2 has been shown to play a crucial role in mitosis in mammalian cells (Hara et al., 2006; Matthews et al., 2012; Motegi and Sugimoto, 2006; Niiya et al., 2006) and in cytokinesis in both fly and mammalian systems (Chalamalasetty et al., 2006; Nishimura and Yonemura, 2006; Prokopenko et al., 1999; Tatsumoto et al., 1999; Yuce et al., 2005). More specifically, the human homologue of Pebble, Ect2, was recently shown to be activated in prophase, where the protein accumulates in the cytoplasm, activating Rho to drive mitotic cell rounding. Therefore, in looking for an upstream trigger driving assembly of the mitotic cell cortex in *Drosophila* cells, I began with Pebble. To study the actin cortex in cells with reduced levels of Pebble activity, I used UAS-lifeactGFP as a read out, and expressed a gene-specific RNAi hairpin under the control of *pnr*-GAL. As previously reported (Prokopenko et al., 1999), this led to a robust failure in cytokinesis, which in this system affected every cell studied (see below).

In movies of lifeactGFP in interphase cells with reduced levels of *Pebble* expression microvilli were observed. In addition, filamentous actin was still seen accumulating at the level of adherens junctions throughout

the cell cycle. At intermediate levels, there was a subtle accumulation of filamentous actin demarking cell margins and, at more basal levels, gaps were observed between neighbouring cells (Figure 4.2.1.1 B cells surrounding mitotic cell marked with a yellow asterisk). Interestingly, as *Pebble* RNAi cells entered prophase these microvilli persisted, even though these were quickly lost at the equivalent stage in control and Diaphanous RNAi cells (Figure 4.2.1.1 and Figure 3.3.10). Strikingly, however, as *Pebble* RNAi cells entering mitosis failed to accumulate basal filamentous actin and failed to undergo normal mitotic rounding, since cell area appeared increased (Figure 4.2.1.1 compare panels A and B for cells in prophase). By metaphase however, *Pebble* RNAi cells had rounded up, and had lost their most apical medial mesh of f-actin. Moreover, like Diaphanous RNAi cells, these cells failed to assemble a metaphase actin cortex (Figure 4.2.1.1 compare A with B and Figure 3.3.10 metaphase panels).

While the majority of cells failed to assemble a cytokinesis ring as they exited mitosis, there were exceptions in which a cleavage furrow was initiated and constricted almost to completion, before regressing to cause a failure in cytokinesis (Figure 4.2.1.1 B anaphase/telophase and late cytokinesis panels) (Castrillon and Wasserman, 1994). Given the striking similarities between the mitotic defects seen in *Pebble* and Diaphanous RNAi cells, we wondered whether Diaphanous activity and localization might be affected by RNAi-induced reductions in *Pebble* expression. To address this idea we stained control and *Pbl* dsRNA expressing *nota* flies using antibodies against Diaphanous protein and  $\alpha$ -tubulin. We also used TRITC-conjugated Phalloidin and DAPI to label filamentous actin and DNA. As a control, we performed the same staining for *nota* expressing dsRNA against Diaphanous. In interphase cells expressing *Pbl* RNAi failed to concentrate Dia at a junctional level, although junctional filamentous actin was still present (Figure 4.2.1.2). Moreover, it was clear from this analysis that *Pbl* RNAi mitotic cells failed to assemble a metaphase actin cortex, as observed for *Dia* RNAi metaphase cells (Figure 4.2.1.3 upper panels). *Dia* was no longer present

at the cell cortex both in Pbl and Dia RNAi metaphase cells (Figure 4.2.1.3 lower panels and Figure 4.2.1.5). When we measured the ratio of cortex/cytoplasm of Dia staining in metaphase cells (the gray-scale average was measured in a single z slice at the intermediate level of cells using imageJ), we observed significant differences in the average cortical accumulation of Diaphanous in Pbl and Dia RNAi cells compared to the control. In control cells, the average ratio was  $1.32 \pm 0.179$ , in Pbl RNAi cells  $1.13 \pm 0.13$  and in Dia RNAi cells  $0.97 \pm 0.13$  (Figure 4.2.1.5). These data suggest that cortical Dia recruitment and Dia function are dependent on Pebble function. Moreover, a few Pebble RNAi cells were able to build a defective cytokinesis ring (Lehner, 1992; Prokopenko et al., 1999), where after anaphase a defective accumulation of filamentous actin accumulated at the presumptive furrow canal. In these circumstances Diaphanous accumulation appeared to be defective (Figure 4.2.1.4). This could explain the subsequent failure of cytokinesis observed in our movies (Figure 4.2.1.1 B), for Pebble RNAi cells were able to initiate the formation of a contractile ring upon mitotic exit.

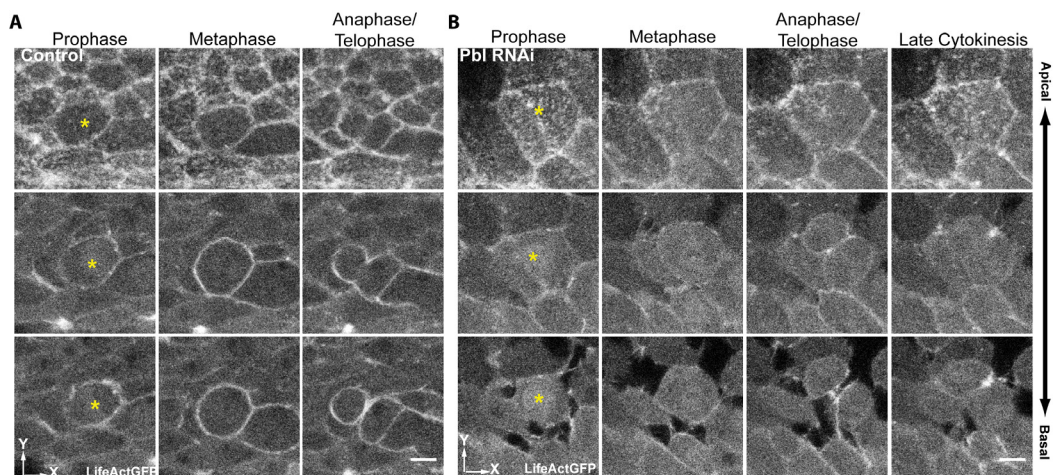


**Figure 4.2.1. 1. RNAi mediated silencing of Pbl impairs the assembly of an actin cortex in mitosis.** Images show actin filaments in apical, intermediate and basal sections of *nota* at different stages of mitosis, marked with a yellow asterisk. Cells are shown that express lifeact-GFP from the *Pnr* promoter in the absence (A) or presence (B) of a UAS-Pbl RNAi transgene. Scale Bars: 5  $\mu$ M.

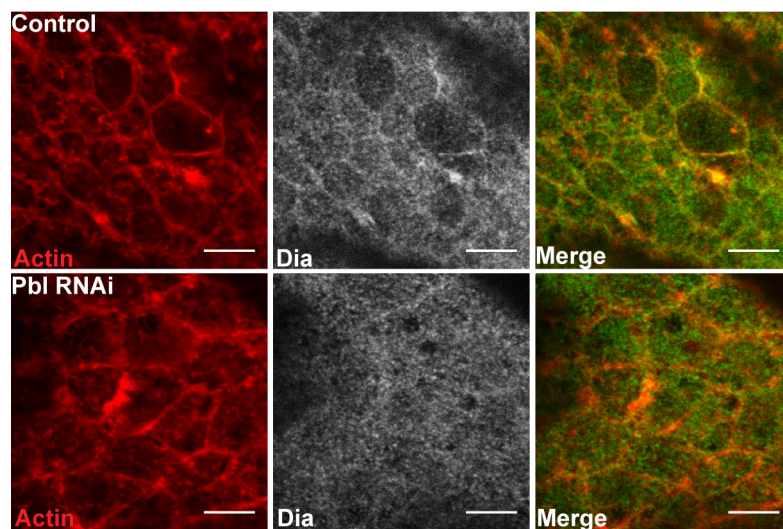


**Figure 4.2.1. 2. Pebble controls Dia at the level of junctional F-actin.** Apical top view of control interphase cells exhibit Dia at the junctional level. Pbl RNAi cells fail to localize Dia at the level of junctional F-actin. Scale bars: 5  $\mu$ m.

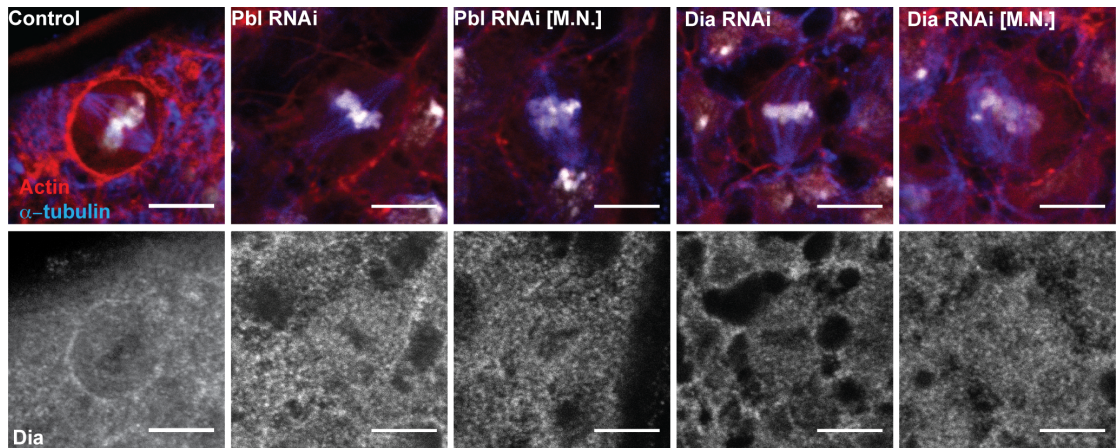


**Figure 4.2.1. 3. Pebble is required for Dia cortical accumulation of cells in mitosis.** Intermediate top view of control cells shows a strong accumulation of cortical Diaphanous. Cortical localization of Dia is lost both in tissues expressing Pbl and Dia dsRNA. Scale Bars: 5  $\mu$ m.

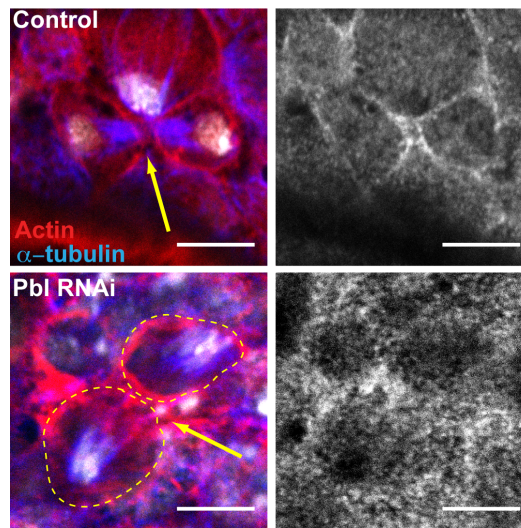


**Figure 4.2.1. 4. Dia recruitment to the furrow canal is impaired in Pbl dsRNA expressing tissues.** Top view of control cells in cytokinesis show a strong accumulation of Dia at the furrow canal (yellow arrow). Pbl dsRNA expressing cells fail to accumulate Dia at the presumptive furrow canal (yellow arrow). Yellow dashed line marks two new daughter cells Scale Bars: 5  $\mu$ m.

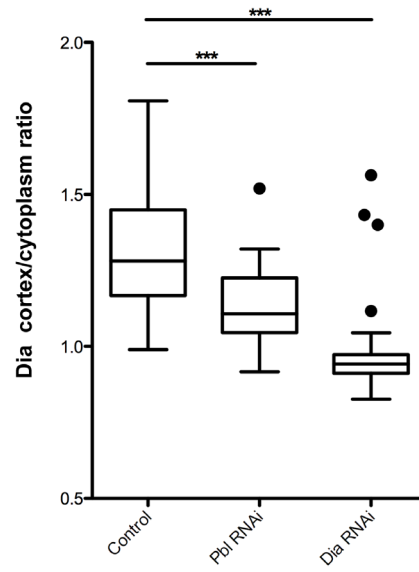


**Figure 4.2.1. 5. Cortical localization of Dia in metaphase cells is compromised in Pbl RNAi expressing cells.** Graph of intermediate single plane ratio of mean gray values of Dia cortex/cytoplasm in control, Pbl and Dia dsRNA expressing metaphase cells. (Mean±S.D. Control: 1.32±0.18. Pbl RNAi: 1.13±0.13. Dia RNAi: 0.97±0.13 N=40).

A large number of studies (Matthews et al., 2012; Morita et al., 2005; Niiya et al., 2006; Prokopenko et al., 1999; Somers and Saint, 2003; Su et al., 2011; Tatsumoto et al., 1999; Wolfe et al., 2009; Yuce et al., 2005) show that Pebble can act via Rho1 to regulate both actin and Myosin in both interphase and mitosis. To better determine whether Pebble regulates Myosin II during mitosis as reported for other systems, we used the same approach to study the localization and activation of Spaghetti squash (sqh), the fly homolog of Myosin Light Chain II, in cells expressing Pebble dsRNA. First, we stained the nota of control, Pbl and Dia dsRNA expressing tissues with antibodies for active, phosphorylated Sqh (S19) and  $\alpha$ -tubulin. TRITC-conjugated Phalloidin was used to visualize filamentous actin and DAPI, DNA.

In the control, the metaphase cell cortex was entirely decorated with pMyo (Figure 4.2.1.6), leading to an average pMyo cortex/cytoplasm ratio of  $1.69 \pm 0.29$ ). This cortical accumulation of pMyo was abrogated in Pbl and Dia RNAi cells (Figure 4.2.1.8). The average cortex/cytoplasm ratio of pMyo reach values of  $1.25 \pm 0.15$  and  $1.19 \pm 0.22$ , respectively. Not only did most Pbl cells fail to establish an actomyosin ring following mitotic exit, but pMyo appeared more dispersed than it did in control cells (Figure 4.2.1.7) in the few escapers that managed to initiate the formation of a contractile ring and cleavage furrow. These data clearly suggest that Pbl is required for the remodelling of the actomyosin cortex of mitotic cells of the notum acting upstream to Diaphanous. The goal of this experiment however, was to determine whether Pebble is required upstream of pMyosin in the generation of the mitotic actomyosin cortex. The fact that pMyo localization was dependent on Diaphanous presents a problem here, since it prevented us from determining whether Pebble acts on pMyo directly or through its effect on Dia. However, in the representative images shown, it is clear that pMyo levels are lower in Pebble RNAi cells than in the Dia control, where pMyo is often seen on small dots at the spindle poles, presumably marking centrosomes (Figure 4.2.1.6), as expected if Myosin was activated in a cell with a weak cortex, enabling it to be stripped off by the action of Dynein (Zheng et al., 2013). However, to help resolve the role of Pebble in Myosin activation, we decided to



study the effect of Rho1 and the remodelling of the actomyosin cortex in epithelial cells during mitosis.

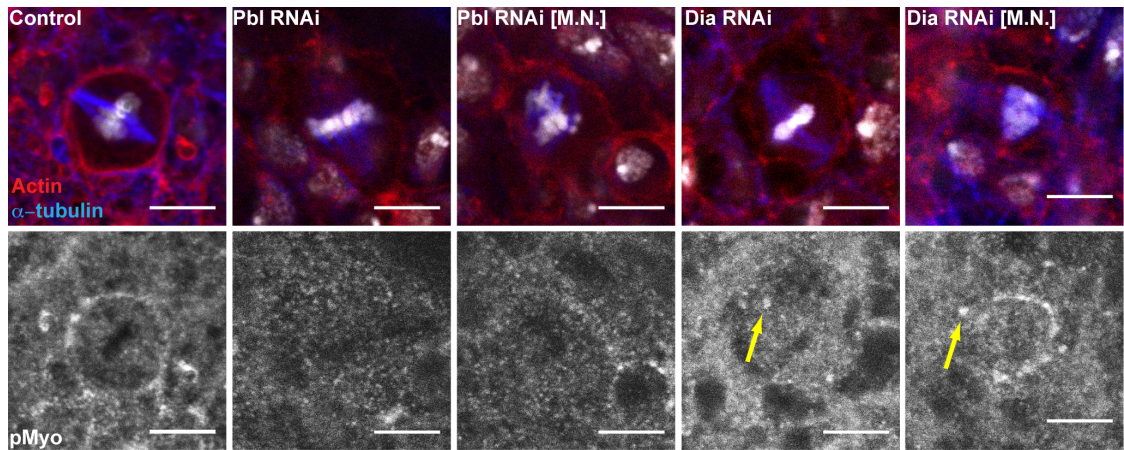


**Figure 4.2.1. 6. Pebble is required for activation and cortical accumulation of myosin.** Intermediate top view of control cells shows a strong accumulation of cortical activated myosin. Tissues expressing Pbl RNAi are deprived of cortical pMyosin. In Dia RNAi expressing tissues pMyosin is concentrated in the presumptive centrosomes (yellow arrows) indicating that myosin activation is not abrogated. [M.N.] multinucleated cells. Scale Bars: 5  $\mu$ m.

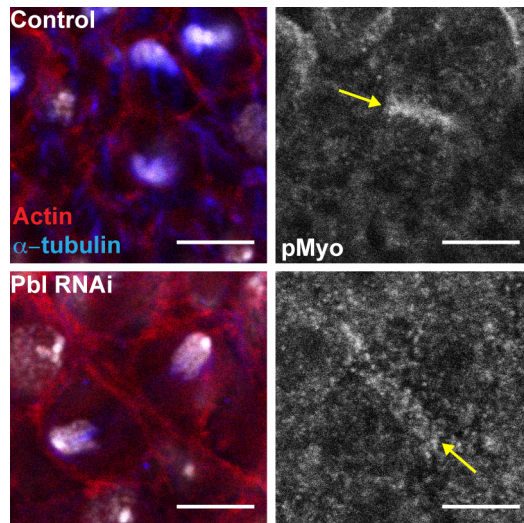


**Figure 4.2.1. 7. Activation of myosin at the furrow canal is compromised in Pbl RNAi expressing cells.** Top view of control cells in cytokinesis show a strong accumulation of pMyosin at the furrow canal (yellow arrow). Pbl dsRNA expressing cells show a severe decrease of activated Myosin at the furrow canal (yellow arrow). Scale Bars: 5  $\mu$ m.

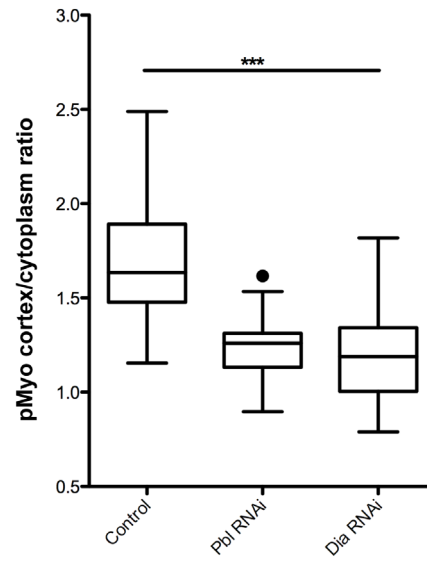


**Figure 4.2.1. 8. Cortical activation of myosin in metaphase cells is compromised in Pbl RNAi expressing cells.** Graph of intermediate single plane ratio of mean gray values of pMyosin cortex/cytoplasm in control, Pbl and Dia dsRNA expressing metaphase cells. (Mean±S.D. Control: 1.69±0.29. Pbl RNAi: 1.25±0.15. Dia RNAi: 1.19±0.22 N=40).

#### 4.2.2. Rho1 is required for Dia and Myosin II activation in mitosis

To better understand which are the players involved in the remodeling of the actomyosin cortex in mitosis we next focused our attention on the likely Pebble effector, Rho1. This was an obvious target since Pebble interacts genetically with Rho1 (Prokopenko et al., 1999) and recruits Rho to the cortex during cell division. Moreover, in mammalian cells Rho is essential for the Pebble/Ect2 dependent changes in cell shape and cortical rigidity that occur upon entry into mitosis (Maddox and Burridge, 2003; Matthews et al., 2012). To study the function of Rho1 in the remodeling of actin and Myosin in mitotic epithelial cells of the fly notum we took advantage of a dominant negative form of Rho (RhoDN) to disrupt specifically Rho function (Hacker and Perrimon, 1998; Prokopenko et al., 1999; Strutt et al., 1997) under the control of *pnr*-GAL4 expression. Since this dominant negative construct is extremely toxic, its expression was attenuated by Gal80ts to enable us to study the mitotic role of Rho1. Flies were left at 18 degrees Celsius until 6-8 hours before notum dissection, where upon pupa were transferred to an incubator with a temperature of 29 degrees Celsius. We then stained the nota of control and RhoDN expressing tissues with antibodies against Dia, phosphorylated Myosin and  $\alpha$ -tubulin. To visualize filamentous actin and DNA we used TRITC conjugated Phalloidin and DAPI, respectively.

Interphase cells expressing RhoDN show a punctuated accumulation of junctional filamentous actin associate with puncta of Dia protein (Figure 4.2.2.1). Similar to Pebble RNAi cells, mitotic cells expressing RhoDN were able to round up upon entry into mitosis. However, the mitotic actin cortex was severely affected in these cells, leading to a heterogeneous accumulation cortical filamentous actin, with areas of low actin accumulation (Figure 4.2.2.2). Additionally, we observed cells with increased DNA content and larger mitotic spindles undergoing mitosis (Figure 4.2.2.2) indicating a failure in cytokinesis and consecutively becoming multinucleated - a phenotype long associated with reductions in Rho1 activity (Prokopenko et al., 1999). Interestingly,

Dia appeared to accumulate in mitotic cells that exhibited clear gaps in their cortical actin staining and in multinucleated cells. Importantly, this suggests that although Dia activity is impaired following the inhibition of Rho1, its localization in metaphase is only marginally affected. To quantify the extent Diaphanous delocalization in following the inhibition of Rho activity, we measured the levels of Dia at the cell cortex in metaphase cells, in a single XZ image at the intermediate level of cells, in control and RhoDN expressing tissues. This revealed a small but significant decrease in the level of the Dia cortex/cytoplasm ratio in the RhoDN compared to the control: with an average of  $1.16 \pm 0.11$  compared to  $1.32 \pm 0.18$  of control cells. This was not statistically significantly different from that observed in metaphase cells depleted of Pbl ( $1.13 \pm 0.13$ ) (Figure 4.2.2.6), suggesting that Dia accumulation in RhoDN tissues is impaired and that Rho was required both for Dia cortical localization and its activation. Nevertheless, the actin and Dia localization phenotype of RhoDN was consistently less strong than that of Pbl RNAi.

Most studies on the role of Rho in the cell cycle have concentrated on its function during cytokinesis. In dividing cells of the fly notum expressing RhoDN we observed cells forming a contractile ring comparable to control cells and in these cases we could also observe a slight accumulation of Dia at the cleavage furrow (Figure 4.2.2.3). However, in all cases, the two new daughter cells exhibited severe cell shape defects that made it difficult to assess whether these cells eventually failed cytokinesis, like equivalent cells in Pbl RNAi tissues (Figure 4.2.1.7). However, these results suggest that Rho1 inhibition, like the depletion of Pebble, leads to a profound defect in the assembly of the actomyosin cortex upon mitotic entry, a partial defect in furrow formation at mitotic exit and a very reproducible failure in cell division.

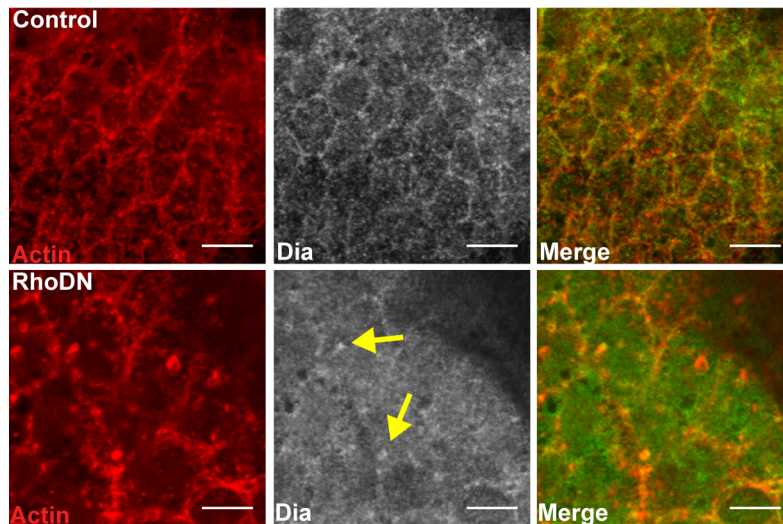


**Figure 4.2.2. 1. Rho1 controls filamentous actin assembly and Dia at junctional level.** Apical top view of control interphase exhibits F-actin and Dia at the junctional level. RhoDN expressing tissues exhibit punctuate accumulation of junctional F-actin and Dia (yellow arrows). Scale bars: 5  $\mu$ m.

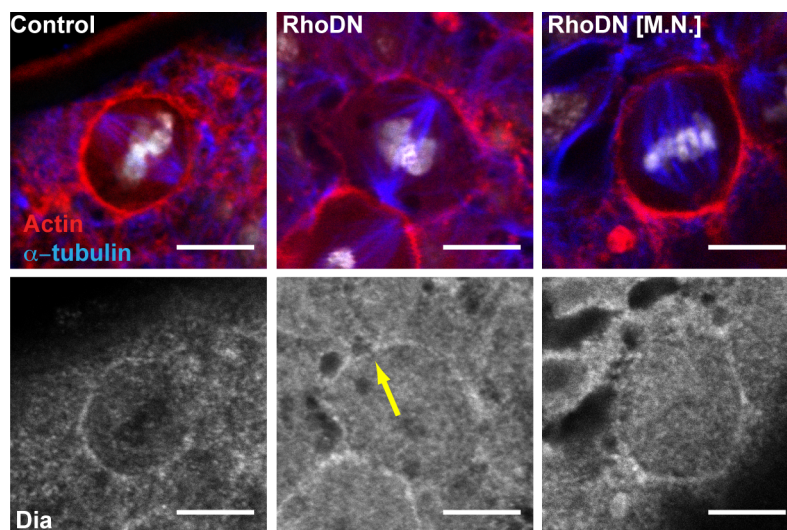


**Figure 4.2.2. 2. Cortical localization of Dia is marginally affected in metaphase cells expressing a dominant negative form of Rho.** Intermediate top views of metaphase cells expressing RhoDN show an accumulation of cortical Dia in domains with modest actin filaments (yellow arrow). [M.N.] multinucleated cells. Scale Bars: 5  $\mu$ m.

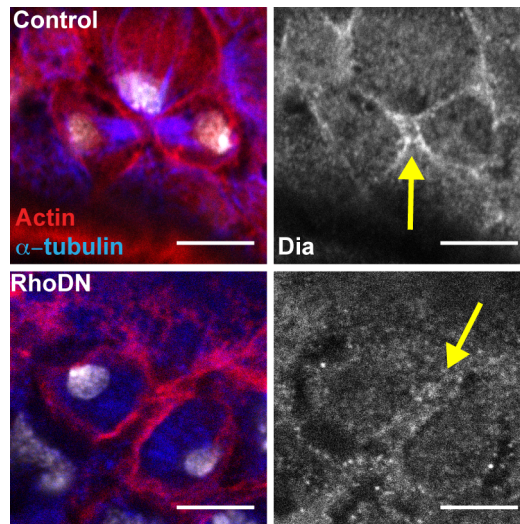


**Figure 4.2.2. 3. Rho1 controls Dia accumulation at the furrow canal.** Top view of control cells in cytokinesis show a strong accumulation of Dia at the furrow canal (yellow arrow). RhoDN expressing cells show decreased Dia accumulation at the furrow canal (yellow arrow). Scale Bars: 5  $\mu$ m.



Rho kinase (Rok) is an effector of Rho activity and the primary output of Rok activity is the phosphorylation of non-muscle myosin light regulatory chain (sqh) consequently, disruption of Rho1 activity via RhoDN expression leads to defects in Myosin II activity (Bloor and Kiehart, 2002). Mitotic cells in RhoDN expressing tissues exhibited a severe decrease in pMyo levels at the cell cortex when compared with control cells (Figure 4.2.2.4). Even though cells were able to round up and establish an actin cortex, the cell cortex was severely deprived of pMyo. As before to quantify this effect we measured cortical versus cytoplasmic pMyo in the nota of control and RhoDN expressing tissues. The cortex/cytoplasm ratio of pMyo of RhoDN expressing metaphase cells was  $1.09 \pm 0.16$  compared to  $1.69 \pm 0.29$  of control cells (Figure 4.2.2.7) clearly indicating that metaphase cells had no active Myosin II at the cell cortex. Moreover, pMyo was not seen at small dots at mitotic spindle poles (presumably the centrosomes) following Rho1 inhibition as it was in Dia RNAi cells. Interestingly, the levels of pMyo in mitotic RhoDN cells were significantly ( $p < 0.01$ , Mann-Whitney statistical test) lower than those observed in Pbl RNAi cells ( $1.25 \pm 0.15$ ). This difference was striking since Dia levels were similar to those seen in Pbl RNAi cells (Figure 4.2.2.6). If anything, levels of cortical Dia appeared higher in RhoDN expressing cells than in Pbl RNAi cells, as did levels of cortical filamentous actin. Conversely, phosphorylated spaghetti squash could be seen in cells expressing RhoDN that formed a cleavage furrow (Figure 4.2.2.5). However, its organization was severely altered, and did not appear to have condensed into a ring-like structure. These data suggest that Rho1 has dual roles. It functions to activate Myosin II upon entry into mitosis, and later at cytokinesis to recruit Dia to the cleavage furrow.



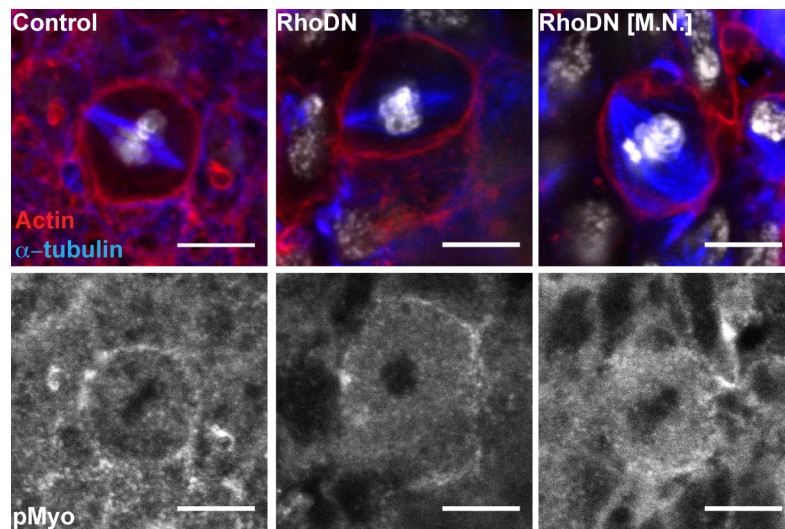


**Figure 4.2.2. 4. Rho1 is required for the activation of myosin at the cell cortex of cells in mitosis.** Intermediate top views of metaphase cells expressing RhoDN show impaired accumulation of activated myosin at the cell cortex. [M.N.] multinucleated cells. Scale Bars: 5  $\mu$ m.

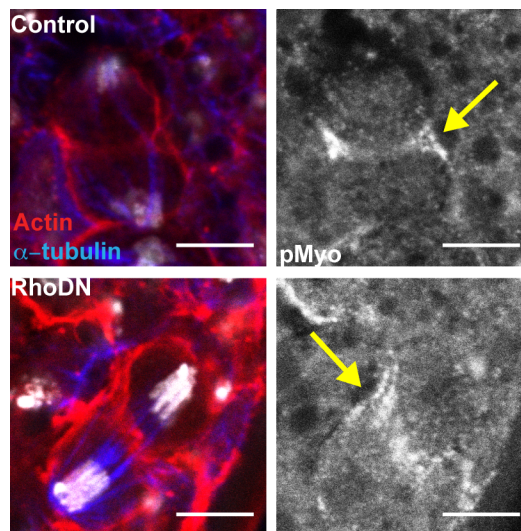


**Figure 4.2.2. 5. Phosphorylated Myosin II concentrates at the furrow canal of cells with compromised Rho1 function.** Top view of control cells in cytokinesis concentrate pMyosin at the furrow canal (yellow arrow). RhoDN expressing cells performing cytokinesis concentrate pMyosin at the furrow canal (yellow arrow). Scale Bars: 5  $\mu$ m.

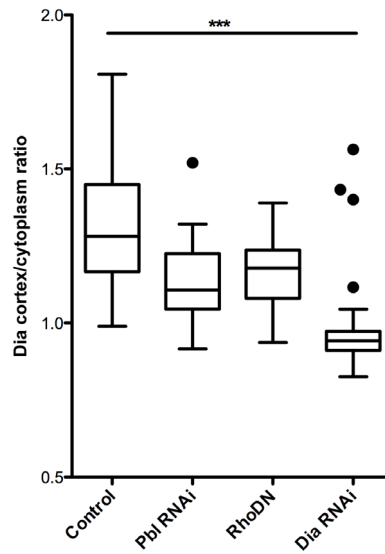


**Figure 4.2.2. 6. Cortical localization of Dia in metaphase cells is compromised in RhoDN expressing cells.** Graph of intermediate single plane ratio of mean gray values of Dia cortex/cytoplasm in control, Pbl, RhoDN Dia dsRNA expressing metaphase cells. (Mean±S.D. Control: 1.32±0.18. Pbl RNAi: 1.13±0.13. RhoDN: 1.16±0.11. Dia RNAi: 0.97±0.13 N=40).

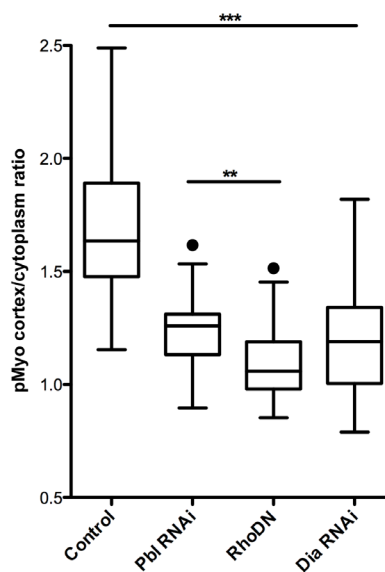


**Figure 4.2.2. 7. Cortical activation of myosin in metaphase cells is compromised in RhoDN expressing cells.** Graph of intermediate single plane ratio of mean gray values of pMyosin cortex/cytoplasm in control, Pbl, RhoDN and Dia dsRNA expressing metaphase cells. (Mean±S.D. Control: 1.69±0.29. Pbl RNAi: 1.25±0.15. RhoDN: 1.09±0.16 Dia RNAi: 1.19±0.22 N=40).

#### 4.2.3. Cdc42 polarizes Dia at the cell cortex in mitosis.

The binding of formins to the GTPase-binding domain (GBD) of GTP-loaded Rho-GTPases activates the proteins by releasing the interaction between the Diaphanous inhibitory domain (DID) and Diaphanous autoregulatory domain (DAD). However, activation is noticeably incomplete (Li and Higgs, 2003; Maiti et al., 2012) suggesting that other factors are required to fully activate formins. Given that RhoDN expressing mitotic cells were still able to build an actin cortex and the most striking defect in these cells was the lack of activated Myosin II, it was important to explore the possibility that additional factors downstream of Pbl might collaborate with Rho in the localization and activation of Diaphanous at the cell cortex in mitotic cells of the fly notum. Following this rationale we focused our attention on the role of Cdc42, effector of Ect2 (Tatsumoto et al., 1999). Importantly, Cdc42 is also implicated in actin filament formation in adherens junctions and within filopodia of the same cells (Georgiou and Baum, 2010), and is implicated in formin-mediated actin filament formation in yeast and microtubule kinetochore attachment in mitotic animal cells (Dong et al., 2003; Yasuda et al., 2004).

To better understand the role of this RhoGTPase in mitosis of epithelial cells of the notum we took advantage of the same approach used to study the role of Pbl. First, we generated movies of cells expressing dsRNA against Cdc42 together with lifeactGFP under the control of the *pnr*-GAL4 driver. Overall Cdc42 RNAi cells behaved identically to control cells in interphase and like the control were able to complete cell division. We did not observe any multinucleate cells. Importantly, however, although Cdc42 RNAi cells were able to build an actin cortex upon entry into mitosis, this appeared to be mechanically unstable as evidenced by the appearance of blebs. Such structures are almost never seen in the central plane of control cells during metaphase (Figure 4.2.3.1). Additionally, we also noticed blebs at the furrow, sign of furrow canal instability (King et al., 2010), indicating Cdc42 function is

indeed disrupted.

To better understand the role of Cdc42 in actomyosin remodeling during mitosis we next studied Dia and pMyo in mitotic cells depleted for Cdc42. Despite the presence of bleb like cortical defects, cells lacking Cdc42 activity as the result of RNAi were able to round up upon entry to mitosis (Figure 4.2.3.2). In interphase, Dia accumulates along junctional actin filaments (Figure 3.3.8), in Cdc42 RNAi tissues junctional Dia is lost although cells still presented filamentous actin at the level of adherens junctions (Figure 4.2.3.2). Moreover, the recruitment of Dia to the metaphase cortex was also severely compromised in Cdc42 RNAi cells (Figure 4.2.3.3). To quantify this effect we measured the ratio of cortical versus cytoplasmic levels of Dia in Cdc42 RNAi cells and control cells. These data revealed a severe decrease of Dia accumulation at the cell cortex since the average cortical/cytoplasm ratio was  $1.1 \pm 0.1$ , significantly lower ( $p < 0.01$ , Mann-Whitney statistical test) than that seen in RhoDN expressing cells (Figure 4.2.3.7). These data suggest that Cdc42 helps to direct Dia to the mitotic cell cortex. While every cell with reduced levels of Cdc42 activity we observed managed to complete cytokinesis, in fixed samples, they exhibit defects in the recruitment of Dia to cytokinetic furrow compared to control cells (Figure 4.2.3.4). However, it is possible that these reduced levels of Dia were sufficient to perform cytokinesis.

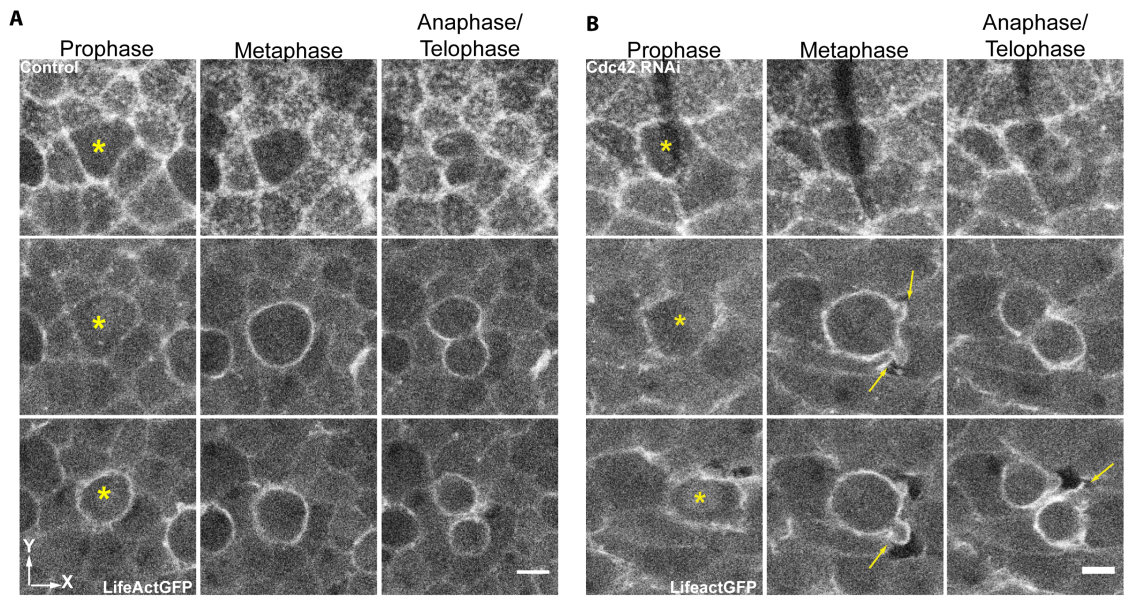


**Figure 4.2.3. 1. RNAi mediated silencing of Cdc42 compromise cell shape stability.** Images show actin filaments in apical, intermediate and basal sections of nota at different stages of mitosis, marked with a yellow asterisk. Cells are shown that express lifeact-GFP from the Pnr promoter in the absence (A) or presence (B) of a UAS-Cdc42 RNAi transgene where metaphase and anaphase/telophase cells exhibit bleb-like deformations (yellow arrows). Scale Bars: 5  $\mu$ M.



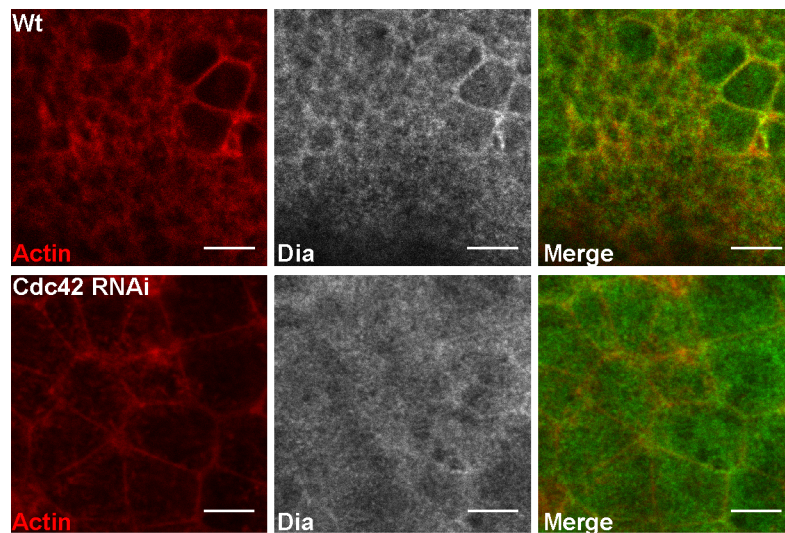


**Figure 4.2.3. 2. Cdc42 controls Dia junctional localization.** Apical top view of control interphase exhibit Dia at the junctional level. Cdc42 RNAi cells fail to localize Dia at the level of junctional F-actin. Scale bars: 5  $\mu$ m.

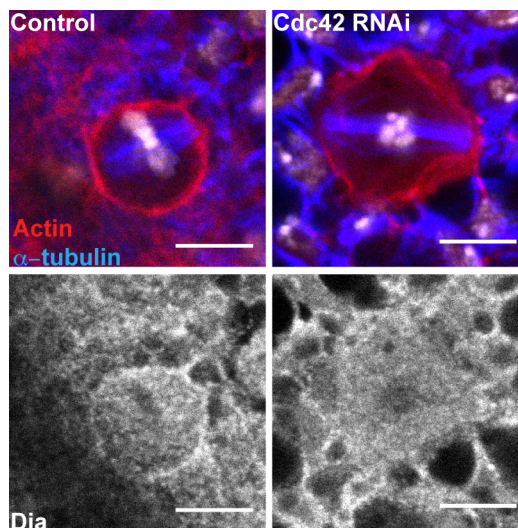


**Figure 4.2.3. 3. Cdc42 is required for cortical Dia localization in mitosis.** Intermediate top view of control cells shows a strong accumulation of cortical Diaphanous. Cortical localization of Dia is lost in tissues expressing Cdc42 dsRNA. Scale bars: 5  $\mu$ m.

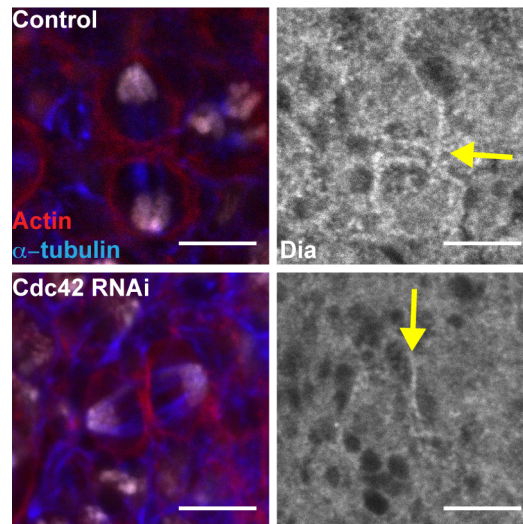


**Figure 4.2.3. 4. Dia recruitment to the furrow canal is impaired in Cdc42 dsRNA expressing tissues.** Top view of control cells in cytokinesis show a strong accumulation of Dia at the furrow canal (yellow arrow). Cdc42 dsRNA expressing cells show a subtle accumulation of Dia at the furrow canal (yellow arrow). Scale Bars: 5  $\mu$ m.

In *Drosophila*, in most cases Rok activation thought to be triggered downstream of active Rho1 (Dawes-Hoang et al., 2005; Hacker and Perrimon, 1998; Kolsch et al., 2007; Nikolaidou and Barrett, 2004). Given the significant role of Cdc42 in the polarization of Dia at the cell cortex in mitotic cells, I wanted to assess the role of Cdc42 in Myosin II activation during mitosis. To do so, we characterized the levels of phosphorylated Spaghetti squash at the cortex of cells in mitosis. It was clear from this analysis that pMyosin (as measured by phosphorylated Sqh) accumulated to high levels at the cortex of Cdc42 RNAi cells even though the average cortex/cytoplasm ratio ( $1.42 \pm 0.23$ ) was significantly lower ( $p < 0.001$ , Mann-Whitney statistical test) than that seen in the control ( $1.69 \pm 0.29$ ) (Figure 4.2.3.8). Thus, cells had significantly ( $p < 0.001$ , Cdc42 RNAi vs RhoDN;  $p < 0.01$ , Cdc42 RNAi vs Pbl RNAi OneWay Anova, Dunn's Multiple Comparison test) more phosphorylated sqh at the cell cortex when compared with cells expressing RhoDN construct ( $1.09 \pm 0.16$ ) or with Pbl RNAi cells ( $1.25 \pm 0.15$ ). In addition, levels of phosphorylated Sqh at the furrow canal appeared to be unperturbed at cytokinesis, even if their organization appeared defective. These results support the hypothesis that the primary function of Cdc42 in mitosis is the polarization of Dia, while Rho1 is required for the activation of Dia and Myosin II actin downstream of RhoGEF Pebble.



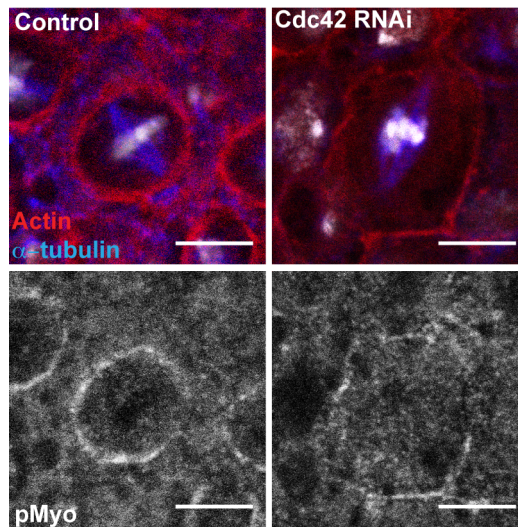


**Figure 4.2.3. 5. Cortical localization of pMyosin is slightly affected in metaphase cells expressing Cdc42 RNAi.** Intermediate top views of metaphase cells expressing Cdc42 RNAi show a mild accumulation of cortical pMyosin. Scale bars: 5  $\mu$ m.

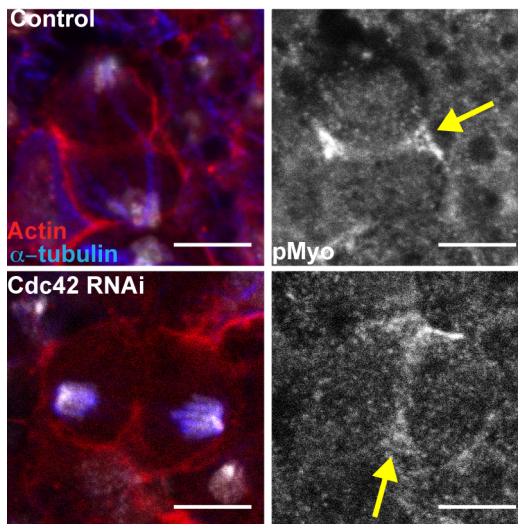


**Figure 4.2.3. 6. Phosphorylated myosin concentrates at the furrow canal of cells with compromised Cdc42 function.** Top view of control cells in cytokinesis concentrate pMyosin at the furrow canal (yellow arrow). Cdc42 RNAi expressing cells performing cytokinesis concentrate pMyosin at the furrow canal (yellow arrow). Scale Bars: 5  $\mu$ m.

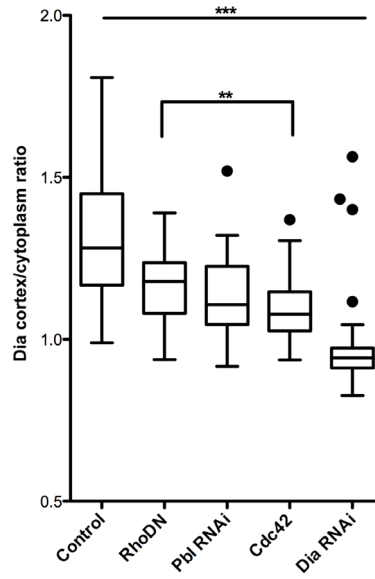


**Figure 4.2.3. 7. Cortical localization of Dia in metaphase cells is compromised in Cdc42 RNAi expressing cells.** Graph of intermediate single plane ratio of mean gray values of Dia cortex/cytoplasm in control, RhoDN Pbl, Cdc42 and Dia dsRNA expressing metaphase cells. (Mean±S.D. Control: 1.32±0.18. Pbl RNAi: 1.13±0.13. RhoDN: 1.16±0.11. Cdc42 RNAi: 1.1±0.1. Dia RNAi: 0.97±0.13 N=40).

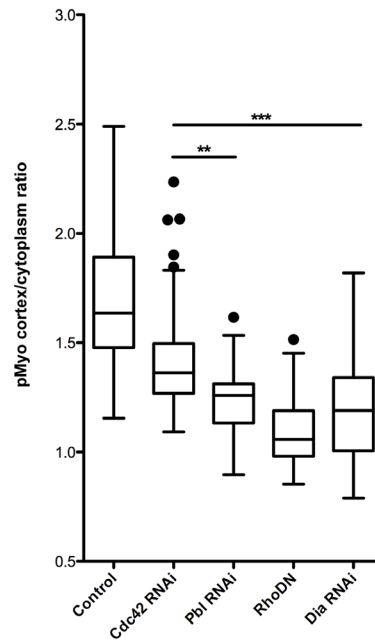


**Figure 4.2.3. 8. Cortical activation of myosin in metaphase cells is slightly compromised in Cdc42 RNAi expressing cells.** Graph of single plane ratio of mean gray values of pMyosin cortex/cytoplasm in control, Cdc42, Pbl, RhoDN and Dia dsRNA expressing metaphase cells. (Mean±S.D. Control: 1.69±0.29. Cdc42 RNAi: 1.42±0.23 Pbl RNAi: 1.25±0.15. RhoDN: 1.09±0.16 Dia RNAi: 1.19±0.22 N=40).

### 4.3. Conclusions

In this chapter, I analyzed the possible candidates regulating Dia activity in the assembly of an actin cortex in mitosis. In particular, we investigated the role of Pbl, a RhoGEF previously shown to be essential for cytokinesis (Grosshans et al., 2005; Prokopenko et al., 1999) and actomyosin-dependent changes in mitotic progression (Matthews et al., 2012) and its effectors Rho and Cdc42 GTPase also involved in the process of actomyosin ring contraction in cytokinesis, actomyosin-dependent changes in mitosis and positive regulators of Dia (Narumiya and Yasuda, 2006). To test the role of these actin regulators we expressed gene-specific dsRNA against Pbl, Dia, Cdc42 and RhoDN form in the *pnr* domain.

In mammalian cells Ect2 (homolog of *Drosophila* Pbl) is required for the assembly of a rigid actin cortex and acts upstream of Rho to activate myosin II to drive cell rounding in mitosis (Matthews et al., 2012). Similarly, in the developing notum Pbl plays the same role, suggesting that Pbl/Ect2 play a conserved role in actomyosin-dependent processes in mitosis and cytokinesis. In addition, I showed that Pbl is required for the cortical recruitment of Dia and activate Myosin II of cells in mitosis. These results point to a molecular pathway where Cdk1 activates Pbl in cells entering mitosis (Matthews et al., 2012) and downstream effectors, e.g. Rho, control the recruitment and activation of Dia and Myosin II. Surprisingly, I identified a concerted molecular mechanism in the recruitment and activation of Dia performed by Cdc42 and Rho, respectively. In yeast, regulation of formins is thought to be dependent of multiple events, like: recruitment of the formin which is dependent of Cdc42p, a specific phosphorylation of the GBD which is dependent of Pkc1p downstream of Rho1p, and the binding of a Rho protein to the GDB, dependent of Rho3p and/or Rho4p (Dong et al., 2003). This implies that the control of formins in animal cells in the process of cell division is highly conserved and dependent of multiple events.

## **5. PEBBLE, CELL SHAPE CHANGES AND THE CONTROL OF APKC/CDC42 LOCALIZATION.**

### **5.1. Introduction**

In this chapter I will explore the Pbl-Cdc42 pathway regulating Diaphanous activity in mitosis suggested by the work in previous Chapters. More specifically, I will look at the link between the RhoGEF Pebble, Cdc42 (Oceguera-Yanez et al., 2005) and the polarity proteins aPKC and Par6, which function together with Cdc42 in a range of processes (Hutterer et al., 2004; Motegi and Sugimoto, 2006).

The polarized aspect of many eukaryotic epithelial cells is clearly manifested in their shape. Work in many systems suggests that the actin cytoskeleton plays a role in the establishment of polarity itself and in the elaboration of their polarized form. This is true in eukaryotic cells from yeast to humans. Interestingly, Cdc42, aPKC and Par6 have a conserved function in the establishment of a polarity axis and in its execution in the development of a polarized form. In both cases, this is achieved through regulation of the actin cytoskeleton in ways that are poorly understood. To study this dialogue between cell shape changes and polarity in mitotic cells the aim of experiments reported in this Chapter was to: 1) examine the spatial distribution of polarity proteins aPKC, Par6 known partners of Cdc42 for epithelial cells of the fly notum during the transition from interphase to mitosis; 2) characterize the function of polarity proteins aPKC, Par6 and Cdc42 in the establishment of a round shape in mitosis and in the reorganization of an actin cortex; 3) determine how Pbl influences aPKC and Cdc42 activities; 4) determine how polarity proteins affect Dia distribution. Finally, we challenge our model by expressing constitutively active forms of Cdc42 and Dia and study the effects on remodeling of the actin cortex and cell shape in and out of mitosis.

## 5.2. Cdc42/Par6/aPKC complex repolarizes in mitosis.

In epithelial cells, Cdc42 has been implicated in the control of actin filament dynamics (Genova et al., 2000; Georgiou and Baum, 2010) as well in the establishment and maintenance of epithelial cell polarity (Joberty et al., 2000; Lin et al., 2000; Petronczki and Knoblich, 2001; Wodarz et al., 2000; Yamanaka et al., 2001). In each case, Cdc42 has been found to work together with its binding partners Par6 and aPKC. In our studies we identified Cdc42 as a regulator of Dia localization in mitotic cells (Chapter 4) which is required for the generation of a stable metaphase cortex. Given the intimate association of Cdc42 RhoGTPase and polarity proteins like Par6 and aPKC, we hypothesized that polarity proteins might function along with Cdc42 in the control of cortical remodeling in mitosis. To address this question we took advantage of antibodies raised against aPKC, V5 and Cdc42. We also used transgenic flies expressing Par6 tagged with GFP and Cdc42 tagged with V5 under the control of *pnr*-GAL4 expression. These tools enabled us to analyze the localization of aPKC and Cdc42 in epithelial cells.

In interphase epithelial cells of the fly notum we detected the presence of aPKC and Cdc42 at the apical region (Figure 5.2.1), as previously described (Hutterer et al., 2004). Similarly, using a transgenic fly expressing Par6 tagged with GFP under the control of *pnr*-GAL4, we observed Par6 protein accumulating at the apical side of interphase epithelial cells (Figure 5.2.5 and 5.2.6). Upon entry into mitosis, a large pool of aPKC, Par6 and Cdc42 was found to remain at the apical side. Interestingly, these proteins were also found accumulating more basally, along regions of the cortex of mitotic cells level with the mitotic spindle (Figure 5.2.2-5.2.6). In prophase, this was evident as a subtle accumulation of Cdc42 and Par6 (Figure 5.2.2, 5.2.3, 5.2.5 and 5.2.6) within intermediate planes, where aPKC showed a stronger accumulation (Figure 5.2.4). By metaphase, however, Cdc42, aPKC and Par6 had accumulated to relatively high levels within the intermediate region of cells (Figure 5.2.2-5.2.6). At telophase Cdc42 could be seen localized at

the furrow canal (Figure 5.2.2, 5.2.3), while aPKC and Par6 appeared to resume their apical localization (Figure 5.2.4-5.2.6). This change in the profile of polarity proteins like aPKC, Par6 and Cdc42 Rho GTPase upon mitotic entry suggests that the change in cell shape that accompanies entry into mitosis is accompanied by a change in apical-basal polarity (see Chapter 6), and raises the possibility that these two events are coupled. This Chapter explores the possibility that changes in the profile of the Cdc42/aPKC/Par6 complex is coupled to changes in shape and actin cortex assembly.

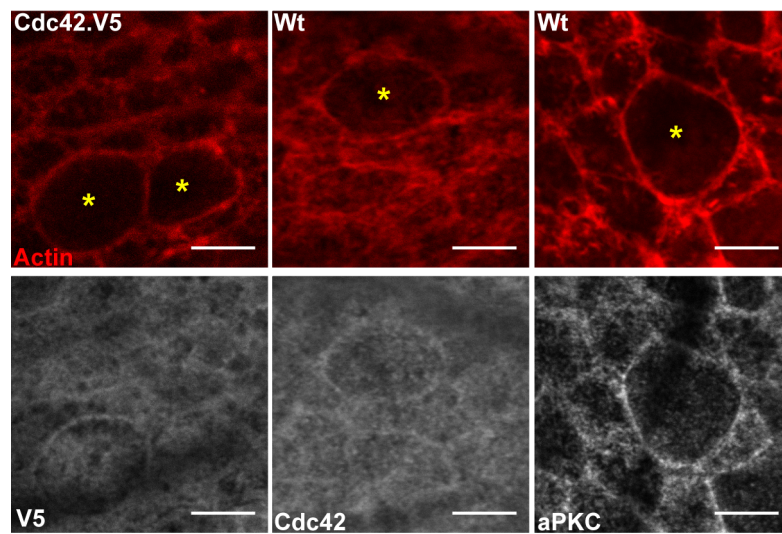


**Figure 5.2. 1. Cdc42 and aPKC localize at the apical side of epithelial cells in interphase and mitosis.** Yellow asterisk marks mitotic cell. Scale bars: 5  $\mu$ m.

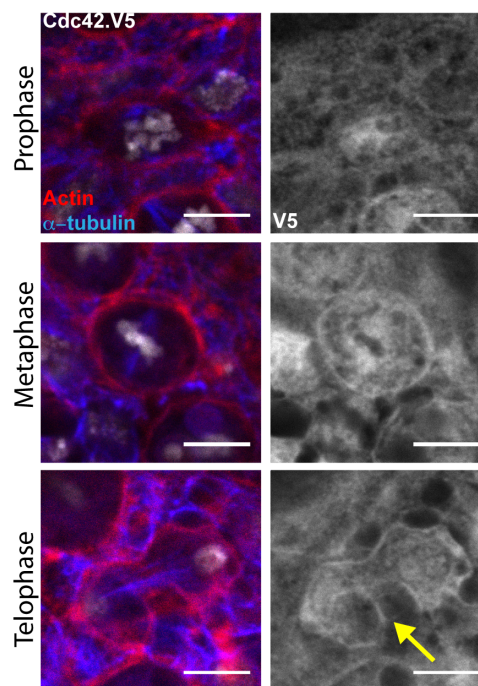


**Figure 5.2. 2. Cdc42 extend the apical localization to intermediate domains in mitosis.** Intermediate top view of cells expressing Cdc42 tagged with V5 in different stages of mitosis. Yellow arrow indicates furrow canal. Scale bars: 5  $\mu$ m.



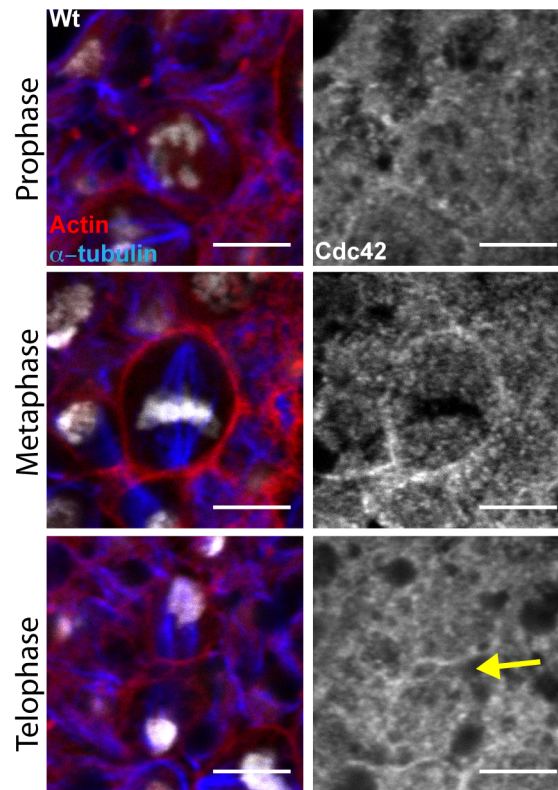


**Figure 5.2. 3. Cdc42 extend the apical localization to intermediate domains in mitosis.** Intermediate top view of wild type cells in different stages of mitosis. Yellow arrow indicates furrow canal. Scale bars: 5  $\mu$ m.

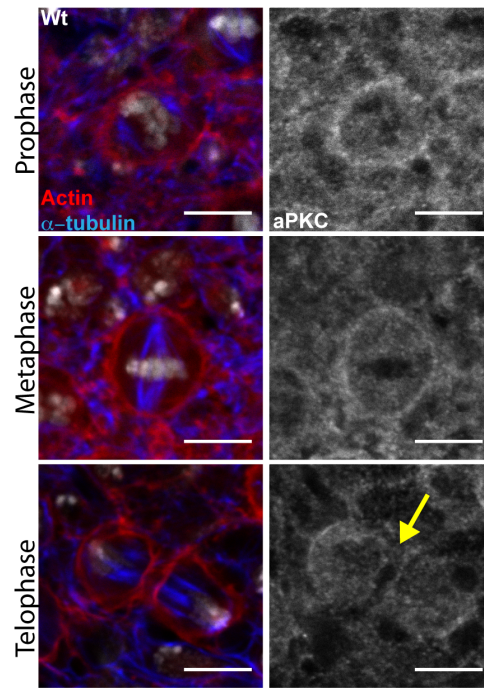


**Figure 5.2. 4. aPKC extend the apical localization to intermediate domains in mitosis.** Intermediate top view of wild type cells in different stages of mitosis. Yellow arrow indicates furrow canal. Scale bars: 5  $\mu$ m.

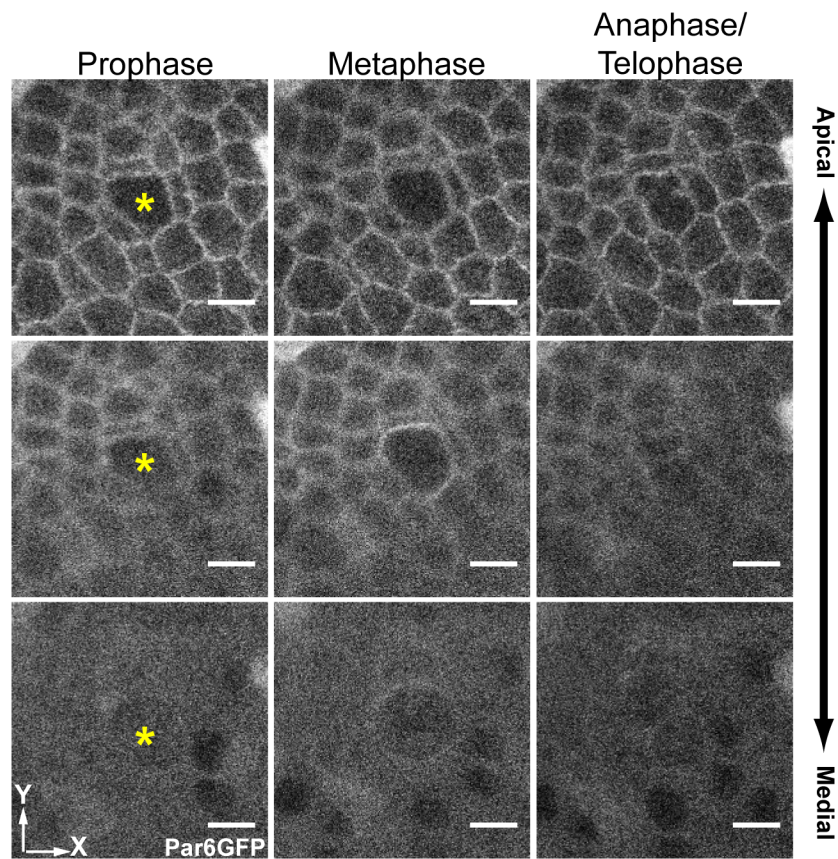


**Figure 5.2. 5. Par6 extend the apical localization to intermediate domains in mitosis.** Images show Par6 from apical to intermediate sections of notum at different stages of mitosis, marked with a yellow asterisk. Cells are shown that express Par6GFP from the Pnr promoter. Scale Bars: 5  $\mu$ M.

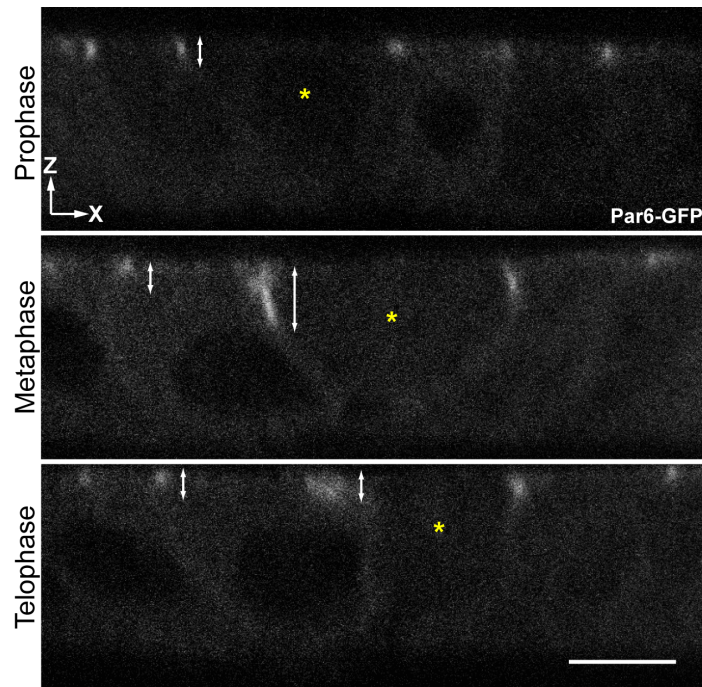


**Figure 5.2. 6. Par6 extend the apical localization to intermediate domains in mitosis.** Side view of cells expressing Par6 tagged with GFP in different stages of mitosis. Yellow asterisk indicates mitotic cell. White double sided arrow indicate Par6 domain. Scale bars: 5  $\mu\text{m}$ .

### 5.3. aPKC/Par6/Cdc42 control mitotic cell shape

To understand whether there is a role for polarity proteins and Cdc42 Rho GTPase in the remodelling of the actin cytoskeleton during mitosis in epithelial cells of the fly notum, we challenged the system by inducing the loss of Par6, aPKC and Cdc42 using gene-specific RNAi, loss of function mutant alleles generated using the MARCM technique (Wu and Luo, 2006) and thermo sensitive mutant alleles.

In chapter 4 I analyzed the role of Cdc42 in *nota* expressing a gene-specific RNAi hairpin against Cdc42. From these results I concluded that Cdc42 helps to localize Dia in mitosis to generate its characteristically stable actin cortex (Figure 4.2.3.1, 4.2.3.3 and 4.2.3.7). Having taken advantage of flies expressing dsRNAi against Cdc42 under the control of *pnr*-GAL4 expression to reveal a role for Cdc42 in the control of mitotic cell shape stability (Figure 5.3.1) it was important to confirm these results using a classical genetic loss of function approach. To do so, I used the MARCM system to generate for GFP-marked loss of function clones for *cdc42*, using a well-studied allele (Fehon et al., 1997). Movies revealed that *cdc42*<sup>3</sup> (a lethal missense mutant allele) mutant cells expressing  $\alpha$ -tubulin-GFP as a marker bleb at metaphase, whereas control cells (wild type cells solely marked for  $\alpha$ -tubulin-GFP) retain a smooth and stable rounded form throughout metaphase (Figure 5.3.2). These results phenocopy the cell shape instability in tissues expressing Cdc42 dsRNA (Figure 5.3.1). When the number of metaphase cells that bleb or show significant cell shape deformations was quantified (Figure 5.3.5), it was clear that there was a significant 40% increase in the incidence of cell shape deformation in Cdc42 RNAi expressing cells relative to a control.

Moesin is the sole member of the ERM (Ezrin, Radixin, Moesin) family of cytoskeletal regulators that link the actin cytoskeleton to the plasma membrane (Fehon et al., 2010). Our group together with others (Carreno et al., 2008; Kunda et al., 2008a) has demonstrated an important role for Moesin in the regulation of cell shape in mitosis. Considering the cell shape phenotype of mitotic cells expressing dsRNAi

against Cdc42 this suggested the possibility that Cdc42 might mediate its effects through the regulation of Moesin activity in mitotic epithelial cells. To test this hypothesis I stained the nota of control and disrupt activity of Cdc42 flies for the active phosphorylated form of Moesin (pT559-Moesin). Disrupting Cdc42 activity had no effect on the accumulation of active Moesin at the cell cortex when compared to the control (Figure 5.3.7), clearly suggesting that Moesin function acts independently of Cdc42 activity. Thus, Cdc42 plays an essential role in cell shape stability, presumably affecting cortical actin organization via Dia repolarization, independently of Moesin function.

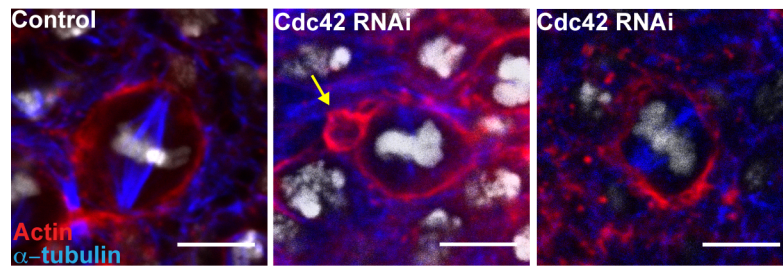


**Figure 5.3. 1. Cdc42 is required for cell shape stability in mitosis.** Intermediate top view of control cells in metaphase with a round smooth shape and metaphase cells expressing Cdc42 RNAi with shape defects and with heterogeneous actin cortex. Scale bars: 5  $\mu$ m.

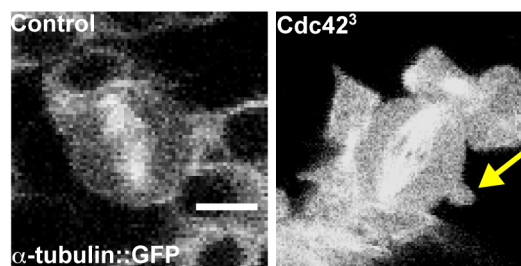


**Figure 5.3. 2. Cdc42 is required for cell shape stability in mitosis.** Intermediate top view of control cells expressing  $\alpha$ -tubulin-GFP in metaphase with a round smooth shape and metaphase cells expressing Cdc42 RNAi and  $\alpha$ -tubulin-GFP with shape defects. Yellow arrow indicates cell bleb. Scale bars: 5  $\mu$ m.



In order to investigate whether polarity proteins act in concert with Cdc42 in the process of actin remodeling in mitosis, we followed the same approach previously described for Cdc42 function analysis in mitotic epithelial cells, focusing on the function of aPKC and Par6. To address this we took advantage of gene-specific RNAi hairpin against aPKC and Par6, and an aPKC thermo-sensitive allele (Guilgur et al., 2012), which enabled us to modulate *in vivo* aPKC activity simply by changing the temperature at which flies were reared. The toxicity of the gene-specific hairpin expression against aPKC was alleviated by expression of Gal80ts, and flies were reared at 18°C and changed to 29°C 6-7 hours before notum dissection. As observed for mitotic cells with disrupted Cdc42 activity, cells hemizygous for aPKC (aPKCts/DF(2R)l4) or expressing dsRNA targeting aPKC under the control of the *pnr*-GAL4 driver exhibited cell shape defects. These included deformation of the metaphase cell cortex and the heterogeneous accumulation of cortical actin (Figure 5.3.3). We quantified the number of cells with the aforementioned cell shape defects in the hemizygous (aPKCts/DF(2R)l4), heterozygous (aPKCts/+) and wild type fly notum. Again, this revealed a 40% increase in the number of metaphase cells with shape defects in the notum of hemizygous aPKC flies relative to the heterozygous control (Figure 5.3.6). In addition, as observed for Cdc42 RNAi cells, the loss of aPKC activity did not impair either the phosphorylation or the localization of Moesin in mitotic cells (Figure 5.3.8).

To study the role of Par6 in actin organization and cell shape in mitosis we used transgenic flies expressing gene-specific RNA hairpin against Par6. Again, in an attempt to alleviate the toxicity of the Par6 dsRNA expression, we combined the *pnr*-GAL4 with the Gal80ts. However, in this case we were unable to identify conditions in which there was a sufficient reduction in activity to see a phenotype, but not so much as to cause lethality. To overcome this experimental obstacle we returned to the method of hairpin expression solely under the control of *pnr*-GAL4 expression modulating the strength of expression by rearing flies at 18°C



followed by 6-7 hours at 29°C prior to dissection. Under these conditions we manage to identify a few cells in the fly notum in mitosis. In each case, cell shape and the actin cortex were severely compromised (Figure 5.3.4), in a similar manner to that described for aPKC and Cdc42 (Figure 5.3.1 and Figure 5.3.3). These results suggest that aPKC and Par6 act in close association with Cdc42 in the regulation of cortical actin and cell shape dynamics in mitotic cells of the fly notum.

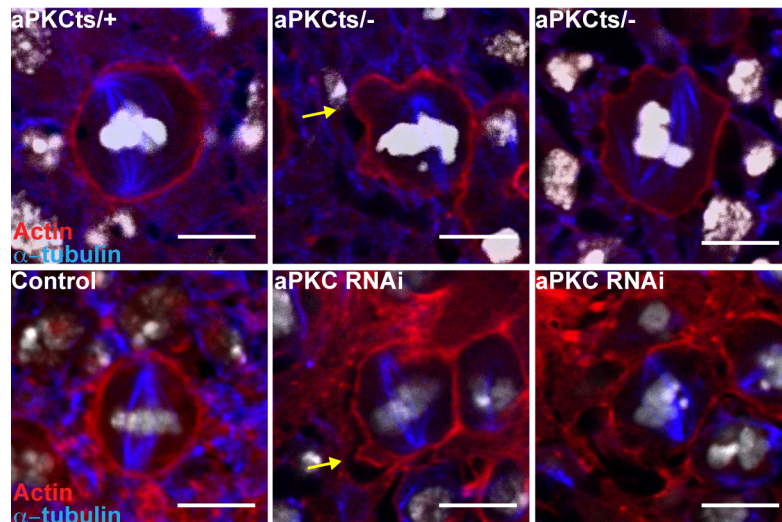


**Figure 5.3. 3. aPKC is required for cell shape stability in mitosis.** Intermediate top view of control cells in metaphase with a round smooth shape and metaphase cells of hemizygous aPKCs or expressing aPKC RNAi with shape defects and with heterogeneous actin cortex. Yellow arrow indicates cell bleb. Scale bars: 5  $\mu$ m.

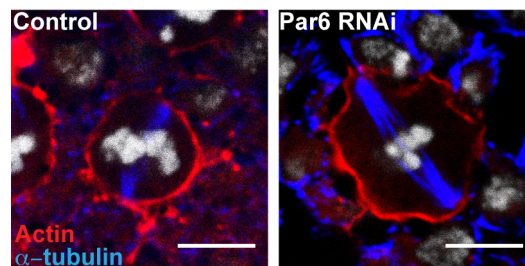


**Figure 5.3. 4. Par6 is required for cell shape stability in mitosis.** Intermediate top view of control cells in metaphase with a round smooth shape and metaphase cells expressing Par6 RNAi with shape defects. Scale bars: 5  $\mu$ m.

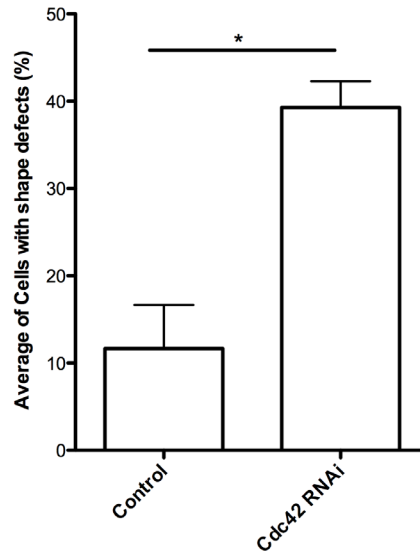


Figure 5.3. 5. Percentage of cells with cell shape defects in metaphase for control and Cdc42 RNAi expressing cells. P-value < 0.5. N= 25.

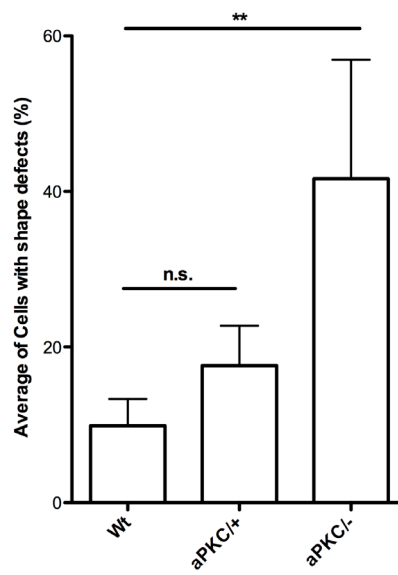
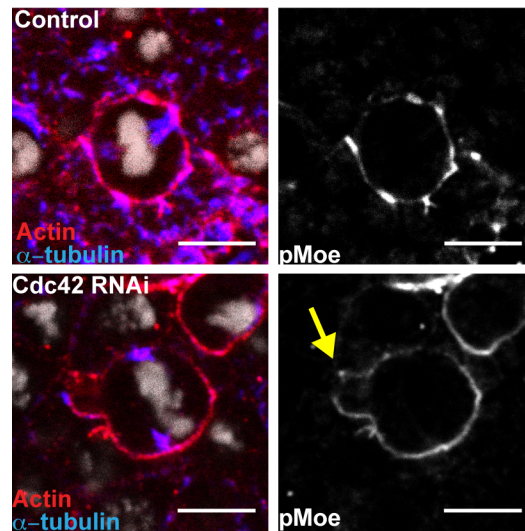
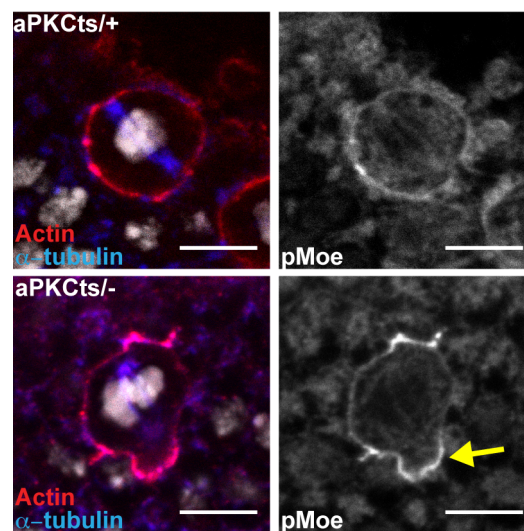


Figure 5.3. 6. Percentage of cells with cell shape defects in metaphase for wild type and heterozygous and hemizygous aPKCts nota. P-value < 0.01. N= 25.



**Figure 5.3. 7. Moesin activation and localization is not dependent of Cdc42 activity.** Intermediate top view of control cells in metaphase with a round smooth shape and activated moesin decorating the cell cortex and metaphase cells expressing Cdc42 RNAi with shape defects (yellow arrow) and activated moesin decorating the cell cortex. Scale bars: 5  $\mu$ m.



**Figure 5.3. 8. Moesin activation and localization is not dependent of aPKC activity.** Intermediate top view of heterozygous aPKCs cells in metaphase with a round smooth shape and activated moesin decorating the cell cortex and metaphase hemizygous aPKCs cells with shape defects (yellow arrow) and activated moesin decorating the cell cortex. Scale bars: 5  $\mu$ m.

Yasuda and colleagues (Yasuda et al., 2004) have shown that Cdc42 and its effector mDia3 function together in mitosis to regulate the attachment of microtubules to kinetochores in human cells. While we did not observe obvious spindle defects in cells with compromised Cdc42, aPKC or Par6, through our characterization of the effects of cortical actin organization in cells depleted for Cdc42 or aPKC we came across unexpected defects in chromosome missegregation (Figure 5.3.9). In this case, cells exhibit lagging chromosomes. This result suggests that additionally to the requirement of Cdc42 and aPKC in cortical actin remodeling, these proteins are likely to have a second function in flies, as suggested previously by Yasuda and colleagues, in chromosome segregation. In this case, however, the defect appears to be in the resolution of sister chromatids or in chromosome condensation late in anaphase. More work is required to determine if this is related to Diaphanous, actin and the process described by Yasuda and colleagues.

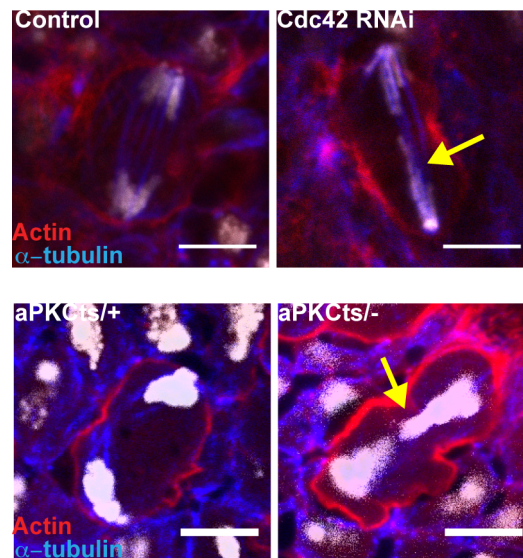


**Figure 5.3. 9. Cdc42 and aPKC control chromosome segregation.** Intermediate top views of cells in anaphase for control Cdc42 RNAi heterozygous and hemizygous aPKCs. Cells with compromised function for Cdc42 and aPKC show lagging chromosomes in anaphase/telophase (yellow arrow). Scale bars: 5  $\mu$ m.

#### **5.4. Pebble and Cdc42 controls aPKC localization in mitosis.**

Several groups (Oceguera-Yanez et al., 2005; Tatsumoto et al., 2003; Yasuda et al., 2006) have studied the role of Ect2, the mammalian homolog of Pbl, in the activation and function of Cdc42 in mitosis. Interestingly, in the study performed by Oceguera-Yanez and colleagues (2005) it was demonstrated that Cdc42 activation reaches a peak at metaphase while Rho increases in anaphase and peaks in telophase in a Ect2 dependent fashion. This study implies Pbl/Ect2 differentially regulating the Rho GTPases in different stages of the cell cycle. While I observed something similar, in this thesis I present data to show that Pbl is required for the remodeling of the actomyosin cortex upon mitotic entry, affecting F-actin, Myosin activation and Dia localization, while Cdc42 appears to preferentially speak to Dia and Rho to Myosin. These data suggest the hypothesis that Pbl regulates Cdc42 binding partners Par6 and aPKC in metaphase to control actin remodeling via Dia. To test this idea I used an antibody against aPKC as a marker to follow the polarization of aPKC, Cdc42 and Par6 (Hutterer et al., 2004) and the behavior of these proteins in interphase and mitotic cells in the presence or absence of Pebble.

In Pbl RNAi tissues, aPKC was still observed at the apical side of cells (Figure 5.4.1), although the domain appeared to be less demarcated than that seen in control cells. At most intermediate levels though, aPKC was lost from the cortex of Pebble RNAi cells (Figure 5.4.2). By quantifying the level of cortical aPKC at the level of the spindle we were able to see a significant decrease in its accumulation in Pbl RNAi tissues compared to the control (on average the cortex/cytoplasm ratio of aPKC in control cells was  $1.44 \pm 0.25$  and  $1.16 \pm 0.13$  in Pbl RNAi tissues (Figure 5.4.5)). Moreover, punctuate accumulations of aPKC were observed at the intermediate level of metaphase Pebble RNAi cells in regions with no actin cortex (Figure 5.4.2), suggesting that is not a non-specific result due



to the loss of actin cortex.

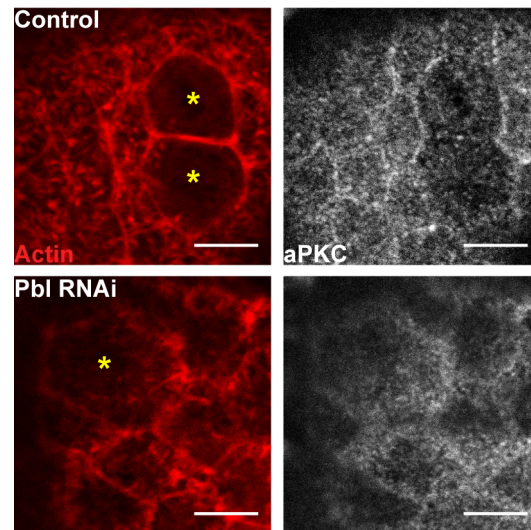


**Figure 5.4. 1. Apical localization of aPKC is dependent of Pbl activity.** Apical top view of cells in interphase and mitosis (yellow asterisk marks mitotic cells). aPKC localizes at the apical region of control cells. Apical localization of aPKC is compromised in Pbl RNAi expressing cells. Scale bars: 5  $\mu$ m.

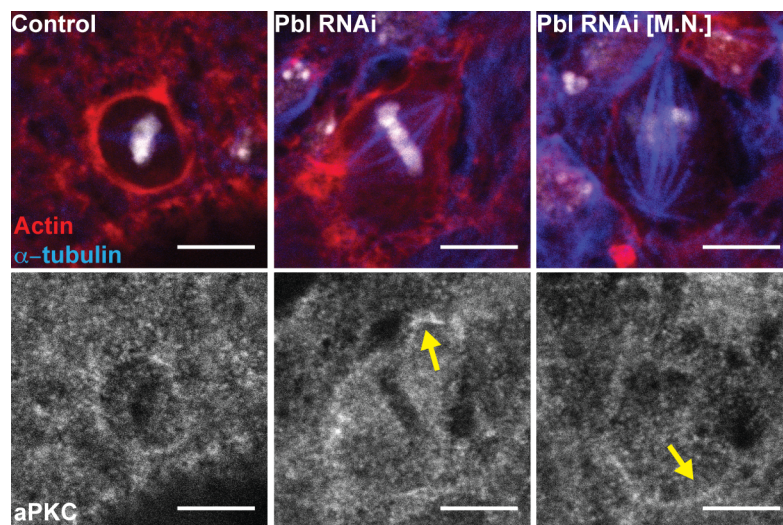


**Figure 5.4. 2. Pbl controls intermediate localization of aPKC in mitosis.** Intermediate top view of metaphase cells. aPKC localizes at the cortex of control cells. Intermediate localization of aPKC is compromised in Pbl RNAi expressing cells. Yellow arrow marks regions of punctuated accumulation of intermediate aPKC in regions severely deprived of filamentous actin. [M.N.] multinucleated cells. Scale bars: 5  $\mu$ m.



In *Drosophila* Cdc42 plays an essential role in the establishment of apical basal polarity. Although Cdc42 is thought not to be required for the kinase activity of aPKC, Cdc42 binding to Par6/aPKC complex is essential for the establishment of epithelial polarity (Hutterer et al., 2004). To better understand if Cdc42 is involved in the establishment of apical-basal polarity of mitotic cells in the notum we again focused on the behaviour of aPKC in interphase and mitotic cells in tissues with compromised Cdc42 activity. In tissues expressing Cdc42 RNAi, there was a very small amount of aPKC still present at the apical side of cells in interphase and mitotic cells (Figure 5.4.3). In addition, for cells in mitosis the aPKC was lost from intermediate planes in Cdc42 RNAi expressing tissues (Figure 5.4.4). We quantified the loss of aPKC at intermediate level of metaphase cells. This revealed that there is a significant decrease in intermediate aPKC ( $1.21 \pm 0.30$ ) in tissues expressing Cdc42 RNAi when compared to control cells ( $1.44 \pm 0.25$ ) (Figure 5.4.5).

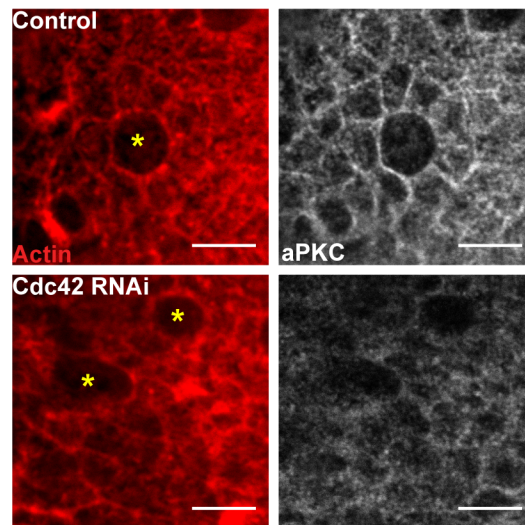


**Figure 5.4. 3. Apical localization of aPKC is dependent of Cdc42 activity.** Apical top view of cells in interphase and mitosis (yellow asterisk marks mitotic cells). aPKC localizes at the apical region of control cells. Apical localization of aPKC is compromised in Cdc42 RNAi expressing cells. Scale bars: 5  $\mu$ m.

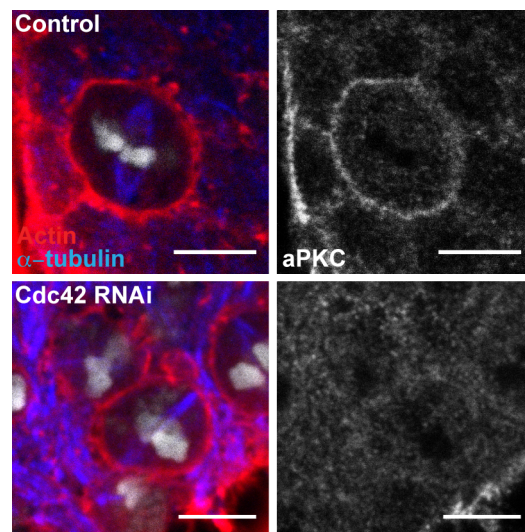


**Figure 5.4. 4. Cdc42 controls intermediate localization of aPKC in mitosis.** Intermediate top view of metaphase cells. aPKC localizes at the cortex of control cells. Intermediate localization of aPKC is compromised in Cdc42 RNAi expressing cells. Scale bars: 5  $\mu$ m.

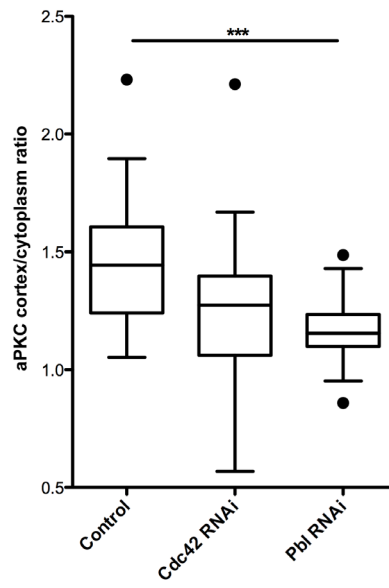


**Figure 5.4. 5. Cortical localization of aPKC in metaphase cells is compromised in Cdc42 and Pbl RNAi expressing cells.** Graph of intermediate single plane ratio of mean gray values of Dia cortex/cytoplasm in control, Pbl, Cdc42 dsRNA expressing metaphase cells. (Mean±S.D. Control: 1.44±0.25. Pbl RNAi: 1.16±0.13. Cdc42 RNAi: 1.21±0.30. N=30).

## 5.5. aPKC/Cdc42 controls Dia localization in mitosis

In mitotic cells expressing Cdc42 or Pbl dsRNA, aPKC failed to become redistributed at the intermediate cortex in the spindle plane. Additionally, tissues with compromised aPKC function showed cell shape defects in mitotic cells similar to Cdc42 RNAi expressing tissues. Given the intimate relationship between Cdc42 and polarity proteins and the establishment of apical-basal polarity it seemed possible that these polarity proteins could function together with Cdc42 (Figure 5.5.1 and Figure 5.5.3) in regulating the localization of Dia at the cortex of mitotic epithelial cells. To test this idea we stained the notum of aPKCs hemizygous mutants for Dia protein. As seen in cells depleted for Pbl or Cdc42, Dia was less abundant at the metaphase cortex of these cells (Figure 5.5.2). We quantified this decrease, and the average ratio of cortex/cytoplasm of Dia in aPKCs hemizygous mutants was found to be comparable to that seen in Pbl and Cdc42 RNAi cells (an average ratio of  $1.11 \pm 0.15$ ,  $1.13 \pm 0.13$  and  $1.10 \pm 0.1$  for aPKC, Pbl, and Cdc42 respectively) Thus, in the fly notum, the accumulation of Dia at intermediate planes of the metaphase cortex is likely regulated, downstream of Pebble, via Cdc42 and its association with polarity proteins.

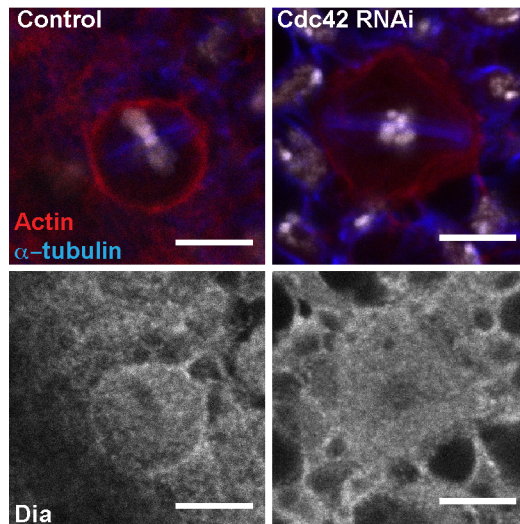


**Figure 5.5. 1. Cdc42 is required for cortical Dia localization in mitosis.** Intermediate top view of control cells shows a strong accumulation of cortical Diaphanous. Cortical localization of Dia is lost in tissues expressing Cdc42 dsRNA. Scale bars: 5  $\mu$ m.

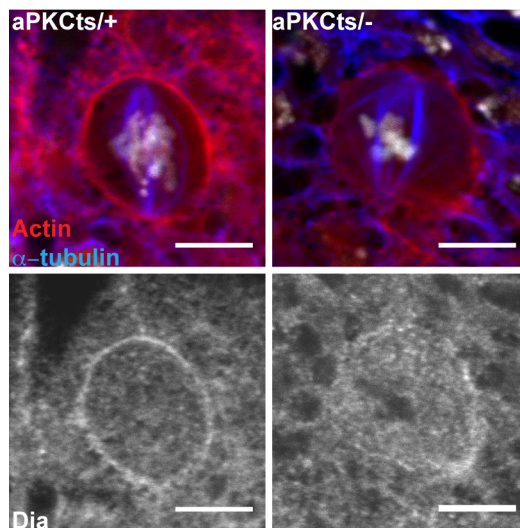


**Figure 5.5. 2. aPKC is required for cortical Dia localization in mitosis.** Intermediate top view of metaphase heterozygous aPKCs cells shows a strong accumulation of cortical Diaphanous. Cortical localization of Dia is lost in hemizygous aPKCs metaphase cells. Scale bars: 5  $\mu$ m.

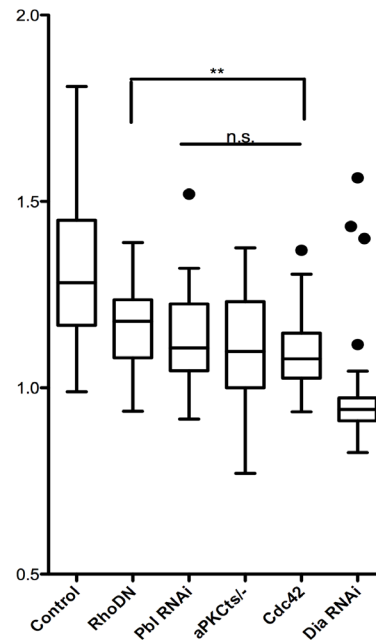


**Figure 5.5. 3. Cortical localization of Dia in metaphase cells is compromised in hemizygous aPKCts.** Graph of intermediate single plane ratio of mean gray values of Dia cortex/cytoplasm in control, RhoDN Pbl, Cdc42, hemizygous aPKCts and Dia dsRNA expressing metaphase cells. (Mean±S.D. Control: 1.32±0.18. Pbl RNAi: 1.13±0.13. RhoDN: 1.16±0.11. hemizygous aPKCts: 1.11±0.15 Cdc42 RNAi: 1.1±0.1. Dia RNAi: 0.97±0.13 N=40).

## **5.6. S.O.P. cells depend on Dia and Cdc42 activity for the remodeling of cortical actin in mitosis.**

To further understand the contribution of Dia for the remodelling of cortical actin in mitosis and the putative regulation of this actin nucleator through the activity of Cdc42 we took advantage of the *Neuralized* promoter, *pnr*-GAL4 and *Neuralized*-Gal4 drivers in combination with UAS-GFP<sub>GMA</sub> to image actin filaments in isolated sensory organ precursor cells (SOPs) in the notum. Using this approach we aimed to study the requirements of Dia and Cdc42 in the remodelling of cortical actin in specialized cells and challenge the system using gain and loss of function experiments. Importantly, these cells undergo an asymmetric division that involves the orientation of the mitotic spindle in response to an extrinsic cue, enabling us to test whether this affects the structural requirements of the metaphase cortex.

To study the requirement of Dia in the remodelling of the actin cortex in SOP cells we followed the actin behaviour of these cells taking advantage of flies expressing UAS-GFP<sub>GMA</sub> under the control of *Neuralized* promoter compared to control *nota* and *nota* expressing dsRNA against Dia and Arp3 using the *pnr*-GAL4 driver. Surprisingly, mitotic Dia RNAi SOP cells underwent mitotic rounding on schedule and were virtually indistinguishable from control cells in form even though these cells failed to build an actin cortex. As described above for epithelial cells of the notum, however, Dia was essential for the formation of an actin cortex in SOPs (Figure 5.6.1). By contrast, disrupting Arp3 activity had no effect on the shape of interphase cells and cells in mitosis presented an actin cortex similar to control cells. To quantify the actin phenotype in Dia RNAi SOP cells, we calculated the cortical/cytoplasm ratio for filamentous actin as they entered mitosis and exited mitosis. Like epithelial cells, these SOP cells depleted of Dia failed to build an actin cortex upon mitotic entry (Figure 5.6.2). These results clearly indicate that Dia is the main mitotic actin regulator in mitosis independently of cell type

in *Drosophila*. Interestingly, however, when I expressed dsRNA against Dia using the *Neuralized*-GAL4 driver, SOP cells exhibited a phenotype similar to that seen in epithelial cells with disrupted Cdc42 activity. Since *Neuralised* expression comes on later than *Pannier* in notum development (Calleja et al., 2000; Romain et al., 1993) the RNAi-induced depletion of a structural protein like Dia using gene-specific hairpin RNA is likely to be less dramatic than that seen under the *Pannier*-Gal4 driver. These data imply that a partial loss of cortical actin can lead to cortical instabilities like those seen in Cdc42 RNAi epithelial cells. When Cdc42 targeted in SOPs through dsRNA expression under the *pnr*-GAL4 driver, a similar phenotype was seen (Figure 5.6.3). These results suggest that Cdc42 supports a minimal threshold of Dia activity required for the correct remodelling of cortical actin culminating in a stiff and stable mitotic cortex, while a more complete depletion of Dia leads to the loss of the entire cortex.



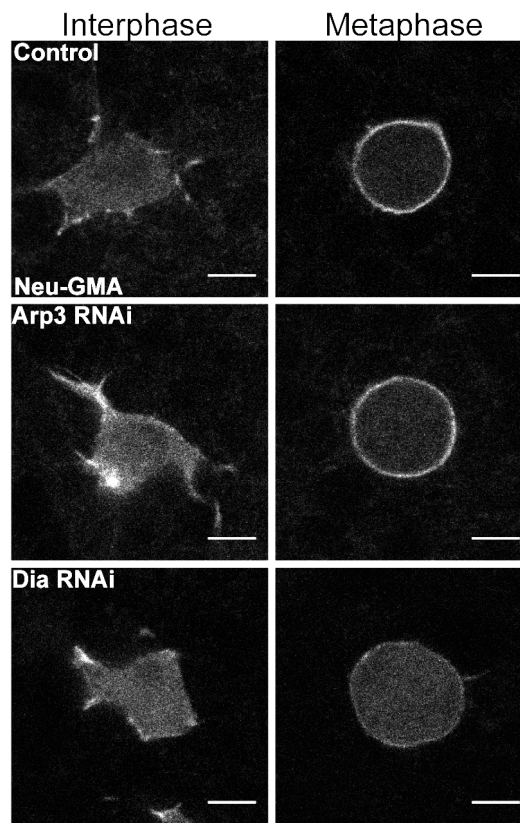


**Figure 5.6. 1. Assembly of a mitotic actin cortex in SOP cells is dependent of Dia activity.** Intermediate top view of interphase and metaphase SOP cells expressing GMAGFP (control cells) and SOP cells expressing UAS-GMA, Arp3 and Dia RNAi. Scale bars: 5  $\mu$ m.

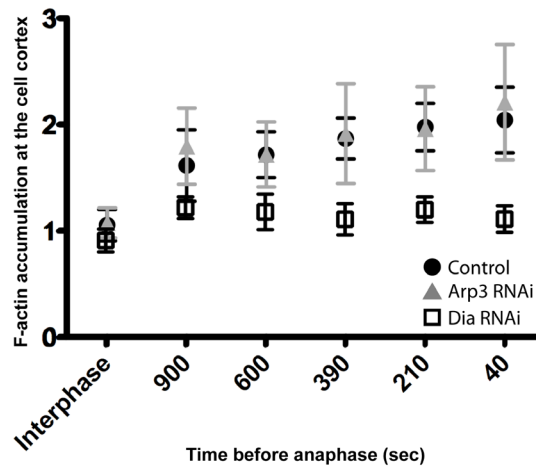


**Figure 5.6. 2. Assembly of an actin cortex is lost in the absence of Dia in SOP cells entering mitosis.** Y values indicate the ratio of mean gray values of filamentous actin intensity at the cortex/cytoplasm of epithelial cells expressing Neu-GMAGFP at interphase and at different times (X: time in seconds) in mitosis previously to anaphase. (Values plotted: mean±S.D.). N=25

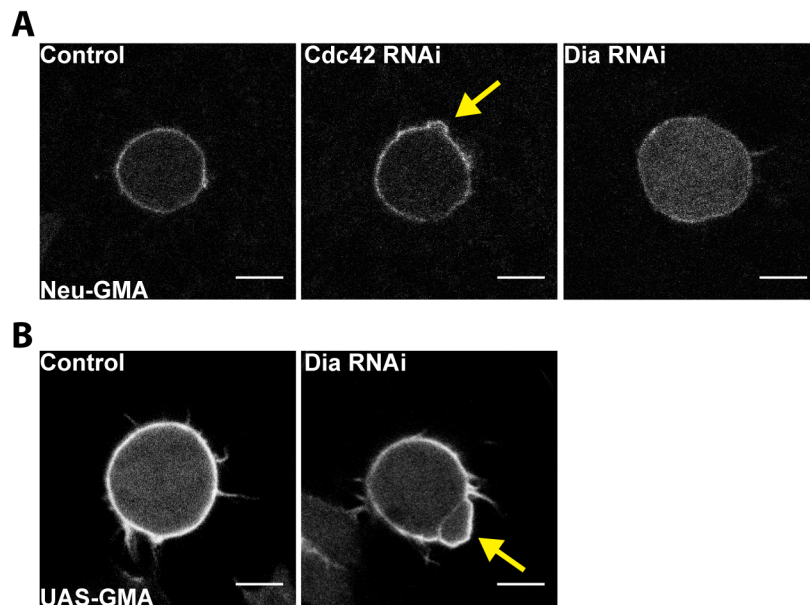


**Figure 5.6. 3. Partial loss of Dia phenocopies Cdc42 mitotic shape defects in SOP mitotic cells.** Intermediate top view of SOP metaphase cells. (A) control cell expressing GMAGFP under the control of *Neu* promoter and Cdc42 and Dia RNAi expressing cells under the control of *pnr*-GAL4. (B) control cell expressing GMA under the control of *Neu*-GAL4 and Dia RNAi expressing cell also under the control of *Neu*-GAL4. Yellow arrow marks cell shape defects. Scale bars: 5  $\mu$ m.

## 5.7. Comparing Cdc42 and Dia gain of function.

The results described above suggest that Dia and Cdc42 play a fundamental role in the formation of the mitotic actin cortex. If the two proteins act together in this process, the expression of constitutively active forms of Cdc42 and Dia should promote the formation of excessive cortical actin. To test this hypothesis, we overexpressed a constitutively active form of Cdc42, Cdc42.V12 and a constitutively active form of Dia, Dia.CA under the *Neu*-GAL4 or *pnr*-GAL4 drivers. Given the high toxicity of these active constructs we combined them with the Gal80ts, reared flies at 18°C before transferring them to 29°C for 5-6 hours before dissection.

The expression of Cdc42.V12 in mitotic epithelial cells was sufficient to induce thickening of the actin cortex (Figure 5.7.1). Nonetheless, these cells appeared to have a similar shape and area to control cells. Similarly, epithelial cells in tissues expressing Dia.CA had thicker actin cortices compared to controls. However, in this case, cells often had an altered shape and were considerably smaller. To determine if Dia was considerably enriched at the cortex of cells expressing constitutive active forms of Cdc42 and Dia, we stained the nota of control and Cdc42.V12 and Dia.CA expressing tissues for Dia and assessed the accumulation of the protein at the cell cortex by measuring the cortex/cytoplasm ratio of the Dia signal. Interestingly, we failed to detect any differences in these ratios compared to the control (Figure 5.7.2). It is possible that thus, while Cdc42 is required to recruit Dia to the intermediate cell cortex, cortical levels of Dia may not respond to quantitative changes in Cdc42 levels. It is possible that Rho1 contributes to this process.

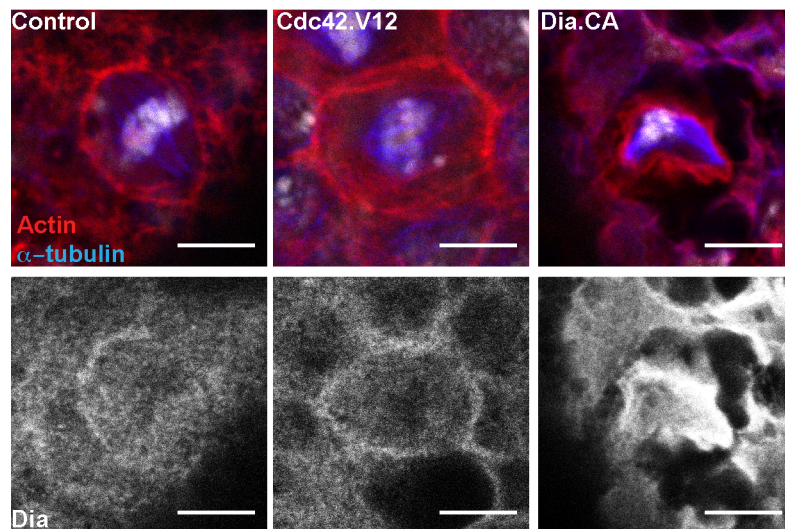


**Figure 5.7. 1. Constitutively active forms of Cdc42 and Dia promote excessive accumulation of cortical actin.** Intermediate top view of control metaphase cells has a defined actin cortex. Cells expressing a constitutively active form of Cdc42 show a thicker actin cortex. Cells expressing a constitutively active form of Dia show a thicker actin cortex and are smaller in size. Scale bars: 5  $\mu$ m.

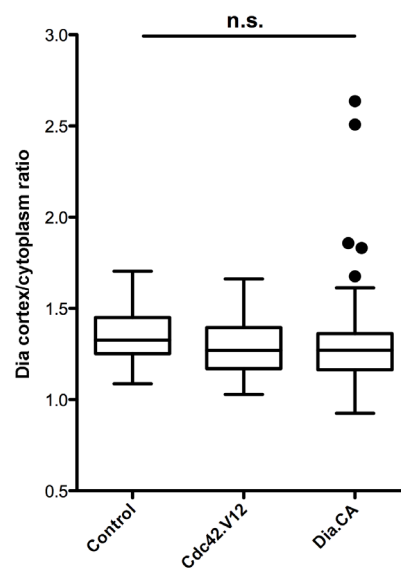


**Figure 5.7. 2. Cortical localization of Dia in metaphase cells expressing constitutively active forms of Cdc42 and Dia.** Graph of intermediate single plane ratio of mean gray values of Dia cortex/cytoplasm in control, Cdc42.V12 and Dia.CA expressing metaphase cells.

As an additional test for a link between Cdc42 and Dia activity in the remodelling of the actin cortex for cells in mitosis we imaged SOP cells of the fly notum expressing Cdc42.V12 and Dia.CA under control of the *Neu*-GAL4 driver. Using UAS-GMA to visualize isolated SOP cells, it was clear that cells expressing Cdc42.V12 in metaphase had a thicker actin cortex compared to control cells; as observed in epithelial cells. Moreover, the shape of cells was highly unstable, leading to the formation of several blebs during the period between mitotic entry and anaphase (Figure 5.7.3). Interestingly, in a few cases, metaphase cells expressing Cdc42.V12 also exhibited actin-based protrusions at the intermediate level. This suggests the possibility that Cdc42.V12 can also drive activation of Arp2/3 in mitosis (Georgiou and Baum, 2010) and/or downstream regulators of filopodial formation (Figure 5.7.3 right panels). When Dia.CA was expressed in SOPs, the cortically thickening induced was much greater than that observed in Cdc42.V12 expressing cells. Again, this rendered the cortex extremely unstable, leading to continuous blebbing in metaphase (Figure 5.7.3). In many cases violent blebbing events caused blebs to detach from the cell (Figure 5.7.3 right panel), presumably leading to a gradual loss in the volume of Dia.CA SOP cells.

In Chapter 3 we showed that cells that failed to build an actin cortex due to the loss of Dia activity showed decreased spindle stability. To better understand the effects of the actin cortex on spindle stability we drove the expression of Centrosomin (Cnn) tagged with GFP (together with Dia.CA using the *Neuralised*-GAL4 driver using the GAL80ts to restrict expression until to 4-5 hours before pupal dissection). Cnn is a centrosomal protein that is present in mitotic centrosomes at all developmental stages (Megraw et al., 1999), enabling us to study the effects of the treatment on spindle stability in control and Dia.CA cells. Interestingly, we failed to detect any increase on spindle instability depicted previously by the increased angle displacement in cells expressing Dia.CA. Instead the mitotic spindle tended to tilt along the apical basal axis of the cell (Figure 5.7.4). This effect on spindle alignment is hard to understand, but could be most simply explained as the result of the observed decrease in the intermediate area of mitotic

cells expressing Dia.CA compared to control cells (Figure 5.7.3), forcing the spindle to switch its alignment. These results reveal the importance of finely tuning actin organization at the cell cortex in mitosis via the regulation of Dia activity, and of balancing the rates of actin nucleation via Dia (Rho and Cdc42) and Arp2/3 (Cdc42), and of Myosin activation (Rho and Rok). Coordinating these activities may be the function of Pbl.

Finally, we imaged cells in interphase expressing both Cdc42.V12 and Dia.CA and noticed that overexpression of constitutively active forms of Cdc42 and Dia are both sufficient to drive cell rounding as seen upon entry into mitosis (Figure 5.7.5). This suggests that the activation of Cdc42 and Dia is likely to play an important role in driving mitotic rounding, even if in the context of a normal division the process can be driven by changes in adhesion and osmotic swelling in the absence of an actomyosin cortex.

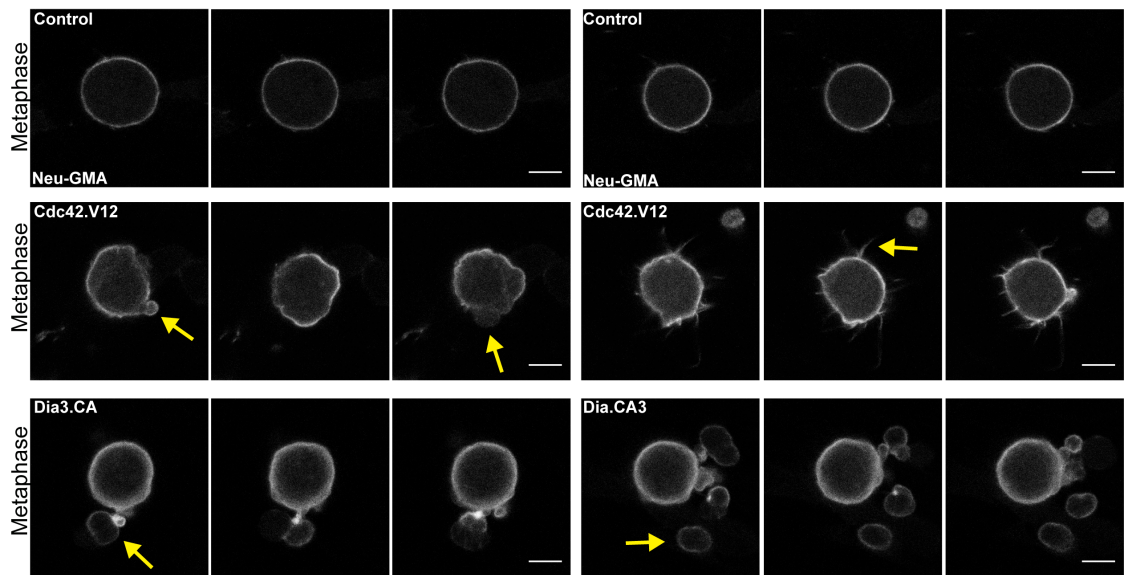


**Figure 5.7. 3. Constitutively active forms of Cdc42 and Dia promote excessive accumulation of cortical actin and cell blebbing in SOP cells.** Intermediate top view of control metaphase cells has a defined actin cortex. Cells expressing a constitutively active form of Cdc42 show a thicker actin cortex cell blebbing (yellow arrow left panel) and intermediate protrusions (yellow arrow right panel). Cells expressing a constitutively active form of Dia show a thicker actin cortex and violent cell blebbing (yellow arrow left panel) with cell detachment (yellow arrow right panel). Time frames of 40 seconds apart. Scale bars: 5  $\mu$ m.

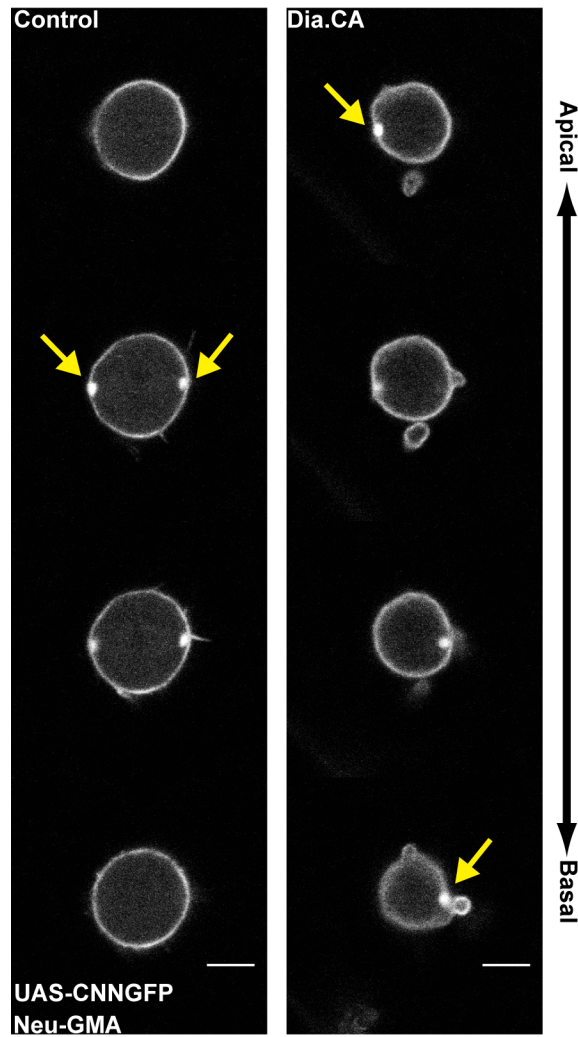


**Figure 5.7. 4. Constitutively active forms of Dia impair spindle orientation along apicobasal axis.** Images show actin filaments marked by UAS-GMA and centrosomes marked by UAS-CNNGFP in apical, intermediate and basal sections of a SOP metaphase cell. Yellow arrow marks centrosomes. Scale bars: 5  $\mu$ m.



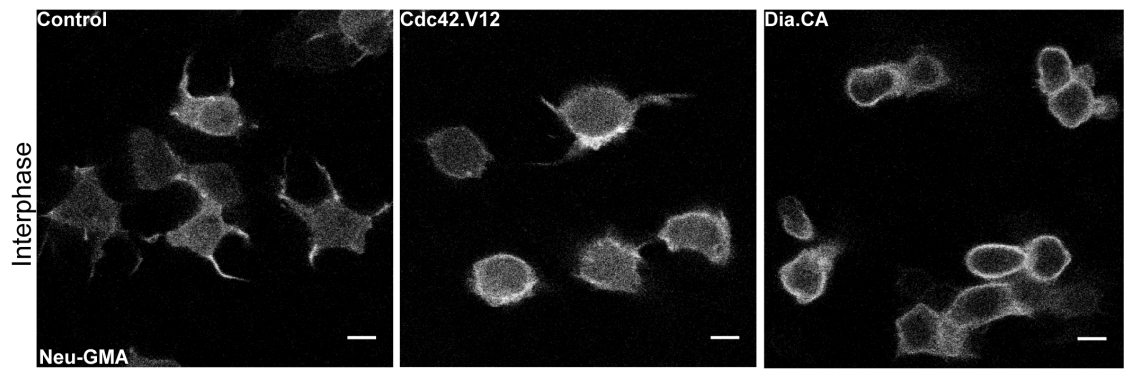


**Figure 5.7. 5. Constitutively active forms of Cdc42 and Dia are sufficient to drive cell rounding in interphase.** Intermediate top view of control cells in interphase show cell protrusions. Cdc42 and Dia constitutively active expression in SOP cells drive cell rounding in interphase cells and assembly of an actin cortex Scale bars: 5  $\mu$ m.

## 5.8. Conclusions

In this chapter I have characterized the organization of the aPKC/Par6/Cdc42 complex in mitotic cells of the developing notum downstream of Pbl. This reveals a potential role for the regulation of actin organization in mitosis dependent on the function of polarity proteins, specifically aPKC/Par6/Cdc42. I found that, coupled to cells entering mitosis the organization of the aPKC/Par6/Cdc42 complex is altered, extending their apical domain to more lateral domains of the mitotic cell and to be dependent of Pbl activity. I used RNAi lines against aPKC, Par6 and Cdc42 along with loss of function alleles for Cdc42 and aPKC to test the role of this polarity complex in mitosis. In all cases I found that mitotic cell shape was severely compromised associated to defects in the actin cortex of these cells.

Interactions between Par complex proteins and RhoGTPases are essential for the proper regulation of cell and cytoskeletal polarity in a wide variety of polarized cells (Anderson et al., 2008; Georgiou and Baum, 2010; Georgiou et al., 2008; Nishimura et al., 2005; Pegtel et al., 2007; Schwamborn and Puschel, 2004; Zhang and Macara, 2006). Together these results suggest that the molecular mechanisms required for the polarization of the cell cytoskeleton have been recycled and adapted for different biological processes ranging from gene expression (Louvet and Percipalle, 2009) to dramatic cell shape changes in mitosis. However, to the best of our knowledge this is the first time the Par complex to have a role regulating Dia activity. These observations strengthen the analogy between the multiple events for the regulation of yeast formins (Dong et al., 2003) and in animal cells, where the recruitment is dependent of Cdc42 and aPKC, presumably like yeast PKC1p an atypical PKC in animal cells might be required for specific phosphorylation of formins, and Rho binding the GBD domain essential for formin activation. Finally I showed that constitutively active forms of Cdc42 phenocopy to a great extent the phenotype of a constitutively active form of Dia, both in mitosis and interphase cells. To note that

expression of these constitutively active forms of Cdc42 and Dia is sufficient to drive cell rounding in interphase cells supporting the role of these proteins in actin-dependent cell shape changes in mitosis. Interestingly, in Cdc42 constitutively active experiments I found the formation of cell protrusions at the intermediate level of metaphase cells. Although Arp2/3 does not play a major role in the assembly of an actin cortex in mitosis this should be tested further before ruling out a role for Arp2/3 in mitosis. The scalability of the contraction process can be regulated by the orientation of actin filaments (Reymann et al., 2012; Reymann et al., 2010). The increased cell contraction in mitotic cells expressing a constitutively active form of Dia suggest that a functional actin cortex is a result of a fine tuning of levels of F-actin at the cell cortex and architecture. This architecture is possibly regulated by the combined activity of primarily Dia and to smaller extent Arp2/3. Failing in obtaining such fine equilibrium has severe consequences in the orientation of the mitotic spindle.(Yasuda et al., 2004) (Yasuda et al., 2004)

## **6. CHARACTERIZATION OF APICAL-BASAL POLARITY IN MITOTIC EPITHELIAL CELLS.**

### **6.1. Introduction**

Epithelial cells are highly polarised. In *Drosophila* they have been proposed to have at least four distinct cortical domains based upon the localization of conserved polarity complexes: an apical domain, a junctional domain, a lateral domain and a basal domain. Modifications in the activity of polarity factors can alter the size of apical, junctional, lateral and basal domains to change cell organization and behavior (St Johnston and Sanson, 2011). In my studies I showed that mitotic entry is accompanied by a change in the localization of the Par proteins aPKC and Par6, together with their binding partner Cdc42, and by a parallel change in cell shape and cytoskeletal organization. Given that the control of apical-basal polarity domains is established and maintained by a network of positive and negative interactions between different cortical polarity proteins, these observed changes might reflect larger shifts in cortical polarity. Thus, the aim of this chapter is to characterize the distributions of apical, junctional and lateral domains in mitotic epithelial cells.

## **6.2. Differential positioning of adherens junctions and Baz/Par3 associated with mitosis.**

In epithelial cells Baz is localised to the junctional domain by exclusion from the apical domain, mediated through Crumbs and the aPKC/Par6/Cdc42 complex (Morais-de-Sa et al., 2010; Walther and Pichaud, 2010). In Chapter 5 I characterized the repolarization of the aPKC/Par6/Cdc42 complex in mitosis, which upon mitotic entry extend their apical domains to more intermediate sides of the cell. This extension of the apical domain via aPKC/Par6/Cdc42 is expected to have an impact on the junctional domain, specifically through aPKC phosphorylation of Baz/Par3 and, consequently, on adherens junctions marked by DE-Cadherin. To follow adherens junctions during mitotic progression in epithelial cells of the fly notum I took advantage of GFP trap fly lines, where the GFP tag is associated with the endogenous gene DE-Cadherin and Bazooka in the fly genome expressed under its own promoter, and a UAS-BazmRFP transgenic line to follow the localization of Baz/Par3 expressed under the control of *pnr*-GAL4 expression.

In movies of these animals I observed a basal shift in the position of adherens junctions marked by DE-CadherinGFP during mitosis. In prophase and following mitotic exit, adherens junctions were seen at the same levels as those seen in neighbouring interphase cells (Figure 6.2.1 and 6.2.2). A similar shift was seen in metaphase in flies expressing tagged versions of Baz. Again reversed as cells exited mitosis (Figure 6.2.3 and 6.2.4). These parallel changes in the position of DE-Cadherin and Bazooka were confirmed in cells expressing DE-Cadherin-GFP and Baz-mRFP. These data show that discrete adherens junctions are maintained in mitosis despite the change in the localisation of Cdc42 and Par6 and aPKC. In addition, however, the extension of Cdc42/PAR polarity domains to the intermediate part of the cell is associated with a slight basal shift in the position of adherens junctions and Baz in cells entering mitosis.



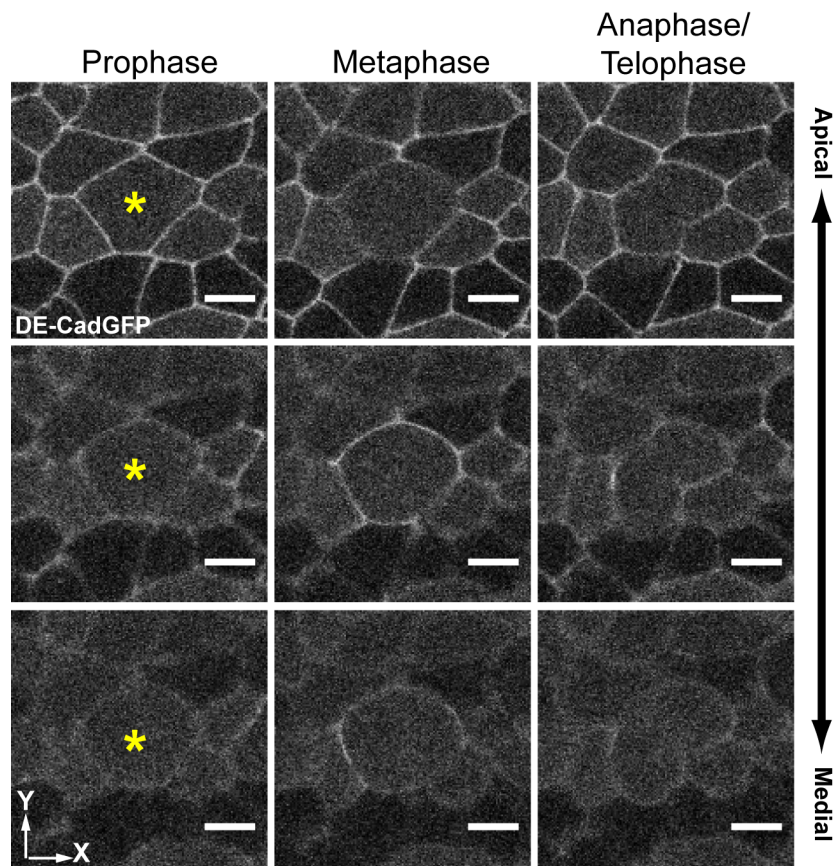


**Figure 6.2. 1. DE-Cadherin shifts position in mitosis.** Images show top view of DE-Cadherin apical and intermediate sections of nota at different stages of mitosis, marked with a yellow asterisk. Cells are shown that express DE-CadherinGFP from the Pnr promoter. Scale Bars: 5  $\mu$ M.

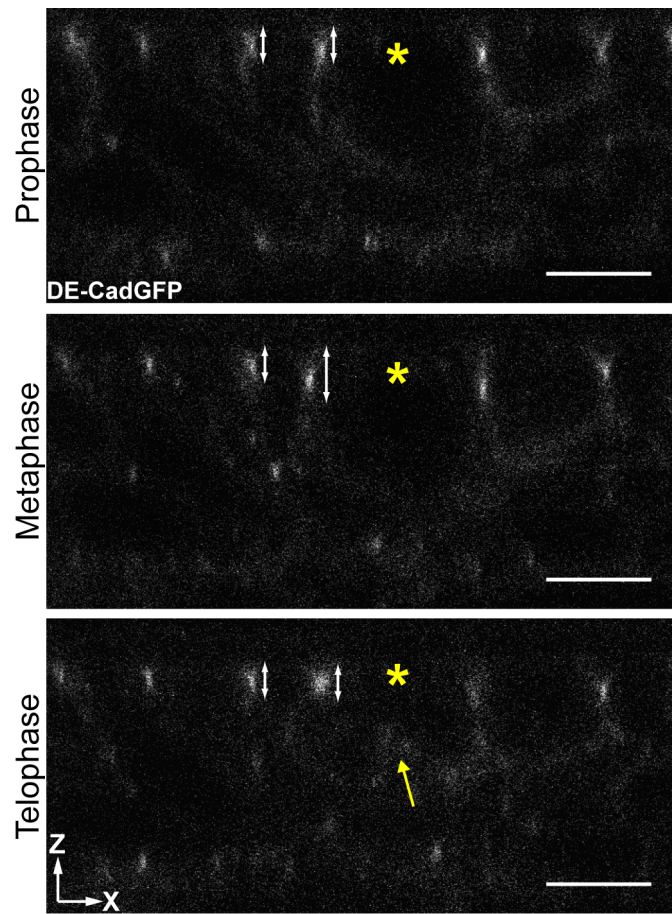


**Figure 6.2. 2. Cadherin shifts position in mitosis.** Side view of cells expressing DE-Cadherin tagged with GFP in different stages of mitosis. Yellow asterisk indicates mitotic cell. White double sided arrow indicates DE-Cadherin localization in interphase and mitotic cells. Yellow arrow marks furrow canal. Scale bars: 5  $\mu$ m.



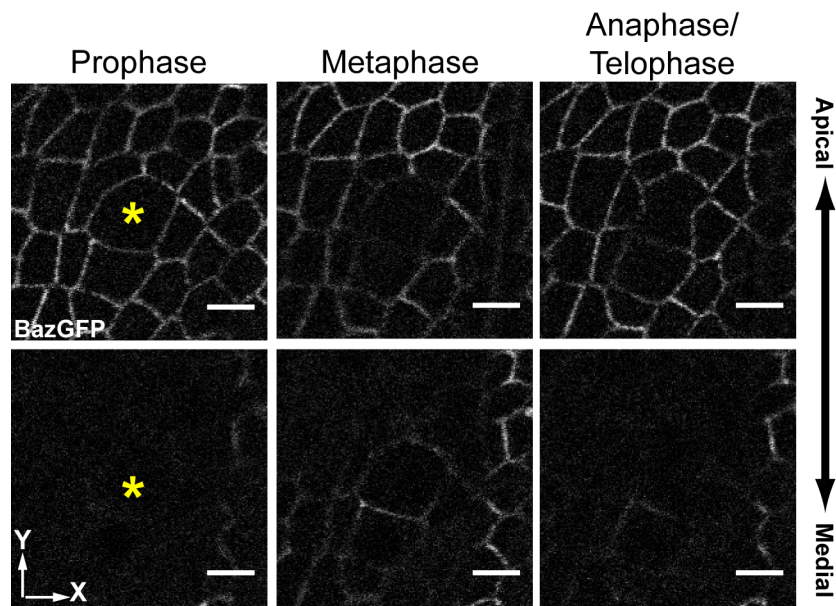


**Figure 6.2. 3. Bazooka localisation undergoes a basal shift in mitosis.** Images show top view of Bazooka apical and intermediate sections of nota at different stages of mitosis, marked with a yellow asterisk. Cells are shown that express BazGFP. Scale Bars: 5  $\mu$ M.

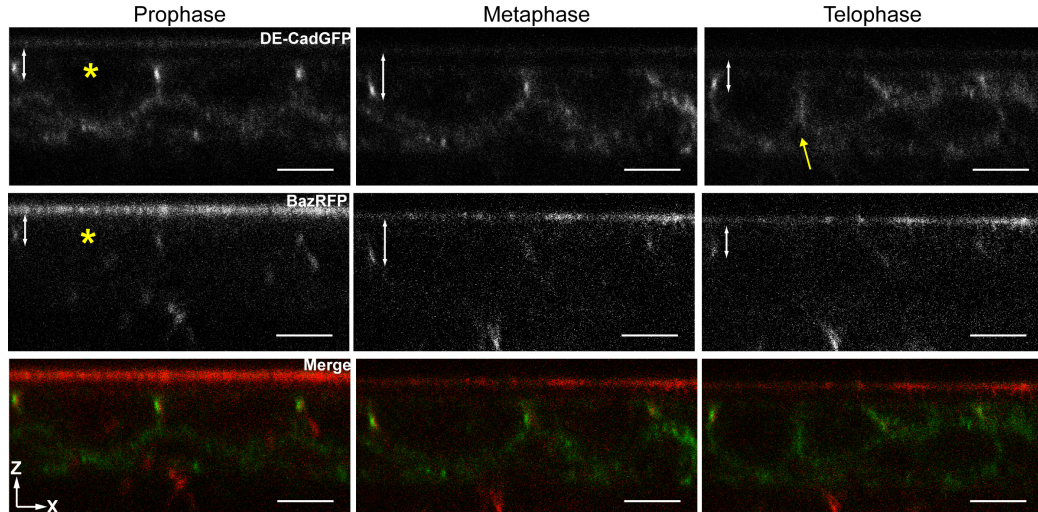


**Figure 6.2. 4. DE-Cadherin and Bazooka undergo parallel basal shifts in their localisation during mitosis.** Side view of cells co-expressing DE-Cadherin tagged with GFP and Bazooka tagged with mRFP in different stages of mitosis. Yellow asterisk indicates mitotic cell. White double sided arrow indicate DE-Cadherin and Bazooka localization. Yellow arrow marks furrow canal. Scale bars: 5  $\mu$ m.

### **6.3. Extension of Crumbs domain decorates the cortex of cells in mitosis**

Crumbs, but not Stardust, have been shown to compete with Baz for the binding of Par6, promoting its exclusion from the apical domain of cells (Morais-de-Sa et al., 2010; Walther and Pichaud, 2010). To understand whether this relationship between Crumbs, Baz and the other PAR proteins is maintained in mitosis, I studied the localization of proteins of the “Crumbs complex” (Bulgakova and Knust, 2009), specifically Crumbs and PatJ, during mitosis in fly epithelial cells. To approach this, I took advantage of antibodies raised against Crumbs and PatJ and stained the nota of *wild type* flies. PatJ localizes at the apical domain of epithelial cell in interphase (Sen et al., 2012), (Figure 6.3.1, note cells surrounding mitotic cell marked with yellow asterisk.). As epithelial cells of the fly nota enter mitosis, PatJ remains at the apical region of cells, retaining its localization along the apical-basal axis of the cell. When I stained cells of the nota for Crumbs, it was visible apically in both in mitotic and non-mitotic (Figure 6.3.2 top panels). However, in mitotic cells, the Crumbs domain extended to the most basal regions of the cell.

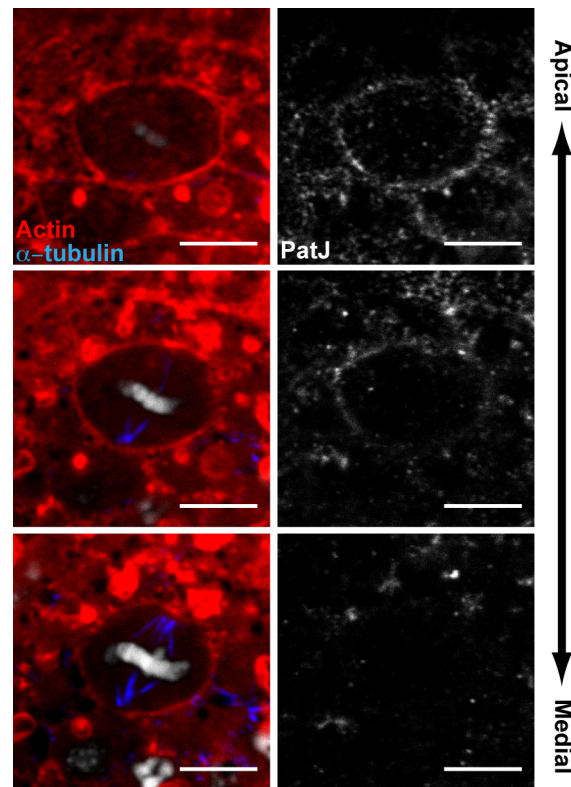


**Figure 6.3. 1. PatJ localization is unperturbed in dividing epithelial cells.** Intermediate top view of wild type cells in metaphase and surrounding interphase cells. Scale bars: 5  $\mu$ m.

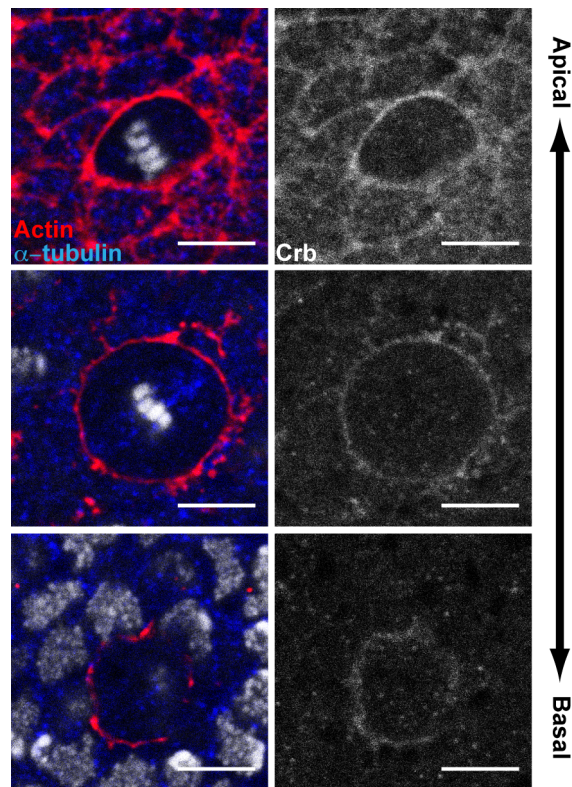


**Figure 6.3. 2. Crumbs extend the apical localization to basal domains in mitosis.**

Intermediate top view of wild type cells in metaphase and surrounding interphase cells. Scale bars: 5  $\mu$ m.

## 6.4. Lgl depolarization in mitosis

*Scribbled*, *discs large* and *lethal giant larvae* are genes that contribute to the establishment of a defined basal-lateral domain in epithelial cells (St Johnston and Ahringer, 2010). In *scrib*, *lgl* and *dlg* mutant embryos, Crb is found at ectopic positions along the basal-lateral membrane and the zonula adherens appears abnormal (Bilder et al., 2000; Bilder and Perrimon, 2000). In light of the previous results, which reveal profound changes in the organisation of apical polarity determinants in mitosis, I wanted to test whether there were parallel changes in the localization of these proteins. To do so, I used a GFP-Dlg flytrap line to mark endogenous Dlg and transgenic flies expressing Lgl tagged with GFP under the control of the *pnr*-GAL4 driver to visualize Lgl.

Dlg localization appeared to be unaltered as cells exited G2 and entered mitosis, although Dlg was visible more basally in rounded prophase and metaphase cells (Figure 6.4.1). Thus, the basal extension of the Crb domain in mitotic cells does not appear to be influence Dlg localization, or vice-versa. This was not unexpected since intermediate Dlg is thought to place a role in orienting the spindle in this plane (Bergstrahl et al., 2013; Nakajima et al., 2013). Conversely, when I imaged the notum of flies expressing LglGFP I noticed a clear change. Lgl was lost from the cortex as cells entered mitosis, and was completely gone from the cortex by metaphase (Figure 6.4.2). Since previous work has identified a mutual antagonism between Crb and Lgl that is mediated by the PAR complex (Fletcher et al., 2012; Tanentzapf and Tepass, 2003), it is possible that the loss of basal Lgl might be promoted by the basal movement of Crumbs and the PAR domain. More work would be required to test this hypothesis.



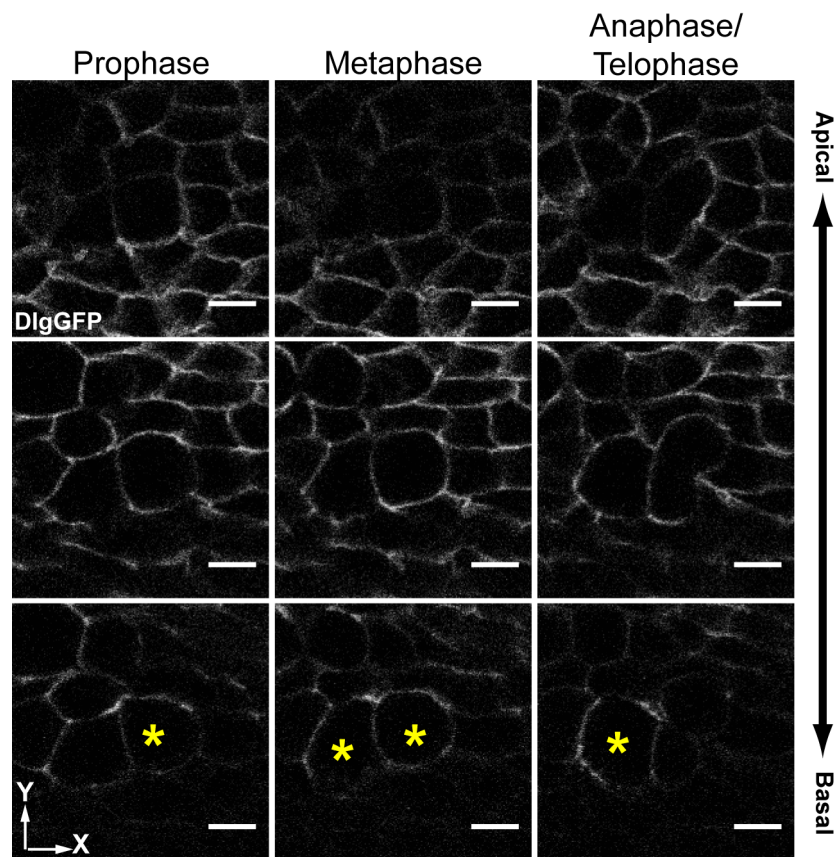


**Figure 6.4. 1. Dlg domain extends to more basal regions of the cell in mitosis.** Images show top view of Dlg apical intermediate and basal sections of nota at different stages of mitosis. Yellow asterisk mark mitotic cells with extended basal domains of Dlg. Cells are shown that express DlgGFP. Scale Bars: 5  $\mu$ M.

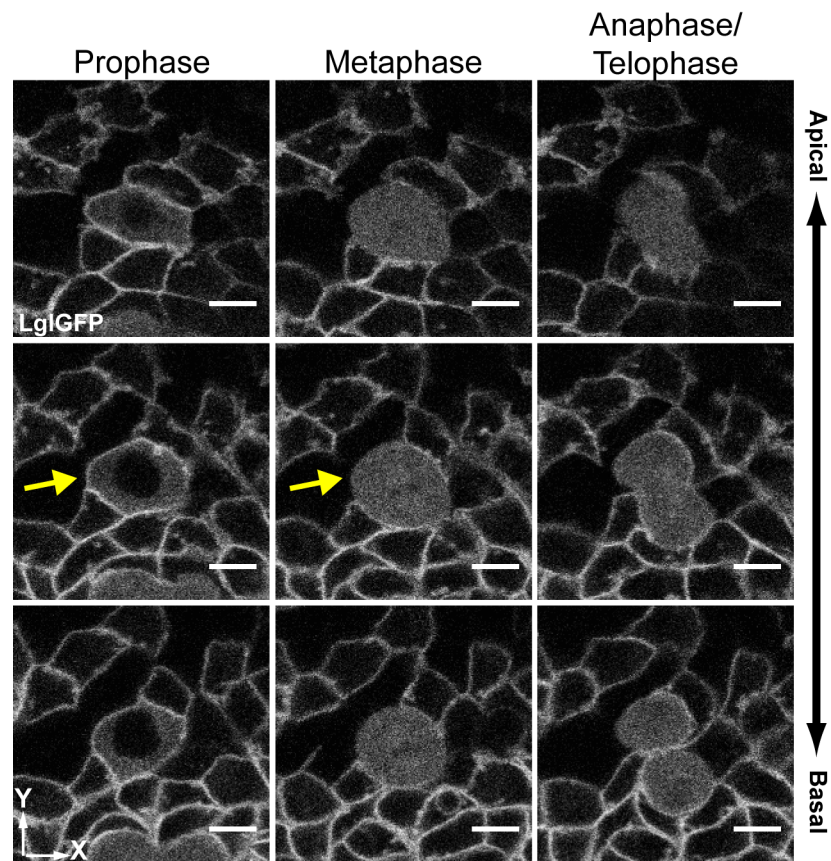


**Figure 6.4. 2. Lgl is depolymerized from the cell cortex in mitosis.** Images show top view of Lgl junctional and basal sections of nota at different stages of mitosis, Yellow arrow marks mitotic cell in prophase with cortical Lgl in prophase and complete depolymerisation in metaphase. Cells are shown that express LglGFP from the Pnr promoter. Scale Bars: 5  $\mu$ M.

## 6.5. Conclusions

In this chapter I characterized the apical-basal polarity of epithelial cells of the developing notum in mitosis. For more than two decades that the first Par genes were identified (Kemphues et al., 1988). Since then extensive work has been performed on their role in cell polarity. However, only recently the focus has been on the organization and function of polarity proteins in symmetric cell division (Bergstralh et al., 2013; Durgan et al., 2011; Guilgur et al., 2012; Jaffe et al., 2008; Nakajima et al., 2013). Recently published work by Bergstralh and colleagues (2013) shows that apical polarity determinants like aPKC, Crb and Baz disappear from the apical cortex of mitotic follicle cells, even though Dlg remains at the lateral cortex suggesting that polarity cues vary between different epithelial cell types and/or developmental processes.

In this chapter I present evidence that in epithelial cells of the developing notum, polarity proteins reside in different domains in mitotic cells compared to their counterparts when resting in interphase. Baz and adherens junctions shift their domains to slightly more basal regions of the cell. These data are consistent with the observation that junctions shift basally in *Drosophila* ventral furrowing. Apically localized aPKC and basal-laterally localized Par-1 restrict Par3/Baz to sub-apical regions, where it directs junctional assembly (Benton and St Johnston, 2003; Harris and Peifer, 2004, 2005; McGill et al., 2009; Morais-de-Sa et al., 2010; Walther and Pichaud, 2010). During *Drosophila* gastrulation shifts in the position of adherens junctions that depend on the relative ratio of Bazooka/Par1 play an important role in morphogenesis. Interestingly, in aPKC mutant embryos this basal shift still occurs, although the disassembly of apical junctional margins, to provide correct apical cell shape changes, are aPKC-dependent (Wang et al., 2012). To better understand the molecular mechanism that controls junctional shift in dividing cells of the fly notum which might offer a better understanding on the molecular mechanism controlling junctional movement further work



needs to be done, specially addressing the localization and role of Par-1 in mitosis.

In polarity remodelling Baz apical exclusion is sponsored by the combined activity of Crumbs, Par proteins and Cdc42 (Morais-de-Sa et al., 2010; Walther and Pichaud, 2010). The extension of the Crb domain during mitosis might play a role in this junctional shift. The ectopic localization of Crb might be a consequence of the depolymerisation of Lgl also in found mitosis. These results provide a new alternative mode of apical basal remodelling in which the insights should be further analysed, particularly defining the major regulator of polarity remodelling and the roles of all polarity factors in the process of cell division. Collectively, the data presented in this thesis suggests that Pbl might initiate polarity remodelling, acting through Cdc42 altering the apical-basal polarity complexes/proteins from their cortical domains.

## 7. DISCUSSION

### 7.1. Introduction

The aims of this thesis were to identify the mechanisms that control actin organization in epithelial cells entering mitosis. In particular, to identify the actin nucleators involved in the assembly of a new actin cortex and upstream regulators operating in mitosis. My data show that cells in the developing *Drosophila notum* disassemble their interphase actin cytoskeleton as they enter mitosis to assemble a new actin cortex that is nucleated by the formin Diaphanous downstream of a conserved molecular pathway involving Rho GTPases and polarity proteins. This mechanism of *de novo* actin assembly appears to be involved mitotic cortex assembly in both symmetric and asymmetric cell divisions in the developing pupal notum. This, together with related findings in other systems (Castanon et al., 2013), suggests that formin-dependent actin-based cell cortex is likely to be a generic mechanism for the generation of the metaphase cortex. Strikingly, this is the same nucleator previously implicated in cell division (Castrillon and Wasserman, 1994; Severson et al., 2002; Watanabe et al., 2008). This highlights the potential importance of viewing cytokinesis as a stepwise process that begins with mitotic rounding, and ends with cell division, following polar relaxation and the focusing of actomyosin machinery around the spindle midzone.

## **7.2. Cortical actin nucleation in mitosis is a Diaphanous-dependent process**

Epithelial cells of the notum present several polarized actin structures in interphase. These include actin bundles at the most apical side of cells that constitute microvilli, an apical actomyosin mesh, circumferential junctional actin that is associated with adherens junctions, and basal protrusions. When cells enter mitosis these actin structures are remodelled and a new homogenous actin cortex assembles *de novo* (Figure 7.4.1), that is crosslinked to the plasma membrane by activated Moesin (Carreno et al., 2008; Kunda et al., 2008a; Kunda et al., 2012; Roubinet et al., 2011). This dramatic remodelling of the actin cell cortex would be expected to require actin nucleators. To test this I inhibited the activity of two well-studied actin nucleators in *Drosophila*: Arp2/3 (Hudson and Cooley, 2002) and Diaphanous (Afshar et al., 2000; Castrillon and Wasserman, 1994). Inhibition of Dia, but not Arp2/3, was sufficient to prevent the assembly of a mitotic actin cortex both in epithelial and SOP cells. Moreover, I found that Dia localizes at the cortex of mitotic cells while Arp2/3 fails to exhibit a clear localization pattern. Interestingly, cells with inhibited Dia function, despite lacking a mitotic actin cortex were capable of rounding up, although mitotic progression and spindle stability were affected. These results suggest that Dia plays the major role in actin cortical nucleation in mitosis. Importantly, during zebrafish gastrulation division of epiblast cells along the A-V axis is influenced by a cap of filamentous actin that depends on the activity of zDia2 (Castanon et al., 2013) supporting a role for formins in the assembly of the mitotic actin cortex.

Arp2/3 was already shown to be required for a new phenomenon of actin assembly in mitosis: the formation of an actin cluster that revolves horizontally around the cortex at a constant angular speed, and later, after three to four revolutions of the cell, fuses into the contractile ring (Mitsushima et al., 2010). Knockdown of Arp2/3 inhibits the formation of this actin cluster in mammalian cells, however it has no affect on other

actin structures in mitosis (Mitsushima et al., 2010). In the developing notum, I was unable to identify any cytoplasmic actin structures in either live or fixed tissues. This either reflects a cell-type or species specific event or is due to differences in the resolution of imaging used in this work. I tend to favour the first explanation; in the work of Mitsushima and colleagues the occurrence of an actin cluster in mitosis was seen in a subset of cells. Further, although the authors favour the hypothesis that actin cluster appearance correlates with the degree of mitotic cell rounding, the occurrence of this actin cluster was also associated with cancer and immortalized cells, but could not be seen in primary cell culture. In light of these events and the apparent absence of an actin cluster in mitotic cells of the developing notum, which are nearly completely spherical in shape, one can hypothesise that actin organization in mitosis is a tightly regulated mechanism, and that Arp2/3 activity is upregulated in cancer and/or transformed cells with an undiscovered benefit in tumor progression (Fink et al., 2010; Thery et al., 2005). Intriguingly, a small subset of mitotic cells in *nota* lacking Arp2/3 activity exhibited deformations in metaphase that resemble blebs. Additionally, the expression of a constitutively active form of Cdc42 resulted in the formation of protrusions in metaphase cells, indicating that in mitosis Cdc42 may be able to activate Arp2/3 in a mitotic cell. These data suggest that the Arp2/3 complex may aid Dia in the establishment of the mitotic actin cortex. Regardless though, the data presented in this thesis suggest that the role of Arp2/3 in mitosis is minor or redundant.

The differential role of actin nucleators in mitosis suggests that Arp2/3 activity is predominantly required in interphase structures and Dia in mitosis. Arp2/3 generates branched actin structures which are ideal for pushing, e.g during endocytic fission (Derivery et al., 2009), and in the formation of lamellipodia (Ridley, 2011) and filopodia formation (Figure 7.2.1) and finally at mitosis exit during midbody formation (Founounou et al., 2013; Guillot and Lecuit, 2013; Herszterg et al., 2013). Dia generates a population of linear Tropomyosin-coated (Wawro et al., 2007) actin

filaments, which are a good substrate for myosin II-dependent contractility (Reymann et al., 2012; Vignaud et al., 2012) and are easily tethered to the membrane by ERMs (Carreno et al., 2008; Kunda et al., 2008a) to generate a thin shell in metaphase (Clark et al., 2013). Following this rationale the actomyosin cortex of metaphase cells can be seen as a three-dimensional shell (an actin sphere) that collapses to form a contractile ring (an actin circle) at mitotic exit to drive cytokinesis.

Interestingly, the inhibition of Dia and the subsequent loss of an actin cortex in mitosis did not dramatically impair cell shape, since mitotic cells were able to round up. This supports the evidence that rounding is mainly driven by a combination of forces including differences in osmotic pressure (Stewart et al., 2011). The ability of mitotic cells to establish a rounded shape in the absence of an actin cortex might explain the mild effect of loss of Dia on spindle stability and mitotic progression, since mitotic progression in mammalian cells was already shown to be unaffected by the loss of an actin cortex (Lancaster et al., 2013). However, expression of a constitutively active form of Dia increased the accumulation of cortical filamentous actin and led to dramatic blebbing, perhaps due to an increase in actomyosin-generated intracellular pressure (Charras et al., 2006). In these circumstances the mitotic spindle tilted along the apical-basal axis. This could be explained by: 1) the reduction in cell width that results from the increase in cortical contractility may be insufficient to accommodate the spindle, which then preferentially aligns along the Z axis or, 2) the increased actin cortex makes it impossible for the astral microtubules to read cortical cues.

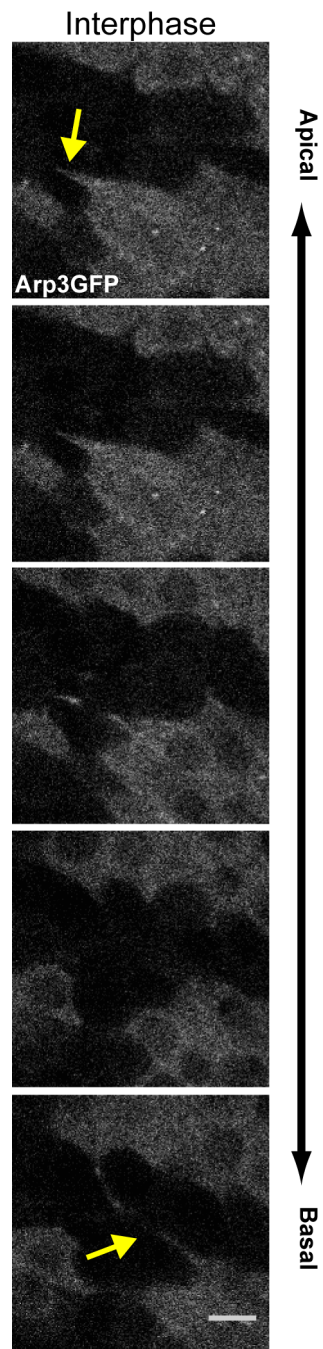


**Figure 7.2. 1. Arp3 is present in intermediate and basal filopodia-like projections.** Top views of intermediate to basal sections of epithelial cells in interphase with protrusions (Yellow arrow) marked by Arp3GFP. Scale Bars: 5  $\mu$ m.

### **7.3. Molecular pathway triggering changes in actin dynamics/organization upon entry into mitosis.**

Cells commit to mitosis by activating the mitotic cyclin-Cdk complexes through a tightly regulated process that involves multiple feedback loops (Lindqvist et al., 2009; Stumpff et al., 2004). Ect2 is a known Cdk1 substrate and a potent actin regulator (Hara et al., 2006; Niiya et al., 2006) that is able to induce changes to both cell shape and cortical mechanics in early mitosis through the activation of RhoA remodeling the actomyosin cytoskeleton (Matthews et al., 2012). Pbl is the fly homolog of vertebrate Ect2. Although threonine T341, a key site of Cdk1/CyclinB-mediated Ect2 phosphorylation, is not conserved in Pbl protein sequence (Hara et al., 2006), the C-terminal is highly conserved (Figure 7.3.1.), and includes T814, another conserved site of Cdk1/CyclinB-mediated phosphorylation (Niiya et al., 2006). Moreover, Andreas van Impel and colleagues showed that C-terminal tail of Pbl protein is crucial for cortical localization, and the selective activation of Rho1- versus Rac-dependent pathways (van Impel et al., 2009). In the fly *notum*, inhibition of Pbl is sufficient to prevent assembly of an actin cortex in mitosis, phenocopying the loss of *Dia*, suggesting a role for Pbl at the cell cortex in mitosis, probably through the activation of Rho GTPases.

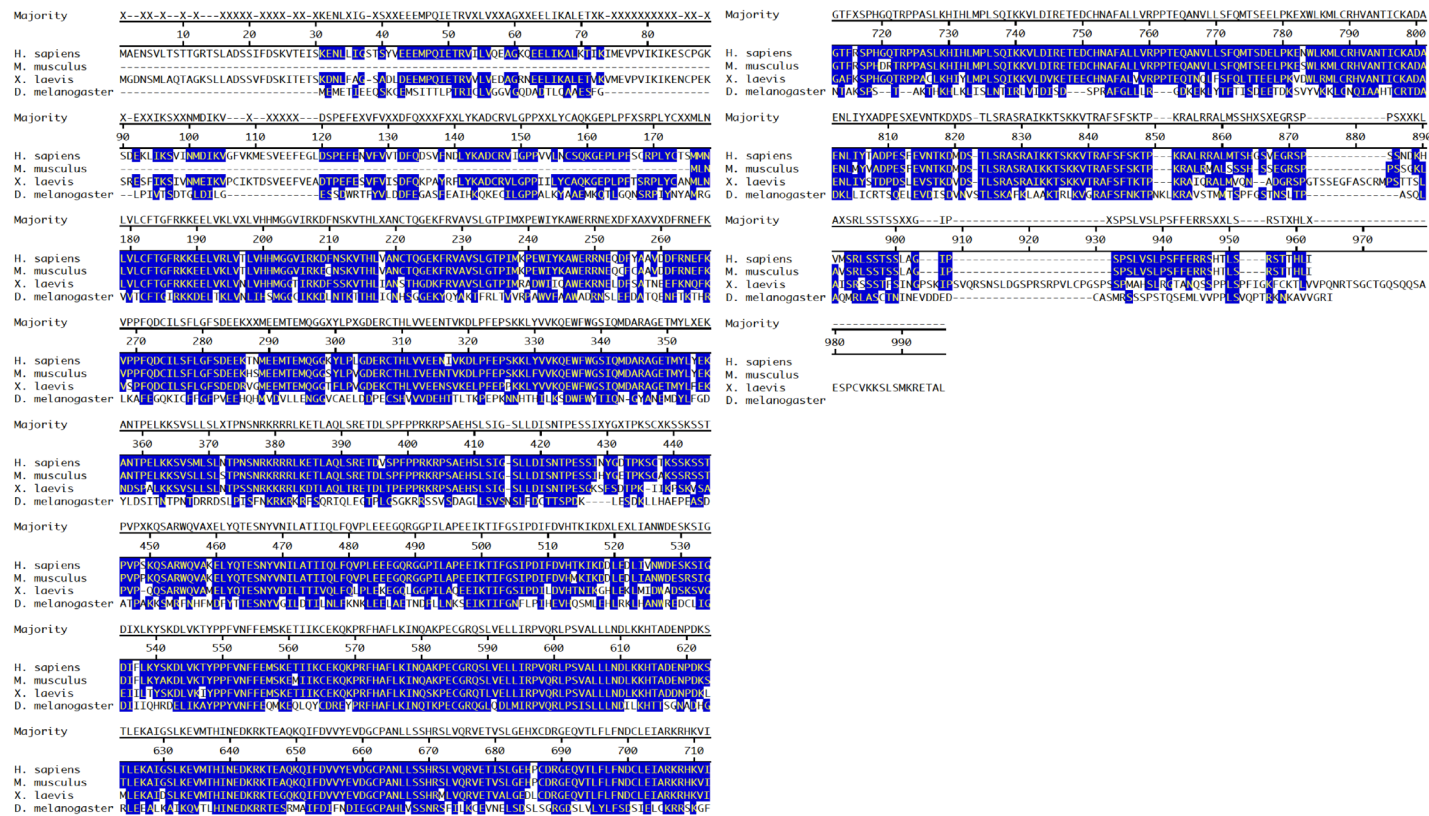


Figure 7.3. 1. Clustal-W alignment report of ECT2 protein sequences for: H. Sapiens; M. musculus; X. laevis and D. melanogaster. Cobalt blue match the Consensus within 2 distance units.



In the developing notum, assembly of a mitotic contractile actin cortex appears to be dependent on a dual function of Pbl (Figure 7.4.1). The inhibition of Rho promotes actin defects and lead to loss of activated non-muscle Myosin II at the cell cortex, though cortical accumulation of Dia is mildly affected. ROCK, a substrate of Rho, phosphorylates LIM Kinases and enhances the ability of LIMKs to phosphorylate cofilin (Maekawa et al., 1999). The fact that inhibition of Rho in the fly notum had a mild effect in the assembly of an actin cortex could also be a consequence of a lesser pool of activated cofilins decreasing overall the severing of actin filaments. Conversely, Cdc42 inhibition does little to alter the distribution or levels of activated myosin but has a significant effect on Dia cortical localization. Strikingly, though, the inhibition of Pbl resulted both in the depletion of cortical activated non-muscle Myosin II and Dia. These data suggest that in mitotic cells of the developing notum Pbl controls the activities of Rho and Cdc42, which may then coordinately regulate *Drosophila* Dia (Dong et al., 2003). Moreover, Rho and Cdc42 have distinct but complementary functions in the assembly of an actomyosin cortex. Cdc42 has been proposed to play a similar role in rat kidney epithelial cells, where its depletion causes an abnormal mitotic cell morphology and defects in the localization of actin and Rho at the equator during cell division (Zhu et al., 2011). Moreover, during wound healing in *Xenopus* embryos Cdc42 and RhoA concentrated around the wound in distinct zones. While RhoA regulates contractility during wound closure, Cdc42 helps to generate the actin filaments required at the site of the wound (Benink and Bement, 2005). Together these results suggest that the combined action of Rho and Cdc42 downstream of Pbl activity is required for the assembly of a functional mitotic actomyosin cortex.

## 7.4. Cortical repolarization in mitosis

As discussed above, in mitotic cells of the developing notum Pbl plays an important role in the assembly of a contractile actin cortex. Importantly, Pbl also controls the mitotic repolarization of Cdc42 and aPKC. In mitosis, aPKC, Par6 and Cdc42 extend their apical domain to more intermediate sides of the cell. Inhibition of Pbl is sufficient to abolish this intermediate extension of Par proteins and Cdc42. Since the loss of either Cdc42 or aPKC is sufficient to prevent cortical Dia accumulation, Pbl appears to play an important role in remodelling cell polarity in epithelial cells entering mitosis via control of the repolarization of Par proteins and Cdc42. However, if we assume that this mitotic polarity remodelling is driven by Pbl, how does the release of this RhoGEF from the nucleus lead to intermediate spreading of Cdc42 and Par proteins, rather than forcing these proteins to decorate the entire cell cortex? One hypothesis for this event to take place might come from the effect of the Par complex on Lgl. Phosphorylation by aPKC inactivates Lgl on the apical side and on the basolateral side, Lgl is active and excludes Par-6 from the cell cortex (Hutterer et al., 2004). Since in mitotic cells of the fly notum the Par complex extends its apical domain to more intermediate regions of the cell and this appears to be concomitant with the complete removal of Lgl from the basolateral domain (depolymerisation of Lgl), one could hypothesize that Lgl removal is fundamental for Dia accumulation at the cell cortex. This would imply that the Par complex acts indirectly in the localization of Dia. Pbl drives changes in the Par complex profile that in turn has profound effect on Lgl polarization that inhibits Dia cortical localization. Answering this question would be aided by imaging of Lgl localization in cell with Pbl, Cdc42 or aPKC knock down. Or the expression of Lgl form that is insensible to aPKC phosphorylation hence maintaining its basolateral localization at all time and measuring levels of Dia cortical localization. Also, we need to consider that the Par complex or simply aPKC and Cdc42 are indeed decorating the entire cell cortex however

the failure to detect such behaviour may be a simple consequence of the difficulties in imaging basally localised proteins. Another possibility could be a difference in the nature of actin organization along the apical-basal axis of the cell. In prophase, one of the first events observed is a basal accumulation of filamentous actin. This would imply that mitotic cells have a basal actin cortex that is composed of recycled branched actin: a product of basal filopodia and adhesion disassembly (Dao et al., 2009), and an intermediate and apical actin cortex, composed of parallel actin filaments product of Dia activity. In this light, it is important to note that although the inhibition of Arp2/3 did not prevent the basal accumulation of filamentous actin in mitotic cells, suggesting that intermediate activation of Dia is sufficient to build a functional actin cortex, a small subset of cells lacking Arp2/3 exhibited an unstable cell shape in metaphase. This could have been due to a loss of basal interphase actin filaments, or due to a needed function of Arp2/3 in the assembly of an actin cortex where a fine tune of different actin structures produced both by Dia and Arp2/3 are needed for a functional actin cortex. Together these results suggest that like the establishment of yeast cell polarity and animal cell migration, a RhoGEF, Rho GTPases and downstream targets regulate mitotic cortical actin assembly in epithelial cells.

The establishment of epithelial polarity in *Drosophila* is dependent on activated Cdc42, which recruits Par6 to the apical cortex to establish the apical compartment. aPKC is recruited by binding to Par6. It then phosphorylates Lgl, restricting its activity to the basolateral side (Hutterer et al., 2004). Given Cdc42's important function in the regulation of epithelial polarity, one might hypothesize that the relocalisation of Cdc42 in mitosis might reflect and help to precipitate a profound change in cell polarity. During mitosis in the developing notum polarity factors from apical, junctional and basal-lateral domains change their localization. While Cdc42 and Par proteins extend their apical domains to more intermediate sides of the cell Crb, an apical polarity factor, is ectopically present around the cell cortex, and Lgl is lost from

the cortex. Strikingly however, PatJ localisation remains unaltered, and Baz and adherens junctions undergo a marginal basally shift in their localisation, and basal determinants like Dlg remain associated with the basolateral membrane (Figure 7.4.1). Currently the extent to which interactions between components of the interphase apical-basal polarity network are altered during mitosis is unclear. Nevertheless, it is possible that the marginal basal shift in the localisation of Baz and adherens junctions is a direct consequence of the more dramatic basal extension of aPKC, Par6 and Cdc42, and Crb (Morais-de-Sa et al., 2010; Walther and Pichaud, 2010). Similarly, the loss of cortical Lgl might be a consequence of the basal extension of the Par domain. These regulatory relationships should be further investigated since the basal extension of Par domain is not enough to cover the all basal-lateral domain of Lgl. Interestingly, the maintenance of Dlg at basolateral membranes despite the loss of Lgl and the shift in the localisation of Cdc42/Par6/aPKC and Crb is likely to be functionally significant, since Dlg is required requirement for the alignment of the mitotic spindle; a function that is separable from its role in epithelial polarity (Bergstralh et al., 2013; Nakajima et al., 2013).

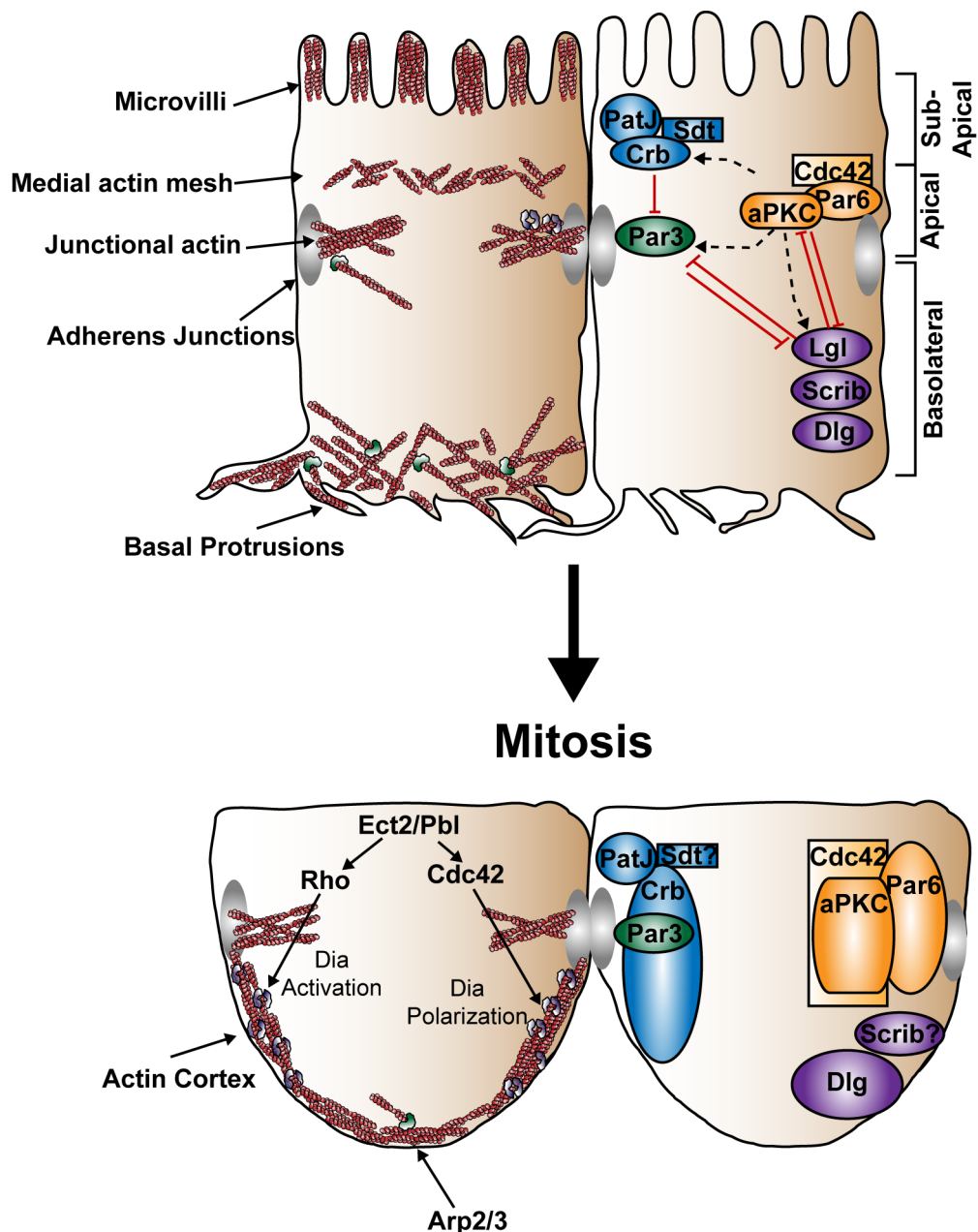


**Figure 7.4. 1. A model for actin regulation in mitosis.** Epithelial cells when entering mitosis change morphology from a columnar like shape to a more round shape. These changes are coupled with the disassembling of actin bundles and consecutively loss of microvilli at the apical side of cells and the assembly of an actin cortex via Diaphanous, downstream of a molecular pathway controlled by Ect2 and the activation of Rho GTPases Rho1 and Cdc42, which activate and polarize Dia, respectively. Junctional actin is maintained. Apico-basal polarity is also remodelled with apical polarity factors like Crb extending to more basal sides of the cell and the aPKC/Par6/Cdc42 complex also extending their apical domains. Baz/Par3 and adherens junctions shift their positions to more basal sides of the cell. Lgl is depolarized and Dlg is maintained to the basolateral side of cells with a slight extension of its domain to more basal sides of the cell.

## 8. OUTLOOK AND FUTURE PERSPECTIVES

In this thesis I presented a novel process of actin regulation in mitosis of epithelial cells, which appears to be dependent of the activity of Diaphanous, downstream of a molecular pathway controlled by the Rho GEF Pbl and Rho GTPases Rho1 and Cdc42. When epithelial cells of the notum enter mitosis cell shape changes are coupled with the remodelling of actin and Myosin II conferring the cell a round shape and a stiff contractile actin cortex. The *novo assembly* of an actin cortex is dependent of Pbl activity, a potent Rho GEF that both affects actin nucleation and Myosin activation in mitosis. The combined activity of Rho1 and Cdc42 GTPases, downstream of Pbl (Prokopenko et al., 1999; Tatsumoto et al., 1999), appear to activate Dia and properly polarized this actin nucleator at the cell cortex. Rho1 also activates Myosin II to promote a contractile actin cortex. Polarity protein aPKC acts similarly to Cdc42 polarizing Dia, supporting the role of the aPKC/Par6/Cdc42 complex in the regulation of the actin cytoskeleton, also in mitosis. In the future, analyses of tissues with perturbed activity of polarity factors will enable to understand the establishment and consecutively function of polarity proteins in the control of the actin cytoskeleton during mitosis. Additionally, a new protocol of fly injection in the notum has been developed in our laboratory by the PhD student Nelio Rodriguez and me, which will enable a further comprehension of the actin cytoskeleton and apico-basal polarity in the process of cell division, taking the advantage of injecting specific drugs in the fly epithelium and followed the effects *in vivo*.

## 9. BIBLIOGRAPHY

- Abreu-Blanco, M.T., Verboon, J.M., and Parkhurst, S.M. (2011). Cell wound repair in *Drosophila* occurs through three distinct phases of membrane and cytoskeletal remodeling. *J Cell Biol* 193, 455-464.
- Adams, A.E., Botstein, D., and Drubin, D.G. (1991). Requirement of yeast fimbrin for actin organization and morphogenesis in vivo. *Nature* 354, 404-408.
- Afshar, K., Stuart, B., and Wasserman, S.A. (2000). Functional analysis of the *Drosophila* diaphanous FH protein in early embryonic development. *Development* 127, 1887-1897.
- Agnes, F., Suzanne, M., and Noselli, S. (1999). The *Drosophila* JNK pathway controls the morphogenesis of imaginal discs during metamorphosis. *Development* 126, 5453-5462.
- Aguda, A.H., Burtnick, L.D., and Robinson, R.C. (2005). The state of the filament. *EMBO Rep* 6, 220-226.
- Ahuja, R., Pinyol, R., Reichenbach, N., Custer, L., Klingensmith, J., Kessels, M.M., and Qualmann, B. (2007). Cordon-bleu is an actin nucleation factor and controls neuronal morphology. *Cell* 131, 337-350.
- Amano, M., Mukai, H., Ono, Y., Chihara, K., Matsui, T., Hamajima, Y., Okawa, K., Iwamatsu, A., and Kaibuchi, K. (1996). Identification of a putative target for Rho as the serine-threonine kinase protein kinase N. *Science* 271, 648-650.
- Anderson, D.C., Gill, J.S., Cinalli, R.M., and Nance, J. (2008). Polarization of the *C. elegans* embryo by RhoGAP-mediated exclusion of PAR-6 from cell contacts. *Science* 320, 1771-1774.
- Artavanis-Tsakonas, S., Rand, M.D., and Lake, R.J. (1999). Notch signaling: cell fate control and signal integration in development. *Science* 284, 770-776.
- Beck, M., Schmidt, A., Malmstroem, J., Claassen, M., Ori, A., Szymborska, A., Herzog, F., Rinner, O., Ellenberg, J., and Aebersold, R. (2011). The quantitative proteome of a human cell line. *Mol Syst Biol* 7, 549.

Bellaiche, Y., Gho, M., Kaltschmidt, J.A., Brand, A.H., and Schweisguth, F. (2001). Frizzled regulates localization of cell-fate determinants and mitotic spindle rotation during asymmetric cell division. *Nat Cell Biol* 3, 50-57.

Benink, H.A., and Bement, W.M. (2005). Concentric zones of active RhoA and Cdc42 around single cell wounds. *J Cell Biol* 168, 429-439.

Benton, R., and St Johnston, D. (2003). Drosophila PAR-1 and 14-3-3 inhibit Bazooka/PAR-3 to establish complementary cortical domains in polarized cells. *Cell* 115, 691-704.

Bergert, M., Chandradoss, S.D., Desai, R.A., and Paluch, E. (2012). Cell mechanics control rapid transitions between blebs and lamellipodia during migration. *Proc Natl Acad Sci U S A* 109, 14434-14439.

Bergstralh, D.T., Lovegrove, H.E., and St Johnston, D. (2013). Discs large links spindle orientation to apical-Basal polarity in Drosophila epithelia. *Curr Biol* 23, 1707-1712.

Bilder, D., Li, M., and Perrimon, N. (2000). Cooperative regulation of cell polarity and growth by Drosophila tumor suppressors. *Science* 289, 113-116.

Bilder, D., and Perrimon, N. (2000). Localization of apical epithelial determinants by the basolateral PDZ protein Scribble. *Nature* 403, 676-680.

Bilder, D., Schober, M., and Perrimon, N. (2003). Integrated activity of PDZ protein complexes regulates epithelial polarity. *Nat Cell Biol* 5, 53-58.

Blanchoin, L., Amann, K.J., Higgs, H.N., Marchand, J.B., Kaiser, D.A., and Pollard, T.D. (2000). Direct observation of dendritic actin filament networks nucleated by Arp2/3 complex and WASP/Scar proteins. *Nature* 404, 1007-1011.

Blanchoin, L., and Pollard, T.D. (2002). Hydrolysis of ATP by polymerized actin depends on the bound divalent cation but not profilin. *Biochemistry* 41, 597-602.

Blanchoin, L., Pollard, T.D., and Hitchcock-DeGregori, S.E. (2001). Inhibition of the Arp2/3 complex-nucleated actin polymerization and branch formation by tropomyosin. *Curr Biol* 11, 1300-1304.



Blaser, H., Reichman-Fried, M., Castanon, I., Dumstrei, K., Marlow, F.L., Kawakami, K., Solnica-Krezel, L., Heisenberg, C.P., and Raz, E. (2006). Migration of zebrafish primordial germ cells: a role for myosin contraction and cytoplasmic flow. *Dev Cell* 11, 613-627.

Block, J., Breitsprecher, D., Kuhn, S., Winterhoff, M., Kage, F., Geffers, R., Duwe, P., Rohn, J.L., Baum, B., Brakebusch, C., *et al.* (2012). FMNL2 Drives Actin-Based Protrusion and Migration Downstream of Cdc42. *Curr Biol*.

Bloor, J.W., and Kiehart, D.P. (2002). *Drosophila* RhoA regulates the cytoskeleton and cell-cell adhesion in the developing epidermis. *Development* 129, 3173-3183.

Boguski, M.S., and McCormick, F. (1993). Proteins regulating Ras and its relatives. *Nature* 366, 643-654.

Bompard, G., Rabeharivelo, G., Cau, J., Abrieu, A., Delsert, C., and Morin, N. (2012). P21-activated kinase 4 (PAK4) is required for metaphase spindle positioning and anchoring. *Oncogene*.

Bosch, M., Le, K.H., Bugyi, B., Correia, J.J., Renault, L., and Carlier, M.F. (2007). Analysis of the function of Spire in actin assembly and its synergy with formin and profilin. *Mol Cell* 28, 555-568.

Brand, A.H., Manoukian, A.S., and Perrimon, N. (1994). Ectopic expression in *Drosophila*. *Methods Cell Biol* 44, 635-654.

Bray, D., and White, J.G. (1988). Cortical flow in animal cells. *Science* 239, 883-888.

Breitsprecher, D., and Goode, B.L. (2013). Formins at a glance. *J Cell Sci* 126, 1-7.

Bretscher, A., Edwards, K., and Fehon, R.G. (2002). ERM proteins and merlin: integrators at the cell cortex. *Nat Rev Mol Cell Biol* 3, 586-599.

Briggs, M.W., and Sacks, D.B. (2003). IQGAP proteins are integral components of cytoskeletal regulation. *EMBO Rep* 4, 571-574.

Bugyi, B., Didry, D., and Carlier, M.F. (2010). How tropomyosin regulates lamellipodial actin-based motility: a combined biochemical and reconstituted motility approach. *EMBO J* 29, 14-26.

Bulgakova, N.A., and Knust, E. (2009). The Crumbs complex: from epithelial-cell polarity to retinal degeneration. *J Cell Sci* 122, 2587-2596.

Cabernard, C. (2012). Cytokinesis in *Drosophila melanogaster*. Cytoskeleton (Hoboken).

Calleja, M., Herranz, H., Estella, C., Casal, J., Lawrence, P., Simpson, P., and Morata, G. (2000). Generation of medial and lateral dorsal body domains by the pannier gene of *Drosophila*. *Development* 127, 3971-3980.

Campellone, K.G., and Welch, M.D. (2010). A nucleator arms race: cellular control of actin assembly. *Nat Rev Mol Cell Biol* 11, 237-251.

Cant, K., Knowles, B.A., Mahajan-Miklos, S., Heintzelman, M., and Cooley, L. (1998). *Drosophila* fascin mutants are rescued by overexpression of the villin-like protein, quail. *J Cell Sci* 111 ( Pt 2), 213-221.

Cant, K., Knowles, B.A., Mooseker, M.S., and Cooley, L. (1994). *Drosophila* singed, a fascin homolog, is required for actin bundle formation during oogenesis and bristle extension. *J Cell Biol* 125, 369-380.

Carlier, M.F., and Pantaloni, D. (1986). Direct evidence for ADP-Pi-F-actin as the major intermediate in ATP-actin polymerization. Rate of dissociation of Pi from actin filaments. *Biochemistry* 25, 7789-7792.

Carlier, M.F., Pantaloni, D., Evans, J.A., Lambooy, P.K., Korn, E.D., and Webb, M.R. (1988). The hydrolysis of ATP that accompanies actin polymerization is essentially irreversible. *FEBS Lett* 235, 211-214.

Carminati, J.L., and Stearns, T. (1997). Microtubules orient the mitotic spindle in yeast through dynein-dependent interactions with the cell cortex. *J Cell Biol* 138, 629-641.

Carramusa, L., Ballestrem, C., Zilberman, Y., and Bershadsky, A.D. (2007). Mammalian diaphanous-related formin Dia1 controls the organization of E-cadherin-mediated cell-cell junctions. *J Cell Sci* 120, 3870-3882.

Carreno, S., Kouranti, I., Glusman, E.S., Fuller, M.T., Echard, A., and Payre, F. (2008). Moesin and its activating kinase Slik are required for cortical stability and microtubule organization in mitotic cells. *J Cell Biol* 180, 739-746.

Castanon, I., Abrami, L., Holtzer, L., Heisenberg, C.P., van der Goot, F.G., and Gonzalez-Gaitan, M. (2012). Anthrax toxin receptor 2a controls mitotic spindle positioning. *Nat Cell Biol* 15, 28-39.

Castanon, I., Abrami, L., Holtzer, L., Heisenberg, C.P., van der Goot, F.G., and Gonzalez-Gaitan, M. (2013). Anthrax toxin receptor 2a controls mitotic spindle positioning. *Nat Cell Biol* 15, 28-39.

Castrillon, D.H., and Wasserman, S.A. (1994). Diaphanous is required for cytokinesis in *Drosophila* and shares domains of similarity with the products of the limb deformity gene. *Development* 120, 3367-3377.

Cavodeassi, F., Modolell, J., and Gomez-Skarmeta, J.L. (2001). The Iroquois family of genes: from body building to neural patterning. *Development* 128, 2847-2855.

Chalamalasetty, R.B., Hummer, S., Nigg, E.A., and Sillje, H.H. (2006). Influence of human Ect2 depletion and overexpression on cleavage furrow formation and abscission. *J Cell Sci* 119, 3008-3019.

Chalmers, A.D., Pambos, M., Mason, J., Lang, S., Wylie, C., and Papalopulu, N. (2005). aPKC, Crumbs3 and Lgl2 control apicobasal polarity in early vertebrate development. *Development* 132, 977-986.

Chang, F., Drubin, D., and Nurse, P. (1997). cdc12p, a protein required for cytokinesis in fission yeast, is a component of the cell division ring and interacts with profilin. *J Cell Biol* 137, 169-182.

Charras, G.T., Coughlin, M., Mitchison, T.J., and Mahadevan, L. (2008). Life and times of a cellular bleb. *Biophys J* 94, 1836-1853.

Charras, G.T., Hu, C.K., Coughlin, M., and Mitchison, T.J. (2006). Reassembly of contractile actin cortex in cell blebs. *J Cell Biol* 175, 477-490.

Chen, W.T. (1981). Mechanism of retraction of the trailing edge during fibroblast movement. *J Cell Biol* 90, 187-200.

Chen, Z., Borek, D., Padrick, S.B., Gomez, T.S., Metlagel, Z., Ismail, A.M., Umetani, J., Billadeau, D.D., Otwinowski, Z., and Rosen, M.K. (2010). Structure and control of the actin regulatory WAVE complex. *Nature* 468, 533-538.

Chereau, D., Boczkowska, M., Skwarek-Maruszewska, A., Fujiwara, I., Hayes, D.B., Rebowski, G., Lappalainen, P., Pollard, T.D., and

Dominguez, R. (2008). Leiomodin is an actin filament nucleator in muscle cells. *Science* **320**, 239-243.

Chesarone, M.A., DuPage, A.G., and Goode, B.L. (2010). Unleashing formins to remodel the actin and microtubule cytoskeletons. *Nat Rev Mol Cell Biol* **11**, 62-74.

Chesarone, M.A., and Goode, B.L. (2009). Actin nucleation and elongation factors: mechanisms and interplay. *Curr Opin Cell Biol* **21**, 28-37.

Clark, A.G., Dierkes, K., and Paluch, E.K. (2013). Monitoring actin cortex thickness in live cells. *Biophys J* **105**, 570-580.

Cohen, M., Georgiou, M., Stevenson, N.L., Miodownik, M., and Baum, B. (2010). Dynamic filopodia transmit intermittent Delta-Notch signaling to drive pattern refinement during lateral inhibition. *Dev Cell* **19**, 78-89.

Connell, M., Cabernard, C., Ricketson, D., Doe, C.Q., and Prehoda, K.E. (2011). Asymmetric cortical extension shifts cleavage furrow position in *Drosophila* neuroblasts. *Mol Biol Cell* **22**, 4220-4226.

Cowan, C.R., and Hyman, A.A. (2007). Acto-myosin reorganization and PAR polarity in *C. elegans*. *Development* **134**, 1035-1043.

Cramer, L.P. (2010). Forming the cell rear first: breaking cell symmetry to trigger directed cell migration. *Nat Cell Biol* **12**, 628-632.

Cramer, L.P., and Mitchison, T.J. (1997). Investigation of the mechanism of retraction of the cell margin and rearward flow of nodules during mitotic cell rounding. *Mol Biol Cell* **8**, 109-119.

Cramer, L.P., Siebert, M., and Mitchison, T.J. (1997). Identification of novel graded polarity actin filament bundles in locomoting heart fibroblasts: implications for the generation of motile force. *J Cell Biol* **136**, 1287-1305.

Dao, V.T., Dupuy, A.G., Gavet, O., Caron, E., and de Gunzburg, J. (2009). Dynamic changes in Rap1 activity are required for cell retraction and spreading during mitosis. *J Cell Sci* **122**, 2996-3004.

Das, M., Drake, T., Wiley, D.J., Buchwald, P., Vavylonis, D., and Verde, F. (2012). Oscillatory dynamics of Cdc42 GTPase in the control of polarized growth. *Science* **337**, 239-243.

Dawes-Hoang, R.E., Parmar, K.M., Christiansen, A.E., Phelps, C.B., Brand, A.H., and Wieschaus, E.F. (2005). folded gastrulation, cell shape change and the control of myosin localization. *Development* 132, 4165-4178.

Derivery, E., Sousa, C., Gautier, J.J., Lombard, B., Loew, D., and Gautreau, A. (2009). The Arp2/3 activator WASH controls the fission of endosomes through a large multiprotein complex. *Dev Cell* 17, 712-723.

DeRosier, D.J., and Tilney, L.G. (2000). F-actin bundles are derivatives of microvilli: What does this tell us about how bundles might form? *J Cell Biol* 148, 1-6.

Dietzl, G., Chen, D., Schnorrer, F., Su, K.C., Barinova, Y., Fellner, M., Gasser, B., Kinsey, K., Oppel, S., Scheiblauer, S., *et al.* (2007). A genome-wide transgenic RNAi library for conditional gene inactivation in *Drosophila*. *Nature* 448, 151-156.

Dominguez, R., and Holmes, K.C. (2011). Actin structure and function. *Annu Rev Biophys* 40, 169-186.

Dong, Y., Pruyne, D., and Bretscher, A. (2003). Formin-dependent actin assembly is regulated by distinct modes of Rho signaling in yeast. *J Cell Biol* 161, 1081-1092.

Durgan, J., Kaji, N., Jin, D., and Hall, A. (2011). Par6B and atypical PKC regulate mitotic spindle orientation during epithelial morphogenesis. *J Biol Chem* 286, 12461-12474.

Eden, S., Rohatgi, R., Podtelejnikov, A.V., Mann, M., and Kirschner, M.W. (2002). Mechanism of regulation of WAVE1-induced actin nucleation by Rac1 and Nck. *Nature* 418, 790-793.

Eisenmann, K.M., Harris, E.S., Kitchen, S.M., Holman, H.A., Higgs, H.N., and Alberts, A.S. (2007). Dia-interacting protein modulates formin-mediated actin assembly at the cell cortex. *Curr Biol* 17, 579-591.

Elliott, D.A., and Brand, A.H. (2008). The GAL4 system : a versatile system for the expression of genes. *Methods Mol Biol* 420, 79-95.

Etienne-Manneville, S. (2004). Cdc42--the centre of polarity. *J Cell Sci* 117, 1291-1300.

Etienne-Manneville, S., and Hall, A. (2001). Integrin-mediated activation of Cdc42 controls cell polarity in migrating astrocytes through PKCzeta. *Cell* 106, 489-498.

Etienne-Manneville, S., and Hall, A. (2002). Rho GTPases in cell biology. *Nature* 420, 629-635.

Evangelista, M., Blundell, K., Longtine, M.S., Chow, C.J., Adames, N., Pringle, J.R., Peter, M., and Boone, C. (1997). Bni1p, a yeast formin linking cdc42p and the actin cytoskeleton during polarized morphogenesis. *Science* 276, 118-122.

Evangelista, M., Pruyne, D., Amberg, D.C., Boone, C., and Bretscher, A. (2002). Formins direct Arp2/3-independent actin filament assembly to polarize cell growth in yeast. *Nat Cell Biol* 4, 260-269.

Evangelista, M., Zigmond, S., and Boone, C. (2003). Formins: signaling effectors for assembly and polarization of actin filaments. *J Cell Sci* 116, 2603-2611.

Evezika, O.C., Younger, N.S., Lu, J., Kaiser, D.A., Corbin, Z.A., Nolen, B.J., Kovar, D.R., and Pollard, T.D. (2009). Incompatibility with formin Cdc12p prevents human profilin from substituting for fission yeast profilin: insights from crystal structures of fission yeast profilin. *J Biol Chem* 284, 2088-2097.

Fededa, J.P., and Gerlich, D.W. (2012). Molecular control of animal cell cytokinesis. *Nat Cell Biol* 14, 440-447.

Fehon, R.G., McClatchey, A.I., and Bretscher, A. (2010). Organizing the cell cortex: the role of ERM proteins. *Nat Rev Mol Cell Biol* 11, 276-287.

Fehon, R.G., Oren, T., LaJeunesse, D.R., Melby, T.E., and McCartney, B.M. (1997). Isolation of mutations in the Drosophila homologues of the human Neurofibromatosis 2 and yeast CDC42 genes using a simple and efficient reverse-genetic method. *Genetics* 146, 245-252.

Field, C.M., Wuhr, M., Anderson, G.A., Kueh, H.Y., Strickland, D., and Mitchison, T.J. (2011). Actin behavior in bulk cytoplasm is cell cycle regulated in early vertebrate embryos. *J Cell Sci* 124, 2086-2095.

Fink, J., Carpi, N., Betz, T., Betard, A., Chebah, M., Azioune, A., Bornens, M., Sykes, C., Fetler, L., Cuvelier, D., *et al.* (2010). External forces control mitotic spindle positioning. *Nat Cell Biol* 13, 771-778.

Fletcher, G.C., Lucas, E.P., Brain, R., Tournier, A., and Thompson, B.J. (2012). Positive feedback and mutual antagonism combine to polarize Crumbs in the *Drosophila* follicle cell epithelium. *Curr Biol* 22, 1116-1122.

Founounou, N., Loyer, N., and Le Borgne, R. (2013). Septins regulate the contractility of the actomyosin ring to enable adherens junction remodeling during cytokinesis of epithelial cells. *Dev Cell* 24, 242-255.

Fowler, W.E., and Aebi, U. (1983). A consistent picture of the actin filament related to the orientation of the actin molecule. *J Cell Biol* 97, 264-269.

Fox, D.T., and Peifer, M. (2007). Abelson kinase (Abl) and RhoGEF2 regulate actin organization during cell constriction in *Drosophila*. *Development* 134, 567-578.

Friedl, P., Borgmann, S., and Bocker, E.B. (2001). Amoeboid leukocyte crawling through extracellular matrix: lessons from the *Dictyostelium* paradigm of cell movement. *J Leukoc Biol* 70, 491-509.

Furukawa, R., and Fechheimer, M. (1997). The structure, function, and assembly of actin filament bundles. *Int Rev Cytol* 175, 29-90.

Fyrberg, E.A., Kindle, K.L., Davidson, N., and Kindle, K.L. (1980). The actin genes of *Drosophila*: a dispersed multigene family. *Cell* 19, 365-378.

Fyrberg, E.A., Mahaffey, J.W., Bond, B.J., and Davidson, N. (1983). Transcripts of the six *Drosophila* actin genes accumulate in a stage- and tissue-specific manner. *Cell* 33, 115-123.

Galletta, B.J., and Cooper, J.A. (2009). Actin and endocytosis: mechanisms and phylogeny. *Curr Opin Cell Biol* 21, 20-27.

Genova, J.L., Jong, S., Camp, J.T., and Fehon, R.G. (2000). Functional analysis of Cdc42 in actin filament assembly, epithelial morphogenesis, and cell signaling during *Drosophila* development. *Dev Biol* 221, 181-194.

George, S.P., Wang, Y., Mathew, S., Srinivasan, K., and Khurana, S. (2007). Dimerization and actin-bundling properties of villin and its role in the assembly of epithelial cell brush borders. *J Biol Chem* 282, 26528-26541.

Georgiou, M., and Baum, B. (2010). Polarity proteins and Rho GTPases cooperate to spatially organise epithelial actin-based protrusions. *J Cell Sci* 123, 1089-1098.

Georgiou, M., Marinari, E., Burden, J., and Baum, B. (2008). Cdc42, Par6, and aPKC regulate Arp2/3-mediated endocytosis to control local adherens junction stability. *Curr Biol* 18, 1631-1638.

Girao, H., Geli, M.I., and Idrissi, F.Z. (2008). Actin in the endocytic pathway: from yeast to mammals. *FEBS Lett* 582, 2112-2119.

Glotzer, M. (2001). Animal cell cytokinesis. *Annu Rev Cell Dev Biol* 17, 351-386.

Goehring, N.W., Trong, P.K., Bois, J.S., Chowdhury, D., Nicola, E.M., Hyman, A.A., and Grill, S.W. (2011). Polarization of PAR proteins by advective triggering of a pattern-forming system. *Science* 334, 1137-1141.

Goldstein, B., and Hird, S.N. (1996). Specification of the anteroposterior axis in *Caenorhabditis elegans*. *Development* 122, 1467-1474.

Goley, E.D., and Welch, M.D. (2006). The ARP2/3 complex: an actin nucleator comes of age. *Nat Rev Mol Cell Biol* 7, 713-726.

Gomez-Skarmeta, J.L., Diez del Corral, R., de la Calle-Mustienes, E., Ferre-Marco, D., and Modolell, J. (1996). Araucan and caupolican, two members of the novel iroquois complex, encode homeoproteins that control proneural and vein-forming genes. *Cell* 85, 95-105.

Gonczy, P., and Rose, L.S. (2005). Asymmetric cell division and axis formation in the embryo. *WormBook*, 1-20.

Goode, B.L., and Eck, M.J. (2007). Mechanism and function of formins in the control of actin assembly. *Annu Rev Biochem* 76, 593-627.

Green, R.A., Paluch, E., and Oegema, K. (2012). Cytokinesis in Animal Cells. *Annu Rev Cell Dev Biol*.

Grosshans, J., Wenzl, C., Herz, H.M., Bartoszewski, S., Schnorrer, F., Vogt, N., Schwarz, H., and Muller, H.A. (2005). RhoGEF2 and the



formin Dia control the formation of the furrow canal by directed actin assembly during *Drosophila* cellularisation. *Development* **132**, 1009-1020.

Guilgur, L.G., Prudencio, P., Ferreira, T., Pimenta-Marques, A.R., and Martinho, R.G. (2012). *Drosophila* aPKC is required for mitotic spindle orientation during symmetric division of epithelial cells. *Development* **139**, 503-513.

Guillot, C., and Lecuit, T. (2013). Adhesion disengagement uncouples intrinsic and extrinsic forces to drive cytokinesis in epithelial tissues. *Dev Cell* **24**, 227-241.

Hacker, U., and Perrimon, N. (1998). DRhoGEF2 encodes a member of the Dbl family of oncogenes and controls cell shape changes during gastrulation in *Drosophila*. *Genes Dev* **12**, 274-284.

Hakeda-Suzuki, S., Ng, J., Tzu, J., Dietzl, G., Sun, Y., Harms, M., Nardine, T., Luo, L., and Dickson, B.J. (2002). Rac function and regulation during *Drosophila* development. *Nature* **416**, 438-442.

Hall, A. (1998). Rho GTPases and the actin cytoskeleton. *Science* **279**, 509-514.

Hall, A. (2005). Rho GTPases and the control of cell behaviour. *Biochem Soc Trans* **33**, 891-895.

Hall, A. (2012). Rho family GTPases. *Biochem Soc Trans* **40**, 1378-1382.

Hall, A., and Nobes, C.D. (2000). Rho GTPases: molecular switches that control the organization and dynamics of the actin cytoskeleton. *Philos Trans R Soc Lond B Biol Sci* **355**, 965-970.

Hamill, O.P., and Martinac, B. (2001). Molecular basis of mechanotransduction in living cells. *Physiol Rev* **81**, 685-740.

Hanakam, F., Albrecht, R., Eckerskorn, C., Matzner, M., and Gerisch, G. (1996). Myristoylated and non-myristoylated forms of the pH sensor protein hisactophilin II: intracellular shuttling to plasma membrane and nucleus monitored in real time by a fusion with green fluorescent protein. *EMBO J* **15**, 2935-2943.

Hannemann, S., Madrid, R., Stastna, J., Kitzing, T., Gasteier, J., Schonichen, A., Bouchet, J., Jimenez, A., Geyer, M., Grosse, R., *et al.*

(2008). The Diaphanous-related Formin FHOD1 associates with ROCK1 and promotes Src-dependent plasma membrane blebbing. *J Biol Chem* 283, 27891-27903.

Hara, T., Abe, M., Inoue, H., Yu, L.R., Veenstra, T.D., Kang, Y.H., Lee, K.S., and Miki, T. (2006). Cytokinesis regulator ECT2 changes its conformation through phosphorylation at Thr-341 in G2/M phase. *Oncogene* 25, 566-578.

Hariharan, I.K., Hu, K.Q., Asha, H., Quintanilla, A., Ezzell, R.M., and Settleman, J. (1995). Characterization of rho GTPase family homologues in *Drosophila melanogaster*: overexpressing Rho1 in retinal cells causes a late developmental defect. *EMBO J* 14, 292-302.

Harris, E.S., Li, F., and Higgs, H.N. (2004). The mouse formin, FRLalpha, slows actin filament barbed end elongation, competes with capping protein, accelerates polymerization from monomers, and severs filaments. *J Biol Chem* 279, 20076-20087.

Harris, K.P., and Tepass, U. (2008). Cdc42 and Par proteins stabilize dynamic adherens junctions in the *Drosophila* neuroectoderm through regulation of apical endocytosis. *J Cell Biol* 183, 1129-1143.

Harris, T.J., and Peifer, M. (2004). Adherens junction-dependent and -independent steps in the establishment of epithelial cell polarity in *Drosophila*. *J Cell Biol* 167, 135-147.

Harris, T.J., and Peifer, M. (2005). The positioning and segregation of apical cues during epithelial polarity establishment in *Drosophila*. *J Cell Biol* 170, 813-823.

Hartenstein, V., and Posakony, J.W. (1990). A dual function of the Notch gene in *Drosophila* sensillum development. *Dev Biol* 142, 13-30.

Hartwig, J.H., and Stossel, T.P. (1975). Isolation and properties of actin, myosin, and a new actinbinding protein in rabbit alveolar macrophages. *J Biol Chem* 250, 5696-5705.

Heasman, S.J., and Ridley, A.J. (2008). Mammalian Rho GTPases: new insights into their functions from in vivo studies. *Nat Rev Mol Cell Biol* 9, 690-701.

Heil-Chapdelaine, R.A., Adames, N.R., and Cooper, J.A. (1999). Formin' the connection between microtubules and the cell cortex. *J Cell Biol* 144, 809-811.

Heitzler, P., and Simpson, P. (1991). The choice of cell fate in the epidermis of *Drosophila*. *Cell* 64, 1083-1092.

Heng, Y.W., and Koh, C.G. (2010). Actin cytoskeleton dynamics and the cell division cycle. *Int J Biochem Cell Biol* 42, 1622-1633.

Herszterg, S., Leibfried, A., Bosveld, F., Martin, C., and Bellaiche, Y. (2013). Interplay between the dividing cell and its neighbors regulates adherens junction formation during cytokinesis in epithelial tissue. *Dev Cell* 24, 256-270.

Higgs, H.N., and Pollard, T.D. (2000). Activation by Cdc42 and PIP(2) of Wiskott-Aldrich syndrome protein (WASp) stimulates actin nucleation by Arp2/3 complex. *J Cell Biol* 150, 1311-1320.

Homem, C.C., and Peifer, M. (2008). Diaphanous regulates myosin and adherens junctions to control cell contractility and protrusive behavior during morphogenesis. *Development* 135, 1005-1018.

Hotulainen, P., and Lappalainen, P. (2006). Stress fibers are generated by two distinct actin assembly mechanisms in motile cells. *J Cell Biol* 173, 383-394.

Hudson, A.M., and Cooley, L. (2002). Understanding the function of actin-binding proteins through genetic analysis of *Drosophila* oogenesis. *Annu Rev Genet* 36, 455-488.

Hussain, N.K., Jenna, S., Glogauer, M., Quinn, C.C., Wasiak, S., Guipponi, M., Antonarakis, S.E., Kay, B.K., Stossel, T.P., Lamarche-Vane, N., *et al.* (2001). Endocytic protein intersectin-I regulates actin assembly via Cdc42 and N-WASP. *Nat Cell Biol* 3, 927-932.

Hutterer, A., Betschinger, J., Petronczki, M., and Knoblich, J.A. (2004). Sequential roles of Cdc42, Par-6, aPKC, and Lgl in the establishment of epithelial polarity during *Drosophila* embryogenesis. *Dev Cell* 6, 845-854.

Hwang, E., Kusch, J., Barral, Y., and Huffaker, T.C. (2003). Spindle orientation in *Saccharomyces cerevisiae* depends on the transport of microtubule ends along polarized actin cables. *J Cell Biol* 161, 483-488.

Innocenti, M., Gerboth, S., Rottner, K., Lai, F.P., Hertzog, M., Stradal, T.E., Frittoli, E., Didry, D., Polo, S., Disanza, A., *et al.* (2005). Abi1 regulates the activity of N-WASP and WAVE in distinct actin-based processes. *Nat Cell Biol* 7, 969-976.

Izaddoost, S., Nam, S.C., Bhat, M.A., Bellen, H.J., and Choi, K.W. (2002). *Drosophila* Crumbs is a positional cue in photoreceptor adherens junctions and rhabdomeres. *Nature* 416, 178-183.

Jacinto, A., Wood, W., Woolner, S., Hiley, C., Turner, L., Wilson, C., Martinez-Arias, A., and Martin, P. (2002). Dynamic analysis of actin cable function during *Drosophila* dorsal closure. *Curr Biol* 12, 1245-1250.

Jaffe, A.B., Kaji, N., Durgan, J., and Hall, A. (2008). Cdc42 controls spindle orientation to position the apical surface during epithelial morphogenesis. *J Cell Biol* 183, 625-633.

Jenkins, N., Saam, J.R., and Mango, S.E. (2006). CYK-4/GAP provides a localized cue to initiate anteroposterior polarity upon fertilization. *Science* 313, 1298-1301.

Joberty, G., Petersen, C., Gao, L., and Macara, I.G. (2000). The cell-polarity protein Par6 links Par3 and atypical protein kinase C to Cdc42. *Nat Cell Biol* 2, 531-539.

Johnson, D.I. (1999). Cdc42: An essential Rho-type GTPase controlling eukaryotic cell polarity. *Microbiol Mol Biol Rev* 63, 54-105.

Joseph, J.M., Fey, P., Ramalingam, N., Liu, X.I., Rohlf, M., Noegel, A.A., Muller-Taubenberger, A., Glockner, G., and Schleicher, M. (2008). The actinome of *Dictyostelium discoideum* in comparison to actins and actin-related proteins from other organisms. *PLoS One* 3, e2654.

Kaksonen, M., Sun, Y., and Drubin, D.G. (2003). A pathway for association of receptors, adaptors, and actin during endocytic internalization. *Cell* 115, 475-487.

Kaksonen, M., Toret, C.P., and Drubin, D.G. (2005). A modular design for the clathrin- and actin-mediated endocytosis machinery. *Cell* 123, 305-320.

Kaksonen, M., Toret, C.P., and Drubin, D.G. (2006). Harnessing actin dynamics for clathrin-mediated endocytosis. *Nat Rev Mol Cell Biol* 7, 404-414.

Kemphues, K.J., Priess, J.R., Morton, D.G., and Cheng, N.S. (1988). Identification of genes required for cytoplasmic localization in early *C. elegans* embryos. *Cell* 52, 311-320.

Kerkhoff, E. (2006). Cellular functions of the Spir actin-nucleation factors. *Trends Cell Biol* 16, 477-483.

Kessels, M.M., and Qualmann, B. (2002). Syndapins integrate N-WASP in receptor-mediated endocytosis. *EMBO J* 21, 6083-6094.

Khurana, S., and George, S.P. (2011). The role of actin bundling proteins in the assembly of filopodia in epithelial cells. *Cell Adh Migr* 5, 409-420.

Kimura, K., Ito, M., Amano, M., Chihara, K., Fukata, Y., Nakafuku, M., Yamamori, B., Feng, J., Nakano, T., Okawa, K., *et al.* (1996). Regulation of myosin phosphatase by Rho and Rho-associated kinase (Rho-kinase). *Science* 273, 245-248.

Kindle, K.L., and Firtel, R.A. (1978). Identification and analysis of Dictyostelium actin genes, a family of moderately repeated genes. *Cell* 15, 763-778.

King, J.S., Veltman, D.M., Georgiou, M., Baum, B., and Insall, R.H. (2010). SCAR/WAVE is activated at mitosis and drives myosin-independent cytokinesis. *J Cell Sci* 123, 2246-2255.

Kiyomitsu, T., and Cheeseman, I.M. (2013). Cortical Dynein and asymmetric membrane elongation coordinately position the spindle in anaphase. *Cell* 154, 391-402.

Kobielak, A., Pasolli, H.A., and Fuchs, E. (2004). Mammalian formin-1 participates in adherens junctions and polymerization of linear actin cables. *Nat Cell Biol* 6, 21-30.

Kolsch, V., Seher, T., Fernandez-Ballester, G.J., Serrano, L., and Leptin, M. (2007). Control of Drosophila gastrulation by apical localization of adherens junctions and RhoGEF2. *Science* 315, 384-386.

Kondo, T., and Hayashi, S. (2013). Mitotic cell rounding accelerates epithelial invagination. *Nature*.

Kooh, P.J., Fehon, R.G., and Muskavitch, M.A. (1993). Implications of dynamic patterns of Delta and Notch expression for cellular interactions during *Drosophila* development. *Development* *117*, 493-507.

Kovacs, E.M., Goodwin, M., Ali, R.G., Paterson, A.D., and Yap, A.S. (2002). Cadherin-directed actin assembly: E-cadherin physically associates with the Arp2/3 complex to direct actin assembly in nascent adhesive contacts. *Curr Biol* *12*, 379-382.

Kovacs, E.M., Verma, S., Ali, R.G., Ratheesh, A., Hamilton, N.A., Akhmanova, A., and Yap, A.S. (2011). N-WASP regulates the epithelial junctional actin cytoskeleton through a non-canonical post-nucleation pathway. *Nat Cell Biol* *13*, 934-943.

Kovar, D.R., Harris, E.S., Mahaffy, R., Higgs, H.N., and Pollard, T.D. (2006). Control of the assembly of ATP- and ADP-actin by formins and profilin. *Cell* *124*, 423-435.

Kovar, D.R., Kuhn, J.R., Tichy, A.L., and Pollard, T.D. (2003). The fission yeast cytokinesis formin Cdc12p is a barbed end actin filament capping protein gated by profilin. *J Cell Biol* *161*, 875-887.

Kovar, D.R., and Pollard, T.D. (2004). Insertional assembly of actin filament barbed ends in association with formins produces piconewton forces. *Proc Natl Acad Sci U S A* *101*, 14725-14730.

Krause, M., Dent, E.W., Bear, J.E., Loureiro, J.J., and Gertler, F.B. (2003). Ena/VASP proteins: regulators of the actin cytoskeleton and cell migration. *Annu Rev Cell Dev Biol* *19*, 541-564.

Kunda, P., and Baum, B. (2009). The actin cytoskeleton in spindle assembly and positioning. *Trends Cell Biol* *19*, 174-179.

Kunda, P., Craig, G., Dominguez, V., and Baum, B. (2003). Abi, Sra1, and Kette control the stability and localization of SCAR/WAVE to regulate the formation of actin-based protrusions. *Curr Biol* *13*, 1867-1875.

Kunda, P., Pelling, A.E., Liu, T., and Baum, B. (2008a). Moesin controls cortical rigidity, cell rounding, and spindle morphogenesis during mitosis. *Curr Biol* *18*, 91-101.

Kunda, P., Rodrigues, N.T., Moeendarbary, E., Liu, T., Ivetic, A., Charras, G., and Baum, B. (2012). PP1-mediated moesin

dephosphorylation couples polar relaxation to mitotic exit. *Curr Biol* 22, 231-236.

Kunda, P., Rohn, J.L., and Baum, B. (2008b). Cell shape: taking the heat. *Curr Biol* 18, R470-472.

Lammers, M., Rose, R., Scrima, A., and Wittinghofer, A. (2005). The regulation of mDia1 by autoinhibition and its release by Rho\*GTP. *EMBO J* 24, 4176-4187.

Lancaster, O.M., Le Berre, M., Dimitracopoulos, A., Bonazzi, D., Zlotek-Zlotkiewicz, E., Picone, R., Duke, T., Piel, M., and Baum, B. (2013). Mitotic rounding alters cell geometry to ensure efficient bipolar spindle formation. *Dev Cell* 25, 270-283.

Laster, S.M., and Mackenzie, J.M., Jr. (1996). Bleb formation and F-actin distribution during mitosis and tumor necrosis factor-induced apoptosis. *Microsc Res Tech* 34, 272-280.

Lazarides, E., and Burridge, K. (1975). Alpha-actinin: immunofluorescent localization of a muscle structural protein in nonmuscle cells. *Cell* 6, 289-298.

Le Borgne, R., Bellaiche, Y., and Schweisguth, F. (2002). Drosophila E-cadherin regulates the orientation of asymmetric cell division in the sensory organ lineage. *Curr Biol* 12, 95-104.

Le Borgne, R., and Schweisguth, F. (2003). Unequal segregation of Neuralized biases Notch activation during asymmetric cell division. *Dev Cell* 5, 139-148.

Lechler, T., Jonsdottir, G.A., Klee, S.K., Pellman, D., and Li, R. (2001). A two-tiered mechanism by which Cdc42 controls the localization and activation of an Arp2/3-activating motor complex in yeast. *J Cell Biol* 155, 261-270.

Lehner, C.F. (1992). The pebble gene is required for cytokinesis in Drosophila. *J Cell Sci* 103 ( Pt 4), 1021-1030.

Leibfried, A., Fricke, R., Morgan, M.J., Bogdan, S., and Bellaiche, Y. (2008). Drosophila Cip4 and WASp define a branch of the Cdc42-Par6-aPKC pathway regulating E-cadherin endocytosis. *Curr Biol* 18, 1639-1648.

Leventis, P.A., Chow, B.M., Stewart, B.A., Iyengar, B., Campos, A.R., and Boulianne, G.L. (2001). *Drosophila* Amphiphysin is a post-synaptic protein required for normal locomotion but not endocytosis. *Traffic* 2, 839-850.

Lewis, A.K., and Bridgman, P.C. (1992). Nerve growth cone lamellipodia contain two populations of actin filaments that differ in organization and polarity. *J Cell Biol* 119, 1219-1243.

Li, F., and Higgs, H.N. (2003). The mouse Formin mDia1 is a potent actin nucleation factor regulated by autoinhibition. *Curr Biol* 13, 1335-1340.

Li, M.G., Serr, M., Edwards, K., Ludmann, S., Yamamoto, D., Tilney, L.G., Field, C.M., and Hays, T.S. (1999). Filamin is required for ring canal assembly and actin organization during *Drosophila* oogenesis. *J Cell Biol* 146, 1061-1074.

Lin, D., Edwards, A.S., Fawcett, J.P., Mbamalu, G., Scott, J.D., and Pawson, T. (2000). A mammalian PAR-3-PAR-6 complex implicated in Cdc42/Rac1 and aPKC signalling and cell polarity. *Nat Cell Biol* 2, 540-547.

Lin, J.J., Warren, K.S., Wamboldt, D.D., Wang, T., and Lin, J.L. (1997). Tropomyosin isoforms in nonmuscle cells. *Int Rev Cytol* 170, 1-38.

Lindberg, U., Schutt, C.E., Goldman, R.D., Nyakern-Meazza, M., Hillberg, L., Rathje, L.S., and Grenklo, S. (2008). Tropomyosins regulate the impact of actin binding proteins on actin filaments. *Adv Exp Med Biol* 644, 223-231.

Lindqvist, A., Rodriguez-Bravo, V., and Medema, R.H. (2009). The decision to enter mitosis: feedback and redundancy in the mitotic entry network. *J Cell Biol* 185, 193-202.

Liu, H.P., and Bretscher, A. (1989). Disruption of the single tropomyosin gene in yeast results in the disappearance of actin cables from the cytoskeleton. *Cell* 57, 233-242.

Longo, F.J., and Chen, D.Y. (1985). Development of cortical polarity in mouse eggs: involvement of the meiotic apparatus. *Dev Biol* 107, 382-394.



Louvet, E., and Percipalle, P. (2009). Transcriptional control of gene expression by actin and myosin. *Int Rev Cell Mol Biol* 272, 107-147.

Luo, L., Liao, Y.J., Jan, L.Y., and Jan, Y.N. (1994). Distinct morphogenetic functions of similar small GTPases: *Drosophila* Drac1 is involved in axonal outgrowth and myoblast fusion. *Genes Dev* 8, 1787-1802.

Luxenburg, C., Pasolli, H.A., Williams, S.E., and Fuchs, E. (2011). Developmental roles for Srf, cortical cytoskeleton and cell shape in epidermal spindle orientation. *Nat Cell Biol* 13, 203-214.

Machacek, M., Hodgson, L., Welch, C., Elliott, H., Pertz, O., Nalbant, P., Abell, A., Johnson, G.L., Hahn, K.M., and Danuser, G. (2009). Coordination of Rho GTPase activities during cell protrusion. *Nature* 461, 99-103.

Machesky, L.M., Atkinson, S.J., Ampe, C., Vandekerckhove, J., and Pollard, T.D. (1994). Purification of a cortical complex containing two unconventional actins from *Acanthamoeba* by affinity chromatography on profilin-agarose. *J Cell Biol* 127, 107-115.

Madaule, P., Eda, M., Watanabe, N., Fujisawa, K., Matsuoka, T., Bito, H., Ishizaki, T., and Narumiya, S. (1998). Role of citron kinase as a target of the small GTPase Rho in cytokinesis. *Nature* 394, 491-494.

Maddox, A.S., and Burridge, K. (2003). RhoA is required for cortical retraction and rigidity during mitotic cell rounding. *J Cell Biol* 160, 255-265.

Maekawa, M., Ishizaki, T., Boku, S., Watanabe, N., Fujita, A., Iwamatsu, A., Obinata, T., Ohashi, K., Mizuno, K., and Narumiya, S. (1999). Signaling from Rho to the actin cytoskeleton through protein kinases ROCK and LIM-kinase. *Science* 285, 895-898.

Magie, C.R., Meyer, M.R., Gorsuch, M.S., and Parkhurst, S.M. (1999). Mutations in the Rho1 small GTPase disrupt morphogenesis and segmentation during early *Drosophila* development. *Development* 126, 5353-5364.

Maiti, S., Michelot, A., Gould, C., Blanchoin, L., Sokolova, O., and Goode, B.L. (2012). Structure and activity of full-length formin mDia1. *Cytoskeleton (Hoboken)* 69, 393-405.

Manseau, L.J., Ganetzky, B., and Craig, E.A. (1988). Molecular and genetic characterization of the *Drosophila melanogaster* 87E actin gene region. *Genetics* 119, 407-420.

Marinari, E., Mehonic, A., Curran, S., Gale, J., Duke, T., and Baum, B. (2012). Live-cell delamination counterbalances epithelial growth to limit tissue overcrowding. *Nature*.

Martin, A.C., Kaschube, M., and Wieschaus, E.F. (2009). Pulsed contractions of an actin-myosin network drive apical constriction. *Nature* 457, 495-499.

Martin-Blanco, E., Pastor-Pareja, J.C., and Garcia-Bellido, A. (2000). JNK and decapentaplegic signaling control adhesiveness and cytoskeleton dynamics during thorax closure in *Drosophila*. *Proc Natl Acad Sci U S A* 97, 7888-7893.

Matsudaira, P. (1991). Modular organization of actin crosslinking proteins. *Trends Biochem Sci* 16, 87-92.

Matsui, T., Amano, M., Yamamoto, T., Chihara, K., Nakafuku, M., Ito, M., Nakano, T., Okawa, K., Iwamatsu, A., and Kaibuchi, K. (1996). Rho-associated kinase, a novel serine/threonine kinase, as a putative target for small GTP binding protein Rho. *EMBO J* 15, 2208-2216.

Matthews, H.K., Delabre, U., Rohn, J.L., Guck, J., Kunda, P., and Baum, B. (2012). Changes in ect2 localization couple actomyosin-dependent cell shape changes to mitotic progression. *Dev Cell* 23, 371-383.

Mattila, P.K., and Lappalainen, P. (2008). Filopodia: molecular architecture and cellular functions. *Nat Rev Mol Cell Biol* 9, 446-454.

Mattison, C.P., Stumpff, J., Wordeman, L., and Winey, M. (2011). Mip1 associates with both the Mps1 kinase and actin, and is required for cell cortex stability and anaphase spindle positioning. *Cell Cycle* 10, 783-793.

Mayer, M., Depken, M., Bois, J.S., Julicher, F., and Grill, S.W. (2010). Anisotropies in cortical tension reveal the physical basis of polarizing cortical flows. *Nature* 467, 617-621.

McGavin, M.K., Badour, K., Hardy, L.A., Kubiseski, T.J., Zhang, J., and Siminovitch, K.A. (2001). The intersectin 2 adaptor links Wiskott Aldrich

Syndrome protein (WASp)-mediated actin polymerization to T cell antigen receptor endocytosis. *J Exp Med* 194, 1777-1787.

McGill, M.A., McKinley, R.F., and Harris, T.J. (2009). Independent cadherin-catenin and Bazooka clusters interact to assemble adherens junctions. *J Cell Biol* 185, 787-796.

Medina, E., Williams, J., Klipfell, E., Zarnescu, D., Thomas, G., and Le Bivic, A. (2002). Crumbs interacts with moesin and beta(Heavy)-spectrin in the apical membrane skeleton of *Drosophila*. *J Cell Biol* 158, 941-951.

Megraw, T.L., Li, K., Kao, L.R., and Kaufman, T.C. (1999). The centrosomin protein is required for centrosome assembly and function during cleavage in *Drosophila*. *Development* 126, 2829-2839.

Mendes Pinto, I., Rubinstein, B., Kucharavy, A., Unruh, J.R., and Li, R. (2012). Actin depolymerization drives actomyosin ring contraction during budding yeast cytokinesis. *Dev Cell* 22, 1247-1260.

Mitchison, T.J., and Cramer, L.P. (1996). Actin-based cell motility and cell locomotion. *Cell* 84, 371-379.

Mitsushima, M., Aoki, K., Ebisuya, M., Matsumura, S., Yamamoto, T., Matsuda, M., Toyoshima, F., and Nishida, E. (2010). Revolving movement of a dynamic cluster of actin filaments during mitosis. *J Cell Biol* 191, 453-462.

Mizuno, H., Higashida, C., Yuan, Y., Ishizaki, T., Narumiya, S., and Watanabe, N. (2011). Rotational movement of the formin mDia1 along the double helical strand of an actin filament. *Science* 331, 80-83.

Moon, S.Y., and Zheng, Y. (2003). Rho GTPase-activating proteins in cell regulation. *Trends Cell Biol* 13, 13-22.

Morais-de-Sa, E., Mirouse, V., and St Johnston, D. (2010). aPKC phosphorylation of Bazooka defines the apical/lateral border in *Drosophila* epithelial cells. *Cell* 141, 509-523.

Morita, K., Hirono, K., and Han, M. (2005). The *Caenorhabditis elegans* ect-2 RhoGEF gene regulates cytokinesis and migration of epidermal P cells. *EMBO Rep* 6, 1163-1168.

Moseley, J.B., and Goode, B.L. (2006). The yeast actin cytoskeleton: from cellular function to biochemical mechanism. *Microbiol Mol Biol Rev* 70, 605-645.

Motegi, F., and Sugimoto, A. (2006). Sequential functioning of the ECT-2 RhoGEF, RHO-1 and CDC-42 establishes cell polarity in *Caenorhabditis elegans* embryos. *Nat Cell Biol* 8, 978-985.

Mullins, R.D., Heuser, J.A., and Pollard, T.D. (1998a). The interaction of Arp2/3 complex with actin: nucleation, high affinity pointed end capping, and formation of branching networks of filaments. *Proc Natl Acad Sci U S A* 95, 6181-6186.

Mullins, R.D., Kelleher, J.F., Xu, J., and Pollard, T.D. (1998b). Arp2/3 complex from *Acanthamoeba* binds profilin and cross-links actin filaments. *Mol Biol Cell* 9, 841-852.

Munro, E., Nance, J., and Priess, J.R. (2004). Cortical flows powered by asymmetrical contraction transport PAR proteins to establish and maintain anterior-posterior polarity in the early *C. elegans* embryo. *Dev Cell* 7, 413-424.

Nakajima, Y., Meyer, E.J., Kroesen, A., McKinney, S.A., and Gibson, M.C. (2013). Epithelial junctions maintain tissue architecture by directing planar spindle orientation. *Nature* 500, 359-362.

Nance, J., and Zallen, J.A. (2011). Elaborating polarity: PAR proteins and the cytoskeleton. *Development* 138, 799-809.

Narumiya, S., and Yasuda, S. (2006). Rho GTPases in animal cell mitosis. *Curr Opin Cell Biol* 18, 199-205.

Naumanen, P., Lappalainen, P., and Hotulainen, P. (2008). Mechanisms of actin stress fibre assembly. *J Microsc* 231, 446-454.

Neidt, E.M., Scott, B.J., and Kovar, D.R. (2009). Formin differentially utilizes profilin isoforms to rapidly assemble actin filaments. *J Biol Chem* 284, 673-684.

Neisch, A.L., Speck, O., Stronach, B., and Fehon, R.G. (2010). Rho1 regulates apoptosis via activation of the JNK signaling pathway at the plasma membrane. *J Cell Biol* 189, 311-323.

Niiya, F., Tatsumoto, T., Lee, K.S., and Miki, T. (2006). Phosphorylation of the cytokinesis regulator ECT2 at G2/M phase stimulates association of the mitotic kinase Plk1 and accumulation of GTP-bound RhoA. *Oncogene* 25, 827-837.

Nikolaidou, K.K., and Barrett, K. (2004). A Rho GTPase signaling pathway is used reiteratively in epithelial folding and potentially selects the outcome of Rho activation. *Curr Biol* *14*, 1822-1826.

Nishimura, T., Yamaguchi, T., Kato, K., Yoshizawa, M., Nabeshima, Y., Ohno, S., Hoshino, M., and Kaibuchi, K. (2005). PAR-6-PAR-3 mediates Cdc42-induced Rac activation through the Rac GEFs STEF/Tiam1. *Nat Cell Biol* *7*, 270-277.

Nishimura, Y., and Yonemura, S. (2006). Centralspindlin regulates ECT2 and RhoA accumulation at the equatorial cortex during cytokinesis. *J Cell Sci* *119*, 104-114.

Nobes, C.D., and Hall, A. (1995). Rho, rac, and cdc42 GTPases regulate the assembly of multimolecular focal complexes associated with actin stress fibers, lamellipodia, and filopodia. *Cell* *81*, 53-62.

Oceguera-Yanez, F., Kimura, K., Yasuda, S., Higashida, C., Kitamura, T., Hiraoka, Y., Haraguchi, T., and Narumiya, S. (2005). Ect2 and MgcRacGAP regulate the activation and function of Cdc42 in mitosis. *J Cell Biol* *168*, 221-232.

Oliferenko, S., and Balasubramanian, M.K. (2002). Astral microtubules monitor metaphase spindle alignment in fission yeast. *Nat Cell Biol* *4*, 816-820.

Olofsson, B. (1999). Rho guanine dissociation inhibitors: pivotal molecules in cellular signalling. *Cell Signal* *11*, 545-554.

Osman, M.A., Konopka, J.B., and Cerione, R.A. (2002). Iqg1p links spatial and secretion landmarks to polarity and cytokinesis. *J Cell Biol* *159*, 601-611.

Ostap, E.M. (2008). Tropomyosins as discriminators of myosin function. *Adv Exp Med Biol* *644*, 273-282.

Otomo, T., Otomo, C., Tomchick, D.R., Machius, M., and Rosen, M.K. (2005). Structural basis of Rho GTPase-mediated activation of the formin mDia1. *Mol Cell* *18*, 273-281.

Otto, J.J., Kane, R.E., and Bryan, J. (1980). Redistribution of actin and fascin in sea urchin eggs after fertilization. *Cell Motil* *1*, 31-40.

Paluch, E.K., and Raz, E. (2013). The role and regulation of blebs in cell migration. *Curr Opin Cell Biol* *25*, 582-590.

Paul, A.S., and Pollard, T.D. (2009). Energetic requirements for processive elongation of actin filaments by FH1FH2-formins. *J Biol Chem* 284, 12533-12540.

Pegtel, D.M., Ellenbroek, S.I., Mertens, A.E., van der Kammen, R.A., de Rooij, J., and Collard, J.G. (2007). The Par-Tiam1 complex controls persistent migration by stabilizing microtubule-dependent front-rear polarity. *Curr Biol* 17, 1623-1634.

Peng, J., Wallar, B.J., Flanders, A., Swiatek, P.J., and Alberts, A.S. (2003). Disruption of the Diaphanous-related formin Drf1 gene encoding mDia1 reveals a role for Drf3 as an effector for Cdc42. *Curr Biol* 13, 534-545.

Petronczki, M., and Knoblich, J.A. (2001). DmPAR-6 directs epithelial polarity and asymmetric cell division of neuroblasts in *Drosophila*. *Nat Cell Biol* 3, 43-49.

Phillips, G.N., Jr., Lattman, E.E., Cummins, P., Lee, K.Y., and Cohen, C. (1979). Crystal structure and molecular interactions of tropomyosin. *Nature* 278, 413-417.

Piekny, A., Werner, M., and Glotzer, M. (2005). Cytokinesis: welcome to the Rho zone. *Trends Cell Biol* 15, 651-658.

Pollard, T.D. (1986). Rate constants for the reactions of ATP- and ADP-actin with the ends of actin filaments. *J Cell Biol* 103, 2747-2754.

Pollard, T.D. (1990). Actin. *Curr Opin Cell Biol* 2, 33-40.

Pollard, T.D. (2007). Regulation of actin filament assembly by Arp2/3 complex and formins. *Annu Rev Biophys Biomol Struct* 36, 451-477.

Pollard, T.D., and Borisy, G.G. (2003). Cellular motility driven by assembly and disassembly of actin filaments. *Cell* 112, 453-465.

Pollard, T.D., and Cooper, J.A. (2009). Actin, a central player in cell shape and movement. *Science* 326, 1208-1212.

Pollard, T.D., and Wu, J.Q. (2010). Understanding cytokinesis: lessons from fission yeast. *Nat Rev Mol Cell Biol* 11, 149-155.

Pring, M., Evangelista, M., Boone, C., Yang, C., and Zigmond, S.H. (2003). Mechanism of formin-induced nucleation of actin filaments. *Biochemistry* 42, 486-496.

Prokopenko, S.N., Brumby, A., O'Keefe, L., Prior, L., He, Y., Saint, R., and Bellen, H.J. (1999). A putative exchange factor for Rho1 GTPase is required for initiation of cytokinesis in *Drosophila*. *Genes Dev* 13, 2301-2314.

Pruyne, D., Evangelista, M., Yang, C., Bi, E., Zigmond, S., Bretscher, A., and Boone, C. (2002). Role of formins in actin assembly: nucleation and barbed-end association. *Science* 297, 612-615.

Pruyne, D., Legesse-Miller, A., Gao, L., Dong, Y., and Bretscher, A. (2004). Mechanisms of polarized growth and organelle segregation in yeast. *Annu Rev Cell Dev Biol* 20, 559-591.

Quilliam, L.A., Lambert, Q.T., Mickelson-Young, L.A., Westwick, J.K., Sparks, A.B., Kay, B.K., Jenkins, N.A., Gilbert, D.J., Copeland, N.G., and Der, C.J. (1996). Isolation of a NCK-associated kinase, PRK2, an SH3-binding protein and potential effector of Rho protein signaling. *J Biol Chem* 271, 28772-28776.

Quinlan, M.E., Heuser, J.E., Kerkhoff, E., and Mullins, R.D. (2005). *Drosophila* Spire is an actin nucleation factor. *Nature* 433, 382-388.

Ramain, P., Heitzler, P., Haenlin, M., and Simpson, P. (1993). *pannier*, a negative regulator of *achaete* and *scute* in *Drosophila*, encodes a zinc finger protein with homology to the vertebrate transcription factor GATA-1. *Development* 119, 1277-1291.

Ratheesh, A., and Yap, A.S. (2012). A bigger picture: classical cadherins and the dynamic actin cytoskeleton. *Nat Rev Mol Cell Biol*.

Rauzi, M., Lenne, P.F., and Lecuit, T. (2010). Planar polarized actomyosin contractile flows control epithelial junction remodelling. *Nature*.

Razzaq, A., Robinson, I.M., McMahon, H.T., Skepper, J.N., Su, Y., Zelhof, A.C., Jackson, A.P., Gay, N.J., and O'Kane, C.J. (2001). Amphiphysin is necessary for organization of the excitation-contraction coupling machinery of muscles, but not for synaptic vesicle endocytosis in *Drosophila*. *Genes Dev* 15, 2967-2979.

Reymann, A.C., Boujemaa-Paterski, R., Martiel, J.L., Guerin, C., Cao, W., Chin, H.F., De La Cruz, E.M., Thery, M., and Blanchoin, L. (2012).

Actin network architecture can determine myosin motor activity. *Science* 336, 1310-1314.

Reymann, A.C., Martiel, J.L., Cambier, T., Blanchoin, L., Boujemaa-Paterski, R., and Thery, M. (2010). Nucleation geometry governs ordered actin networks structures. *Nat Mater* 9, 827-832.

Ridley, A.J. (2001). Rho GTPases and cell migration. *J Cell Sci* 114, 2713-2722.

Ridley, A.J. (2011). Life at the leading edge. *Cell* 145, 1012-1022.

Ridley, A.J., Schwartz, M.A., Burridge, K., Firtel, R.A., Ginsberg, M.H., Borisy, G., Parsons, J.T., and Horwitz, A.R. (2003). Cell migration: integrating signals from front to back. *Science* 302, 1704-1709.

Riedl, J., Crevenna, A.H., Kessenbrock, K., Yu, J.H., Neukirchen, D., Bista, M., Bradke, F., Jenne, D., Holak, T.A., Werb, Z., *et al.* (2008). Lifeact: a versatile marker to visualize F-actin. *Nat Methods* 5, 605-607.

Robertson, A.S., Smythe, E., and Ayscough, K.R. (2009). Functions of actin in endocytosis. *Cell Mol Life Sci* 66, 2049-2065.

Rogers, S.L., Wiedemann, U., Stuurman, N., and Vale, R.D. (2003). Molecular requirements for actin-based lamella formation in *Drosophila* S2 cells. *J Cell Biol* 162, 1079-1088.

Rohatgi, R., Ho, H.Y., and Kirschner, M.W. (2000). Mechanism of N-WASP activation by CDC42 and phosphatidylinositol 4, 5-bisphosphate. *J Cell Biol* 150, 1299-1310.

Romero, S., Le Clainche, C., Didry, D., Egile, C., Pantaloni, D., and Carlier, M.F. (2004). Formin is a processive motor that requires profilin to accelerate actin assembly and associated ATP hydrolysis. *Cell* 119, 419-429.

Rose, R., Weyand, M., Lammers, M., Ishizaki, T., Ahmadian, M.R., and Wittinghofer, A. (2005). Structural and mechanistic insights into the interaction between Rho and mammalian Dia. *Nature* 435, 513-518.

Rosenblatt, J., Cramer, L.P., Baum, B., and McGee, K.M. (2004). Myosin II-dependent cortical movement is required for centrosome separation and positioning during mitotic spindle assembly. *Cell* 117, 361-372.



Roubinet, C., Decelle, B., Chicanne, G., Dorn, J.F., Payrastre, B., Payre, F., and Carreno, S. (2011). Molecular networks linked by Moesin drive remodeling of the cell cortex during mitosis. *J Cell Biol* 195, 99-112.

Ryu, J.R., Echarri, A., Li, R., and Pendergast, A.M. (2009). Regulation of cell-cell adhesion by Abi/Diaphanous complexes. *Mol Cell Biol* 29, 1735-1748.

Sagot, I., Klee, S.K., and Pellman, D. (2002). Yeast formins regulate cell polarity by controlling the assembly of actin cables. *Nat Cell Biol* 4, 42-50.

Sakamori, R., Das, S., Yu, S., Feng, S., Stypulkowski, E., Guan, Y., Douard, V., Tang, W., Ferraris, R.P., Harada, A., *et al.* (2012). Cdc42 and Rab8a are critical for intestinal stem cell division, survival, and differentiation in mice. *J Clin Invest* 122, 1052-1065.

Salbreux, G., Charras, G., and Paluch, E. (2012). Actin cortex mechanics and cellular morphogenesis. *Trends Cell Biol* 22, 536-545.

Samora, C.P., Mogessie, B., Conway, L., Ross, J.L., Straube, A., and McAinsh, A.D. (2011). MAP4 and CLASP1 operate as a safety mechanism to maintain a stable spindle position in mitosis. *Nat Cell Biol*.

Sanchez, F., Tobin, S.L., Rdest, U., Zulauf, E., and McCarthy, B.J. (1983). Two *Drosophila* actin genes in detail. Gene structure, protein structure and transcription during development. *J Mol Biol* 163, 533-551.

Sandquist, J.C., Kita, A.M., and Bement, W.M. (2011). And the dead shall rise: actin and Myosin return to the spindle. *Dev Cell* 21, 410-419.

Saotome, I., Curto, M., and McClatchey, A.I. (2004). Ezrin is essential for epithelial organization and villus morphogenesis in the developing intestine. *Dev Cell* 6, 855-864.

Sasamura, T., Kobayashi, T., Kojima, S., Qadota, H., Ohya, Y., Masai, I., and Hotta, Y. (1997). Molecular cloning and characterization of *Drosophila* genes encoding small GTPases of the rab and rho families. *Mol Gen Genet* 254, 486-494.

Sato, M., and Saigo, K. (2000). Involvement of pannier and u-shaped in regulation of decapentaplegic-dependent wingless expression in developing *Drosophila notum*. *Mech Dev* 93, 127-138.

Schmidt, A., and Hall, A. (2002). Guanine nucleotide exchange factors for Rho GTPases: turning on the switch. *Genes Dev* 16, 1587-1609.

Schonegg, S., and Hyman, A.A. (2006). CDC-42 and RHO-1 coordinate acto-myosin contractility and PAR protein localization during polarity establishment in *C. elegans* embryos. *Development* 133, 3507-3516.

Schwamborn, J.C., and Puschel, A.W. (2004). The sequential activity of the GTPases Rap1B and Cdc42 determines neuronal polarity. *Nat Neurosci* 7, 923-929.

Schwanhaussner, B., Busse, D., Li, N., Dittmar, G., Schuchhardt, J., Wolf, J., Chen, W., and Selbach, M. (2011). Global quantification of mammalian gene expression control. *Nature* 473, 337-342.

Sechi, A.S., and Wehland, J. (2004). ENA/VASP proteins: multifunctional regulators of actin cytoskeleton dynamics. *Front Biosci* 9, 1294-1310.

Sedzinski, J., Biro, M., Oswald, A., Tinevez, J.Y., Salbreux, G., and Paluch, E. (2011). Polar actomyosin contractility destabilizes the position of the cytokinetic furrow. *Nature* 476, 462-466.

Segal, M., and Bloom, K. (2001). Control of spindle polarity and orientation in *Saccharomyces cerevisiae*. *Trends Cell Biol* 11, 160-166.

Sen, A., Nagy-Zsver-Vadas, Z., and Krahn, M.P. (2012). *Drosophila* PATJ supports adherens junction stability by modulating Myosin light chain activity. *J Cell Biol* 199, 685-698.

Severson, A.F., Baillie, D.L., and Bowerman, B. (2002). A Formin Homology protein and a profilin are required for cytokinesis and Arp2/3-independent assembly of cortical microfilaments in *C. elegans*. *Curr Biol* 12, 2066-2075.

Shemesh, T., Otomo, T., Rosen, M.K., Bershadsky, A.D., and Kozlov, M.M. (2005). A novel mechanism of actin filament processive capping by formin: solution of the rotation paradox. *J Cell Biol* 170, 889-893.

Simpson, P. (2007). The stars and stripes of animal bodies: evolution of regulatory elements mediating pigment and bristle patterns in *Drosophila*. *Trends Genet* 23, 350-358.

Simpson, P., Woehl, R., and Usui, K. (1999). The development and evolution of bristle patterns in *Diptera*. *Development* 126, 1349-1364.

Skau, C.T., Neidt, E.M., and Kovar, D.R. (2009). Role of tropomyosin in formin-mediated contractile ring assembly in fission yeast. *Mol Biol Cell* 20, 2160-2173.

Smith, P.R., Fowler, W.E., Pollard, T.D., and Aebi, U. (1983). Structure of the actin molecule determined from electron micrographs of crystalline actin sheets with a tentative alignment of the molecule in the actin filament. *J Mol Biol* 167, 641-660.

Snapper, S.B., Takeshima, F., Anton, I., Liu, C.H., Thomas, S.M., Nguyen, D., Dudley, D., Fraser, H., Purich, D., Lopez-Illasaca, M., *et al.* (2001). N-WASP deficiency reveals distinct pathways for cell surface projections and microbial actin-based motility. *Nat Cell Biol* 3, 897-904.

Somers, W.G., and Saint, R. (2003). A RhoGEF and Rho family GTPase-activating protein complex links the contractile ring to cortical microtubules at the onset of cytokinesis. *Dev Cell* 4, 29-39.

Song, B.D., and Schmid, S.L. (2003). A molecular motor or a regulator? Dynamin's in a class of its own. *Biochemistry* 42, 1369-1376.

Sotillos, S., Diaz-Meco, M.T., Caminero, E., Moscat, J., and Campuzano, S. (2004). DaPKC-dependent phosphorylation of Crumbs is required for epithelial cell polarity in *Drosophila*. *J Cell Biol* 166, 549-557.

St Johnston, D., and Ahringer, J. (2010). Cell polarity in eggs and epithelia: parallels and diversity. *Cell* 141, 757-774.

St Johnston, D., and Sanson, B. (2011). Epithelial polarity and morphogenesis. *Curr Opin Cell Biol*.

Stearns, T. (1997). Motoring to the finish: kinesin and dynein work together to orient the yeast mitotic spindle. *J Cell Biol* 138, 957-960.

Stevenson, R.P., Veltman, D., and Machesky, L.M. (2012). Actin-bundling proteins in cancer progression at a glance. *J Cell Sci* 125, 1073-1079.

Stewart, M.P., Helenius, J., Toyoda, Y., Ramanathan, S.P., Muller, D.J., and Hyman, A.A. (2011). Hydrostatic pressure and the actomyosin cortex drive mitotic cell rounding. *Nature* 469, 226-230.

Strutt, D.I., Weber, U., and Mlodzik, M. (1997). The role of RhoA in tissue polarity and Frizzled signalling. *Nature* 387, 292-295.

Stumpff, J., Duncan, T., Homola, E., Campbell, S.D., and Su, T.T. (2004). *Drosophila* Wee1 kinase regulates Cdk1 and mitotic entry during embryogenesis. *Curr Biol* 14, 2143-2148.

Su, K.C., Takaki, T., and Petronczki, M. (2011). Targeting of the RhoGEF Ect2 to the equatorial membrane controls cleavage furrow formation during cytokinesis. *Dev Cell* 21, 1104-1115.

Svitkina, T.M., Bulanova, E.A., Chaga, O.Y., Vignjevic, D.M., Kojima, S., Vasiliev, J.M., and Borisy, G.G. (2003). Mechanism of filopodia initiation by reorganization of a dendritic network. *J Cell Biol* 160, 409-421.

Sweeney, H.L., and Houdusse, A. (2010). Structural and functional insights into the Myosin motor mechanism. *Annu Rev Biophys* 39, 539-557.

Tanentzapf, G., and Tepass, U. (2003). Interactions between the crumbs, lethal giant larvae and bazooka pathways in epithelial polarization. *Nat Cell Biol* 5, 46-52.

Tatsumoto, T., Sakata, H., Dasso, M., and Miki, T. (2003). Potential roles of the nucleotide exchange factor ECT2 and Cdc42 GTPase in spindle assembly in *Xenopus* egg cell-free extracts. *J Cell Biochem* 90, 892-900.

Tatsumoto, T., Xie, X., Blumenthal, R., Okamoto, I., and Miki, T. (1999). Human ECT2 is an exchange factor for Rho GTPases, phosphorylated in G2/M phases, and involved in cytokinesis. *J Cell Biol* 147, 921-928.

Thery, M., and Bornens, M. (2008). Get round and stiff for mitosis. *HFSP J* 2, 65-71.

Thery, M., Racine, V., Pepin, A., Piel, M., Chen, Y., Sibarita, J.B., and Bornens, M. (2005). The extracellular matrix guides the orientation of the cell division axis. *Nat Cell Biol* 7, 947-953.

Tilney, L.G., Tilney, M.S., and Guild, G.M. (1996). Formation of actin filament bundles in the ring canals of developing *Drosophila* follicles. *J Cell Biol* 133, 61-74.

Tobin, S.L., Zulauf, E., Sanchez, F., Craig, E.A., and McCarthy, B.J. (1980). Multiple actin-related sequences in the *Drosophila melanogaster* genome. *Cell* 19, 121-131.

Tolliday, N., VerPlank, L., and Li, R. (2002). Rho1 directs formin-mediated actin ring assembly during budding yeast cytokinesis. *Curr Biol* 12, 1864-1870.

Toshima, J.Y., Toshima, J., Kaksonen, M., Martin, A.C., King, D.S., and Drubin, D.G. (2006). Spatial dynamics of receptor-mediated endocytic trafficking in budding yeast revealed by using fluorescent alpha-factor derivatives. *Proc Natl Acad Sci U S A* 103, 5793-5798.

Trichet, L., Le Digabel, J., Hawkins, R.J., Vedula, S.R., Gupta, M., Ribault, C., Hersen, P., Voituriez, R., and Ladoux, B. (2012). Evidence of a large-scale mechanosensing mechanism for cellular adaptation to substrate stiffness. *Proc Natl Acad Sci U S A*.

Usui, K., and Kimura, K. (1993). Sequential emergence of the evenly spaced microchaetes on the notum of *Drosophila*. *Dev Genes Evol* 203, 151–158.

van Impel, A., Schumacher, S., Draga, M., Herz, H.M., Grosshans, J., and Muller, H.A. (2009). Regulation of the Rac GTPase pathway by the multifunctional Rho GEF Pebble is essential for mesoderm migration in the *Drosophila* gastrula. *Development* 136, 813-822.

Vasiliev, J.M., Omelchenko, T., Gelfand, I.M., Feder, H.H., and Bonder, E.M. (2004). Rho overexpression leads to mitosis-associated detachment of cells from epithelial sheets: a link to the mechanism of cancer dissemination. *Proc Natl Acad Sci U S A* 101, 12526-12530.

Vavylonis, D., Kovar, D.R., O'Shaughnessy, B., and Pollard, T.D. (2006). Model of formin-associated actin filament elongation. *Mol Cell* 21, 455-466.

Veltman, D.M., and Insall, R.H. (2010). WASP family proteins: their evolution and its physiological implications. *Mol Biol Cell* 21, 2880-2893.

Vignaud, T., Blanchoin, L., and Thery, M. (2012). Directed cytoskeleton self-organization. *Trends Cell Biol*.

Wahlstrom, G., Lahti, V.P., Pispä, J., Roos, C., and Heino, T.I. (2004). *Drosophila* non-muscle alpha-actinin is localized in nurse cell actin bundles and ring canals, but is not required for fertility. *Mech Dev* 121, 1377-1391.

Waller, B.J., and Alberts, A.S. (2003). The formins: active scaffolds that remodel the cytoskeleton. *Trends Cell Biol* 13, 435-446.

Walther, R.F., and Pichaud, F. (2010). Crumbs/DaPKC-dependent apical exclusion of Bazooka promotes photoreceptor polarity remodeling. *Curr Biol* 20, 1065-1074.

Wang, Y.C., Khan, Z., Kaschube, M., and Wieschaus, E.F. (2012). Differential positioning of adherens junctions is associated with initiation of epithelial folding. *Nature* 484, 390-393.

Wang, Y.L. (1991). Dynamics of the cytoskeleton in live cells. *Curr Opin Cell Biol* 3, 27-32.

Watanabe, G., Saito, Y., Madaule, P., Ishizaki, T., Fujisawa, K., Morii, N., Mukai, H., Ono, Y., Kakizuka, A., and Narumiya, S. (1996). Protein kinase N (PKN) and PKN-related protein rhotaphilin as targets of small GTPase Rho. *Science* 271, 645-648.

Watanabe, N., Madaule, P., Reid, T., Ishizaki, T., Watanabe, G., Kakizuka, A., Saito, Y., Nakao, K., Jockusch, B.M., and Narumiya, S. (1997). p140mDia, a mammalian homolog of *Drosophila* diaphanous, is a target protein for Rho small GTPase and is a ligand for profilin. *EMBO J* 16, 3044-3056.

Watanabe, S., Ando, Y., Yasuda, S., Hosoya, H., Watanabe, N., Ishizaki, T., and Narumiya, S. (2008). mDia2 induces the actin scaffold for the contractile ring and stabilizes its position during cytokinesis in NIH 3T3 cells. *Mol Biol Cell* 19, 2328-2338.

Wawro, B., Greenfield, N.J., Wear, M.A., Cooper, J.A., Higgs, H.N., and Hitchcock-DeGregori, S.E. (2007). Tropomyosin regulates elongation by formin at the fast-growing end of the actin filament. *Biochemistry* 46, 8146-8155.

Wegner, A., and Isenberg, G. (1983). 12-fold difference between the critical monomer concentrations of the two ends of actin filaments in physiological salt conditions. *Proc Natl Acad Sci U S A* 80, 4922-4925.

Werner, A., Disanza, A., Reifenberger, N., Habeck, G., Becker, J., Calabrese, M., Urlaub, H., Lorenz, H., Schulman, B., Scita, G., *et al.* (2013). SCFFbxw5 mediates transient degradation of actin remodeller Eps8 to allow proper mitotic progression. *Nat Cell Biol* 15, 179-188.

Wiesner, S., Helfer, E., Didry, D., Ducouret, G., Lafuma, F., Carlier, M.F., and Pantaloni, D. (2003). A biomimetic motility assay provides insight into the mechanism of actin-based motility. *J Cell Biol* 160, 387-398.

Wodarz, A., Ramrath, A., Grimm, A., and Knust, E. (2000). *Drosophila* atypical protein kinase C associates with Bazooka and controls polarity of epithelia and neuroblasts. *J Cell Biol* 150, 1361-1374.

Wolfe, B.A., Takaki, T., Petronczki, M., and Glotzer, M. (2009). Polo-like kinase 1 directs assembly of the HsCyk-4 RhoGAP/Ect2 RhoGEF complex to initiate cleavage furrow formation. *PLoS Biol* 7, e1000110.

Wood, W., Jacinto, A., Grose, R., Woolner, S., Gale, J., Wilson, C., and Martin, P. (2002). Wound healing recapitulates morphogenesis in *Drosophila* embryos. *Nat Cell Biol* 4, 907-912.

Woolner, S., and Papalopulu, N. (2012). Spindle Position in Symmetric Cell Divisions during Epiboly Is Controlled by Opposing and Dynamic Apicobasal Forces. *Dev Cell*.

Wu, C., Lytvyn, V., Thomas, D.Y., and Leberer, E. (1997). The phosphorylation site for Ste20p-like protein kinases is essential for the function of myosin-I in yeast. *J Biol Chem* 272, 30623-30626.

Wu, J.S., and Luo, L. (2006). A protocol for mosaic analysis with a repressible cell marker (MARCM) in *Drosophila*. *Nat Protoc* 1, 2583-2589.

Xu, J., Wang, F., Van Keymeulen, A., Herzmark, P., Straight, A., Kelly, K., Takuwa, Y., Sugimoto, N., Mitchison, T., and Bourne, H.R. (2003). Divergent signals and cytoskeletal assemblies regulate self-organizing polarity in neutrophils. *Cell* 114, 201-214.

Xu, T., and Rubin, G.M. (1993). Analysis of genetic mosaics in developing and adult *Drosophila* tissues. *Development* 117, 1223-1237.

Xu, Y., Moseley, J.B., Sagot, I., Poy, F., Pellman, D., Goode, B.L., and Eck, M.J. (2004). Crystal structures of a Formin Homology-2 domain reveal a tethered dimer architecture. *Cell* 116, 711-723.

Yam, P.T., Wilson, C.A., Ji, L., Hebert, B., Barnhart, E.L., Dye, N.A., Wiseman, P.W., Danuser, G., and Theriot, J.A. (2007). Actin-myosin

network reorganization breaks symmetry at the cell rear to spontaneously initiate polarized cell motility. *J Cell Biol* 178, 1207-1221.

Yamanaka, T., Horikoshi, Y., Sugiyama, Y., Ishiyama, C., Suzuki, A., Hirose, T., Iwamatsu, A., Shinohara, A., and Ohno, S. (2003). Mammalian Lgl forms a protein complex with PAR-6 and aPKC independently of PAR-3 to regulate epithelial cell polarity. *Curr Biol* 13, 734-743.

Yamanaka, T., Horikoshi, Y., Suzuki, A., Sugiyama, Y., Kitamura, K., Maniwa, R., Nagai, Y., Yamashita, A., Hirose, T., Ishikawa, H., *et al.* (2001). PAR-6 regulates aPKC activity in a novel way and mediates cell-cell contact-induced formation of the epithelial junctional complex. *Genes Cells* 6, 721-731.

Yamane, J., Ohnishi, H., Sasaki, H., Narimatsu, H., Ohgushi, H., and Tachibana, K. (2011). Formation of microvilli and phosphorylation of ERM family proteins by CD43, a potent inhibitor for cell adhesion: cell detachment is a potential cue for ERM phosphorylation and organization of cell morphology. *Cell Adh Migr* 5, 119-132.

Yasuda, S., Ocegüera-Yanez, F., Kato, T., Okamoto, M., Yonemura, S., Terada, Y., Ishizaki, T., and Narumiya, S. (2004). Cdc42 and mDia3 regulate microtubule attachment to kinetochores. *Nature* 428, 767-771.

Yasuda, S., Taniguchi, H., Ocegüera-Yanez, F., Ando, Y., Watanabe, S., Monypenny, J., and Narumiya, S. (2006). An essential role of Cdc42-like GTPases in mitosis of HeLa cells. *FEBS Lett* 580, 3375-3380.

Yoshizaki, H., Ohba, Y., Kurokawa, K., Itoh, R.E., Nakamura, T., Mochizuki, N., Nagashima, K., and Matsuda, M. (2003). Activity of Rho-family GTPases during cell division as visualized with FRET-based probes. *J Cell Biol* 162, 223-232.

Yuce, O., Piekny, A., and Glotzer, M. (2005). An ECT2-centralspindlin complex regulates the localization and function of RhoA. *J Cell Biol* 170, 571-582.

Zanet, J., Stramer, B., Millard, T., Martin, P., Payre, F., and Plaza, S. (2009). Fascin is required for blood cell migration during *Drosophila* embryogenesis. *Development* 136, 2557-2565.



Zeitlinger, J., and Bohmann, D. (1999). Thorax closure in *Drosophila*: involvement of Fos and the JNK pathway. *Development* 126, 3947-3956.

Zelhof, A.C., Bao, H., Hardy, R.W., Razzaq, A., Zhang, B., and Doe, C.Q. (2001). *Drosophila* Amphiphysin is implicated in protein localization and membrane morphogenesis but not in synaptic vesicle endocytosis. *Development* 128, 5005-5015.

Zhang, H., and Macara, I.G. (2006). The polarity protein PAR-3 and TIAM1 cooperate in dendritic spine morphogenesis. *Nat Cell Biol* 8, 227-237.

Zheng, Z., Wan, Q., Liu, J., Zhu, H., Chu, X., and Du, Q. (2013). Evidence for dynein and astral microtubule-mediated cortical release and transport of Galphai/LGN/NuMA complex in mitotic cells. *Mol Biol Cell* 24, 901-913.

Zhu, X., Wang, J., Moriguchi, K., Liow, L.T., Ahmed, S., Kaverina, I., and Murata-Hori, M. (2011). Proper regulation of Cdc42 activity is required for tight actin concentration at the equator during cytokinesis in adherent mammalian Cells. *Exp Cell Res*.

Zigmond, S.H. (2004). Formin-induced nucleation of actin filaments. *Curr Opin Cell Biol* 16, 99-105.

Zulauf, E., Sanchez, F., Tobin, S.L., Rdest, U., and McCarthy, B.J. (1981). Developmental expression of a *Drosophila* actin gene encoding actin I. *Nature* 292, 556-558.

Zwaenepoel, I., Naba, A., Da Cunha, M.M., Del Maestro, L., Formstecher, E., Louvard, D., and Arpin, M. (2012). Ezrin regulates microvillus morphogenesis by promoting distinct activities of Eps8 proteins. *Mol Biol Cell* 23, 1080-1094.